

COASTAL ENGINEERING

196

IN JAPAN •

VOL. 1

UNIVERSITY OF HAWAII
LIBRARY

1958

LIBRARY USE ONLY

COMMITTEE OF COASTAL ENGINEERING,
JAPAN SOCIETY OF CIVIL ENGINEERS

DICAL

203

3

~~10~~

LIBRARY

Price ¥ 250. (including domestic mail fare)

PREFACE

Coast prevention from high tide and stormy wave is very important problem in Japan where the states are very serious in many parts of beach and cliff.

Since 1954, the conference on coastal engineering was held every year in this country, and the results of laboratory researches and field observations were reported in the meeting. The proceedings of the conference were published in Japanese edition and some copies of them have been sent abroad. But we have thought it is necessary to publish the English editions of the papers in the purpose of promotion of interchange of knowledge between Japan and other countries.

In the committee meeting of the last year, it was decided to begin to carry out our plan. We selected twelve papers, which seemed to be of general interest, and edited the volume 1 of "Coastal Engineering in Japan". Some of the included papers contain additional parts on the investigations later than the original papers.

Though there are still some financial difficulties, we are thinking on the plan of the publication of following volumes.

The Committee takes this opportunity to thank the authors of the papers and the many others who assisted in the preparation of this volume for publication.

Masashi HOM-MA, Chairman

Committee of Coastal Engineering

Japan Society of Civil Engineers

October, 1958

CONTENTS

1. Yasuo MASHIMA:	
Study on the Typhoon Characteristics in respect of Wave Development and the Distribution of Longshore Current	1
2. Shoitiro HAYAMI:	
Type of Breakers, Wave Steepness and Beach Slope.	21
3. HAYASHI and HATTORI:	
Pressure of the Breaker against a Vertical Wall.	25
4. SATO and KISHI:	
Experimental Study of Wave Run-up on Sea Wall and Shore Slope.	39
5. SHIMANO, HOM-MA and HORIKAWA:	
Effect of a Jetty on Nearshore Currents	45
6. K. HORIKAWA and C. SONU:	
An Experimental Study on the Effect of Coastal Groihs.	59
7. Y. IWAGAKI and T. SAWARAGI:	
Experimental Study on the Equilibrium Slopes of Beaches and Sand Movement by Breaker.	75
8. Yasuo MASHIMA:	
Study on Littoral Drift and Longshore Current.	85
9. T. ISHIHARA, Y. IWAGAKI and M. MURAKAMI:	
On the Investigation of Beach Erosion along the North Coast of Akashi Strait.	97
10. K. SHINOHARA T. TSUBAKI, M. YOSHITAKA and Ch. AGE MORI:	
Sand Transport along a Model Sandy Beach by Wave Action.	111
11. H. FUKUSHIMA and Y. MIZOGUCHI:	
Field Investigation of Suspended Littoral Drift.	131
12. Tamotsu KUBOO:	
Considerations by Fundamental Test of Jetty in River Month.	135

Study on the Typhoon Characteristics in respect of Wave Development and the distribution of Longshore Current.

Yasuo Mashima.

Dr. Eng., M.J.S.C.E. Prof. of
Civil Engineering Department,
Defence Academy, Yokosuka, Japan.

Index

- .. Introduction.
- .. General properties of Typhoon.
- .. The variation of wind direction and velocity in Typhoon region.
- .. Classification of longshore currents.
- .. Currents due to the momentum of wave.
- .. Longshore current due to breakers.
- .. Velocity of longshore current due to the successive breakers.
- .. Conclusion.

1. Introduction.

The essential fact that should be always taken into consideration on the design and construction of maritime structures is the stability of coasts. The coast perpetually repeats its transformation by the actions of tide, tidal currents, wave and longshore currents, and during a long period results often some gradual variations or happens an unexpected erosion or accretion from the construction of coast structures. In order to solve such problems the effects of following items on the coasts should be studied by their observations and theories, and any harmful effects should be treated to decrease as possible.

- (1) Ocean current (2) Tidal current
- (3) Tidal range (4) Waves
- (5) Currents due to waves
 - (a) Rip current, back rash
 - (b) Longshore current
- (6) Effects by the coast structures
- (7) Weather effects to wave, namely local characteristics of wind direction, wind velocity, and its duration, especially those of typhoon.
- (8) Time variation of above every items, that is, they will change in the same locality by year, month or day, so they will be treated statistically.
- (9) Coast characteristics, that is, the coast so changes perpetually that the sizes and properties of coast materials, slopes of beach, sea bottom and coast rocks are to be stable. The extent to harm the coast stabilities by some abrupt change of sea circumstances

depends upon their original states.

Among them, the properties of tropical low atmospheric pressure (typhoon) in regard to wave developments and the fundamental theory of velocity distribution of longshore currents in the near coast region are illustrated in this report.

2. General properties of typhoon.

Among all kinds of the winds in the neighbourhood of Japan, the typhoon accompanies with violent winds and furious waves especially at the south portion of Japan and frequently happens terrible damages to ships, coast and harbours. The typhoon usually travels from the south part to north and then to Aleutian Islands altering its properties to the temperate low atmospheric pressure. The wind of a typhoon has the following characters when we observe it at a locality of coasts.

- (1) Wind directions change corresponding to the center situation of typhoon. They will reverse as the center of typhoon pass through the place and the wind often ceases at the time of passing. If the center passes far from the locality, the direction of wind changes gradually.
- (2) Wind velocities change corresponding to the atmospheric pressure gradient.
- (3) Typhoons often accompany with high tides.
- (4) In the typhoon region, winds are violent and generate raging waves. The wave directions are recognized to be rotative and radial to its center. Out of the region, swell propagates far away.

These conditions have an intimate relations with the elements of typhoon, that is, the center pressure, traveling velocity of typhoon region, the situation of center of typhoon relative to the observation point, area of typhoon region. Here the typhoon region is assumed the scope surrounded by a closed isobaric line where wind

velocity is larger than 5 m/sec. The typhoon region is the wind wave generating area and swells propagate out of this region. In order to estimate whether one point on the coast enters into the typhoon region, it is necessary to use the probability of the typhoon course to pass the point and its properties.

Here some relations between wind direction, wind velocity and its duration time in connection with the observation point and the center of typhoon are calculated as follows using their models and they will be fundamentals of wave estimation in the typhoon regions.

3. The variation of wind direction and velocity in typhoon region.

(A) The case when wind velocity is assumed to have no connection with the travelling velocity of typhoon. The typhoon region is assumed a circle of radius R , its center as the origin of polar coordinates and the situation of the observation point is $P(r, \theta)$. The direction of $\theta = 0$ takes the north direction. If the center travels to the direction α with velocity U , the observation point P is just like to travel to the direction $(\alpha + \pi)$ with the same velocity U . Usually the wind direction in a typhoon region has a counter clockwise revolution and its velocity is not equal in the both sides of travelling direction, so that the typhoon is considered to travel riding on a air current. At first the variation of wind velocity due to the travelling velocity is neglected here.

If at time $t=0$ the position of observation point is (r_0, θ_0) ,

$$\frac{dr \cos(\alpha - \theta)}{dt} = -U \dots (1)$$

$$\frac{dr \sin(\alpha - \theta)}{dt} = 0 \dots (2)$$

From these two formulas

$$\tan(\alpha - \theta) = \frac{r_0 \sin(\alpha - \theta_0)}{-Ut + r_0 \cos(\alpha - \theta_0)} \dots (3)$$

$$r = r_0 \frac{\sin(\alpha - \theta_0)}{\sin(\alpha - \theta)} \dots (4)$$

and

$$r = \sqrt{r_0^2 - 2Ut r_0 \cos(\alpha - \theta_0) + U^2 t^2} \dots (5)$$

Therefore if the initial position $(r_0,$

$\theta_0)$, travelling velocity U and travelling direction α are known, (r, θ) at any time is calculated. The azimuth of the center of the typhoon at P (the observation point) is $\pi + \theta$

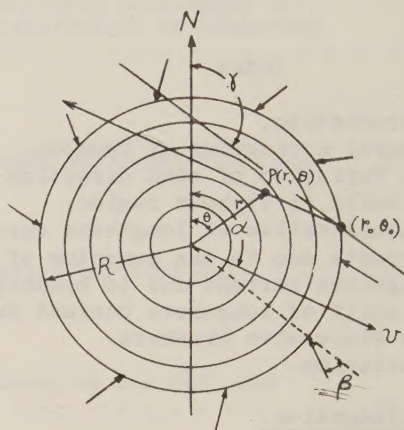


Fig.-1

If the wind direction is assumed to deviate β degree to right hand (in north hemisphere) from the direction of atmospheric pressure gradient, the blow on direction angle is $(\theta + \beta)$ and the blow off direction angle is $(\pi + \theta + \beta)$. β is usually $30^\circ \sim 60^\circ$. Now it is assumed β is not influenced by U . From (3)

$$\theta + \beta = \alpha + \beta - \tan^{-1} \frac{r_0 \sin(\alpha - \theta_0)}{-Ut + r_0 \cos(\alpha - \theta_0)} \dots (6)$$

If the direction angle of the coast line from left to right facing to off shore from the coast is γ , the angle between the blow off direction of the wind and the direction of the coast line is $\xi = \pi + \beta + \theta - \gamma \dots (7)$ as shown in Fig.-2.

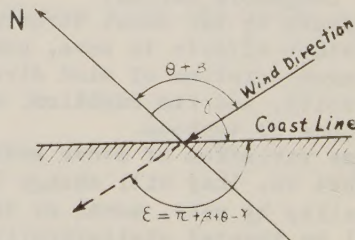


Fig. 2

The wind in the range of $\xi = 0^\circ$ to 180° is a see wind and in $\xi = 180^\circ$ to 360° is a land wind.

If the wind velocity is approximately reversely

proportional to the square of the distance from the center of the typhoon, and velocity V m/sec is

$$V = \frac{K}{r^2} = \frac{K}{r_0^2 - 2vt r_0 \cos(\alpha - \theta_0) + v^2 t^2} \quad \dots (8)$$

where k is the constant of proportion that is considered to relate to the center pressure and the area of the typhoon region, namely the atmospheric pressure gradient, whether the position is in the danger half circle, and the latitude. Accordingly k must be estimated from the observation values. By the above method, the wind direction and the velocity at the observation point of the coast at any time are able to be about estimated from the travelling direction, velocity, area, center position of the typhoon and the direction of the coast line. But actually the travelling direction, velocity, the center pressure and the region of the typhoon are not uniform and vary from time to time. So it must be modified corresponding to these variation. If the circumstances of a typhoon can be supposed by a long period observation, the wind conditions and accordingly the waves caused by the typhoon may be estimated.

In Fig.-3 $\alpha = 45^\circ$, $\beta = 45^\circ$, $\beta = 30^\circ$, $k = 300 \text{ km}^2/\text{hr}$, $\theta_0 = 120^\circ$, the curves are the variations of r and ξ when the typhoon travels off shore parallel with the coast line.

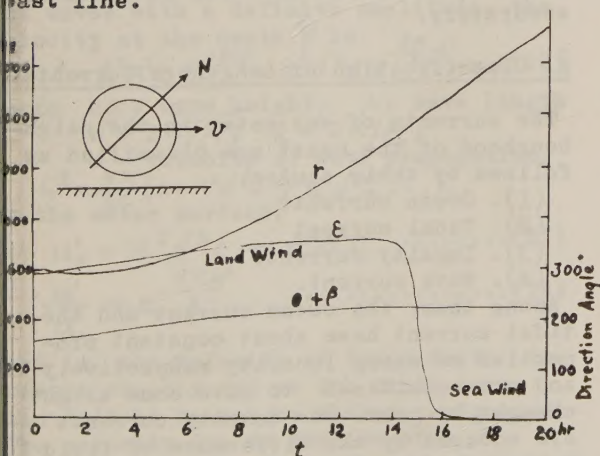


Fig-3

) The case when the typhoon travels with an air current of constant direction. In this case the wind direction and velocity are the resultant of the motion

of an air current and the inverse revolution wind of a reposed typhoon. Therefore the wind directions of both motions are opposite in the left side of the travelling direction of a typhoon and the wind velocity is decreased, and on the contrary the velocity is increased adding both motions in the right side of the typhoon where is called the danger semi-circle. The stream line of air in a typhoon is a spiral of equal deviation when the typhoon is travelling. The direction of a tangent on the air stream line is the wind direction at that point, but the straight line of wind direction does not necessarily coincide with the stream line. Therefore the distance of the straight part of a stream line is to be taken as a fetch.

Now if the wind velocity of (8) and velocity V of an air current in the direction α are added, the resultant wind velocity V_p and its direction τ in direction angle are

$$V_p = \sqrt{V^2 + v^2 - 2Vv \cos(\theta + \beta - \alpha)}$$

$$= \sqrt{V^2 + v^2 - 2Vv \cos\left\{\beta - \tan^{-1} \frac{r_0 \sin(\alpha - \theta_0)}{r_0 \cos(\alpha - \theta_0) - vt}\right\}}$$

$$\tau = \theta + \beta \pm 2 \tan^{-1} \sqrt{\frac{(S - V)(S - V_p)}{S(S - v)}} \quad \dots (9)$$

$$\dots (10)$$

where $S = \frac{1}{2}(V + V_p + v)$ (Plus sign is the case when the typhoon travels to right of the line towards the north.)

The wind direction at the coast is $\xi = \tau + \beta \quad \dots (11)$

By these formulas, the variation of wind directions and velocities with time can be calculated and so the duration time of any wind direction is obtained. When $\alpha = 45^\circ$, $\beta = 60^\circ$, $\theta_0 = 60^\circ$, $r_0 = 500 \text{ km}$, $V = 40 \text{ km/hr}$, the time variation of V_p and ξ at the coast $\gamma = 300^\circ$ is indicated in Fig.-4. From this figure, the relations between wind directions, wind velocities and its duration time are obtained. And by the figure of stream line, the distance to supply the wind energy to waves, or the fetch can be obtained.

For example, when $\alpha = 60^\circ$, $\beta = 60^\circ$, $V = 40 \text{ km/hr}$, $V = k/r^2$, $k = 520 \text{ km}^2/\text{sec}$, the stream line of a typhoon is Fig.-5.

The time variation of fetch can be gotten from the situation of this stream line in reference to the coast line. When the part near the circumference of the typhoon pass through the observation

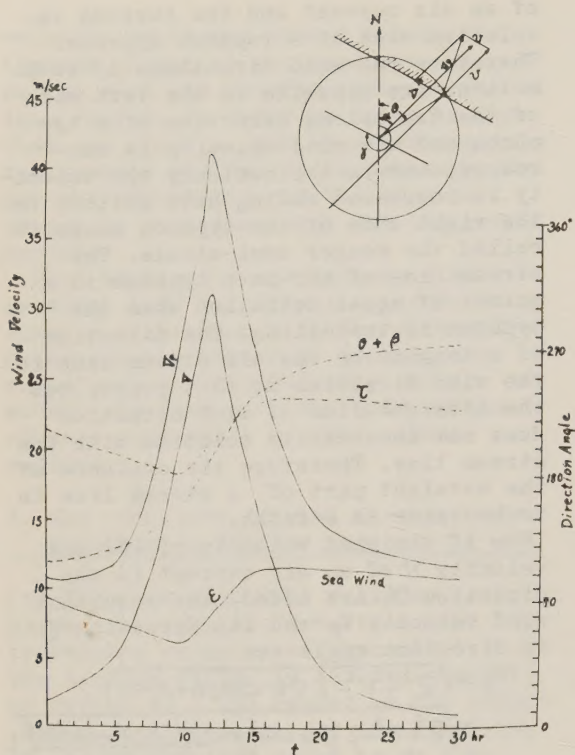


Fig.-4.

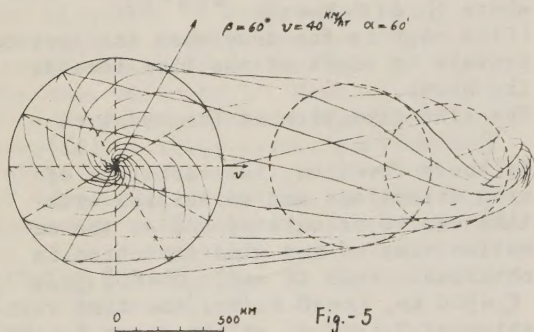


Fig.-5

point, the change of wind directions is slack, but when its center passes there, the wind direction varies suddenly and the wind velocity is so large that occurs raging billows in spite of small fetch. The waves develop by the supply of energy in the initial wind direction and next different wind direction when the wind directions are varying. At this case the waves of the first direction does not get any supply of energy and is in the decay state, but if the wind direction changes slowly, the first

waves are yet faintly present, and the second wave grows gradually. But when the wind direction varies suddenly as the center region of a typhoon, the first, the second and the other waves exist at the same time and results very irregular composite waves.

The above method is applied to the circular model of a typhoon, but it can be similarly applied to the elliptic region of a typhoon or to the temperate low atmospheric pressure region accompanied with a discontinuous line. The diameter of the temperate low pressure region as a wave generating area is about 2000 to 3000 km, and the region of ordinary tropic low pressures has 1000 to 2000 km diameter. However the area of Japan Sea is about 1500 x 700 km and the Pacific Ocean about 10000 x 10000 km. So the fetch can usually take the distance to the opposite shore in Japan Sea and the similar water basin, but in the Pacific Ocean the wind regions contain only one part of the total area, so that the fetch depends upon the locality and properties of the wind regions. With respect to these problems, the temperate low pressure region with a discontinuous line is very different from the typhoon. Above the general circumstances of the fetch, the variation of wind direction, wind velocity and its duration time of the typhoon are treated in order to carry out the wave estimations accurately.

4. Classification of Longshore Currents.

The currents of sea water in the neighbourhood of the coast are classified as follows by their causes.

- (1). Ocean current.
- (2). Tidal current
- (3). Density current.
- (4). Wave current.

Among them, the ocean current and the tidal current have about constant properties at every locality respectively and are considered to have some slight changes by year. The density currents are occurred by the difference of field densities due to the temperature and salinity of sea water, and the contributions of river water, etc. and depends mainly upon the long period weather variation. Above three kinds of currents have not large velocities near coasts except at the complicated

topography as narrow straits. However the fourth current due to the waves exist where waves exist and depends upon the wave conditions. Accordingly the velocity and direction of this current change always by position and time. Especially near coast where conditions change suddenly, therefore the circumstances of the currents are not uniform. So they should be treated statistically in connection with winds which are the cause of waves in order to demand the general properties of the current. And the facts that the velocity of currents is large near coasts, they have intense turbulences due to the wave breaking and the directions of the currents vary from normal to parallel with the coast line, have great influences upon the stability of the coast. On the open ocean, the current accompanied with the waves by the prevailing wind will be the cause of the ocean currents. In the following articles, the currents due to waves near coast and their variation caused by the properties of coast will be stated systematically according to the wave conditions, and especially the distribution of the longshore current will be expressed.

Currents due to the momentum of waves.

According to Stokes' theory of deep sea waves with a definite amplitude, the velocity at the depth h' is

$$u' = k^2 a^2 c e^{-2kh'} = \pi^2 \sigma^2 c e^{-\frac{2\pi}{\lambda} h'} \dots (12)$$

where $2a$: wave height, λ : wave length
 $\sigma = 2a/\lambda$, $k = 2\pi/\lambda$,
 c = velocity of wave propagation,
 $c^2 = \frac{g\lambda}{2\pi} (1 + \pi^2 \sigma^2 + \frac{5}{4} \pi^4 \sigma^4 + \dots)$
 the water surface,

$$u'_0 = \pi^2 \sigma^2 c = k^2 a^2 c \dots (13)$$

$$\frac{u'}{u'_0} = e^{-\frac{4\pi h'}{\lambda}} \dots (14)$$

that is, the velocity at large depth decreases rapidly and at the depth more than $\lambda/2$ it cannot be almost recognized. The velocity due to the momentum of waves with a definite amplitude at shallow water is as the mean value u' between the wave length

$$\begin{aligned} u' &= \frac{1}{2} k^2 a^2 c \frac{\cosh 2k(h-h')}{\sinh^2 kh} \\ &= \frac{1}{2} \left(\frac{2\pi a}{\lambda} \right)^2 c \frac{\cosh \frac{4\pi}{\lambda} (h-h')}{\sinh^2 \frac{2\pi h}{\lambda}} \dots (15) \end{aligned}$$

the surface

$$\left. \begin{aligned} u'_0 &= \frac{1}{2} k^2 a^2 c (1 + \coth^2 kh) \\ \text{At the sea bottom} \\ u'_b &= \frac{1}{2} k^2 a^2 c (\coth^2 kh - 1) \end{aligned} \right\} \dots (16)$$

The mean velocity u'_m of depth h is

$$u'_m = k^2 a^2 c \frac{\coth kh}{2kh} = \frac{\pi \left(\frac{2a}{\lambda} \right)^2}{4 \left(\frac{h}{\lambda} \right)} \sqrt{\frac{g\lambda}{2\pi}} \coth \frac{2\pi h}{\lambda} \dots (17)$$

The discharge by this velocity is

$$Q = h u'_m B \dots (18)$$

where

h = depth, B = length of wave crest line.

This discharge is due to that the progressive velocity at the wave crest is larger than the regressive velocity at the wave trough. When the waves approach the shallower sea propagating to the coast, and increase their wave steepnesses, and then at last break, the water volume that can not be sustained in waves will move to the part of smaller discharge and result in a longshore current or rip current.

The velocity distribution of the current due to waves at various coasts will be as follows.

(1) Straight and upright coast.

In the case that the equal depth lines are parallel with the coast and wave direction is perpendicular to the coast, if the waves do not break coming to the coast, they will reflect 100 per cent at the upright coast and result a clapotis. So the progressive momentum of waves will disappear. If the waves break on the way, the secondary waves will be formed according to the break conditions and they will reflect at the coast to build the clapotis of themselves. The released water from the waves by breaking will grow at last to the off shore current.

(2) Straight and inclined coast.

It is assumed that the equal depth lines are parallel with the coast and the wave direction is perpendicular to the coast. When the waves come near the coast, they will break and the released water will remain so long that their water head will be risen to balance the water volume with the off shore discharge. This counter currents will flow along the bottom and it will tend to form some sand ridges where the forward current and the counter current will encounter with equilibrium. If the sand ridges are once formed, they will be

apt to fix the breaker line and promote their formation. As there is a limit of sand diameter to rest corresponding to the current velocity, after a long period of the same wave condition, the sand ridge will develop more and more shallower, but it will stop their development as the sand diameter has the larger limit to some extent. The discharge will flow off shore uniformly over the ridge or will concentrate on its discontinuous point to cut the ridges.

(3) Straight and upright coast, equal depth contour lines are parallel with coast and wave direction is oblique to the coast.

When the waves reach to the coast without breaking, they will reflect 100 per cent, so as to have the direction of the reflective waves that the angle of incidence equals to the angle of reflection by Fermat's principle. It is assumed that the angle between the crest line direction of waves and the coast line is α , and the particle velocities of progression of both the incident waves and reflective waves will be decomposed to the component velocities of parallel and normal to the coast.

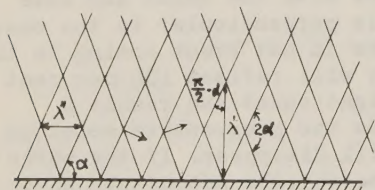


Fig-6.

It will be able to think that the normal components of the incident and reflective waves will build the stationary wave and disappear their progressive property, but the parallel components will maintain the progressive wave motion on which wave height is double the incident wave, wave length λ' is equal to $\lambda / \sin \alpha$ and its period is same as the incident waves. Therefore by using $k \sin \alpha$ for k , $\lambda / \sin \alpha$ for λ and $2a \sin \alpha$ for a in formulas (15) (16) and (17), the velocity due to the parallel momentum with coast will be found. So there are nodes of the wave at the distance $(\frac{1}{4} + \frac{n}{2}) \frac{\lambda}{\cos \alpha}$ from the coast and loop at $\frac{n}{2} \frac{\lambda}{\cos \alpha}$. The parallel velocity at the loop will be

$$u'_p = 2k^2 a^2 c \frac{\cosh\{2k(h-h')\} \sin \alpha \sin^4 \alpha}{\sinh^2(kh \sin \alpha)} \dots (19)$$

where

$$c = \sqrt{\frac{g}{k \sin \alpha}} \tanh(kh \sin \alpha)$$

At the surface

$$u'_{p0} = 2k^2 a^2 c \{1 + \coth^2(kh \sin \alpha)\} \sin^4 \alpha$$

At the sea bottom

$$u'_{pb} = 2k^2 a^2 c \{\coth^2(kh \sin \alpha) - 1\} \sin^4 \alpha$$

The average velocity for depth h will be

$$\begin{aligned} u'_{pm} &= 4k^2 a^2 c \frac{\coth(kh \sin \alpha)}{2kh \sin \alpha} \sin^4 \alpha \\ &= 2k^2 a^2 c \frac{\coth(kh \sin \alpha)}{kh} \sin^3 \alpha \dots (20) \\ &= \pi \left(\frac{2a}{\lambda}\right)^2 \sin^3 \alpha \sqrt{\frac{g\lambda}{2\pi \sin \alpha}} \coth\left(\frac{2\pi}{\lambda} h \sin \alpha\right) \end{aligned}$$

There will not exist any parallel velocities at the node where the surface does not appear wave forms. The parallel velocity at a distance y from the coast will be considered that two progressive waves which half wave height is $a \sin \alpha$ and wave length $\lambda' = \lambda / \sin \alpha$ will progress to the same direction with a phase difference $4\pi y / \lambda'$. Here is $\lambda' = \lambda / \cos \alpha$. Therefore the wave form will be

$$\begin{aligned} \zeta &= a \sin \alpha \sin(kx - \sigma t) \\ &\quad + a \sin \alpha \sin(kx - \sigma t + \frac{4\pi y}{\lambda'}) \\ &= a \sin \alpha [\{\sin(kx \sin \alpha) \\ &\quad + \sin(kx \sin \alpha + 2ky \cos \alpha)\} \cos \sigma t \\ &\quad - \{\cos(kx \sin \alpha) + \cos(kx \sin \alpha \\ &\quad + 2ky \cos \alpha)\} \sin \sigma t] \\ &= a \sin \alpha \sqrt{2\{1 + \cos(2ky \cos \alpha)\}} \\ &\quad \times \sin\{kx \sin \alpha + ky \cos \alpha - \sigma t\} \dots \dots \dots (21) \end{aligned}$$

Using $a \sin \alpha \sqrt{2\{1 + \cos(2ky \cos \alpha)\}}$ for half wave height and $k \sin \alpha$ for wave length in formulas (15) -- (17), the parallel velocity with the coast due to this resultant wave will be as follows. The mean velocity for a wave length will be

$$\begin{aligned} u'_p &= a^2 k^2 \sin^4 \alpha \{1 + \cos(2ky \cos \alpha)\} \sqrt{\frac{g}{k \sin \alpha}} \tanh(kh \sin \alpha) \\ &\quad \times \frac{\cosh\{2k \sin \alpha (h - h')\}}{\sinh^2(kh \sin \alpha)} \dots \dots (22) \end{aligned}$$

At the surface

$$U'_{p0} = a^2 k^2 \sin^4 \alpha \{1 + \cos(2ky \cos \alpha)\} \{1 + \coth^2(kh \sin \alpha)\} \times \sqrt{\frac{g}{k \sin \alpha} \tanh(kh \sin \alpha)} \dots (23)$$

At the sea bottom

$$U'_{pb} = a^2 k^2 \sin^4 \alpha \{1 + \cos(2ky \cos \alpha)\} \{ \coth^2(kh \sin \alpha) - 1 \} \sqrt{\frac{g}{k \sin \alpha} \tanh(kh \sin \alpha)} \dots (24)$$

The mean velocity for the depth h is

$$U'_{pm} = \frac{a^2 k^2}{kh} \sin^3 \alpha \{1 + \cos(2ky \cos \alpha)\} \times \sqrt{\frac{g}{k \sin \alpha} \coth(kh \sin \alpha)} \dots (25)$$

where $k = 2\pi/\lambda$.

The variation of these velocities in the normal direction to the coast will be found for y . It will change with wave length $y = \lambda/2 \cos \alpha \dots (26)$

For $2ky \cos \alpha = 2\pi$.

The value of $\{1 + \cos(2ky \cos \alpha)\}$ in formulas 22)-(25) varies as follows.

$y = 0$ (at coast)	2
$y = \lambda/8 \cos \alpha$	1
$y = \lambda/4 \cos \alpha$	0
$y = 3\lambda/8 \cos \alpha$	1
$y = \lambda/2 \cos \alpha$	2

At the loop $y = \frac{n}{2} \frac{\lambda}{\cos \alpha}$, the parallel velocity is max. and at the node

$y = (\frac{1}{4} + \frac{n}{2}) \frac{\lambda}{\cos \alpha}$ it is minimum. The parallel discharge Q at the range from $y = 0$ to $y = \lambda/4 \cos \alpha$ will be

$$Q = h \int_0^{\lambda/4 \cos \alpha} U'_{pm} dy$$

$$= \frac{k k^2 a^2 \lambda \sin^3 \alpha}{k h \cos \alpha} \sqrt{\frac{g}{k \sin \alpha} \coth(kh \sin \alpha)} \dots (27)$$

Therefore the mean velocity U'_{mp} at this width is

$$\begin{aligned} U'_{mp} &= \frac{Q}{\lambda h} = \frac{k^2 a^2}{k h} \sin^3 \alpha \sqrt{\frac{g}{k \sin \alpha} \coth(kh \sin \alpha)} \\ &= \frac{\pi}{2} \left(\frac{2a}{\lambda} \right)^2 \sin^3 \alpha \sqrt{\frac{g \lambda}{2\pi \sin \alpha} \coth\left(\frac{2\pi h}{\lambda} \sin \alpha\right)} \dots (28) \end{aligned}$$

(4) Straight, but bent at one point and upright coast.

If the straight coast bends β degrees and the angle between the wave crest line and the coast line I is α as in Fig.-7, the angle between the wave crest line and the coast line II will be $\pi - (\beta - \alpha)$. In order to compare the velocities at coast I and II, applying $\pi - (\beta - \alpha)$ instead of α in formula (28)

$$\frac{U'_{mpI}}{U'_{mpII}} = \left\{ \frac{\sin \alpha}{\sin(\beta - \alpha)} \right\}^{\frac{5}{2}} \sqrt{\frac{\coth\left(\frac{2\pi h}{\lambda} \sin \alpha\right)}{\coth\left\{\frac{2\pi h}{\lambda} \sin(\beta - \alpha)\right\}}} \dots (29)$$

When $\alpha = \beta - \alpha$, namely $\beta = 2\alpha$, $U'_{mpI} = U'_{mpII}$ and their directions are opposite. If h/λ is sufficient large, the parallel velocity at coast I will be larger than one at coast II when $\alpha > \beta - \alpha$ or $2\alpha > \beta$, but if h/λ is small, the velocity at coast II will be some times larger. These variation is indicated in Fig.-8.

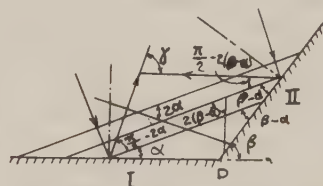


Fig- 7.

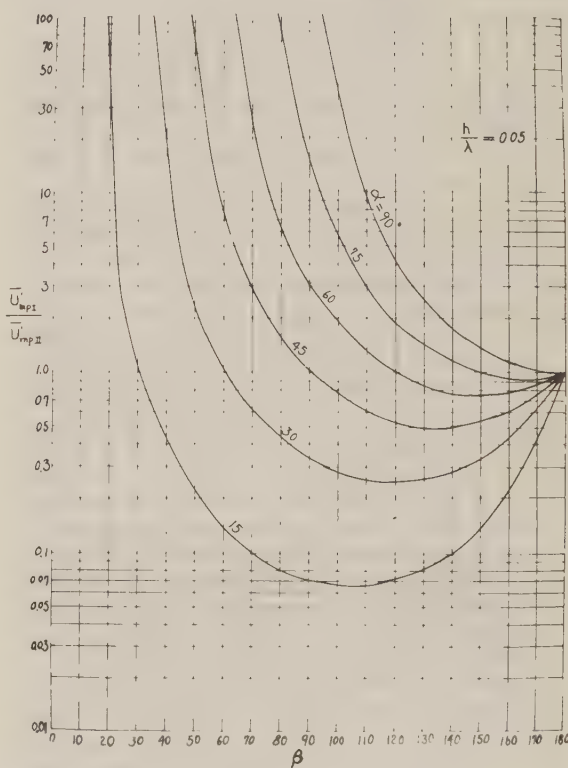


Fig- 8

If it is assumed that the parallel mean velocity in (28) with coast I and II are U_1 and U_2 respectively and the current toward the right side facing off shore at coast is expressed (+) and towards the left side (-), when $\beta = 0$, $U_1 = U_2$ and they will have

same direction, when $\beta = \alpha$, $U_1 > U_2, U_2 = 0$. The velocity of $+U_1$ will be decreased in the vicinity of point P and at coast II there will occur (+) current due to the reflective wave when $2\alpha > \pi/2$ and its velocity will change according to the angle to the coast II. When $2\alpha < \frac{\pi}{2}$, the reflection wave will leave from the coast II and its refractive wave will arrive at the coast II, so that the current will flow off shore.

When $2\alpha = \pi/2$, it is supposed that the reflective wave will propagate parallel with the coast II and decay on the way of propagation decreasing its velocity, so that the discharge will vary to a horizontal flow and spread widely.

When $\beta > \alpha$, the velocities will become $+U_1$ and $-U_2$ and their discharges meeting at point P will flow off shore from P or wash away to the region of smaller velocity. When $\alpha > \pi/2$, the wave at I is one due to land winds and at II to sea wind, resulting non uniform wave conditions, so that the above formulas cannot be applied at once. For the encounter and reflection of waves do not occur at I and do only at II.

When $\beta < \alpha$, the velocities will become $+U_1$ and $+U_2$, and $\alpha > \alpha - \beta$, so the mean velocity at I is larger than that at II and the discharge due to their difference will remain adjacent P and flow out off shore or parallel with II.

When $\beta < 0$; If $\alpha + \beta < \pi/2$, it will be $+U_1 < +U_2$. As the velocity at II from point P will be larger, there will occur the supplemental current from the open sea. When $\alpha + \beta = \pi/2$, $+U_2$ will be max. When $\alpha + \beta > \pi/2$, the incidental waves will leave from II and only their refractive waves will arrive at II.

In the general coast, the depth varies irregularly and the equal depth contours have not any uniform figures. Therefore the directions of wave propagation will refract and the wave height and wave length will vary accordingly. So the height and length of the waves should be corrected by using the refraction diagram and found velocity distributions by the incident wave direction. In addition the currents along the coast varies towards the normal to the coast, so the relation of flow out and supplement should be estimated by their variation.

(5) Upright curved coast and the depth is constant.

When the waves arrive at the coast without breaking, they will reflect 100 per cent. Here it is assumed that the tangent line at one point O on the coast in Fig.-9 as x-axis and the angle between the x-axis and wave crest line as α_0 .

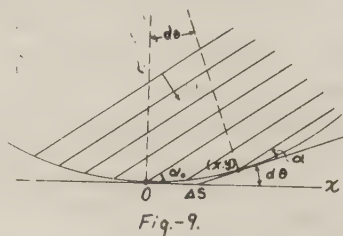


Fig.-9.

The reflective waves at this point will propagate with angle $(2\pi - \alpha_0)$ to x-axis and occur the parallel current at this point. Now consider the current at a voluntary point (x, y) on the coast. The figure of the coast is assumed to be expressed $y = f(x)$ and the angle between the tangent at (x, y) and x-axis equals θ . So

$$\tan \theta = dy/dx = f'(x)$$

If the angle between the wave crest line at (x, y) and the coast line is assumed α ,

$$\alpha = \alpha_0 - \theta = \alpha_0 - \tan^{-1} \left(\frac{dy}{dx} \right) = \alpha_0 - \tan^{-1} f'(x) \quad \dots \dots \dots (30)$$

By applying this α to the formulas (22)--(25), it will be found the velocity distribution. When the velocity will decrease with x , namely the coast curve is concave off shore, the discharge due to the wave will decrease along the coast, so its difference will develop as the longshore current. For example, if the coast curve is a circle expressed by $y = r - \sqrt{r^2 - x^2}$,

$$\alpha = \alpha_0 - \tan^{-1} \frac{x}{\sqrt{r^2 - x^2}}, \text{ where } r = \text{radius of the circle.}$$

In this case, the velocity will decrease along the coast and the difference of the discharge will result in a steady current following the topography.

(6) Straight and inclined coast. Equal depth contours are parallel with the coast and the direction of wave propagation is oblique to the coast line.

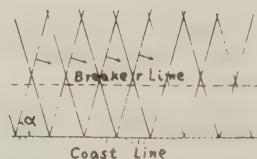


Fig.-10

When the wave approaches to the coast, there occurs longshore currents due to the breakers. Here we consider the state of current before the wave breaks. When the wave breaks, water particles will run out of the circuit of wave motion and deform the wave forms. According to degree of breaking, the waves of smaller wave steepness with the same period as before will remain secondarily and this wave reflect at the coast to turn a reflective wave. Therefore the states of current inside and outside of the breaker line will be different. Now it is assumed that the part of incident wave breaks and the other part of it propagates to turn a reflective wave and the height of the reflective wave is p times of the incident wave height. Then it is assumed that in the narrow region of coast, waves propagate straightly so that the incident angle equals to the reflective angle. And the wave lengths of the incident wave and reflective wave are equal, for the propagation velocity is constant at the same place where the depth is constant.

If the half height of the incident wave is a ,
 incident wave ... $a \sin(kx - \sigma t)$
 reflective wave... $pa \sin(kx - \sigma t)$ } ..(31)
 where $k = 2\pi/\lambda$, $\sigma = 2\pi/T$

It is assumed that the angle between the wave crest line and the coast line is α as in Fig.-10, and the coast line is x -axis and the perpendicular line to it is y -axis. The wave form of the parallel component with the coast is

$$\zeta = a \sin \alpha \sin(kx - \sigma t) + pa \sin \alpha \sin\{kx - \sigma t + \frac{4\pi \cos \alpha}{\lambda} y\} \dots\dots(32)$$

where $k = \frac{2\pi}{\lambda} \sin \alpha$

The wave form of the normal component is

$$\begin{aligned} \zeta_n &= a \cos \alpha \sin(ky + \sigma t) + pa \cos \alpha \sin(ky - \sigma t) \\ &= -a(1-p) \cos \alpha \sin(ky - \sigma t) + 2a \cos \alpha \sin ky \cos \sigma t \\ &= a(1+p) \cos \alpha \sin ky \cos \sigma t \\ &\quad + a(1-p) \cos \alpha \cos ky \sin \sigma t \dots(33) \end{aligned}$$

where $k = \frac{2\pi \cos \alpha}{\lambda}$
 If formula (32) is transformed, we get

$$\begin{aligned} \zeta &= a \sin \alpha \sin(kx \sin \alpha - \sigma t) \\ &\quad + pa \sin \alpha \sin\{kx \sin \alpha - \sigma t + 2ky \cos \alpha\} \end{aligned}$$

$$\begin{aligned} &= (1+p) a \sin \alpha \cos(ky \cos \alpha) \sin(kx \sin \alpha + ky \cos \alpha - \sigma t) \\ &\quad - (1-p) a \sin \alpha \sin(ky \cos \alpha) \cos(kx \sin \alpha + ky \cos \alpha - \sigma t) \dots\dots\dots(34) \end{aligned}$$

where

$$k = \frac{2\pi}{\lambda}$$

This formula expresses the resultant wave of two progressive waves advancing to $+x$ direction, so that the velocity by this wave will be derived by composition of the currents due to each wave.

The velocity due to the mean momentum in a wave length is as follows from (15) (16) and (17),

$$U'_p = \frac{k^2 a^2}{2} \sin^4 \alpha \{1 + p^2 + 2p \cos(2ky \cos \alpha)\} \times C \frac{\cosh\{2k(h-h') \sin \alpha\}}{\sinh^2(kh \sin \alpha)} \dots(35)$$

At the surface $h' = 0$,

$$U'_{op} = \frac{k^2 a^2}{2} \sin^4 \alpha \{1 + p^2 + 2p \cos(2ky \cos \alpha)\} \times \{1 + \coth^2(kh \sin \alpha)\} C$$

At the sea bottom $h' = h$,

$$U'_{bp} = \frac{k^2 a^2}{2} \sin^4 \alpha \{1 + p^2 + 2p \cos(2ky \cos \alpha)\} \times \{\coth^2(kh \sin \alpha) - 1\} C \dots(36)$$

where

$$C = \sqrt{\frac{g}{k \sin \alpha} \tanh(kh \sin \alpha)}$$

The mean velocity for depth h is

$$U'_{mp} = \frac{k^2 a^2}{2kh} \sin^3 \alpha \{1 + p^2 + 2p \cos(2ky \cos \alpha)\} \times \sqrt{\frac{g}{k \sin \alpha} \coth(kh \sin \alpha)} \dots\dots(37)$$

The variation towards y depends upon $\{1 + p^2 + 2p \cos(2ky \cos \alpha)\}$. When $p=1$ and $y = \lambda/4 \cos \alpha$, $U'_{mp} = 0$ and this varies in the wave length $y = \lambda/2 \cos \alpha$. That is

$$y=0 \quad U'_{mp} = \frac{(1+p)^2}{2} \frac{k^2 a^2}{kh} \sin^3 \alpha \sqrt{\frac{g}{k \sin \alpha} \coth(kh \sin \alpha)}$$

$$y = \frac{\lambda}{8 \cos \alpha} \quad U'_{mp} = \frac{1+p^2}{2} \quad " \quad " \quad "$$

$$y = \frac{\lambda}{4 \cos \alpha} \quad U'_{mp} = \frac{(1-p)^2}{2} \quad " \quad " \quad "$$

$$y = \frac{3\lambda}{8 \cos \alpha} \quad U'_{mp} = \frac{1+p^2}{2} \quad " \quad " \quad "$$

$$y = \frac{\lambda}{2 \cos \alpha} \quad U'_{mp} = \frac{(1+p)^2}{2} \quad " \quad " \quad "$$

Integrating (37) for y and dividing it by the width, mean velocity is

$$\overline{U}_{mp} = \frac{1+p^2 k^2 a^2}{2 kh} (\sin \alpha)^{\frac{5}{2}} \sqrt{\frac{g}{k}} \coth(kh \sin \alpha) \dots\dots\dots (38)$$

As above, when there are partly reflective waves, the mean velocity is derived by multiplying the term containing the coefficient of reflection p to the formula of total reflection. The discharge of this case is

$$Q = B h \overline{U}_{mp} \dots\dots\dots (39)$$

which varies between the position of max. velocity $y = \pi \lambda / 2 \cos \alpha$ and one of min. velocity $y = (\frac{1}{4} + \frac{\pi}{2}) \frac{\lambda}{\cos \alpha}$. From the wave conditions near coast, the distribution of longshore current due to these waves can be derived by the above idea. Generally the velocity of this longshore current is larger as h/λ is smaller, wavesteepness is larger and angle α between the crest line and coast line is larger.

Moreover in regard to the coefficient of reflection, Healy's experiment was reported before.

6. Longshore current due to breakers.

Accompanying with the energy supply by winds, the wave height will increase and the wave steepness will grow. When waves approach to the shallower coast, the wave steepness will grow by the decrease of wave length due to the decrease of wave propagation velocity. In any way after the development of these states, wave forms cannot be maintained by themselves and result in breakers. By breaking the wave transforms to the waves having smaller energy when they lose one portion or whole of their energy. The part of energy thrown out from breakers moves the water and originate the longshore current and one part increases the turbulence of water and turns at last to heat energy, and besides other part is consumed to push up sea water on beaches growing the rip current. When the rate of supplied part of energy from breakers and one of the mechanical energy loss by the friction of longshore current on sea bottom are equal, the current will be steady.

Therefore the conditions of development of longshore current due to breakers are supposed as follows.

- (1) The outbreak of breakers are limited in some definite region and their directions are uniform.
- (2) The narrower the region of long-

shore current, the stronger the current.

- (3) When the direction of wave propagation is oblique to the coast, the current is strong.
- (4) The longshore current is strong when the rate of thrown out energy from breaker and the rate of energy consumption for the development of longshore current are large.
- (5) The current is strong when the duration time of breaker is long.

The velocity of longshore current due to breakers has been derived by Putnum, Munk and Traylor's formula⁽¹⁾ and Nagai's one.⁽²⁾

As described in 5, the longshore currents are classified to the current due to the momentum of wave, that is accompanied with the wave form and the current due to breakers, that is accompanied with the transformation of wave form. The longshore currents accompanied with the transformation of waves are stated below.

When the waves transform without breaking, the velocity of the current accompanied with the wave is expressed in (17) as the mean for one wave length and the depth, and its direction coincides with one of the wave propagation. Now in unit width, the waves are assumed to be transformed from one point to other without breaking. Here the subscript 1 and 2 indicate the first point and the second one respectively.

The discharge is

$$q = h U'_m = \frac{k a^2 c}{2} \coth kh \dots (40)$$

Therefore

$$q_1 = \frac{k_1 a_1^2 c_1}{2} \coth k_1 h_1$$

$$q_2 = \frac{k_2 a_2^2 c_2}{2} \coth k_2 h_2$$

then $Q = q_1 - q_2$ is the discharge which does not accompany with the wave and it has to supply in this section.

Using $c^2 = \frac{g}{k} \tanh kh$, $k = \frac{2\pi}{\lambda}$ in (40)

$$q = \sqrt{\frac{\pi}{2}} a^2 \sqrt{\frac{g}{\lambda}} \coth \frac{2\pi h}{\lambda}$$

If the wave height and length vary depending upon the variation of depth and other reason, the changes of Q are found by above formula.

Next we consider the case of the wave transformation by breaking. When waves propagate to the coast, the period does not change, but wave velocity decreases gradually with the decrease of depth.

It is assumed that the waves break at depth h_1 and secondary waves originate at depth h_2 . The wave lengths at each depth are λ_1 and λ_2 .

From the period $T = \lambda/c$

$$\frac{1}{\lambda_1} \sqrt{\frac{g\lambda_1}{2\pi} \tanh \frac{2\pi h_1}{\lambda_1}} = \frac{1}{\lambda_2} \sqrt{\frac{g\lambda_2}{2\pi} \tanh \frac{2\pi h_2}{\lambda_2}}$$

therefore

$$\lambda_2 = \lambda_1 \frac{\tanh \frac{2\pi h_2}{\lambda_2}}{\tanh \frac{2\pi h_1}{\lambda_1}} \dots\dots(41)$$

By this formula, wave length λ_2 can be found when the depth h_2 is observed. The propagation velocity C_2 is

$$C_2 = \sqrt{\frac{g\lambda_2}{2\pi} \tanh \frac{2\pi h_2}{\lambda_2}}$$

In order to indicate the degree of breaker, the decrease of wave height is used and assumed as $\frac{a_2}{a_1} = S \dots(42)$

The decrease of wave height by breaking $2a_1 - 2a_2 = 2a_1(1-S)$

When $S=0$, the secondary wave does not originate at all, but when $S=1$, the wave height does not transform at all. The momentum of wave before breaking is

$$M_1 = \pi \rho a_1^2 C_1 \coth k_1 h_1 \dots\dots(43)$$

for a wave length. Therefore the flow discharge is $\frac{M_1}{T} = \frac{\pi \rho a_1^2 C_1}{T} \coth k_1 h_1$

Putting $\sigma_1 = \frac{k_1 a_1^2}{2} \coth k_1 h_1 = \frac{\pi a_1^2}{\lambda_1} \coth k_1 h_1$

$$\frac{M_1}{T} = \frac{\rho C_1 \sigma_1 \lambda_1}{T} = \rho \sigma_1 C_1^2 \dots(44)$$

and $\sigma_2 = \frac{k_2 a_2^2}{2} \coth k_2 h_2 = \frac{\pi a_2^2}{\lambda_2} \coth k_2 h_2$

From (41) $\lambda_1 \coth k_1 h_1 = \lambda_2 \coth k_2 h_2$

Therefore $\sigma_2 = \pi S^2 a_1^2 \frac{\lambda_1 \coth k_1 h_1}{\lambda_2^2} = \sigma_1 S^2 \frac{\lambda_1^2}{\lambda_2^2}$

The momentum of the secondary wave per unit time is

$$\frac{M_2}{T} = \frac{\rho C_2 \sigma_2 \lambda_2}{T} = \rho \sigma_2 C_2^2 = \rho S^2 \sigma_1 \frac{\lambda_1^2}{\lambda_2^2} C_2^2 \dots\dots(45)$$

If h_1 , λ_1 and h_2 are known, λ_2 and accordingly C_2 are found by (41) and M_2 is calculated using known S .

If it is assumed that when breaking, the water volume thrown out of the wave circuit is the volume at the crest of the depth $\frac{2a_1 - 2a_2}{2} = \frac{2a_1(1-S)}{2} = a_1(1-S)$

from the surface, this volume V can be calculated as follows. Using the wave form

$$\zeta = \frac{k a^2}{2} \coth kh + a \cos k(x-ct) + \frac{k a^2}{2} \coth kh \cos k(x-ct) + \dots\dots$$

and $a_2 = a_1 S$

$$\rho V = 2 \rho \int_0^{x_1} (\zeta - a_1 S) dx$$

Taking to the second term as an approximate value of wave form, from the next formula

$$\zeta - \frac{k a_1^2}{2} \coth kh - a_1 S = a_1 \cos kx - a_1 S = 0$$

x_1 will be found.

Then $\cos kx_1 = S$

$$x_1 = \frac{1}{k} \cos^{-1} S = \frac{\lambda}{2\pi} \cos^{-1} S$$

Therefore

$$\rho V = 2 \rho \int_0^{x_1} (a_1 \cos kx - a_1 S) dx = \frac{2 \rho a_1 S}{k_1} \left\{ \frac{\sqrt{1-S^2}}{S} - \cos^{-1} S \right\}$$

If this broken volume is considered to turn into a current that has a velocity v to the direction of the wave propagation, this momentum is

$$\frac{2 v \rho a_1 S \lambda_1}{2\pi} \left(\frac{\sqrt{1-S^2}}{S} - \cos^{-1} S \right) = \frac{\rho v a_1 \lambda_1}{\pi} (\sqrt{1-S^2} - S \cos^{-1} S)$$

If the angle between the wave crest line and the coast line is α , the parallel momentum with the coast is

$$v \rho V \sin \alpha = \frac{\rho v a_1 \lambda_1}{\pi} \sin \alpha (\sqrt{1-S^2} - S \cos^{-1} S)$$

where V = volume

$\dots\dots(46)$

Accordingly the mass per unit time is

$\frac{\rho V}{T} \sin \alpha$. It is considered that the momentum $M_1 - M_2$ is the decreased momentum by breaking which turn into the momentum of breaker and other.

$$(M_1 - M_2) \sin \alpha = (\rho \sigma_1 C_1^2 - \rho \sigma_1 S^2 \frac{\lambda_1^2}{\lambda_2^2} C_2^2) \sin \alpha = \rho \sigma_1 \sin \alpha (C_1^2 - S^2 \frac{\lambda_1^2}{\lambda_2^2} C_2^2) \dots\dots\dots(47)$$

The secondary wave has a longshore current accompanied with its momentum as described before.

If the difference of the momentum of (46) and (47) is equal to the frictional force W acting on the sea bottom by the longshore current,

$$W = K \rho v^2 \ell = K \rho v^2 \frac{h_b}{m} \dots\dots(48)$$

where

$m = h_b / \ell$; slope of sea bottom
 ℓ ; a distance from coast to the breaker line
 h_b ; depth at breaker line.

If it is considered that the momentum (46) what the broken water has travels at first towards the direction of wave propagation, but at last along the coast, it can be taken $\sin \alpha = 1$ near coast. So at steady condition the momentum of broken water volume per unit time is

$$\rho v \frac{V}{T} = \frac{\rho v a_1 \lambda_1}{\pi T} (\sqrt{1-S^2} - S \cos^{-1} S) \dots (49)$$

And the wave width to come on the coast length dx is $dx \cos \alpha$. Therefore

$$\left\{ \rho d_1 \sin \alpha (C_1^2 - S^2 \frac{\lambda_1^2}{\lambda_2^2} C_2^2) - \frac{\rho v a_1 \lambda_1}{\pi T} (\sqrt{1-S^2} - S \cos^{-1} S) \right\} \cos \alpha dx = K \rho v^2 \frac{h_b}{m} dx$$

Then

$$\begin{aligned} v^2 &= \frac{m \cos \alpha}{K h_b} \left[d_1 C_1^2 \sin \alpha \left\{ 1 - S^2 \left(\frac{\lambda_1}{\lambda_2} \right)^2 \left(\frac{C_2}{C_1} \right)^2 \right\} \right. \\ &\quad \left. - \frac{a_1 C_1}{\pi} (\sqrt{1-S^2} - S \cos^{-1} S) v \right] \\ &= \frac{m C_1 \cos \alpha}{K h_b} \left[d_1 C_1 \sin \alpha \left\{ 1 - S^2 \left(\frac{\lambda_1}{\lambda_2} \right)^2 \left(\frac{C_2}{C_1} \right)^2 \right\} \right. \\ &\quad \left. - \frac{a_1}{\pi} \{ \sqrt{1-S^2} - S \cos^{-1} S \} v \right] \dots (50) \end{aligned}$$

From (41)

$$\begin{aligned} \frac{\lambda_1}{\lambda_2} &= \frac{\tanh k_1 h_1}{\tanh k_2 h_2} \\ \frac{C_2}{C_1} &= \frac{\sqrt{\frac{g}{k_2} \tanh k_2 h_2}}{\sqrt{\frac{g}{k_1} \tanh k_1 h_1}} = \sqrt{\frac{k_1 \tanh k_2 h_2}{k_2 \tanh k_1 h_1}} \\ &= \sqrt{\frac{\lambda_2 \tanh k_2 h_2}{\lambda_1 \tanh k_1 h_1}} \end{aligned}$$

$$\left(\frac{C_2}{C_1} \right)^2 = \frac{\lambda_2 \tanh k_2 h_2}{\lambda_1 \tanh k_1 h_1} = \left(\frac{\lambda_2}{\lambda_1} \right)^2$$

$$\left(\frac{C_2}{C_1} \right)^2 \left(\frac{\lambda_1}{\lambda_2} \right)^2 = 1$$

$$d_1 C_1^2 = \frac{a_1^2}{2} \sqrt{k_1 g \coth k_1 h_1} \sqrt{\frac{g}{k_1} \tanh k_1 h_1} = \frac{a_1^2 g}{2}$$

Therefore from (50)

$$\begin{aligned} v^2 &= \frac{m \cos \alpha}{K h_b} \left[\frac{a_1^2 g}{2} \sin \alpha (1-S^2) - \frac{a_1 C_1}{\pi} (\sqrt{1-S^2} - S \cos^{-1} S) v \right] \\ &= \frac{m a_1 \cos \alpha}{K h_b} \left[\frac{g a_1 \sin \alpha}{2} (1-S^2) - \frac{C_1}{\pi} (\sqrt{1-S^2} - S \cos^{-1} S) v \right] \dots (51) \end{aligned}$$

Assuming the wave height $H_1 = 2a_1$,

$$\begin{aligned} v^2 &= \frac{m H_1 \cos \alpha}{2 K h_b} \left[\frac{g H_1 \sin \alpha}{4} (1-S^2) - \frac{C_1}{\pi} (\sqrt{1-S^2} - S \cos^{-1} S) v \right] \dots (52) \end{aligned}$$

When the wave breaks at wave height H_1 , the wave velocity at the point assume C_b , wave height there H_b .

The approximate condition for wave breaking is $\tanh kh = \frac{ka}{1-k^2 a^2} \div ka$

Accordingly

$$C_b = \sqrt{\frac{g}{k_b} \tanh k_b h_b} = \sqrt{\frac{g k_b a_b}{k_b}} = g a_b = \sqrt{\frac{g H_b}{2}}$$

$$\frac{H_b}{C_b} = \frac{2 a_b}{C_b} = \frac{2 a_b}{\sqrt{g a_b}} = 2 \sqrt{\frac{a_b}{g}} = \sqrt{\frac{2 H_b}{g}}$$

By using these relations

$$\begin{aligned} v^2 &= \frac{m H_b \cos \alpha C_b}{2 K h_b \pi} \left[\frac{g \pi H_b}{4 C_b} \sin \alpha (1-S^2) \right. \\ &\quad \left. - \{ \sqrt{1-S^2} - S \cos^{-1} S \} v \right] \dots (53) \\ &\div \frac{m g^{\frac{1}{2}} H_b^{\frac{3}{2}} \cos \alpha}{2 \sqrt{2} \pi K h_b} \left[\frac{\pi \sqrt{g} H_b}{2 \sqrt{2}} \sin \alpha (1-S^2) \right. \\ &\quad \left. - \{ \sqrt{1-S^2} - S \cos^{-1} S \} v \right] \dots (53') \end{aligned}$$

When the secondary wave does not originate after breaking, that is $S=0$,

$$\begin{aligned} v^2 &= \frac{m H_b C_b \cos \alpha}{2 \pi K h_b} \left[\frac{\pi g H_b \sin \alpha}{4 C_b} - v \right] \\ &= \frac{m \sqrt{g} H_b^{\frac{3}{2}} \cos \alpha}{2 \sqrt{2} \pi K h_b} \left[\frac{\pi \sqrt{g} H_b}{2 \sqrt{2}} \sin \alpha - v \right] \dots (54) \end{aligned}$$

Usually the waves break according the decrease of depth and thereby increase of wave steepness, and then the secondary waved propagate to break as similarly as the initial waves and finally the last wave breaks at beach. Accordingly the velocity of longshore current will be small at the first breaker line and increase larger near coast.

Formula (53) will be solved for v as follows.

$$\begin{aligned} v &= \frac{m H_b C_b \cos \alpha}{4 \pi K h_b} \left\{ \sqrt{(\sqrt{1-S^2} - S \cos^{-1} S)^2} \right. \\ &\quad \left. + \frac{2 \pi^2 g K h_b}{m C_b^2} \tan \alpha \{ (1-S^2) - (\sqrt{1-S^2} - S \cos^{-1} S) \} \right\} \\ &= \frac{m H_b \lambda_b \cos \alpha}{4 \pi K h_b T} \left\{ \sqrt{(\sqrt{1-S^2} - S \cos^{-1} S)^2} \right. \\ &\quad \left. + \frac{2 \pi^2 g K h_b T^2 (1-S^2)}{m \lambda_b^2} \tan \alpha \right. \\ &\quad \left. - (\sqrt{1-S^2} - S \cos^{-1} S) \right\} \dots (55) \end{aligned}$$

When $S = 0$,

$$v = \frac{m H_b C_b \cos \alpha}{4 \pi K h_b} \left\{ \sqrt{1 + \frac{2 \pi^2 g K h_b \tan \alpha}{m C_b^2}} - 1 \right\}$$

$$= \frac{m H_b \lambda_b \cos \alpha}{4 \pi K h_b T} \left\{ \sqrt{1 + \frac{2 \pi^2 g K h_b T^2 \tan \alpha}{m \lambda_b^2}} - 1 \right\} \dots \dots (56)$$

In (55) assume

$$P = \cos \alpha \left\{ \sqrt{(\sqrt{1-S^2} - S \cos' S)^2} \right.$$

$$\left. + \frac{2 \pi^2 g K h_b (1-S^2) \tan \alpha - (\sqrt{1-S^2} - S \cos' S)}{m C_b^2} \right\} \dots \dots (57)$$

Then

$$v = \frac{m H_b \lambda_b}{4 \pi K h_b T} P = \frac{m H_b C_b}{4 \pi K h_b} P \dots (58)$$

And assume

$$\frac{2 \pi^2 g K h_b T^2}{m \lambda_b^2} = K \dots \dots (59)$$

From (56)

$$v = \frac{m H_b C_b \cos \alpha}{4 \pi K h_b} \left\{ \sqrt{1 + K \tan \alpha} - 1 \right\} \dots (56')$$

$$= \frac{\pi g H_b T \cos \alpha}{2 K \lambda_b} \left\{ \sqrt{1 + K \tan \alpha} - 1 \right\}$$

From (55)

$$v = \frac{\pi g H_b T \cos \alpha}{2 K \lambda_b} \left[\sqrt{(\sqrt{1-S^2} - S \cos' S)^2} \right.$$

$$\left. + K (1-S^2) \tan \alpha - (\sqrt{1-S^2} - S \cos' S) \right]$$

$$= \frac{\pi g H_b T}{2 K \lambda_b} P \dots \dots (55')$$

And moreover assume

$$P_K = \frac{\pi g \cos \alpha}{2 K} \left[\sqrt{(\sqrt{1-S^2} - S \cos' S)^2} \right.$$

$$\left. + K (1-S^2) \tan \alpha - (\sqrt{1-S^2} - S \cos' S) \right] \dots (60)$$

$$K = \frac{2 \pi^2 g K h_b T^2}{m \lambda_b^2} = \frac{2 \pi^2 g K h_b}{m C_b^2} \dots (59)$$

From them

$$v = \frac{H_b T}{\lambda_b} P_K = \frac{H_b}{C_b} P_K \dots (61)$$

When $S=0$

$$P_K = \frac{\pi g \cos \alpha}{2 K} \left[\sqrt{1 + K \tan \alpha} - 1 \right] \dots (62)$$

$$\text{From } C_b = \sqrt{\frac{g \lambda_b \tanh \frac{2 \pi h_b}{\lambda_b}}{2 \pi}}$$

$$K = \frac{2 \pi^2 g K h_b}{m C_b^2} = \frac{2 \pi^2 g K h_b 2 \pi}{m g \lambda_b} \coth \frac{2 \pi h_b}{\lambda_b}$$

$$= \frac{4 \pi^3 K h_b}{m \lambda_b} \coth \frac{2 \pi h_b}{\lambda_b}$$

At the very shallow water where $\frac{h_b}{\lambda_b}$ is very small, $\tanh \frac{2 \pi h_b}{\lambda_b} \div \frac{2 \pi h_b}{\lambda_b}$, therefore

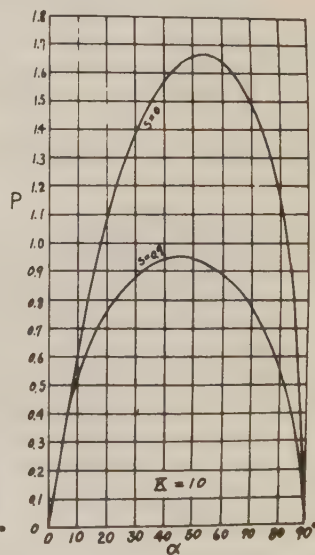
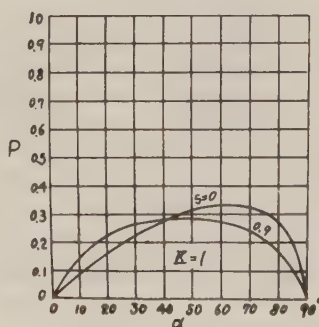
$$K = \frac{2 \pi^2 K}{m}$$

At deep sea where $\frac{h_b}{\lambda_b}$ is large, $\tanh \frac{2 \pi h_b}{\lambda_b} \div 1$

$$K = \frac{4 \pi^3 K h_b}{m \lambda_b} \dots \dots (63)$$

The variations of P and P_K are shown in Fig.-11 and Fig.-12.

Fig.-11.



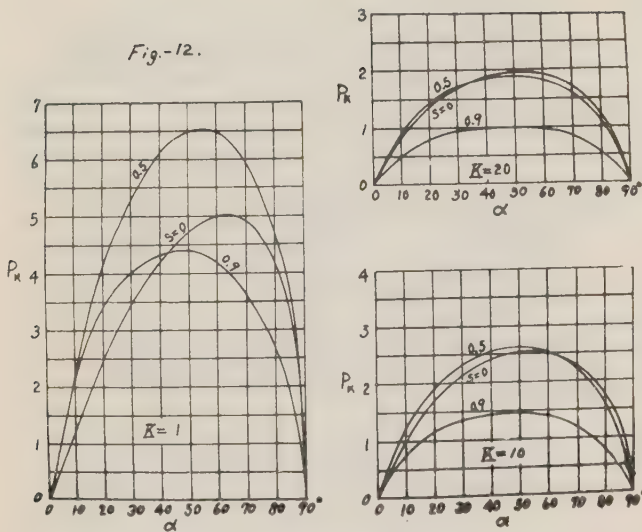
From (56'), α where v will have the max. value by the condition $\frac{dv}{d\alpha} = 0$, should satisfy the next formula.

$$\frac{1}{\tan \alpha} = \frac{K}{4} \left(\tan \alpha - \frac{1}{\tan \alpha} \right)^2$$

So that

$$\tan^4 \alpha + 2 \tan^2 \alpha - \frac{4}{K} \tan \alpha + 1 = 0 \dots (64)$$

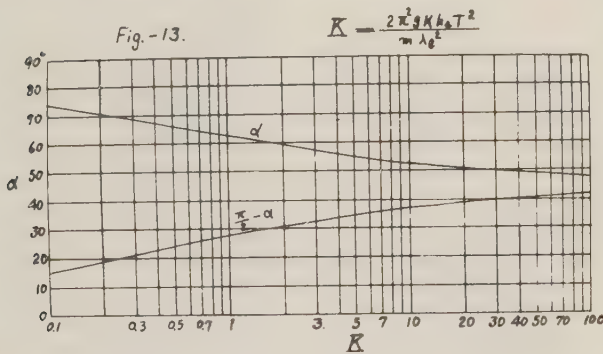
Fig.-12.



Angle α derived from this formula is indicated in the following table.

K	0.1	1	5	10	20
α	74°30'	62°49'	55°13'	52°42'	50°43'
$\frac{\pi}{2}-\alpha$	15 30	27 11	34 47	37 18	39 17
K	40	80	100	infinity	
α	49°11'	48°01'	47°42'	45°00'	
$\frac{\pi}{2}-\alpha$	40 49	41 59	42 18	45 00	

This variation is shown in Fig.-13.



This results are considered to explain the reason of that in the experiment by Shay and Johnson⁽³⁾, the max. volume of littoral drift occurred when the angle between the direction of wave propagation and the beach line was 30 degrees. This angle corresponds to the angle $\frac{\pi}{2}-\alpha$ and K at this condition is contained in $K = 1$ to 3.

From formula (56') that is for $S=0$,

$$K = \frac{\pi g H_b^2 \cos \alpha}{8 h_b v^2} \left(\sin \alpha - \frac{4 \lambda_b v}{\pi g H_b T} \right) \dots (65)$$

Therefore K and then the friction coefficient K from (59) can be obtained from the values of observation.

The discharge q by the longshore current in the region from the breaker line to beach is as follows from (55).

$$q = \frac{l h_b}{2} v = \frac{h_b^2}{2m} v$$

$$= \frac{H_b \lambda_b h_b \cos \alpha}{8 \pi K T} \left[\sqrt{(\sqrt{1-S^2} - S \cos \alpha) S} \right]^2$$

$$+ \frac{2 \pi^2 g K h_b T^2 (1-S^2)}{m \lambda_b^2} \tan \alpha$$

$$- (\sqrt{1-S^2} - S \cos \alpha) S \dots (66)$$

When $S=0$, it becomes to

$$q = \frac{H_b \lambda_b h_b \cos \alpha}{8 \pi K T} \left[\sqrt{1 + \frac{2 \pi^2 g K h_b T^2}{m \lambda_b^2} \tan \alpha} - 1 \right] \dots (67)$$

The period T , wave length λ_b and wave height H_b of breaker, the depth h_b , angle α (angle between the wave crest line and coast line), the friction coefficient on sea bottom K , bottom slope m and degree of breaking S are contained in above formulas of long shore current.

Among them, K and m are the characteristic factors of the coast, T and α can be estimated from the wind direction, wind velocity, fetch and wind duration, and λ_b and H_b are decided from T and h_b . The off shore waves will be decided from weather conditions. When these sufficiently developed waves propagate with more supply of energy or with the frictional effect of sea bottom, they will break at once. These conditions correspond to $1 > S > 0$, and the breakers are defined as spilling breakers.

When the off shore waves which does not sufficiently develop, approach the coast and break all at once near coast, the condition of this breaker corresponds to $S=0$ and the breakers are defined as plunging breakers. The boundary of spilling breakers and plunging breakers has been studied by Iversen and Hayami.⁽⁴⁾

Velocities of longshore current will be large when the waves break near

coast corresponding to $S=0$.

As above mentioned, the wave height and velocity of breaker can be obtained from wave period and depth, and the depth at breaker line h_b and wave length λ_b from the wave height $2a_b$ and wave period T of the breakers. Applying these values to (55) or (56), the velocities of longshore currents can be obtained.

Velocity of longshore current due to the successive breakers.

If the decrease of wave height is defined by $2a_1(1-S)$ when the first breaker $2a_1$ transforms to the secondary wave $2a_2$, the velocity of longshore current originated at this time is obtained from the formula (65). The range of this current is the sea from coast to $l = h_b/m$ offshore. On the constant slope of sea bottom, the waves assume to propagate with the angle α between the wave crest line and coast line.

The distance from the coast is defined as x and the depth at its point as h .

then $h = \frac{x}{l} h_b = m x$.

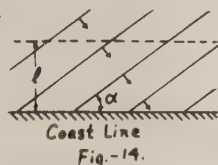
When the wave height $2a_2 = 2Sa_1$, wave length λ_b and depth h_b at $x=l$, the situation where the next breaker may occur will be found as follows.

The relation of depth and wave height at the time of breaking is

$$\begin{aligned} \frac{h_b}{2a} &= \frac{h+d_2}{2a} = \frac{1}{2} \frac{kh}{ka} + \frac{1}{4} ka \coth kh \\ &= \frac{1}{2} \frac{kh}{ka} + \frac{1}{4} \frac{(1+8 \tanh^2 kh - 3 \tanh^4 kh)^{\frac{1}{2}} - (1 + \tanh^2 kh)}{\tanh^2 kh (3 - 2 \tanh^2 kh)} \end{aligned} \quad \dots\dots(68)$$

Applying the next relations

$$\begin{aligned} \frac{2a_2}{2a_1} &= \left(\frac{\lambda_1}{\lambda_2}\right)^{\frac{1}{2}} \\ \frac{\lambda_2}{\lambda_1} &= \frac{\tanh \frac{2\pi h_2}{\lambda_2}}{\tanh \frac{2\pi h_1}{\lambda_1}} \end{aligned} \quad \dots(41)$$



Depth $= d_2 + h_2 = mx$ $d_1 + h_1 = h_b + d_1 = ml$

$$\frac{2a_2}{2a_1} = \left(\frac{\lambda_1}{\lambda_2}\right)^{\frac{1}{2}} = \left\{ \frac{\tanh \frac{2\pi(ml-d_1)}{\lambda_1}}{\tanh \frac{2\pi(mx-d_2)}{\lambda_2}} \right\}^{\frac{1}{2}}$$

Therefore

$$\frac{2a_2}{2a_1} = \left(\frac{\lambda_1}{\lambda_2}\right)^{\frac{3}{2}} = \left\{ \frac{\tanh \frac{2\pi(ml-d_1)}{\lambda_1}}{\tanh \frac{2\pi(mx-d_2)}{\lambda_2}} \right\}^{\frac{3}{2}}$$

$$\frac{2a_2}{\lambda_2} = \frac{2a_1}{\lambda_1} \left\{ \frac{\tanh \frac{2\pi}{\lambda_1}(ml-d_1)}{\tanh \frac{2\pi}{\lambda_2}(mx-d_2)} \right\}^{\frac{3}{2}} \quad \dots(69)$$

$$\text{From } C = \frac{\lambda}{T} = \sqrt{\frac{g\lambda}{2\pi} \tanh \frac{2\pi h}{\lambda}}$$

$$\frac{2\pi\lambda_2}{gT^2} = \tanh \frac{2\pi h_2}{\lambda_2} = \tanh \frac{2\pi}{\lambda_2}(mx-d_2)$$

Substituting (70) into (69).....(70)

$$\begin{aligned} \frac{2a_2}{\lambda_2} &= \frac{2a_1}{\lambda_1} \left\{ \frac{\tanh \frac{2\pi}{\lambda_1}(ml-d_1)}{\frac{2\pi\lambda_2}{gT^2}} \right\}^{\frac{3}{2}} \\ &= \frac{2a_1}{\lambda_1} \left(\frac{gT^2}{2\pi\lambda_2}\right)^{\frac{3}{2}} \left\{ \tanh \frac{2\pi}{\lambda_1}(ml-d_1) \right\}^{\frac{3}{2}} \end{aligned} \quad \dots\dots(71)$$

where

$$d_1 = \frac{k_1 a_1^2}{2} \coth k_1 h_1 = \frac{\pi a_1^2}{\lambda_1} \coth k_1 (ml-d_1)$$

$$\text{Therefore } \tanh k_1 (ml-d_1) = \frac{\pi a_1^2}{\lambda_1 d_1}$$

Accordingly

$$\begin{aligned} \frac{2a_2}{\lambda_2} &= \frac{2a_1}{\lambda_1} \left(\frac{\pi a_1^2}{\lambda_1 d_1}\right)^{\frac{3}{2}} \left(\frac{gT^2}{2\pi\lambda_2}\right)^{\frac{3}{2}} \\ &= \frac{\sqrt{g^3} a_1^4 T^3}{\sqrt{2} d_1^3 \lambda_1^5 \lambda_2^3} = 2a_1 \frac{\lambda_1^{\frac{1}{2}}}{\lambda_2^{\frac{3}{2}}} \quad \dots(72) \end{aligned}$$

And from

$$d_2 = \frac{\pi a_2^2}{\lambda_2} \coth k_2 (mx-d_2) \quad \dots(73)$$

d_2 can be obtained applying a_2 and λ_2 at known depth. Substituting (70) in (73)

$$d_2 = \frac{\pi a_2^2}{\lambda_2} \frac{gT^2}{2\pi\lambda_2} = \frac{g a_2^2 T^2}{2 \lambda_2^2} = \frac{g}{8} \left(\frac{2a_2}{\lambda_2}\right)^2 T^2$$

Then substituting this in (70)(74)

$$\begin{aligned} \frac{2\pi\lambda_2}{gT^2} &= \tanh 2\pi \left(\frac{mx}{\lambda_2} - \frac{d_2}{\lambda_2} \right) \\ &= \tanh \frac{2\pi}{\lambda_2} \left\{ mx - \frac{g}{8} \left(\frac{2a_2}{\lambda_2}\right)^2 T^2 \right\} \end{aligned}$$

In this formula, use (72)

$$\begin{aligned} \frac{2\pi\lambda_2}{gT^2} &= \tanh \frac{2\pi}{\lambda_2} \left\{ mx - \frac{gT^2}{8} \frac{a_1^8 T^6 g^3}{2 \lambda_1^5 d_1^3 \lambda_2^3} \right\} \\ &= \tanh \frac{2\pi}{\lambda_2} \left\{ mx - \frac{g^4 a_1^8 T^8}{16 \lambda_1^5 \lambda_2^3 d_1^3} \right\} \end{aligned}$$

From (74)

$$d_1 = \frac{g}{8} \left(\frac{2a_1}{\lambda_1}\right)^2 T^2$$

Therefore

$$\frac{2\pi\lambda_2}{gT^2} = \tanh \frac{2\pi}{\lambda_2} \left\{ m\chi - \frac{ga_1^2\lambda_1 T^2}{2\lambda_2^3} \right\} \dots\dots\dots(75)$$

When T, a_1, λ_1, m, g and χ in this formula are known, λ_2 can be calculated. So that $2a_2/\lambda_2$ is obtained from (72). In the next we calculate χ where $\frac{2a_2}{\lambda_2}$ will satisfy the condition of breaking (68) when the waves propagate.

The condition (68) means that when

$$ka = \frac{(1+8\tanh^2 kh - 3\tanh^4 kh)^{\frac{1}{2}} - (1+\tanh^2 kh)}{\tanh kh (3-2\tanh^2 kh)} \dots\dots\dots(68')$$

the waves break. Namely the waves break where χ satisfies the relation

$$\frac{2\pi a_2}{\lambda_2} = f(\tanh k_2 h) = f\left\{ \tanh \frac{2\pi}{\lambda_2} (m\chi - \sigma_2) \right\}$$

where f is the function of right side of (68').

From (70) and (75)

$$\begin{aligned} \frac{2\pi\lambda_2}{gT^2} &= \tanh k_2 h = \tanh \frac{2\pi}{\lambda_2} (m\chi - \sigma_2) \\ &= \tanh \frac{2\pi}{\lambda_2} \left(m\chi - \frac{ga_1^2 T^2 \lambda_1}{2\lambda_2^3} \right) \\ &= \tanh \chi \dots\dots\dots(76) \end{aligned}$$

where

$$\chi = \frac{2\pi}{\lambda_2} \left(m\chi - \frac{ga_1^2 T^2 \lambda_1}{2\lambda_2^3} \right)$$

From (68')

$$\frac{2\pi a_2}{\lambda_2} = \frac{2\pi a_1 \lambda_1^{\frac{1}{2}}}{\lambda_2^{\frac{3}{2}}} = \frac{(1+8\tanh^2 \chi - 3\tanh^4 \chi)^{\frac{1}{2}} - (1+\tanh^2 \chi)}{\tanh \chi (3-2\tanh^2 \chi)} \dots\dots\dots(77)$$

χ can be derived from (76) and (77). Namely from (76)

$$\lambda_2 = \frac{gT^2}{2\pi} \tanh \chi$$

Substituting this into (77)

$$\begin{aligned} \frac{(2\pi)^{\frac{5}{2}} a_1 \lambda_1^{\frac{1}{2}}}{g^{\frac{3}{2}} T^3 (\tanh \chi)^{\frac{1}{2}}} &= \frac{(1+8\tanh^2 \chi - 3\tanh^4 \chi)^{\frac{1}{2}} - (1+\tanh^2 \chi)}{3-2\tanh^2 \chi} \\ \text{or} \quad \frac{(2\pi)^{\frac{5}{2}} a_1 \lambda_1^{\frac{1}{2}}}{g^{\frac{3}{2}} T^3} &= \beta_1^{\frac{3}{2}} \frac{2\pi a_1}{\lambda_1} = \pi \beta_1^{\frac{3}{2}} \left(\frac{2a_1}{\lambda_1} \right) \\ &= \frac{(\tanh \chi)^{\frac{1}{2}} \{ (1+8\tanh^2 \chi - 3\tanh^4 \chi)^{\frac{1}{2}} - (1+\tanh^2 \chi) \}}{3-2\tanh^2 \chi} \dots\dots\dots(78) \end{aligned}$$

where $\beta_1 = \frac{2\pi\lambda_1}{gT^2} \dots\dots\dots(79)$

Or substitute (76) into (77)

$$\frac{2\pi a_1 \lambda_1^{\frac{1}{2}}}{\lambda_2^{\frac{3}{2}}} = \frac{\{1+8(\frac{2\pi\lambda_2}{gT^2})^2 - 3(\frac{2\pi\lambda_2}{gT^2})^4\}^{\frac{1}{2}} - \{1+(\frac{2\pi\lambda_2}{gT^2})^2\}}{\frac{2\pi\lambda_2}{gT^2} \{3-2(\frac{2\pi\lambda_2}{gT^2})^2\}} \dots\dots\dots(80)$$

(75) is the relation λ_2 and χ or depth $m\chi$ when T, a_1, λ_1, m and g are known. (76) and (77) is the relation of λ_2 and χ or depth $m\chi$ when the wave breaks. Therefore using χ that satisfies (78) to the next formula

$$\begin{aligned} \lambda_2 &= \frac{gT^2}{2\pi} \tanh \chi \\ \chi &= \frac{2\pi}{\lambda_2} \left\{ m\chi - \frac{ga_1^2 \lambda_1 T^2}{2\lambda_2^3} \right\} \end{aligned}$$

λ_2 and χ or depth $m\chi$ at the breaking point can be obtained. Or applying λ_2 that satisfies (80) to the next formula

$$\lambda_2 = \frac{gT^2}{2\pi} \tanh \frac{2\pi}{\lambda_2} \left\{ m\chi - \frac{ga_1^2 \lambda_1 T^2}{2\lambda_2^3} \right\} \dots\dots\dots(81)$$

Such obtained χ or depth $m\chi$ is the situation of breaking.

Substituting the known λ_2 to

$$2a_2 = 2a_1 \left(\frac{\lambda_1}{\lambda_2} \right)^{\frac{1}{2}}$$

the breaker height can be calculated. It is assumed that the initial first wave height of breaker $H_b = 2a_{0b}$ and after breaking $2S_0 a_{0b} = 2a_1$ and then the secondary wave height of breaker after propagating the distance $\ell - \chi_1$ is $2a_{1\ell}$. In the next the wave height becomes $2S_1 a_{1\ell} = 2a_2$ after breaking and then $2a_{2\ell}$ at breaking after its propagation. These relation is indicated in Fig.-15 and is assumed to continue to the final breaking at the beach.

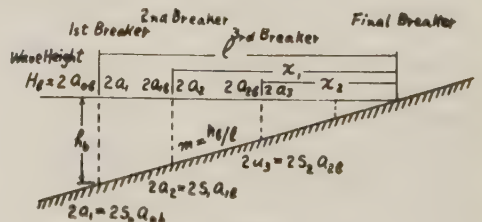


Fig.-15.

In order to calculate λ_2 and χ by (80) and (81) using the known values a_1, λ_1, T

and m , we assume

$$\frac{2 \pi \lambda_2}{g T^2} = \beta_2 \dots\dots\dots(82)$$

and transform (80) and (81) as follows.

$$\pi \beta_1^{\frac{3}{2}} \left(\frac{2a_1}{\lambda_1} \right) = \frac{\beta_2^{\frac{1}{2}} \{ (1+8\beta_2^2-3\beta_2^4)^{\frac{1}{2}} - (1+\beta_2^2) \}}{3-2\beta_2^2} \dots\dots(83)$$

$$\beta_2 = \tanh \left\{ 2\pi \frac{\beta_1}{\beta_2} \frac{m\chi}{\lambda_1} - \frac{\pi^2}{2} \left(\frac{2a_1}{\lambda_1} \right)^2 \frac{\beta_1^3}{\beta_2^4} \right\} \dots\dots\dots(84)$$

Applying the known values β_1 and $\frac{2a_1}{\lambda_1}$, β_2 can be obtained by (83), λ_2 by (82) and the depth of the breaker situation $m\chi$ by (84).

These calculation can be conveniently carried out by the calculation diagrams of Fig.-16, 17 and 18.

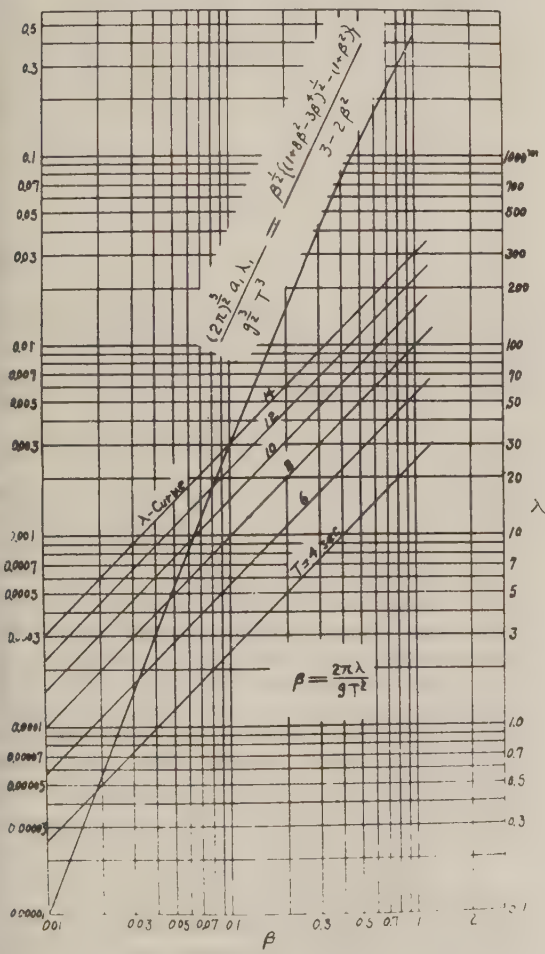


Fig. 16.

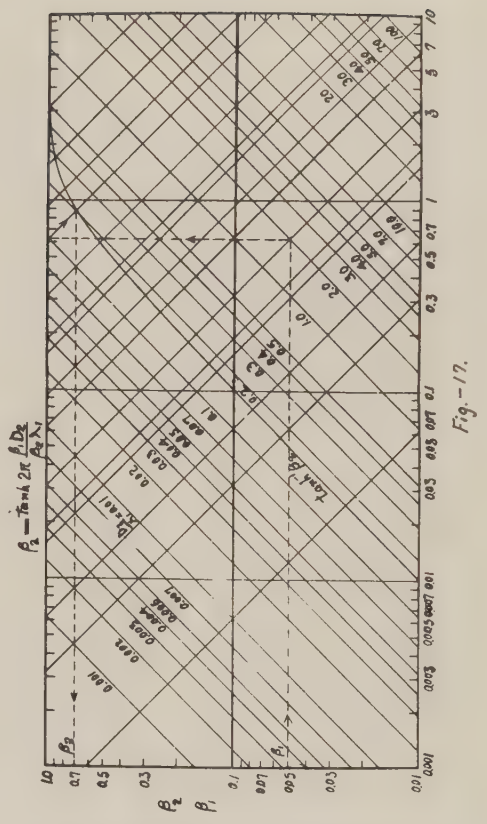


Fig.-17.

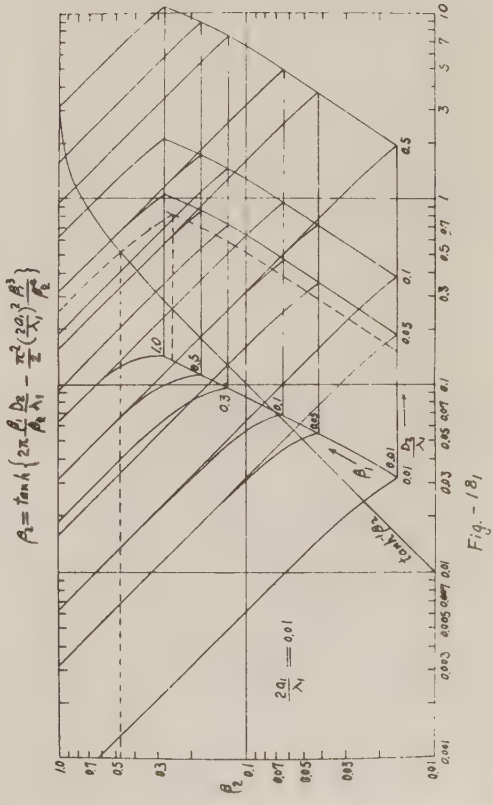


Fig.-18.

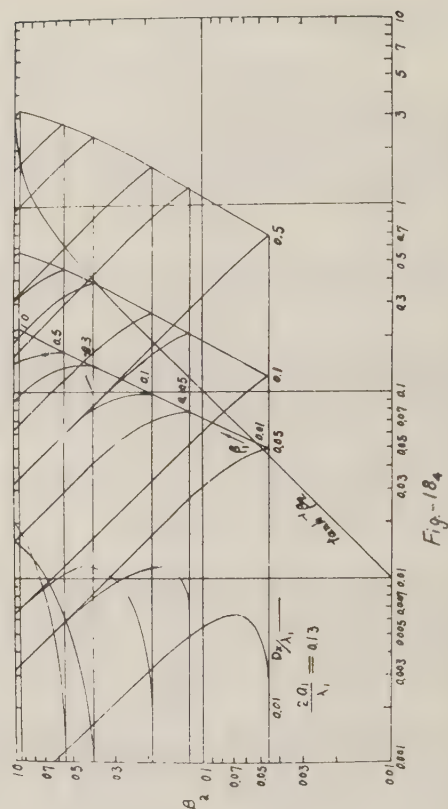
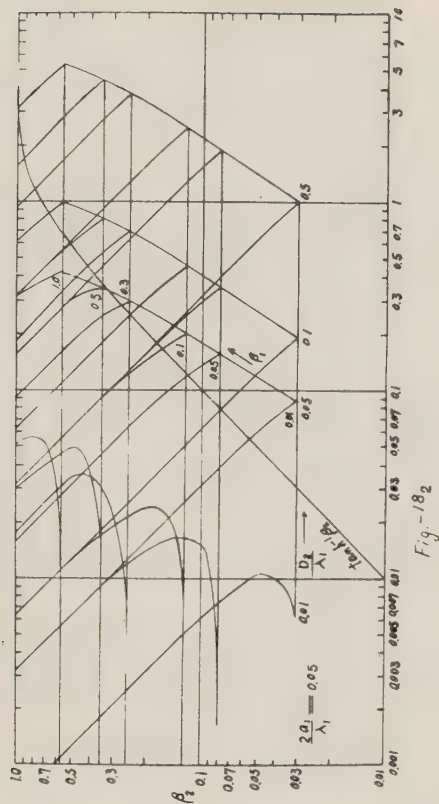
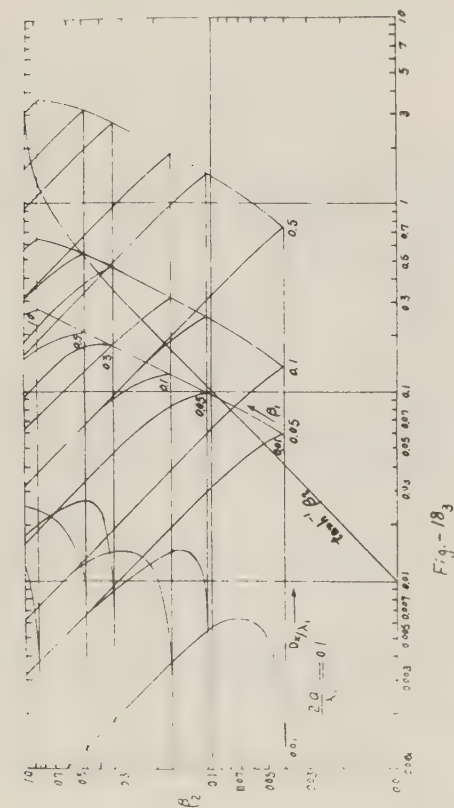


Fig.-16 is the calculation diagram of (83) to ask for β_2 and λ_2 from β_1 and $\frac{2a_1}{\lambda_1}$. Fig.-17 is that of the approximate formula $\beta_2 = \tanh\left(2\pi \frac{\beta_1}{\beta_2} \frac{mx}{\lambda_1}\right)$ of (84) to

ask for $m\chi = D_2$ from β_1 and β_2 , and Fig.-18 is that of (84).

When the waves propagate from the open sea to coast, they usually break their crests slightly and successively, and break violently at a shoal, then they become flat and grow their steepness to break again near coast. Therefore from these general properties of breakers, it is able to assume that the degree of breaking depends on the increase rate of wave height between one wave length.

If the increase rate of wave height is given by I, the assumption can be written as $I = \frac{a_1}{a_2}$ (85)

$$S = \frac{a_2 b}{a_1} \propto I \dots\dots (86)$$

where S = degree of breaking.

If in (81), λ_{1x} is the wave length when $x = x_1$ and λ_{2x} is one when $x = x_1 - \lambda_{1x}$,

$$\frac{2\pi \lambda_{1x}}{gT^2} = \tanh \frac{2\pi}{\lambda_{1x}} \left(m\chi_1 - \frac{ga_1^2 T^2 \lambda_1}{2\lambda_{1x}^3} \right) \quad (87)$$

$$\frac{2\pi \lambda_{2x}}{gT^2} = \tanh \frac{2\pi}{\lambda_{2x}} \left\{ m(\chi_1)_{1x} - \frac{ga_1^2 T^2 \lambda_1}{2\lambda_{2x}^3} \right\} \quad (88)$$

where a_1 , T and λ_1 are the half wave height, period and the wave length respectively at the known position before breaking and here they are taken the values immediately after breaking.

By the wave length λ_{1x} at χ_1 , obtained from (87) and λ_{2x} from (88), the increase rate of wave height between one wave length is obtained.

$$I = \frac{a_2}{a_1} = \left(\frac{\lambda_{1x}}{\lambda_{2x}} \right)^{\frac{1}{2}} \dots (89)$$

When I is small, the breaking process of wave crest does not so much disturb the circuit motion of water particles, that after breaking the waves maintain their critical steepnesses and at the next crest, the same increase rate of wave height will break.

As such all crests break uniformly and slightly and seem as the foaming sea.

In such state $1-S=I-1$

$$S = 2-I = 2 - \left(\frac{\lambda_1}{\lambda_2} \right)^{\frac{1}{2}} \dots (90)$$

This relation is indicated in Fig.-19.

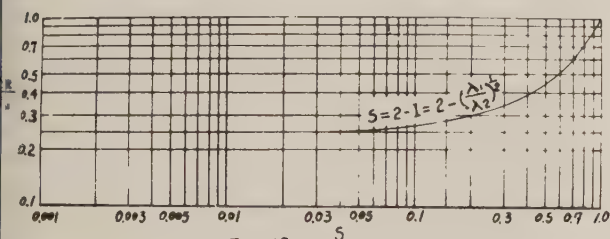


Fig.-19.

Even when the off shore waves are same, I is not constant, for λ_{1x} and λ_{2x} depend upon χ and bottom slope as shown by (87). Then the successive wave heights between one wave length are obtained by (87), (88), (89) and diagrams of (83) and (84), and the degree of breaking is calculated, these values can be plotted against the bottom slope and the wave steepnesses of off shore waves as shown in Fig.-20. By this figure, the boundary line of spilling breakers and plunging breakers indicated by Iversen and Hayami's experiments, has been expressed by the

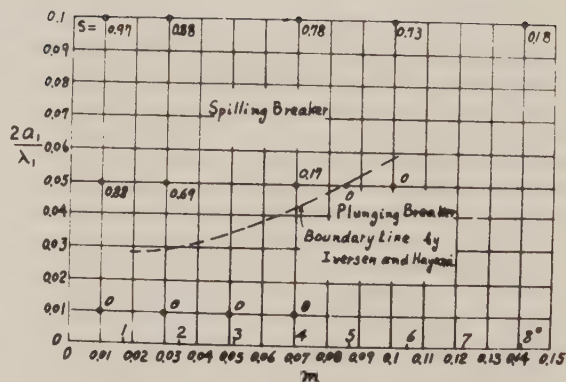


Fig.-20.

boundary of $S = 0$ region. And in the spilling breaker region, S approaches to 1 where it leaves far from the boundary line, and accordingly the state of breakers seems to be able to be expressed by the degree of breaking.

When I is large, it is supposed that the energy of breaker disturbs the circuit motion of subsurface water and decreases the wave height. As it is considered that the nearer I is to 1, the nearer S is to 1 and the larger than 1 I is, the nearer S is to 0, it will be written as follows.

$$S = (2 - I)^n \dots \dots \dots (91)$$

where n is the constant number to be decided by experiment. When the waves coming from open sea to the coast break successively, the velocity U_x of longshore current at distance χ from the coast can be expressed by the following formula by (55).

$$U_x = \sum_{i=0}^n v_i = \sum_{i=0}^n \frac{m H_{\delta i} \lambda_{\delta i} \cos \alpha_i}{4\pi K h_{\delta i} T} \left\{ \left(\sqrt{1 - S_i^2} - S_i \cos^2 S_i \right)^2 + \frac{2\pi^2 g K h_{\delta i} T^2 (1 - S_i^2)}{m \lambda_{\delta i}^2} \tan \alpha_i - \left(\sqrt{1 - S_i^2} - S_i \cos^2 S_i \right) \right\} \dots \dots (92)$$

The velocity distribution of longshore current near coast will be indicated by (92).

8. Conclusion.

The currents near the coast consist of many kinds as described above and are flowing to the composite direction. Accordingly the practical observation method of these currents should be corresponding to its purpose. The observation on the normal and calm sea surface is very easy and convenient for the measurements of the steady ocean flow or the periodic tidal current, but is not reasonable for the current due to wind waves. And the observations in the stormy weather near the coast are very difficult except that the longshore current at the plunging line can be measured by small floats⁽⁶⁾ thrown from the beach and the measurement of wave height and wave length, etc. in a storm are so difficult that they are necessary to be estimated by weather observations. For this purpose, the fundamentals of the wind velocity, its direction, fetch and durations in the typhoon region and the distribution of longshore current are described in this papers.

Acknowledgments:- Grateful acknowledgment is made to the cooperative members of Hokkaido Development Bureau, the Experiment Laboratory of Civil Engineering of Hokkaido Development Bureau, Muroran Development and Construction Department, The Coastal Engineering Committee of J.S.C.E., and Faculty of Technology of Hokkaido University under the auspices of Education Ministry Science Research Fund.

References

- (1) J.A.Putnum, W.H.Munk and M.A. Traylor:- The prediction of longshore current, Trans. Amer. Geophy. Union, Vol.30, No.3, June, 1949.
- (2) S.Nagai:- The study on sea coast groin, Transaction of Coastal engineering Meeting, J.S.C.E., No.2, Nov.1955.
- (3) J.W.Johnson:- Sand transport by littoral currents, Proc. of 5th Hydraulic Conference, Bulletin 34, State University of Iowa, Studies in Engineering, 1953.
- (4) S.Hayami:- Mechanism of Breakers II, Transaction of the 2nd Coastal Engineering Meeting, J.S.C.E., Nov.1955.
- (5) S.Sato:- Study on littoral drift No.4, Report of the Civil Engineering Laboratory, Japan Construction Ministry.
- (6) Y.Mashima:- The stability of Tomakomai Coast, Report of the investigation on Tomakomai Harbour, 1954 and 1955.

This report was published in Japanese on the Transaction of the Research Announcement Meeting on Coastal Engineering No.3, Nov. 1956, J.S.C.E.

Type of Breakers, Wave Steepness and Beach Slope*

By

Shōitirō HAYAMI, Dr. Sc., Kyoto University

Abstract

Beach waves break in two types, the one is spilling and the other is plunging. The main factors which control these breaker types are the off-shore wave steepness and beach slope. In a coordinate plane of beach slope and off-shore steepness, the region of spilling breakers is separated from the region of plunging breakers by a definite curve. In the present paper, this curve is obtained on the experimental basis and some of its implications in beach processes are explained.

In various beach processes including beach erosion, beach sedimentation and the change of beach slope, the role of breakers is very important. Beach waves break in two types, the one is wave type and the other is current type. 3) Usually, the current type breakers are called plunging breakers and the wave type breakers are called spilling breakers. According to the author's investigation, 3) spilling breakers cause beach erosion, while plunging breakers bring beach sedimentation in a movable beach, so that in the study of beach processes it is essential to elucidate the factors which control the type of breakers. When a wave of definite off-shore steepness breaks on a beach, the accumulation of energy causing wave-breaking is considered to be due to the decrease of water depth and the reflection of breakers at the shore; so that the type of breakers will be also governed by these factors. As the off-shore steepness and bottom slope are independent to each other, while the reflection of breakers are rather determined by these factors, it will be reasonable to infer that the type of breakers is mainly

controlled by the off-shore steepness and bottom slope. These factors are all dimensionless quantity.

The breakers in deep water are spilling type and take place when the wave steepness increases to a critical value. In shoaling water of small bottom slope, waves of small off-shore steepness break in plunging type, whereas waves of large off-shore steepness break in spilling type. With the increase of bottom slope, waves of large off-shore steepness tend to break in plunging type. So, in the rectangular coordinate plane representing the bottom slope and off-shore steepness, the region of plunging breakers and the region of spilling breakers will be separated by a definite curve or, strictly speaking, by a definite transitional zone. 4) Along this curve or within this zone, no erosion nor sedimentation occurs, in other words, it represents the equilibrium slope for a wave of specified off-shore steepness. The determination of this critical curve or zone is not only important for the study of breakers, but also has a fundamental meaning in a wide field of beach processes. In this paper, this curve is presented on the basis of experimental data.

2. These years, H. W. Iversen carried out a comprehensive experiment on the breaking of waves in shoaling water, 5) among which important data on the critical curve above noticed were included, though the materials were not so abundant and he did not explicitly stressed their importance in beach processes. The present author and his assistants also made the same sort of experiment independently with him and supplemented his results.

This experiment was made in a

*Abstract of two papers in Japanese (1), (2) cited in references at the end of the present paper.

wave channel of Disaster Prevention Research Institute, Kyoto University. It is of 22m in length, 1m in height and 0.75m in breadth constructed with iron frames and glass plates. At the one end of the channel, waves of about one second in period were generated by a pneumatic wave generator, wave steepness being mainly controlled by a change of wave amplitude. At the other end of the channel, sloping bed of iron plate supported by iron frame was set up. In view of the slope of the ordinary shoreface, the inclination of the sloping bed was made variable through the range from 0° to 3° . Waves in the channel were observed by five electrical wave meters 6) installed along the wave channel and were recorded by an electromagnetic oscillograph. The off-shore wave steepness was calculated from these records. The type of breakers was judged by the photographs taken at the instant of breaking, the time of which was recorded simultaneously by the oscillograph through a synchronous contact of the photographic camera used. The judgement of the type of breakers was made according to the criterion given by Suguet, 4) the double breaker (double *déferlement*) was classified in the group of spilling breakers.

The boundary of two types of breakers was not clear cut, indicating the existence of transitional zone, the breadth of which was, however, relatively narrow in our experiment as well as in Iversen's experiment. The breadth of the transitional zone seems to be of the order of 0.002 in wave steepness. Taking the central value of the transitional zone as the critical wave steepness, the result of our experiment is shown graphically in Fig. 1 together with Iversen's data. The curve in Fig. 1 represents the boundary between spilling breakers and plunging breakers. In movable beaches, sediments will be carried off shore by the waves above this curve and will be carried on shore by the waves below this curve.

3. The transportation of beach sediments occurs in two directions, the one parallel to a shore line and

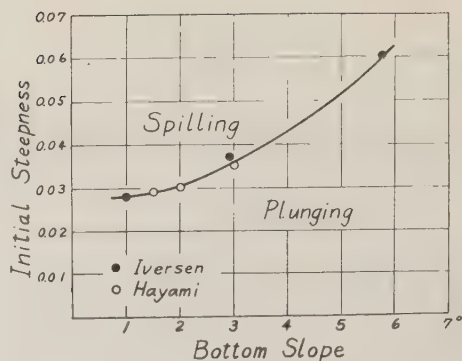


Fig. 1

the other perpendicular to it. Groins constructed perpendicular to a shore line prevent the drift of sediment parallel to a shore line, but the efficiency of groins to prevent beach erosion will decrease greatly for the waves of off-shore steepness greater than the critical steepness. 7)

Different waves of equal off-shore steepness may have different energy according to their amplitude and frequency, so their effect on beach drift also differs according to their wave energy. If the tractive force of the currents associated with breakers is not great enough to move beach sediments, beach slope will not be affected by breakers. Beach slope will be, therefore, mainly determined by the waves of sufficient energy to move beach sediments. The fact 8,9) that the shore slope and the grain size of shore sediments both increase with the increase of prevailing wind force may be accounted for by this reason.

J. W. Johnson classified the beach in two types, the one is normal beach, the other is storm beach, the latter being characterised by the formation of off-shore sand ridges in contrast to the former which has no such one, and pointed out that the off-shore steepness of the waves which separate these two types is about 0.025. 10) This interesting feature will be also explained by the same reasoning: As the slope of the shoreface is usually less than 3° , the transitional steepness

on spilling to plunging breakers
 own in Fig. 1 is nearly 0.03.
 en waves of off-shore steepness
 eater than this critical value
 out in shoreface zone, a part of
 ach sediments will be carried off
 ore and deposits in due places,
 ulting in the formation of sand
 lges, while the breakers of plung-
 g type has no such effect, only
 ntaining the equilibrium slope of
 e shoreface.

The reason why the shoreface or,
 e generally, the continental shelf
 s a slope of 1° - 2° , has not been
 equately explained so far. Accord-
 s to H. U. Sverdrup, 11) W. H. Munk,
 G. Neumann 12) and others, the
 eepness of a wind wave varies with
 e wave age and approaches to a
 eady value of 0.02-0.03 for wave
 e greater than 1.4. The swells
 ginating from such a wind wave
 ll also have a steepness of the
 e order. The observed slope of a
 mal shoreface seems to indicate
 at the shoreface is in equilibrium
 h regards to the action of such a
 e. Similarly, the observed slope
 the continental shelf will be
 lained by the progressive rise of
 e level under the action of breakers
 the same kind.

When an artificial structure is
 constructed on a beach, original
 rfile of the beach will be disturb-
 under the action of breakers. The
 e of this disturbance is sometimes
 uired. It will be scrutinished,
 ve compare the actual profile of
 e beach with the original one which
 e be theoretically infered from the
 ea of waves with the aid of Fig. 1,
 an if the original profile is not
 veysed. 13)

In conclusion, the present author
 likes to express his cordial thanks
 Mr. Hideaki Kunishi and Mr. Akio
 uchi for their kind assistance
 oughout the course of investigation.
 is also indebted to the Ministry
 onstruction and the Ministry of
 eation for their grants-in-aid to
 is work.

References

- 1) Hayami, S.: On the mechanism of breakers, 1. Symposium on Coastal Engineering, No. 1, Committee of Coastal Engineering, Civ. Eng. Soc. Japan, 1954.
- 2) " : On the mechanism of breakers, 2. Symposium on Coast. Eng., No. 2, Committ. Coast. Eng., Civ. Eng. Soc. Japan, 1955.
- 3) Hayami, S., Ishihara, T. and Iwagaki, Y.: Some studies on beach erosions. Dis. Prev. Res. Inst., Kyoto University, Bull., No. 5, 1953.
- 4) Suquet, F.: Étude expérimentale du déferlement de la houle. La Houille Blanche, Vol. 5, 1950.
- 5) Iversen, H. W.: Waves and breakers in shoaling water. Proc. Third Conf. on Coast. Eng., 1952.
- 6) Hayami, S., Yano, K., Adachi, S. and Kunishi, H.: Experimental studies on meteorological tsunamis traveling up the rivers and canals in Osaka City. Dis. Prev. Res. Inst., Bull., No. 9, 1955.
- 7) Hayami, S., Ishihara, T. and Iwagaki, Y.: Basic study on beach erosions of Sennan Coast, 6. Report of Comm. Beach Erosion of Sennan Coast, No. 3, 1953.
- 8) Toyohara, Y.: On the inclination of the strand along a sandy sea-shore, 1. Proc. Imp. Acad., Vol. 14, 1938.
- 9) " : On the inclination of the strand along a sandy sea-shore, 2. Proc. Imp. Acad., Vol. 15, 1939.
- 10) Johnson, J. W.: Scale effects in hydraulic models involving wave motion. Trans. Amer. Geophys. Union, Vol. 30, 1949.
- 11) Sverdrup, H. U., and Munk, W.H.: Wind, sea and swell. U.S. Navy, Hydrograph. O. Publ., No. 601, 1947..
- 12) Neumann, G.: Über die Komplexe Natur des Seeganges. 2 Teil. Das Anwachsen der Wellen unter dem Einfluss des Windes. Deutsche Hydrograph. Zt., Bd. 5, 1952.
- 13) Hayami, S.: On the beach drift of Tomari Bay. Report on beach drift of Tottori Prefecture, 1950.

PRESSURE OF THE BREAKER AGAINST A VERTICAL WALL

Taizo HAYASHI* and Masataro HATTORI**

INTRODUCTION

A knowledge of the wave pressure of the breaker is essential to the design of breakwaters. Although only a few formulae have specifically been published for the wave pressure of the breaker notably by Hiroi,¹⁾ Bagnold²⁾ and Minikin,³⁾ even among the formulae primarily related to the clapotis there are many formulae wherein the expression of the dynamic pressure of waves compatible to the pressure of the breaker is considered, the expression of the dynamic pressure of waves being

$$\frac{P_{dyn}}{w} = f \frac{U^2}{2g} \dots \dots \dots (1)$$

where P_{dyn} / w is the head of the dynamic pressure of waves, $U^2 / 2g$ the head of water at impact and f a coefficient. Although many important formulae for the wave pressure are multi-form, it will be seen that they can conveniently be classified by the expression (1) which is the assumption adopted for the derivation of the formulae for the wave pressure. A summary of the assumptions used for the various formulae for the dynamic pressure against a vertical wall is listed in Table 1 in order of their magnitude. The purpose of this investigation of ours was to find experimentally the most reasonable value of the coefficient f in the expression (1) for the breaker.

Before proceeding with the experimental investigation, preliminary theoretical considerations were made of the dynamic pressure of the breaker starting from the existing theory of the dynamic pressure of a jet.

The experimental investigation was done by the use of the breaker of the solitary wave in order to eliminate the undeterminable effect of the return current caused by the preceded waves

in oscillatory waves.

SYMBOLS

L	Wave length
L_{eff}	Effective wave length of solitary wave
L_{equiv}	Deep-water wave length, equivalent of effective length of solitary wave, by Ippen-Kulin
H	Wave height, crest to trough
H_{equiv}	Deep-water wave height, equivalent of maximum solitary wave height, by Ippen-Kulin
H_u	Maximum solitary wave height at the part of constant depth of experimental channel
H_b	Height of breaker at breaking point
H_0	Height of breaker just before impact to vertical wall
t	Time
g	Acceleration of gravity
w	Unit weight of water
ρ	Density of water
U_w	Wave velocity
U_o	Velocity of orbital motion of water particle at free surface
U	Velocity of water at impact to vertical wall
p	Pressure (gage pressure)
P_o	Absolute pressure of atmosphere
P_{dyn}	Dynamic pressure (gage pressure)
P_{th}	Pressure due to thrust of jet (gage pressure)
f	Coefficient of dynamic pressure
K	Length of column of virtual mass of water
d	Depth of water
d_1, d_2	Depth of water at wall and in front of mound, respectively

* Dr. Eng., Professor of Civil Engineering, Chuo University, Tokyo

** Sc. M., Postgraduate Student, Chuo University, Tokyo

d_u	Depth of water at the part of constant depth of experimental channel	γ	Adiabatic constant of air
d_b	Depth of water at breaking point	M	Dimensionless coefficient in solitary wave theory by Munk, approximately $(3H/d)^{1/2}$
c_1, c_2	Velocity of elastic wave in water and wall, respectively	T_{eff}	Effective period of solitary wave by Bagnold
D	Thickness of air cushion	S	Beach slope
D_{th}	Value of D at $p = P_{th}$		

TABLE 1

EXPRESSION OF DYNAMIC PRESSURE OF WAVES ASSUMED
AT DERIVATION OF VARIOUS FORMULAE FOR WAVE PRESSURE

Author†	Expression of dyn. press. assumed	Value of f in the expression $\frac{P_{dyn}}{w} = f \frac{U^2}{2g}$
Betz (Germany 1936)	$\frac{P_{dyn}}{w} = \frac{1}{g} \frac{c_1 c_2}{c_1 + c_2} U$	$\frac{2}{\frac{c_1}{c_2} + 1} \frac{c_1}{U} \approx \frac{c_1}{U}$
Bagnold (England 1938)	$\frac{P_{dyn.max}}{w} = 0.54 \frac{H}{D} \frac{U^2}{g}$	$1.08 \frac{H}{D}$
Minikin (England 1950)	$\frac{P_{dyn.max}}{w} = 2 \pi m \frac{d_1}{d_2} \frac{H}{L} \frac{U_w^2}{g}$	$4 \pi m \frac{d_1}{d_2} \frac{H}{L}, (m = 32.6)$
Lira (Chile 1927)	$\frac{P_{dyn}}{w} = \frac{2 U_0^2}{g}$	4
Trenjukhinn (USSR 1926)	$P_{dyn} = 0.200 (U_w + U_0)^2 *$	3.92**
Gaillard (USA 1904)	$\frac{P_{dyn.max}}{w} = 1.80 \frac{(U_w + U_0)^2}{2g}$	3.60
Molitor (USA 1935)	$\frac{P_{dyn.max}}{w} = 1.80 \frac{(U_w + U_0)^2}{2g}$	3.60
Latham (England -)	$P_{dyn.max} = 0.125 U_0^2 *$	2.45**
Hiroi (Japan 1907)	$\frac{P_{dyn}}{w} = \frac{U^2}{g}$	2
Engels (Germany -)	$\frac{P_{dyn}}{w} = \frac{U_w^2}{g}$	2
Hansen (Germany 1950)	$\frac{P_{dyn}}{w} = \frac{U_w^2}{g}$	2
Richter (USSR -)	$\frac{P_{dyn}}{w} = \frac{U_0^2}{g}$	2
Kandiba-Toukholka (USSR 1926)	$\frac{P_{dyn}}{w} = 1.6 \frac{U_w^2}{2g}$	1.60

PRELIMINARY THEORETICAL CONSIDERATIONS

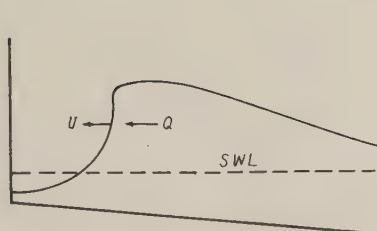
Let us denote the rate of travel of the crest of the breaker just before impact to a vertical

wall by U , the rate of displacement of water mass toward the wall by Q , and the area directly subjected to the breaker by A (Fig. 1). The velocity of water particles just before impact to

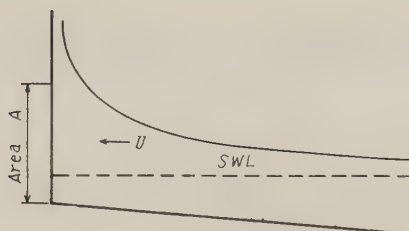
† As to the formulae for wave pressure reference was made to the literature (4) at the end of this paper.

* In the ton-m-sec system.

** Calculated from its original formula by assuming $w = 1.027 \text{ ton/m}^3$



(a) Wave just before impact.



(b) Wave just after impact.

Fig. 1. Nomenclature for the analysis of the pressure of the breaker.

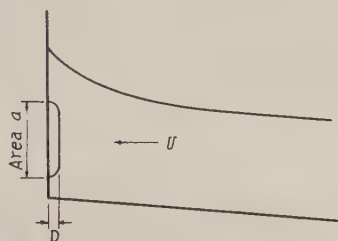


Fig. 2. An idealized case of an air cushion.

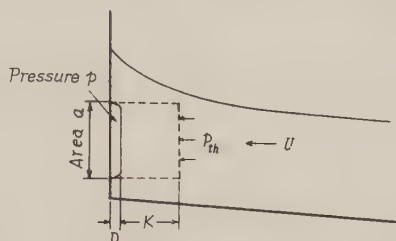


Fig. 3. Virtual mass.

the wall will reasonably be approximated by v . Assuming the state shown in Fig. 1 (b) lasts steadily for a moment and neglecting the pressure upon the upper part of the wall above area A, the whole thrust P_{th} upon area A is approximated as

$$P_{th} = \frac{w}{g} Q U \dots \dots \dots (2)$$

and the average pressure p_{th} as

$$P_{th} = \frac{P_{th}}{A} = \frac{w U^2}{g} \dots \dots \dots (3)$$

In order to take the effect of the air cushion enclosed between the breaker and the wall into account, let us consider an idealized case shown in Fig. 2, where a breaker has made contact with the wall and has enclosed a cushion of air whose area and thickness are a and D , respectively. Near the wall the direction of the fluid velocity is almost upward, the horizontal component of the velocity being almost zero. However, due to the volumetric change of the air cushion, even near the wall a slight horizontal component of velocity u is induced, which is given by

$$-\frac{dD}{dt} = u \dots \dots \dots (4.a)$$

As assumed by Bagnold²⁾, let us assume the virtual mass of water which is associated with the volumetric change of the air cushion in the equivalent form of that of a column of fluid of cross section

equal to the area of the air cushion and of length K (Fig. 3). Then, for the motion of the mass of water

$$\rho a K \frac{du}{dt} = a (P_{th} - p) \dots \dots \dots (4.b)$$

and for the pressure of the enclosed air

$$p + P_0 = (P_{th} + P_0) \left(\frac{D_{th}}{D} \right)^\gamma \dots \dots (4.c)$$

where p is the gage pressure of the enclosed air, P_0 the absolute pressure of the atmosphere, D_{th} the value of D at $p = P_{th}$ and γ the adiabatic constant of air.

Putting

$$D_{th} - D = x \dots \dots \dots (4.d)$$

in the above equation and expanding the equation in a power series of x by assuming $x \ll D_{th}$, we obtain

$$p + P_0 = (P_{th} + P_0) \left(1 + \gamma \frac{x}{D_{th}} + \dots \right) \dots \dots (4.e)$$

Substituting (4.a), (4.d) and (4.e) into (4.b), we obtain

$$\frac{d^2 x}{dt^2} + \frac{\gamma (P_{th} + P_0)}{\rho K D_{th}} x = 0 \dots \dots (4.f)$$

On integration of the above equation we obtain

$$x = A \sin \sqrt{\frac{\delta (P_{th} + P_0)}{\rho K D_{th}}} t + B \cos \sqrt{\frac{\delta (P_{th} + P_0)}{\rho K D_{th}}} t \quad \dots (4.g)$$

from equation (4.d) and (4.a)

$$u = \sqrt{\frac{\delta (P_{th} + P_0)}{\rho K D_{th}}} \left[A \cos \sqrt{\frac{\delta (P_{th} + P_0)}{\rho K D_{th}}} t - B \sin \sqrt{\frac{\delta (P_{th} + P_0)}{\rho K D_{th}}} t \right] \quad \dots (4.h)$$

and from equation (4.e)

$$p - P_{th} = \frac{\delta (P_{th} + P_0)}{D_{th}} \left[A \sin \sqrt{\frac{\delta (P_{th} + P_0)}{\rho K D_{th}}} t + B \cos \sqrt{\frac{\delta (P_{th} + P_0)}{\rho K D_{th}}} t \right] \quad \dots (4.i)$$

In order to determine the integration constants A and B in the above equations, let us next consider the initial conditions:

The pressure of the air cushion at an instant can be regarded to be in equilibrium with that of surrounding fluid p_{th} . However, through many air bubbles between the air cushion and the free surface (see Photo. 1), a passage may suddenly and for a moment lead from the air cushion up to the free atmosphere (Fig. 4), by which passage the pressure of the enclosed air is suddenly released. As soon as the pressure in the passage of the air as well as that of the air cushion is released to

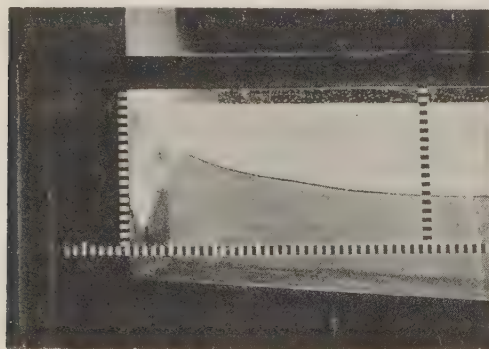


Photo. 1. Breaker just at impact.

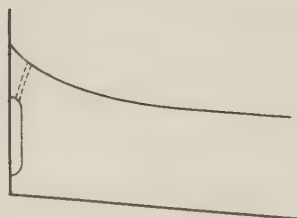


Fig. 4. An air pipe.

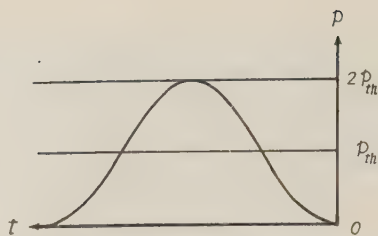


Fig. 5. Pressure variation in the air cushion.

less than that of the surrounding fluid, the passage is closed with water and the air cushion is again under compression of surrounding water. Let us take the origin of time at the instant when the passage is thus closed. Then as the initial conditions we have

$$t = 0 : \quad p = 0 \quad \text{and} \quad u = 0 \quad \dots (5)$$

Then on account of the initial conditions and by the use of equations (4.h) and (4.i), we obtain

$$A = 0 \quad \text{and} \quad B = \frac{-D_{th}}{\delta (P_{th} + P_0)} P_{th}$$

Hence, from equation (4.e), we obtain

$$p = P_{th} - P_{th} \cos \sqrt{\frac{\delta (P_{th} + P_0)}{\rho K D_{th}}} t \quad \dots (6)$$

whence we have

$$p_{max} = 2 P_{th} \quad \dots (7)$$

As is obvious, the pressure variation given by eq. (6) is as shown in Fig. 5. Substituting eq. (3) in eq. (7), we obtain as the tentative conclusion the relation

$$p_{max} = \frac{2 w U^2}{g} \quad \dots (8)$$

and therefore the value of f in the expression (1) as

$$f = 4 \quad \dots (9)$$

It is to be noted that the fundamental equations (4.a), (4.b) and (4.c) are almost the same as those used by Bagnold²⁾ except the difference that p_{th} stands for p_0 . It should also be noted that the initial conditions are the very difference, as the result of which difference the present theoretical considerations may be

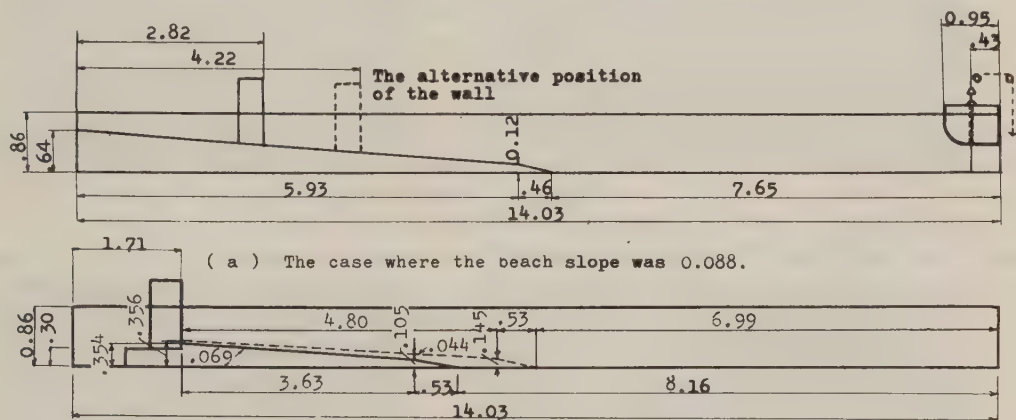
defined as that which deals with an different aspect from what was dealt with by Bagnold.

0.86m deep. The observation section, 10.27m long, was made of 6mm armour-plate glass in panels 0.86m by 1.26m.

EXPERIMENTAL EQUIPMENT AND PROCEDURE

The wave tank is shown in Fig. 6. It was made of reinforced concrete 14.03m long, 1m wide and

In order to eliminate the undeterminable effect of return current caused by the preceded waves in oscillatory waves and to investigate the purely dynamic pressure of each wave in oscilla-



(a) The case where the beach slope was 0.088.

(b) The case where the beach slope was 0.069 or 0.044.

Fig. 6. Wave tank (dimensions in m).

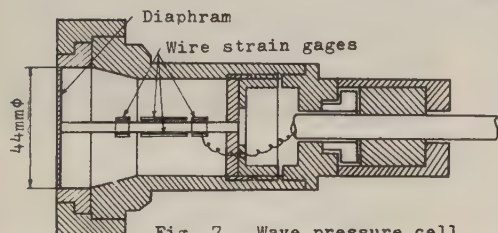


Fig. 7. Wave pressure cell.

tory waves, the solitary wave was generated by means of the sudden drop of a plunger 0.90m long, 0.99m wide, 0.60m deep. the front surface of which consisted of a parabolic curve.

The solitary wave was driven forward along a level floor, made to break, by means of a sloping beach, against a vertical wall, beach slope being 0.088, 0.069 or 0.044 in the course of experiments (Fig. 6).

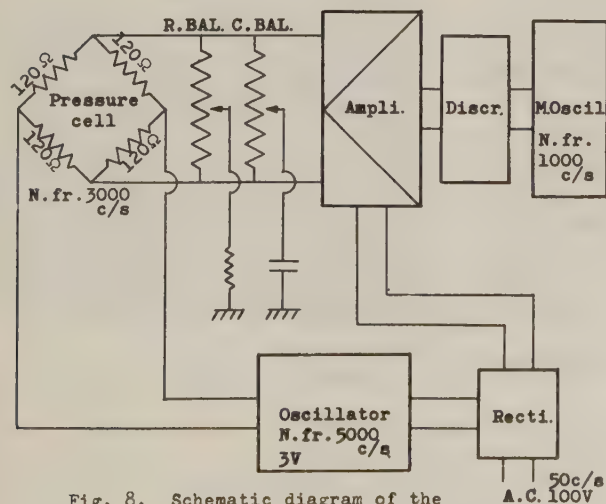


Fig. 8. Schematic diagram of the recording equipments for the wave pressure.

Five calibrated pressure cells were mounted in the bulkhead representing the vertical wall against which the waves were to break. The sensitive surface of the cells 44mm in diameter was flush with the surface of the wall. The pressure cells designed and made at Kyowamusen Kenkyujo Company consisted of a diaphragm and a supporting rod on the sides of which wire strain gages were attached (Fig. 7).

The pressure variation thus picked up by the cells was conveyed to a six-element oscillograph through an amplifier

(Fig. 8).

The motion of the breaker just before and after the impact to the vertical wall was taken with a 16mm Bell and Howell motion-picture camera at its maximum shutter speed of 64 frames per second. By means of switching on and off an electric lamp taken photographically in the motion-picture as well as led electrically to the oscillograph, the motion of the motion-picture was synchronized to that of oscillograph. By the examination of the frames of the motion-picture after developing the film, the speed of impact of the wave, the height and depth of the breaker, and so on were studied.

The solitary wave off the beach slope was recorded also photographically by 35mm Canon camera.

EXPERIMENTAL RESULTS

A typical oscillograph record and the corresponding motion-picture of the impact of a breaker enclosing a thick air cushion are shown in Fig. 9 and Photo. 2.

The longitudinal lines on the oscillogram show the instants when the pictures were taken, the number enclosed by a circle in the oscillogram corresponding to the picture of the same number.

At pressure cell B a sharp initial rise of pressure was followed by a second longer period during which high pressure was maintained, that being the same as reported in the previous investigations, notably by Larras,⁵⁾ Rouville, Besson and Petry,⁶⁾ and Bagnold.²⁾ At cells C, D and E smoother variations of pressure were recorded, to which type of pressure variation our preliminary theoretical considerations were concerned, whereas the theoretical considerations by Bagnold

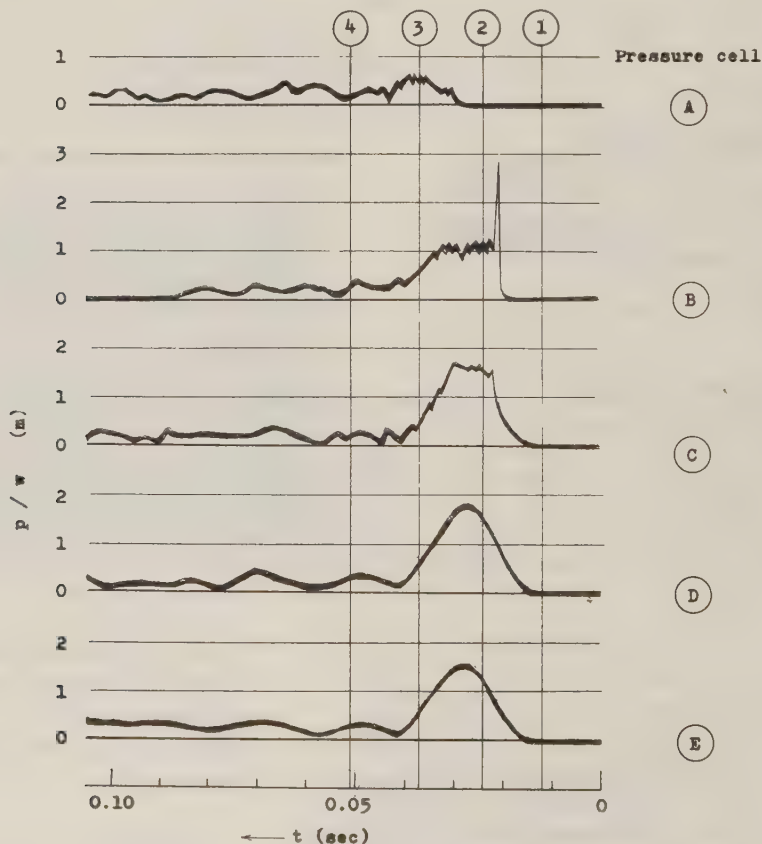
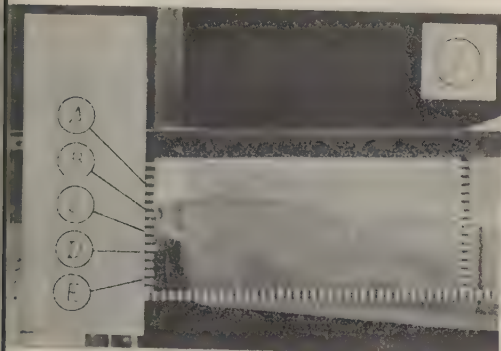


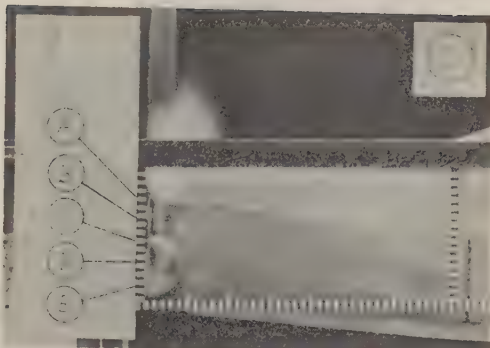
Fig. 9. Oscillograph record of the breaker corresponding to the pictures shown in Photo. 2.

chiefly concerned with the initial shock

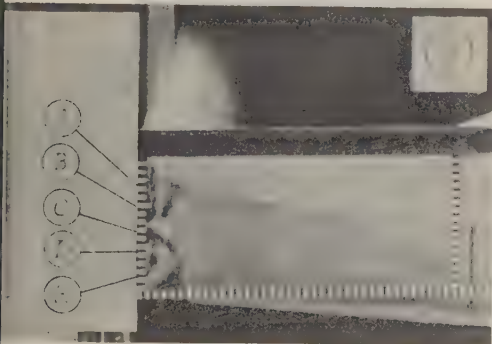
pressure.



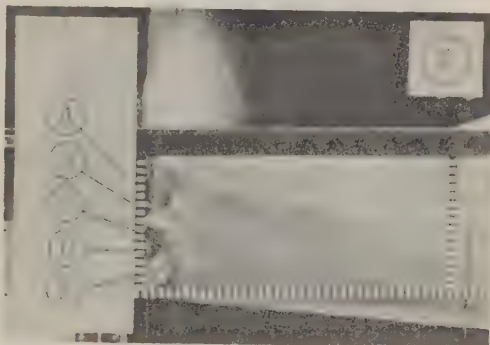
$t = 0.012\text{sec}$. instant just before the impact. Any pressure cell has not yet felt any pressure.



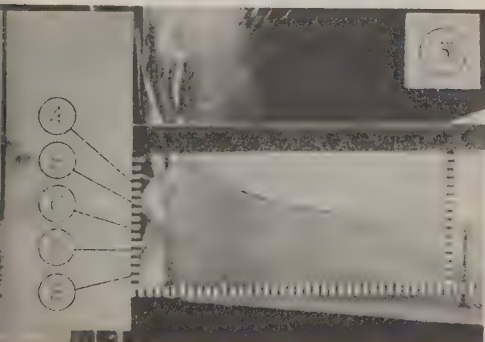
$t = 0.024\text{sec}$. Upon pressure cell B a sharp initial rise of pressure has already passed off and high pressure of a longer period is acting. Upon cell C similar pressure is acting. Upon cells D and E pressure is rising.



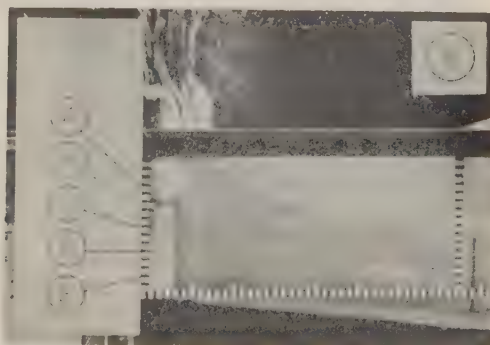
$t = 0.037\text{sec}$. Upon pressure cell A relatively high pressure is acting, but upon cells B, C, D and E high pressure is vanishing.



$t = 0.051\text{sec}$. Pressure upon each pressure cell has almost vanished.

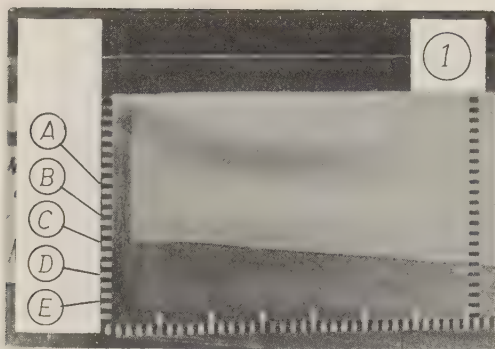


$t = 0.130\text{sec}$. Much spray is bursted upwards, while at each pressure cell pressure has already vanished except hydrostatic pressure.

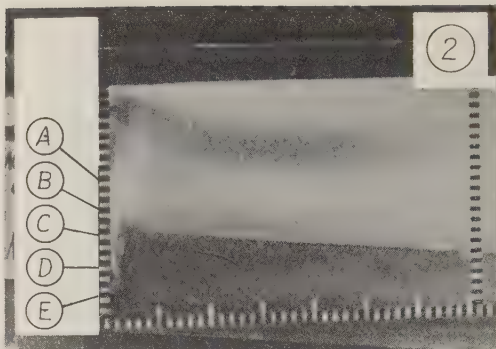


$t = 0.195\text{sec}$. Formation of spray has almost deceased.

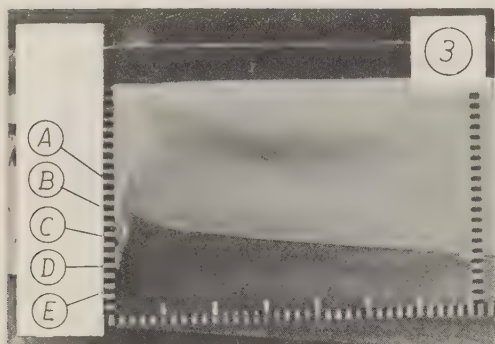
Photo. 2. High speed motion picture of the impact of a breaker, enclosing a thick air cushion, against a vertical wall. (The width of each white or black band of the scales is 1cm. Still water level was at the upper line of the horizontal scale, the initial depth just in front of the wall being 4cm. The center of the five pressure cells A, B, C, D and E were at 25.50cm, 9.90cm, 14.47cm, 9.00cm and 3.54cm, respectively, above the still water level. Test number shown in Table 2 is 9.)



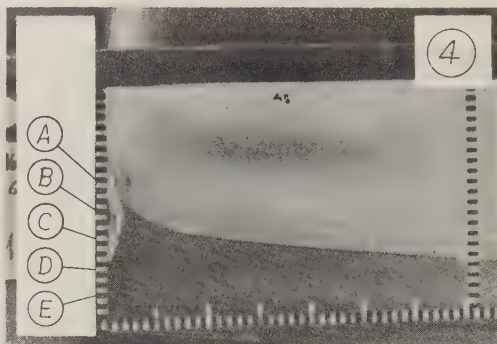
$t = 0.014\text{sec.}$ Just before impact.



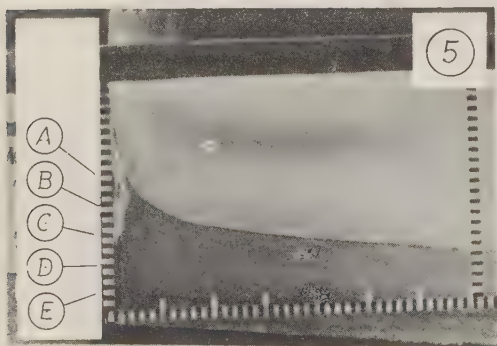
$t = 0.028\text{sec.}$ Upon pressure cells D and E a sharp initial rise of pressure has already passed off.



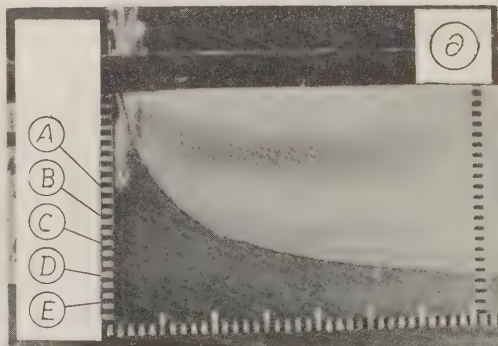
$t = 0.042\text{sec.}$



$t = 0.056\text{sec.}$



$t = 0.069\text{sec}$



$t = 0.158\text{sec.}$

Photo. 3. High speed motion picture of the impact of a breaker, enclosing a thin air cushion, against a vertical wall. (The width of each white or black band of the scales is 1cm. Still water level was at the upper line of the horizontal scale, the initial depth just in front of the wall being 3.3cm. The center of the five pressure cells A, B, C, D and E were at 26.60cm, 20.90cm, 15.30cm, 9.70cm and 4.50cm, respectively, above the still water level. Test number shown in Table 2 is 69.)

Another typical motion picture and the corresponding oscillogram of the impact of a breaker enclosing a thin air cushion are shown in Photo. 3 and Fig. 10. As was reported in the previous works, notably by Bagnold²⁾, Ross⁷⁾ and*

* Denny,⁸⁾ the initial rise of the pressure was very sharp, at pressure cell D at this case, pressure at every pressure cell consisting of sharp waves, to which our preliminary theoretical considerations were not concerned.

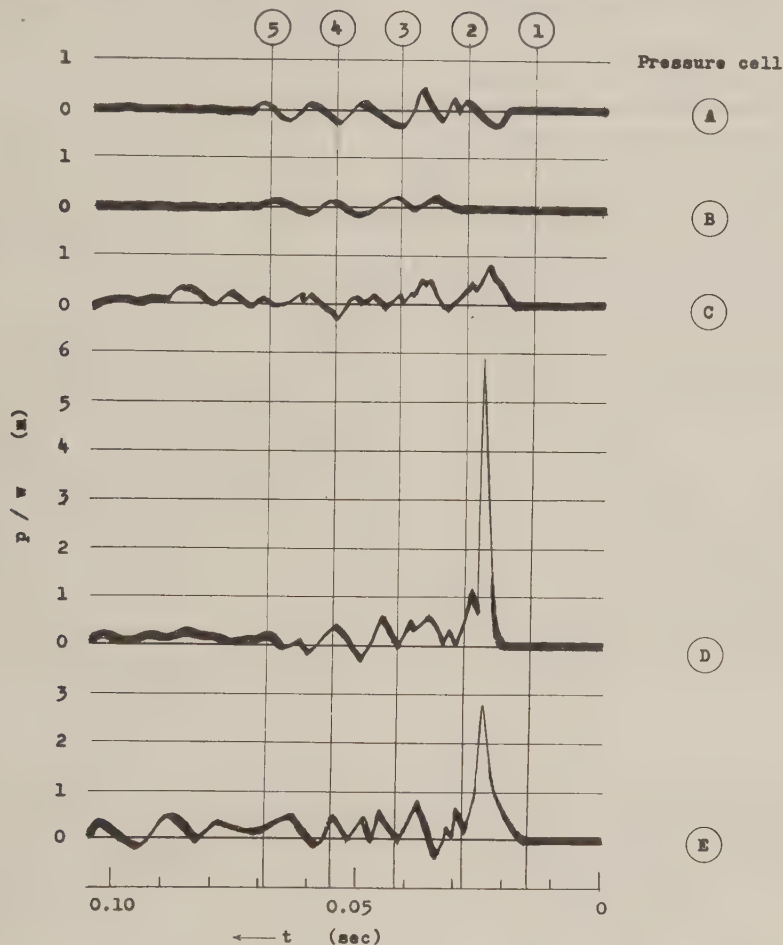


Fig. 10. Oscillograph record of the breaker corresponding to the pictures shown in Photo. 3.

Necessary data covering the entire range of the experiment are shown in Table 2 at the appendix.

In the table, the effective length of the solitary wave was given by Munk's formula⁹⁾

$$L_{\text{eff}} = \frac{2\pi}{M} d_u$$

the period of the periodic waves equivalent of the solitary wave by Bagnold-Munk's formula⁹⁾**

**

$$T_{\text{eff}} = \frac{2\pi}{M} \sqrt{\frac{d_u}{g}}$$

and the wave length and wave height of the deep water oscillatory waves, equivalent of the effective length and the height of the solitary wave, respectively, by Ippen-Kulin's formulae¹⁰⁾

$$L_{\text{equiv}} = L_{\text{eff}} \coth \frac{2\pi d_u}{L_{\text{eff}}}$$

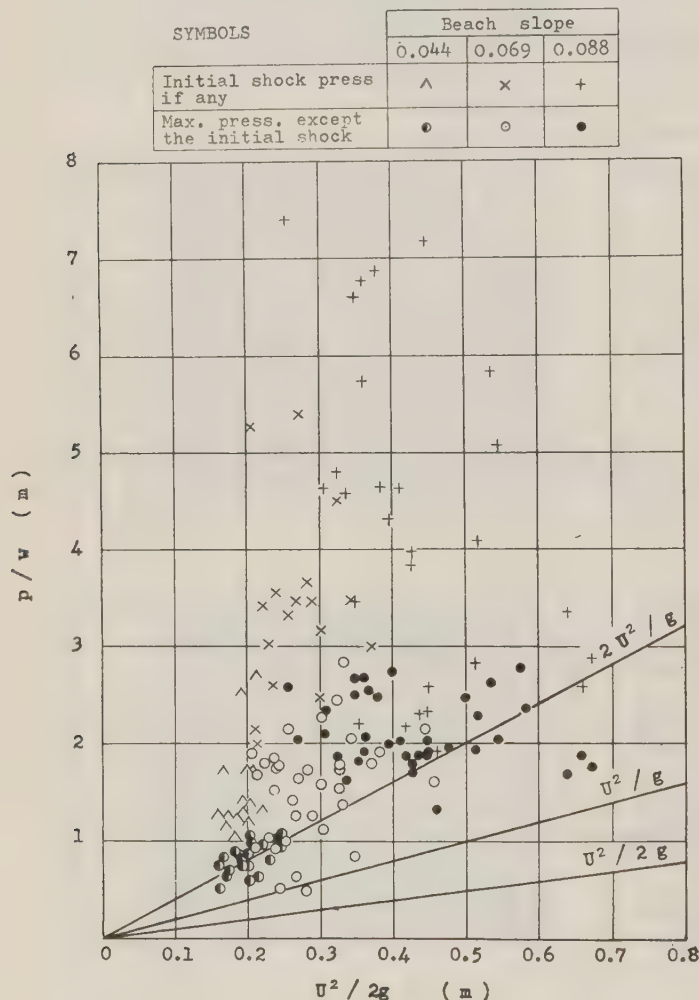
and

$$H_{\text{equiv}} = H_u \left[\tanh \frac{2\pi d_u}{L_{\text{eff}}} \right]^{\frac{1}{2}} \left[1 + \frac{4\pi d_u}{L_{\text{eff}}} \operatorname{cosech} \frac{4\pi d_u}{L_{\text{eff}}} \right]^{\frac{1}{2}}$$

Fig. 11 shows the relation between the dynamic pressure and the velocity head, both being of breakers at impact. In this figure both the shock pressure, if any, and the maximum pressure except the shock pressure, at each run, are shown with different symbols* and compared with theoretical curves.

It has been observed that the shock pressure varies enormously from test to test, it often being much larger than what is given by theoretical curves. However, as far as the maximum pressure except the shock pressure is concerned, it scatters somewhat nearer the theoretical curve given by $p / w = 2 U^2 / g$.

Fig. 11. Relation between the dynamic pressure and the velocity head, both of breakers at impact.



SUMMARY

The wave pressure of the breaker was investigated both theoretically and experimentally.

The theoretical considerations were concerned with a different aspect from the initial shock pressure which Bagnold dealt with. The tentative conclusion of the theoretical considerations which was led from the existing theory of the stationary jet was $p / w = 2 U^2 / g$, where p / w is the maximum pressure of the wave with longer period other than the initial shock and U the velocity of water just at its impact to the vertical wall.

Experiments were made and compared with the tentative conclusion. At the experiments the motion of the breaker just before and just after its impact to a vertical wall was taken with a high speed motion-picture camera while its pressure on the wall was recorded with an oscillograph. In this way it became possible to examine the process of the pressure variation of the breaker on the wall also photographically.

The result of the experiment shows that the initial shock pressure varies so enormously from test to test that it almost seems to have nothing to do with our theoretical considerations. Whereas, as far as the maximum pressure of the wave with longer period other

* That is, as to Fig. 9, for example, the initial pressure rise at pressure cell B and the maximum pressure at cell D were plotted in this figure, the latter being the maximum pressure among all except the initial pressure rise at cell B.

an the initial shock is concerned, it somewhat
as a tendency to gather near the theoretical
urve.

Thus, although data are still insufficient
establish definitely the relation between the
pressure and the velocity head of the breaker at
as impact to a vertical wall, in view of both our
eoretical conclusion and our experimental result
propose as a tentative conclusion of the
resent investigation the relation

$$\frac{p}{w} = \frac{2 U^2}{g}$$

and therefore

$$f = 4$$

with formulae being the same as or close to what
ve been adopted notably by Lira, Trenjukkinn,
illard and Molitor. In comparison with the
conclusions of ours the formula of the breaker
Hiroi gives the pressure of the breaker of
sufficient magnitude.

ACKNOWLEDGEMENT

The authors are grateful to Messrs. T. Imai
and K. Hayashi, both at Hydraulics Laboratory of
uo University, for their assistance.

A part of the expenses of the work was
ndebted to the scientific research fund grant
from the Ministry of Education of Japan during
the period from 1954 to 1957.

REFERENCES

- (1) I. Hiroi: The force and power of waves,
Engineer, 1920, pp. 184-185.
- (2) R. A. Bagnold: Interim report on wave-press-
ure research, Journal of Institution of Civil
Engineers, 1938-39, pp. 202-226.
- (3) R. R. Minikin: Winds, waves and maritime
structures, (Charles Griffin), 1950.
- (4) E. Bruns: Berechnung des Wellenstosses auf
Molen und Wellenbrecher, Jahrbuch der Hafen-
bautechnischen Gesellschaft, (Springer), 1951.
- (5) J. Larras: Le déferlement des lames sur les
jetées verticales, Annales des Ponts et
Chaussées, 1937, pp. 643-680.
- (6) A. de Rouville, P. Besson et P. Pétry: Etat
actuel des études internationales sur les
efforts dus aux lames, Ann. des Ponts et Ch.,
1938, pp. 5-113.
- (7) C. W. Ross: Laboratory study of shock press-
ure of breaking waves, Technical Memorandum
No. 59, Beach Erosion Board, 1955.
- (8) D. F. Denny: Further experiments on wave
pressures, Journ. of Inst. of Civ. Engineers,
1951. pp. 330-345.
- (9) W. H. Munk: The solitary wave and its appli-
cation to surf problems, Ann. of New York
Academy of Science, 1949. pp. 376-424.
- (10) A. T. Ippen and G. Kulin: Shoaling and break-
ing characteristics of the solitary wave.
Technical Report No. 15, Hydrodynamics Labora-
tory, Massachusetts Institute of Technology,
1955.

APPENDIX

Table 2. DATA OF EXPERIMENT.

Test No.	H_u (m)	d_u (m)	L_{equiv} (m)	H_{equiv} (m)	$\frac{H_{equiv}}{L_{equiv}}$	T_{eff} (s)	S	H_b (m)	d_b (m)	H'_b (m)	d_1 (m)	U ($\frac{m}{s}$)	$\frac{U^2}{2g}$ (m)	Max.press.except shock press.		Shock press.			
														Location(m)		$\frac{P}{w}$ (m)	Location(m)		$\frac{P}{w}$ (m)
														Above S.W.L.	Below w.cr.		Above S.W.L.	Below w.cr.	
1	.218	.460	4.74	.233	.049	1.74	.088				.040		.145		1.88		.145		3.50
2	.228	.460	4.67	.244	.052	1.73	.088				.040		.090		1.82		.145		1.88
3	.212	.460	4.78	.226	.047	1.75	.088	.215	.079	.205	.040	2.93	.438	.090	.115	1.88	.145	.060	2.30
4	.225	.460	4.69	.241	.051	1.73	.088	.220	.070	.215	.040	2.30	.270	.145	.070	2.04	No shock		
5	.226	.460	4.67	.242	.052	1.73	.088	.215	.067	.215	.040	3.63	.673	.145	.070	1.77	.145	.070	2.88
6	.220	.460	4.72	.235	.050	1.74	.088	.220	.075	.215	.040	2.63	.353	.145	.070	1.82	.145	.070	2.20
7	.243	.460	4.54	.261	.058	1.70	.088	.225	.072	.220	.040	3.60	.661	.145	.075	1.88	.199	.021	2.56
8	.230	.460	4.64	.247	.053	1.72	.088	.230	.074	.220	.040			.145	.075	1.90	No shock		
9	.245	.460	4.53	.263	.058	1.70	.088	.240	.077	.230	.040	3.19	.520	.090	.140	1.93	.199	.031	2.82
10	.250	.460	4.50	.269	.059	1.70	.088	.240	.079	.230	.040	3.03	.418	.145	.085	1.87	.199	.031	2.18
11	.219	.460	4.72	.234	.050	1.74	.088	.220	.074	.220	.040	2.89	.426	.035	.185	1.70	.145	.075	3.84
12	.223	.460	4.69	.238	.051	1.74	.088	.230	.076	.210	.040	2.96	.447	.145	.065	1.88	.145	.065	2.33

Test No.	H _u (m)	d _u (m)	L _{b,uv} (m)	H _{equi.} (m)	H _{equi.} L _{equi.}	T _{eff} (s)	S	H _b (m)	d _b (m)	H _b (m)	d _l (m)	·U ($\frac{m}{s}$)	U ² 2g (m)	Max. press. except shock press.			Shock press.		
														Location (m)		p w (m)	Location (m)		p w (m)
														Above S.W.L.	Below w.cr.		Above S.W.L.	Below w.cr.	
13	.217	.460	4.73	.232	.049	1.74	.088	.220	.078	.210	.040	2.97	.450	.145	.065	1.91	.145	.065	2.58
14	.222	.460	4.73	.236	.050	1.74	.088	.230	.079	.220	.040	3.06	.478	.145	.075	1.96	No shock		
15	.180	.348	3.46	.193	.056	1.49	.088	.170	.047	.170	.033	2.73	.380	.045	.125	2.50	.097	.073	6.87
16	.179	.348	3.57	.191	.054	1.51	.088				.033								
17	.181	.348	3.46	.194	.056	1.49	.088	.180	.044	.180	.033	3.56	.646	.153	.027	1.68	.097	.083	3.35
18	.195	.348	3.37	.210	.062	1.47	.088				.033								
19	.185	.348	3.44	.198	.058	1.48	.088	.185	.046	.180	.033	2.24	.256	.153	.027	2.58	.097	.083	7.40
20	.196	.348	3.37	.211	.063	1.47	.088				.033								
21	.200	.348	3.35	.215	.064	1.46	.088	.206	.058	.203	.033	2.68	.366	.097	.106	2.54	No shock		
22	.225	.348	3.24	.243	.075	1.44	.088	.205	.055	.205	.033			.097	.108	2.41	No shock		
23	.190	.348	3.40	.204	.060	1.47	.088	.190	.043	.185	.033	2.61	.348	.153	.032	2.67	.097	.088	3.45
24	.178	.348	3.49	.191	.055	1.50	.088	.185	.043	.185	.033	2.61	.348	.045	.140	2.50	.097	.088	6.66
25	.180	.348	3.46	.193	.056	1.49	.088	.185	.046	.182	.033	2.96	.447	.045	.137	2.03	.097	.085	7.18
26	.181	.348	3.46	.194	.056	1.49	.088	.185	.044	.185	.033	2.66	.361	.045	.140	1.93	.097	.088	6.76
27	.180	.348	3.46	.193	.056	1.49	.088	.187	.045	.185	.033	2.66	.361	.097	.088	2.68	.153	.032	5.84
28	.184	.348	3.44	.198	.058	1.48	.088	.188	.047	.187	.033	2.84	.411	.045	.142	2.03	.097	.090	4.63
29	.180	.348	3.46	.193	.056	1.49	.088	.185	.045	.184	.033	2.57	.336	.045	.139	1.62	.097	.087	4.57
30	.138	.429	5.28	.145	.028	1.84	.069	.190	.089	.180	.075	2.56	.334	.099	.081	2.84	No shock		
31	.153	.429	5.03	.161	.032	1.79	.069	.180	.089	.180	.075	2.65	.458	.099	.081	1.61	No shock		
32	.141	.429	5.22	.148	.028	1.83	.069	.190	.089	.180	.075	2.70	.372	.060	.020	1.79	.099	.081	3.00
33	.155	.429	4.96	.164	.033	1.78	.069	.200	.084	.190	.075	2.55	.332	.019	.071	1.37	No shock		
34	.155	.429	4.96	.164	.033	1.78	.069	.190	.084	.190	.075	2.54	.329	.099	.091	1.74	No shock		
35	.153	.429	5.03	.161	.032	1.79	.069	.190	.087	.180	.075	2.60	.345	.060	.120	2.06	.099	.081	3.48
36	.148	.429	5.20	.156	.031	1.82	.069	.190	.086	.190	.075	2.74	.384	.099	.091	1.90	No shock		
37	.161	.429	4.87	.170	.035	1.77	.069	.200	.086	.200	.075	2.95	.444	.099	.101	2.15	No shock		
38	.160	.429	4.93	.170	.035	1.79	.069	.180	.087	.190	.075	2.53	.326	.099	.091	1.78	No shock		
39	.158	.429	4.93	.167	.034	1.78	.069	.200	.086	.190	.075	2.19	.244	.099	.091	1.76	No shock		
40	.158	.429	4.93	.167	.034	1.78	.069	.190	.094	.190	.075	2.53	.327	.099	.091	1.54	No shock		
41	.158	.429	4.93	.167	.034	1.78	.069	.200	.085	.190	.075	2.36	.284	.181	.009	1.73	.099	.091	3.66
42	.168	.429	4.78	.178	.036	1.75	.069	.190	.085	.190	.075	2.51	.322	.181	.009	2.45	.099	.091	4.51
43	.173	.429	4.72	.184	.039	1.74	.069	.210	.094	.210	.075	2.25	.258	.050	.150	2.15	.099	.111	3.32
44	.163	.429	4.85	.172	.036	1.76	.069	.190	.085	.190	.075	2.44	.302	.099	.091	2.27	.181	.009	3.16
45	.166	.429	4.79	.176	.037	1.75	.069	.200	.087	.200	.075	2.44	.302	.160	.040	1.59	.099	.101	2.47
46	.155	.429	4.96	.164	.033	1.78	.069	.180	.089	.190	.075	2.15	.236	.060	.130	1.85	No shock		
47	.110	.395	5.36	.124	.021	1.85	.069	.110	.055	.115	.045	2.19	.245	.049	.066	0.50	No shock		
48	.118	.395	5.07	.123	.024	1.80	.069	.130	.052	.130	.045	2.28	.266	.129	.001	1.25	.090	.040	3.46
49	.106	.395	5.41	.115	.021	1.86	.069	.130	.053	.130	.045	2.29	.266	.090	.040	0.63	No shock		
50	.105	.395	5.36	.109	.020	1.85	.069	.130	.053	.130	.045	2.34	.280	.129	.001	0.49	No shock		
51	.116	.395	5.10	.121	.024	1.81	.069	.130	.053	.130	.045	2.26	.261	.129	.001	1.41	No shock		
52	.113	.395	5.23	.118	.023	1.83	.069	.130	.053	.130	.045	2.11	.227	.090	.040	1.79	.129	.001	3.44
53	.120	.395	4.73	.128	.027	1.74	.069	.140	.053	.140	.045	2.17	.240	.129	.011	1.74	.090	.050	3.56
54	.115	.395	5.17	.120	.023	1.82	.069	.130	.058	.130	.045		.090	.090	.040	0.93	No shock		
55	.145	.395	4.56	.155	.034	1.71	.069	.170	.071	.150	.045	2.17	.239	.002	.148	0.91	No shock		
56	.137	.395	4.71	.144	.037	1.74	.069	.160	.084	.140	.045	2.61	.348	.002	.138	0.84	No shock		
57	.120	.395	5.04	.125	.023	1.80	.069	.140	.075	.135	.045	2.44	.304	.090	.045	1.11	No shock		
58	.120	.395	4.73	.126	.027	1.74	.069	.140	.078	.140	.045	2.03	.209	.090	.050	0.93	.090	.050	2.15
59	.121	.395	4.58	.128	.028	1.71	.069	.140	.073	.140	.045	2.04	.213	.090	.050	1.68	.129	.011	1.99
60	.116	.395	5.14	.121	.024	1.82	.069	.130	.079	.130	.045	2.38	.289	.129	.001	1.26	.090	.040	3.46
61	.118	.395	5.05	.123	.024	1.80	.069	.130	.077	.130	.045	2.15	.236	.090	.040	1.51	.049	.081	2.60
62	.118	.395	5.05	.123	.024	1.80	.069	.140	.080	.130	.045	2.23	.254	.090	.040	0.99	No shock		
63	.115	.395	5.17	.120	.023	1.82	.069	.120	.082	.130	.045	2.12	.229	.049	.081	1.04	.090	.040	3.03
64	.113	.395	5.20	.118	.023	1.82	.069	.125	.081	.135	.045	2.02	.208	.129	.006	1.90	No shock		
65	.115	.395	5.17	.120	.023	1.82	.069	.135	.082	.130	.045	2.30	.270	.049	.081	1.64	.090	.040	5.39
66	.116	.395	5.10	.121	.024	1.81	.069	.130	.080	.130	.045	2.02	.208	.002	.128	0.92	.090	.040	5.27
67	.190	.350	3.43	.204	.060	1.48	.088	.175	.049	.175	.033	2.46	.309	.035	.140	2.34	No shock		
68	.158	.350	3.66	.169	.046	1.53	.088	.160	.039	.155	.033	2.66	.361	.090	.065	1.94	No shock		
69	.162	.350	3.60	.175	.049	1.52	.088	.175	.041	.160	.033	3.24	.535	.125	.035	2.62	.090	.070	5.83
70	.164	.350	3.62	.175	.048	1.52	.088	.165	.041	.165	.033	2.78	.394	.130	.035	1.99	.090	.075	4.31
71	.167	.350	3.59	.178	.050	1.52	.088	.170	.039	.160	.033	2.74	.383	.125	.035	1.92	.090	.070	4.64
72	.158	.350	3.11	.169	.046	1.53	.088	.160	.040	.160	.033	2.89	.426	.125	.035	1.74	.090	.070	3.98
73	.168	.350	3.58	.179	.050	1.52	.088	.170	.034	.160	.033	2.45	.366	.125	.035	2.10	.090	.070	4.63
74	.178	.350	3.50	.191	.055	1.50	.088	.165	.041	.160	.033	3.00	.459	.035	.125	1.32	.070	.090	1.92
75	.173	.350	3.54	.186	.053	1.51	.088	.170	.041	.160	.033	2.51	.322	.125	.035	1.87	.090	.070	4.80
76	.173	.350	3.54	.186	.053	1.51	.088	.180	.040	.160	.033	2.66	.362	.070	.090	2.07	No shock		
77	.174	.350	3.52	.186	.053	1.50	.088	.170	.041	.150	.033	2.80	.400	.060	.090	2.74	No shock		
78	.175	.350	3.51	.188	.054	1.50	.088	.175	.040	.160	.033	3.27	.545	.125	.035	2.04	.090	.070	5.08
79	.170	.350	3.57	.185	.051	1.51	.088	.175	.037	.180	.033	2.16	.238	.145	.035	1.02	No shock		
80		.350					.088	.185	.046	.185	.033	3.18	.517	.035	.150	2.29	.090	.095	4.08
81		.350					.088	.190	.047	.185	.033	3.13	.499	.090	.095	2.48	No shock		
82		.350					.088	.185	.047	.185	.033	3.39	.584	.090	.095	2.36	No shock		
83		.350					.088	.185	.041	.185	.033	3.36	.575	.090	.095	2.77			

Test No.	H _u (m)	d _u (m)	L _{equiv} (m)	H _{equiv} (m)	$\frac{H_{equiv}}{L_{equiv}}$	T _{eff} (s)	S	H _b (m)	d _b (m)	H' _b (m)	d _l (m)	U ($\frac{m}{s}$)	$\frac{U^2}{2g}$ (m)	Max. press. except shock				Shock press.			
														Location(m)		$\frac{P}{W}$ (m)		Location(m)		$\frac{P}{W}$ (m)	
														Above	Below			Above	Below		
														S.W.L.	w.cr.			S.W.L.	w.cr.		
84	.109	.428	6.02	.112	.0186	1.96	.044	.155	.092	.150	.072	2.48	.313	.138	.012	0.69		.095	.055	1.53	
85	.107	.428	6.08	.110	.0183	1.97	.044	.155	.089	.160	.072	2.47	.310	.095	.065	0.90		No	shock		
86	.114	.428	5.85	.118	.0202	1.94	.044	.155	.090	.150	.072	2.42	.297	.059	.091	0.70		.095	.055	1.24	
87	.112	.428	5.92	.116	.0196	1.95	.044	.150	.088	.155	.072	2.20	.247	.095	.060	1.07		No	shock		
88	.102	.428	6.24	.105	.0168	2.00	.044	.151	.083	.145	.072	1.94	.192	.018	.127	0.84		.095	.050	2.52	
89	.103	.428	6.19	.106	.0171	1.99	.044	.152	.088	.145	.072	2.12	.229	.095	.050	0.81		No	shock		
90	.101	.428	6.27	.104	.0166	2.01	.044	.163	.084	.157	.072	1.95	.193	.023	.180	0.74		.095	.062	1.31	
91	.102	.428	6.24	.105	.0168	2.00	.044	.144	.086	.145	.072	1.97	.199	.138	.007	0.73		.095	.050	1.73	
92	.100	.428	6.32	.102	.0162	2.01	.044	.155	.081	.153	.072	2.01	.206	.018	.135	1.00		.138	.015	1.75	
93	.090	.428	6.70	.092	.0137	2.07	.044	.136	.082	.135	.072	1.95	.193	.138	.003	0.80		.095	.040	2.41	
94	.092	.428	6.60	.094	.0142	2.06	.044	.132	.081	.136	.072	1.85	.174	.018	.118	0.70		.095	.041	1.26	
95	.092	.428	6.60	.094	.0142	2.06	.044	.136	.077	.134	.072	1.91	.186	.095	.039	0.87		No	shock		
96	.088	.428	6.77	.089	.0131	2.09	.044	.136	.072	.136	.072	1.82	.170	.059	.077	0.63		.095	.041	1.18	
97	.089	.428	6.73	.090	.0134	2.08	.044	.140	.077	.142	.072	1.97	.199	.059	.083	0.81		.095	.047	1.22	
98	.114	.428	5.85	.118	.0202	1.94	.044	.162	.074	.138	.072	2.50	.320	.138	.000	0.72		No	shock		
99	.115	.428	5.82	.119	.0205	1.93	.044	.153	.086	.148	.072	2.20	.248	.095	.053	0.93		.059	.089	0.95	
100	.110	.428	5.96	.114	.0191	1.94	.044	.167	.080	.169	.072	2.01	.205	.095	.074	1.05		.138	.031	1.39	
101	.084	.417	6.75	.085	.0126	2.08	.044	.124	.070	.126	.061	2.04	.213	.049	.175	0.62		.070	.056	2.73	
102	.081	.417	6.90	.082	.0119	2.10	.044	.124	.070	.121	.061	1.88	.182	.029	.092	0.85		.070	.051	1.03	
103	.081	.417	6.90	.082	.0119	2.10	.044	.131	.069	.121	.061	1.80	.166	.070	.051	0.83		.029	.092	1.72	
104		.417					.044	.128	.068	.126	.061	2.01	.206	.012	.138	0.59		.070	.056	0.91	
105	.078	.417	7.02	.078	.0112	2.12	.044	.116	.066	.116	.061										
106	.090	.417	6.44	.092	.0143	2.03	.044	.133	.074	.141	.061	2.08	.220	.012	.153	0.96		.070	.071	1.33	
107	.091	.417	6.41	.093	.0145	2.03	.044	.131	.078	.126	.061	1.78	.162	.070	.056	0.51		No	shock		
108	.081	.417	6.90	.082	.0119	2.10	.044	.124	.070	.126	.061	1.77	.160	.070	.056	0.75		.029	.097	1.28	
109	.082	.417	6.84	.083	.0121	2.09	.044	.121	.070	.126	.061	1.88	.180	.012	.138	0.87		.029	.097	1.24	

Experimental Study of Wave Run-up on Sea Wall and Shore Slope

by Seiichi Sato, Dr.Eng. and Tsutomu Kishi, Dr.Eng.

(Contribution from the Public Works Research Institute,
Ministry of Construction)

Synopsis. In the first part of this paper, wave run-up on sea wall with slope of 1 : 2 was discussed. Wave run-up considerably increased in height comparing with that on vertical wall and was more sensitive to wave steepness and water depth. Additional experiments were carried out to evaluate the effects of parapet wall set on sloped wall. In the second part, wave run-up on foreshore with slopes of 1 : 9 and 1 : 17 was studied. Run-up on 1 : 9 slope were more sensitive to wave steepness than 1 : 17 slope.

Definitions used in this paper

- R : Run-up height above S.W.L.
(Without parapet)
- R' : Run-up height above S.W.L.
(With parapet)
- H₀ : Height of deep water wave
- H_s : Wave height at the shoreline
- H_b : Breaker height
- L₀ : Length of deep water wave
- (H/L)₀ : Steepness of deep water wave
or initial steepness of wave
- h : Water depth at the toe of slope
- h/L₀ : Shallowness at the toe of the
slope
- L_r : Horizontal distance of wave
run-up on foreshore, i.e., dis-
tance from shoreline to run-up
limit

I. Introduction

Almost every year storm surges caused by typhoon attack our country and greater part of shoreline are protected by sea walls or revetments. Sea walls mostly consist of earth embankment with concrete covering and their surface slopes are generally in the range 1 : 1.5 ~ 1 : 2.

Concerning run-up height on sea wall, it is thought that vertical wall is more favorable than sloping wall. However, sloping wall has advantages of distributing the wave force and reduc-

ing the score at the wall front. A series of experiments on wave run-up have been conducted by the Public Works Research Institute and experimental results on vertical wall was published in 1954.⁽¹⁾ In this paper character of wave run-up on slope of 1 : 2 was studied.

Almost all sea walls are built on shore. Some of them are built on foreshore. In this case wave run-up on shore is one of the basic factor of structure design. From this view point, experiments were carried out on two model beaches with slopes of 1 : 9 and 1 : 17.

II. Experimental procedure

Experiments were carried out in a wave channel 0.6m wide, 0.25m deep and 18.4m long. Waves were generated at one end of the channel by a flatter and model beaches with slopes 1 : 9 and 1 : 17 were built at the other end. They were used for the experiments of wave run-up on shore. For the experiments on sea wall, slope of 1 : 2 was set on model beach with slope of 1 : 17.

III. Results of experiments on slope 1 : 2

In these experiments wave periods were varied from 0.8 sec to 2.25 sec and initial steepnesses of waves covered the range between (H/L)₀ = 0.004 and 0.068.

Run-up height R depends on wave height, wave period and water depth at the toe of the slope. In other word, relative run-up (R/L₀) is a function of wave steepness (H/L)₀ and shallowness (h/L₀). Some examples of experimental results are shown in Fig. 1 and data show relatively less scatter. Complete sets of experiments are shown in Fig.2.

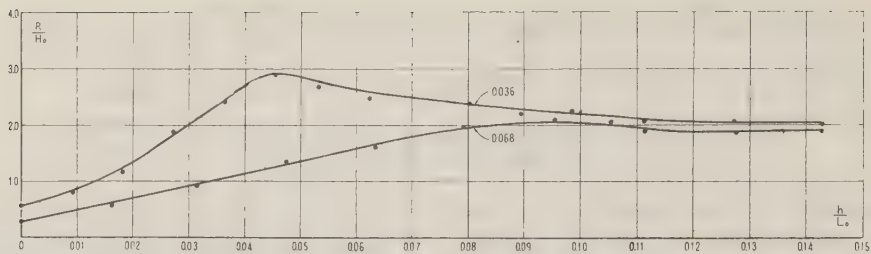


Fig. 1

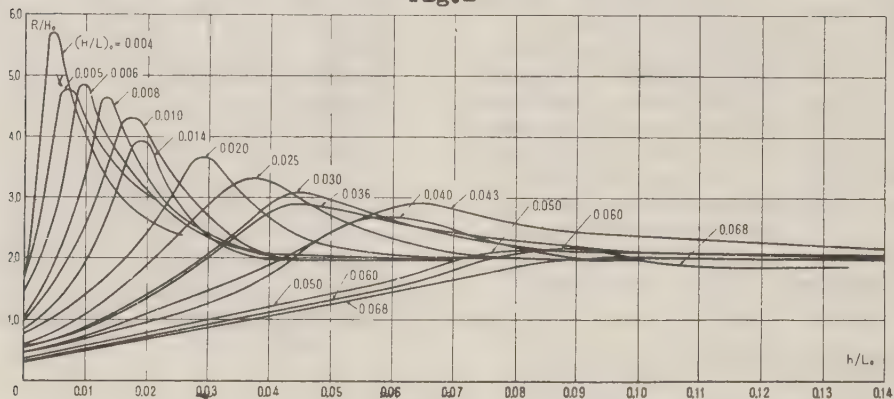


Fig. 2

From the figure following three characteristics could be pointed out.

(1) When wave steepness is maintained constant, value of R/H_0 has its maximum at certain value of shallowness. Such a shallowness decreases as steepness becomes small.

(2) When shallowness is maintained constant, value of R/H_0 is considerably sensitive to wave steepness, especially for smaller shallowness.

(3) When shallowness is larger than 0.08 value of R/H_0 becomes ill sensitive to wave steepness and seems to converge to a constant value.

1) Relation between the maximum run-up $(R/H_0)_{\max}$ and wave steepness $(H/L)_0$.

Relation between $(R/H_0)_{\max}$ and $(H/L)_0$ obtained from 2 is shown in Fig. 3 and

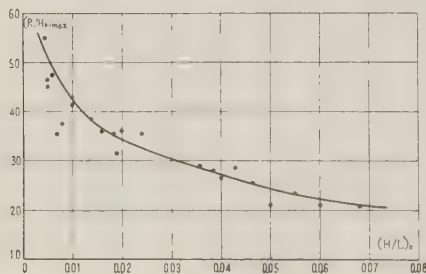


Fig. 3

the smaller wave steepness becomes, the more $(R/H_0)_{\max}$ increases. For example, when $(H/L)_0 = 0.01$ the value $(R/H_0)_{\max} = 4.25$, while $(R/H_0)_{\max} = 2.1$ when $(H/L)_0 = 0.07$. Such a trend is remarkable especially when $(H/L)_0$ is smaller than 0.02.

Positions of sea walls where $(R/H_0)_{\max}$ occur at any steepness are shown in Fig. 4. As shown in the figure (h/L_0) is linearly related with $(H/L)_0$ and this indicates that values of h/H_0 which make $(R/H_0)_{\max}$ are constant, 1.4, independent of wave steepness. This value is slightly greater than that of breaking point.⁽²⁾

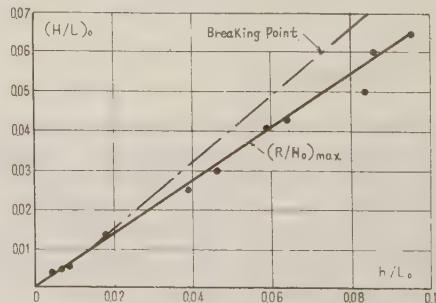


Fig. 4

2) Effect of wave steepness on wave run-up

To determine the effect of wave

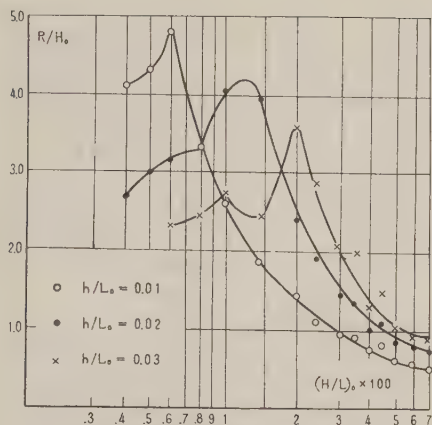


Fig.5 - 1

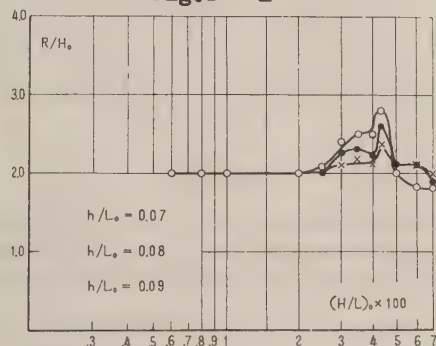


Fig.5 - 3

steepness on wave run-up Figs 5 are prepared. In Figs 5-1-4 relations between R/H_0 and $(H/L)_0$ are shown for several shallownesses. As pointed out by O.Sibul⁽³⁾, it is noticed that there exist certain value of steepness which makes (R/H_0) maximum at any shallowness. Such values of steepness are to be identical with those given in Fig.4.

Effect of steepness is remarkable when shallowness is small and it gradually weakens as shallowness increases. And when shallowness is larger than 0.12 R/H_0 has almost constant value, 2.0.

IV. Effects of parapets on wave run-up

Effects of parapets on wave run-up were studied by setting parapets on slope 1 : 2. Three parapets were used in this experiments and they are shown in Fig.6.

Wave height at uniform depth 25cm was 7cm and various wave steepness was obtained by varying wave period.

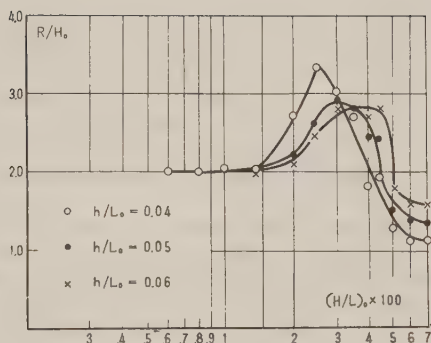


Fig.5 - 2

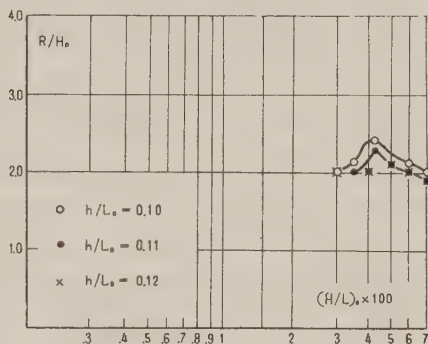
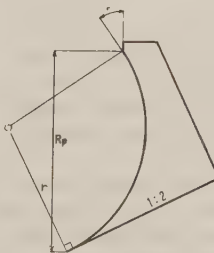


Fig.5 - 4



Parapet	r/H_0	R_p/H_0	$\beta (^{\circ})$
1	1.17	1.86	43
2	1.43	1.94	28
3	0.55	0.75	28

Fig.6

Run-up height R' was determined by observing the critical height where wave began to overflow the parapets.

(1) Height of parapet

The values of ratio (R'/R) corresponding to these three parapets are shown in Fig.7. The values (R'/R) with parapets 1 and 2 are about 0.5~0.6, namely run-up height can be reduced to about half by these parapets, while those with parapet 3 are about 0.8~1.0 and effect of parapet 3 is not noticeable. Relative heights of parapets, (R_p/H_0) , and 1.89, 1.96 and 0.75, respectively. And from the

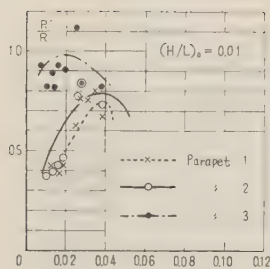


Fig.7 - 1

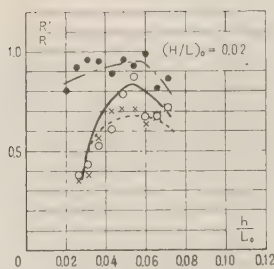


Fig.7 - 2

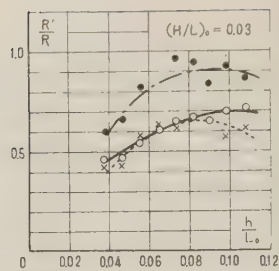


Fig.7 - 3

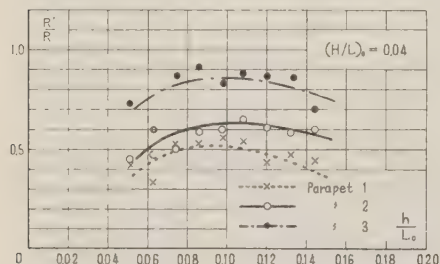


Fig.7 - 4

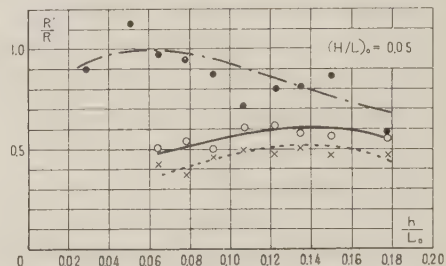


Fig.7 - 5

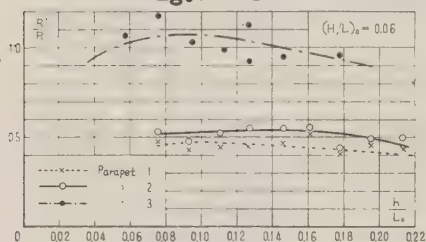


Fig.7 - 6

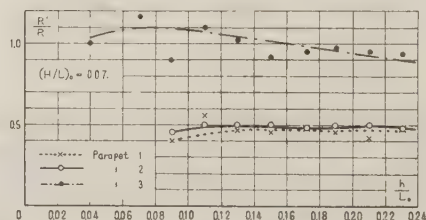


Fig.7 - 7

above results, it is estimated that parapets have considerable effect to reduce wave run-up only when their height exceed incident wave height.

(2) Shape of parapet

Parapets 1 and 2 have nearly same height but are different in their direction angle β . For parapet 1 angle β is 45° , and for parapet 2 it is 28° . In Fig.7 difference of run-up heights with these two parapets is small. This may indicate that angle β has relatively less effect to reduce wave run-up.

V. Wave run-up on foreshore

Experiments were carried out on model beaches with slopes 1 : 9 and 1 : 17. Initial steepnesses of waves were varied from 0.003 to 0.06.

1) Wave run-up

By preliminary plots, run-up height R was found to depend on breaker

height H_b and wave period. So that results of measurements are shown in Fig.8 which gives relations between (R/H_b) and $(H/L)_0$. In the case of slope 1 : 9 (R/H_b) increases as $(H/L)_0$ decreases. For example $R/H_b = 1.0$ when $(H/L)_0$ is 0.003 which $R/H_b = 0.5$ when $(H/L)_0 = 0.04$.

In the case of slope 1 : 17, on the other hand, (R/H_b) are generally smaller than the former and have nearly constant value independent of wave steepness.

2) Wave height at shore line H_s

Wave height at shore line H_s is an important factor in the detailed study of run-up. H_s , also, may depend on breaker height, wave steepness and foreshore slope, as wave run-up. Relations between (H_s/H_b) and $(H/L)_0$ for two slopes are shown in Fig.9. In the case of slope 1 : 9, (H_s/H_b) remarkably varies with wave steepness and it increases as steepness decreases. While in the case of 1 : 17, values of

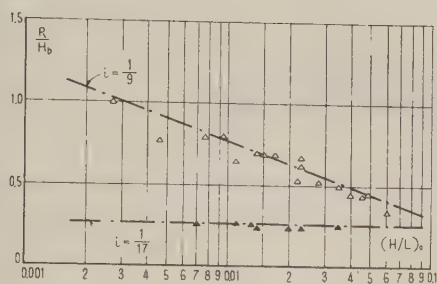


Fig. 8

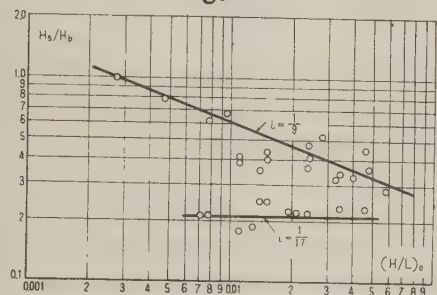


Fig. 9

(H_s/H_b) remain almost constant independent of wave steepness and their mean value is smaller than the former.

3) Attenuation of wave height on foreshore

Attenuations of wave heights on slope of 1 : 9 are shown in Fig. 10. Wave steepnesses used in the experiments vary relatively wide range between 0.008 and 0.04. However attenuation rate shown in Fig. 10 seems to be represented by a curve regardless of various steepnesses. And it may be concluded that wave height at any point of foreshore is lower than the line which connects wave crest at shore line and run-up limit.

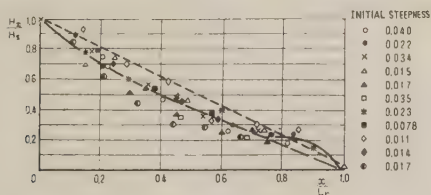


Fig. 10

VI. Conclusion

(1) Wave run-up on slope 1 : 2 is generally greater than that on vertical wall.

(2) When wave steepness is maintained constant, value of R/H_0 has its maximum at certain value of shallowness. Such the shallowness decreases as steepness becomes small. (Fig. 3)

(3) When values of ratio (h/H_0) is 1.4 relative run-up (R/H_0) has its maximum independent of wave steepness. (Fig. 4)

(4) Effect of steepness on wave run-up is remarkable weakens as shallowness increases. And when shallowness is larger than 0.12, (R/H_0) has almost constant value 2.0. (Fig. 5)

(5) Effect of parapet on wave run-up is appreciable only when its height exceeds incident wave height. And difference in shape of parapet is relatively less effective to reduce wave run-up. (Fig. 7)

(6) Wave run-up on foreshore with slope of 1 : 9 is sensitive to wave steepness and it increases as steepness decreases. On the other hand run-up on slope of 1 : 17 is not affected by steepness. (Fig. 8)

(7) Wave heights at shore line are shown in Fig. 9 and they show similar trend to run-up height.

(8) Attenuation of wave height on foreshore with slope of 1 : 9 seems to be represented by a curve independent of steepness. (Fig. 10)

References

- (1) Sato, S. and Kishi, T. : Experimental study on the height of sea wall; Journal of Research of the Public Works Research Institute, July 1954. and Sato, S. and Kishi, T. : Functional design of sea wall (in Japanese), ditto, Sep. 1954.
- (2) Kishi, T. : On the highest progressive wave in shallow water; ditto, March 1957.
- (3) Sibul, O. : Flow over reefs and structures by wave action; Trans. A.G. U., Feb. 1955

EFFECT OF A JETTY ON NEARSHORE CURRENTS

— MODEL EXPERIMENT —

Teizo SHIMANO, Dr. Sc., M.J.S.C.E.
Professor of Civil Engineering, University of Tokyo

Masashi HOM-MA, Dr. Sec., M.J.S.C.E.
Professor of Civil Engineering, University of Tokyo

Kiyoshi HORIKAWA, M.J.S.C.E.
Assistant Professor of Civil Engineering, University of Tokyo

1. Introduction

Our land is surrounded by sea and its long coastline is under the continual actions of waves. This has necessitated the construction of huge protection devices along our coast. Sea walls, groins or breakwaters have been built to counteract the disasters caused by high tides, Tsunamis, and beach erosion. As a means of ensuring the tranquillity of anchorage basin, breakwaters have become a common feature of most of the Japanese ports which are immediately exposed to the ocean, Jetties serve to facilitate the discharge of floods, the maintenance of navigation channels, and defense against waves.

As a matter of fact, these hydraulic constructions cannot be fully effective unless they are made compatible with the local requirements - particularly in relation to waves. Extensive research has been conducted by many coastal engineers which has contributed to solving some of the complications involved in beach-zone hydraulics. Primarily, this report intends to deal with the effects of coastal jetties, i.e. to pursue the mechanism of beach erosion brought about by the existence of coastal jetties which were originally constructed to afford protection to a beach. An example of this may be seen at the Niigata coast.

As waves shoal, their profiles are deformed by the effect of depth, the crest lines tend to be parallel to the shoreline by refraction, and they finally break releasing a large amount of mass transport which causes littoral current and, in most cases, littoral drift. The phenomenon takes on a vastly different aspect, however, when an artificial factor such as a jetty is employed. The waves may increase their heights by clashing at the jetty, develop their disturbance by the interference of reflecting waves, and further run along the length of the jetty and concentrate near its root, finally giving rise to a flow away

from the jetty. The bed materials, disturbed by breakers, may be carried as littoral drift and cause erosion. On the lee-side of the jetty waves may undergo refraction as well, as diffraction and cause a seaward flow along the jetty which is essentially related to erosion and accretion of sand in the beach area. Any artificial interference in a natural condition may cause an unbalance of the existing equilibrium and either erosion or accretion - at best local - may result. My research has attempted to clarify the fundamental aspects of this phenomenon and contribute to minimizing the damage resulting from the construction of coastal jetties.

2. Experimental equipment and procedures

The wave basin used in the experiment was 7 m long, 2.5 m wide, and 0.4 m deep and was equipped at one end with a flutter-type wave generator which could be operated with a desired period and amplitude. At the other end of the basin was built a board model beach of 1/10 slope with its toe perpendicular to the wave orthogonals. The depth of water was kept at 25 cm and the waves had periods varying between 0.5 and 0.9 seconds. The converted deep-water steepness, δ_0 , ranged between 0.03 and 0.10.

The jetty was simulated by a board placed vertically in varying directions and lengths from the shoreline (Figure 1). However, the variety of the cases was restricted due to the lack of space. The flow velocities were measured by paper floats and averaged to obtain representative values.

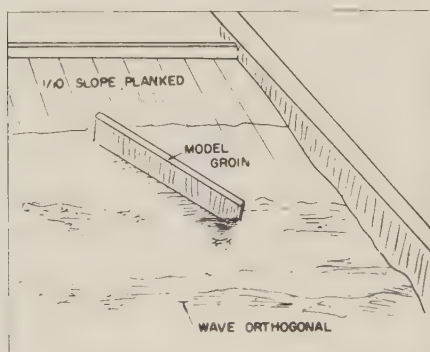


Fig - 1

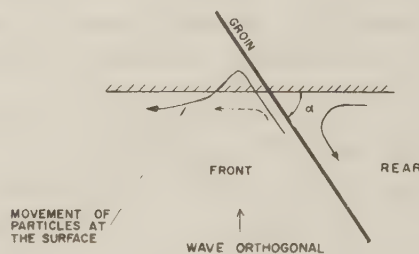


Fig - 2

3. Observations

Remarkable differences were observed between the two sides of the jetty (Figure 2).

On the front side the oncoming waves struck the jetty wall and reflected, causing interference with subsequent waves and, as a result, strong local disturbances. The waves were also found to run along the jetty, break, and concentrate toward the root of the jetty in a state of turbulent flow. The manner of breaking and plunging of the waves varied sharply according to the direction of the jetty, i. e. the

angle between the jetty and the shoreline, α , as well as to the characteristics of the coming waves. The accounts for the influence of reflecting waves. The breakers at the side of the jetty were considerably higher than those without a jetty, regardless of its direction. Figure 3 shows that the breaker heights also increase rapidly as the angle decreases. For α less than about 45° the breaking resembled that of a jumping wave, and there was significant disturbance on the bottom. After breaking, the surface layer of the wave mass ran along the jetty far beyond the shoreline and then receded. The bottom layer was turned in the direction of the alongshores flow as shown by the dotted curve in Figure 2. No change was observed in the position of the breaker line. Before breaking, the wave mass near the jetty was found to move in a direction parallel to the jetty, but the influence of the jetty was weakened as the distance from it was increased, and the wave mass tended to move in a direction perpendicular to the shoreline. However, this wave mass was abruptly turned at the breaker line in the direction of the alongshore flow, demonstrating the extensive influence of the jetty. A fairly steady alongshore flow was observed in the surf zone, its velocity was greater near the shoreline than near the breaker line.

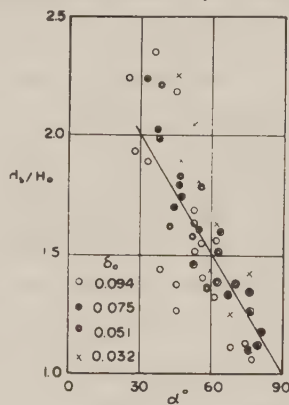


Fig - 3

On the lee-side of the jetty wave diffraction was clearly observed and, strictly speaking, it accompanied a refraction. Here the flow was directed toward the jetty and then ran seaward along it at a greater velocity. Near the root of the jetty was observed an almost fixed dead-water zone beside a disturbance caused by the interference of waves and flow. The diffraction was complicated because of the flow directed against oncoming waves. The breaker line was also not as simple as that on the front side of the jetty. It was imagined that a flow away from the jetty or a movement of a water mass oscillating perpendicularly to the shoreline ought to exist beyond the jetty, but this could not be confirmed because of the limitation in the beach length available, Eddies and zones were found near the tip of the jetty.

The general movement of beach material may be estimated on the basis of the above observations. On the front side of the jetty the disturbances in the bed materials near the breaker line may also be varied according to the direction of the jetty as well as the characteristics of the waves. The beach adjoining the root of the jetty may be washed by the running-up of the surface portion of the wave mass; the range of washing in the vicinity of the root of the jetty may largely depend on the wave steepness, but the influence of the jetty direction

must not be overlooked. An example is shown in Figure 4 where R_d denotes the elevation above the still-water level for the jetty direction α . The bed materials, disturbed by breakers, may be carried by the along-shore flow either along the bottom or in suspension. Consequently, without compensating beach materials supplied from some other location, erosion may occur. On the lee-side of the jetty erosion may start near the far-

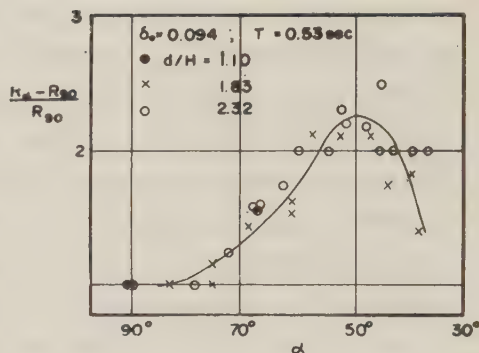


Fig - 4

thest end of the area of influence of the jetty; the eroded materials may be carried toward the root of the jetty, or further along the jetty by a rapid flow; and the scouring of the jetty foundation may also result. The materials thus eroded may be either lost in deep water or accreted near the tip of the jetty.

4. Analysis of the results

a) Characteristics of the flows on the front side of the jetty.

As described in the preceding chapter, an alongshore flow results from the waves progressing perpendicularly toward the shoreline and the jetty placed on the beach at angles smaller than 90° to the shoreline. The size of this flow is regarded as being closely related to the amount of littoral drift.

The size of the alongshore flow may depend on the angle between the jetty direction and the shoreline, α , the depth of water at the tip of the jetty, d , the beach slope, i , and the bottom roughness. Excluding the effects of viscosity and bottom roughness, the following relationship is obtained:

$$\varphi(\alpha, \delta_s, d/H_0, v/C_0, i) = 0 \dots \dots \dots (1)$$

where $\delta_s = H/L_0$ is the deep-water wave steepness, H_0 and L_0 denoting the deep-water wave height and period respectively; v/C_0 is the rate of the flow velocity to the deep-water wave celerity. We now proceed to examine the relationships between these non-dimensional factors on the basis of the experiment observations for the particular case of $i = 1/10$.

The cause of this flow is mainly attributed to the fact that the direction of the jetty does not conform with the orthogonals of oncoming waves, but it is also related to the amount of the mass transported by breakers into the surf zone. On the other hand, the waves are veered in the jetty direction, α , in the vicinity of the jetty but this effect is gradually weakened as the distance from the jetty increases. Denoting the mean volume of the mass transported by breakers progressing perpendicularly to the shoreline by Q_b , and the mean

volume of the mass which is veered in the direction α after breaking and reflecting at the jetty wall by Q_b , the following relationship between Q_b and $Q_{b,\alpha}$ may be given (Figure 5):

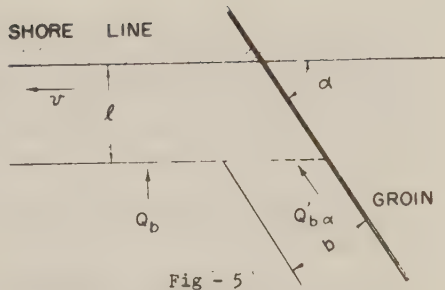


Fig - 5

$$Q_{b,\alpha} = Q_b \cdot \sin \alpha \cdot f(\alpha, d/H_0, \delta_0, i) \dots\dots(2)$$

Assuming that the effect of the jetty is confined within a distance b , i.e. that there exists a uniform flow in the direction α in the strip of width b immediately adjoining the jetty wall, we can form the equation of continuity between the flows along the jetty and the shoreline, in a channel of a triangular section in the surf zone:

$$Q_{b,\alpha} \cdot b \cdot \cos \alpha = \frac{1}{2} h_b \cdot l \cdot \rho \dots\dots\dots(3)$$

where only the alongshore component of $Q_{b,\alpha}$ has been regarded as responsible for the alongshore flow; h denotes the depth at the breaker line, h_b the width of the surf zone, i.e. the distance between the shoreline and the breaker line, and ρ the density of water.

Further, considering

$$Q_b = \frac{\rho C_b \pi}{L_b} \frac{H_b^2}{4} \coth \frac{2\pi h_b}{L_b} \dots\dots\dots(4)$$

and

$$l = h_b / i \dots\dots\dots(5)$$

we obtain

$$v = \frac{\pi}{2} C_b \left(\frac{H_b}{h_b} \right) \frac{b}{L_b} \sin \alpha \cdot \cos \alpha \cdot \coth \frac{2\pi h_b}{L_b} \cdot i \cdot f \dots\dots\dots(6)$$

where the subscript b indicates the values corresponding to the breakers. Putting $b = L_0 K'$, and $K = K' f$, and since $C_b = L_b / T_b$, $C_0 = L_0 / T_0$, and $T_b = T_0$, we obtain

$$\frac{v}{C_0} = \frac{\pi}{2} \left(\frac{H_b}{h_b} \right)^2 \sin \alpha \cdot \cos \alpha \cdot \coth \frac{2\pi h_b}{L_b} \cdot i \cdot K \dots\dots\dots(7)$$

Since $i = 1/10$, equation (7) is reduced to

$$\frac{v}{C_0} = \frac{\pi}{40} \left(\frac{H_b}{h_b} \right)^2 \sin 2\alpha \cdot \coth \frac{2\pi h_b}{L_b} \cdot K \dots\dots\dots(8)$$

In equation (8) H_b/h_b , h_b/L_b and C are determined by the deep-water characteristics, and v can be measured. K must be expressed in relation to the other factors and since it is non-dimensional, we may formulate

$$K = F(\delta_o, \alpha, d/H_o) \dots\dots\dots(9)$$

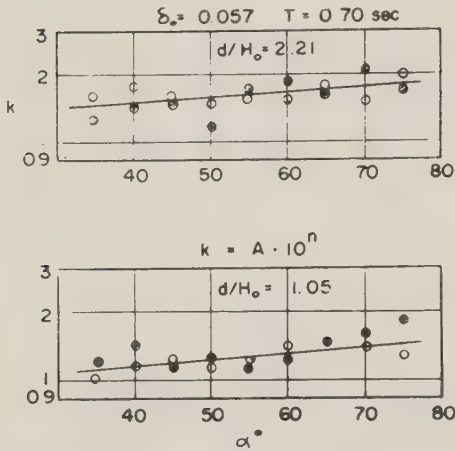


Fig - 6

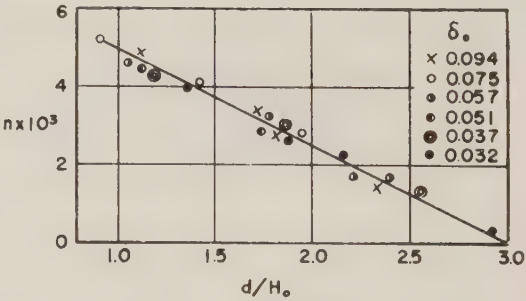


Fig - 7

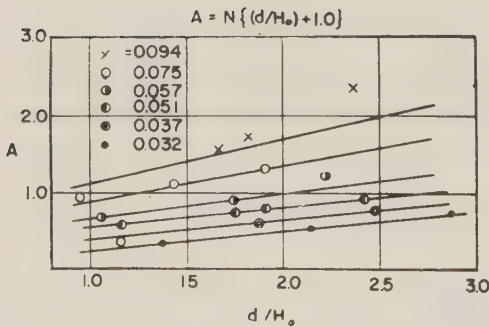


Fig - 8

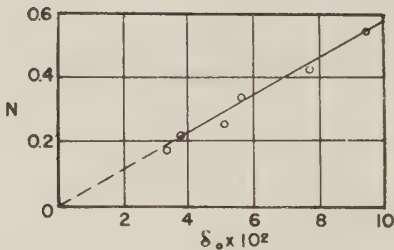


Fig - 9

Examining the value of K by the experiment data, as shown in Figures 6, 7, 8 and 9, K may be approximated by

$$K = 5.9 \delta_o \{ (d/H_o) + 1 \} \cdot e^{\frac{1}{4} \{ 3 - (d/H_o) \}} \dots\dots\dots(10)$$

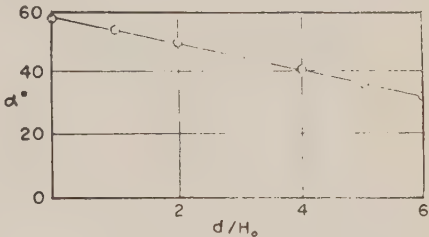
where α is expressed in radians. Therefore, equation (8) can be rewritten as

$$\frac{v}{C_o} = \frac{\pi}{40} \left(\frac{H_b}{h_b} \right)^2 \sin^2 \alpha \cdot \coth \frac{2\lambda h_b}{L_b} \left[5.9 \delta_o \left\{ \left(\frac{d}{H_o} \right) + 1 \right\} \cdot e^{\frac{1}{4} \{ 3 - (d/H_o) \}} \right] \dots\dots\dots(11)$$

Our experiment data used in examining the values of K covers the range between 0.9 and 0.3 for d/H_0 and the data for the remaining range have been extrapolated for convenience and left for a future investigation. The data for the range between 0° and 30° for α have not been determined so that equation (11) only indicates the general trend of the phenomenon in this range. The factor K must also depend on i but it does not appear in the equation because it has been replaced by $i = 1/10$. It must be pointed out that the slope of our model beach was steeper than would actually be round, and that the section of the alongshore flow is rather small. This fact must have resulted in the observation of values of flow greater than those actually expected. The effects of the beach slope should be examined by experimental procedures and for greater accuracy the bottom roughness should also be investigated.

Table - 1

d/H_0	0	1	2	3	4	5
α	57.8	53.8	49.5	45	40.5	36.2



d at $v = \max$ while δ_0 kept constant

Fig - 10

Table 1 shows the directions of the jetty for which the flow velocities attain the maximum values for each different wave; it has been diagramed in Figure 10. The values for $d/H_0 = 0, 4$, and 5 were also computed for comparison. α is about equal to 60° for $d/H_0 = 0$ and then gradually decreases with an increase of d/H_0 . Our experiment has determined that the maximum value lies between 4° and 55° . This variation of α is doubtful; it may converge to a definite value with an increase in d/H_0 . It is also doubtful that the trend found in the figure can be extended to the range $0 < d/H_0 < 1$.

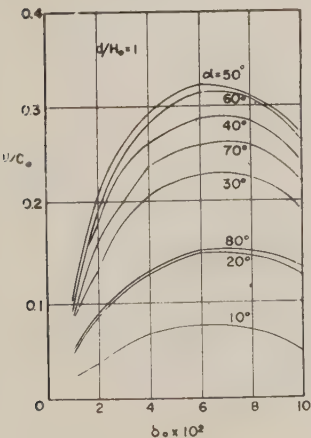


Fig - 11

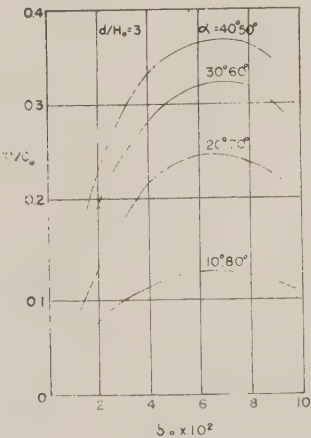


Fig - 12

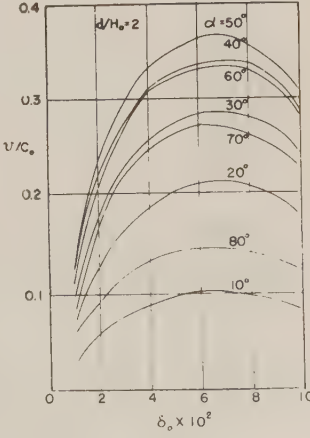


Fig - 13

Figure 11, 12 and 13 show the relationships between v/C_0 and δ_0 for three different values of d/H_0 1.0, 2.0 and 3.0 where α is given as a parameter. The angles for which v/C_0 attains the maximum values corresponding to a particular value of d/H_0 were determined in the preceding analysis, and here it was further found that v/C_0 also attains the maximum values at $\delta \doteq 0.06$ for any angle α . This appears to result from the fact that the waves of higher deep-water steepness, extremely unstable and liable to breaking, may be subject to the effects of the jetty to a lesser degree. Considering that v/C_0 tends, on the whole, to increase with an increase of d/H_0 , the maximum values of v/C_0

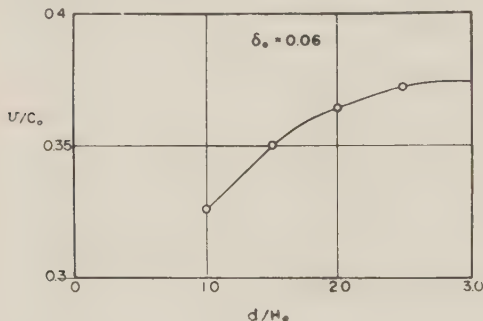


Fig - 14

have been checked in relation to each value of d/H_0 for $\delta = 0.06$, as diagramed in Figure 14. It shows that for small values of d/H_0 the increase of v/C_0 is rapid but that the increase of v/C_0 almost ceases for approximately $d/H_0 \approx 3$, signifying the existence of an asymptote. The influence of d/H_0 greater than 3 is noticeably reduced, and the wave characteristics and the angles seem to predominate instead. On the other hand, in view of the rapid increase of v/C_0 for $d/H_0 < 1$, it is estimated that the length of the jetty may be an extremely significant factor.

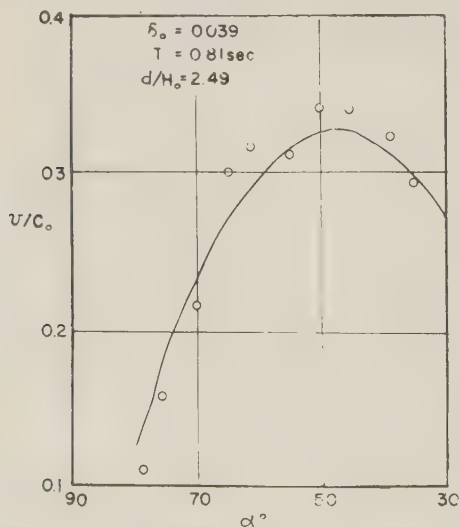


Fig - 15

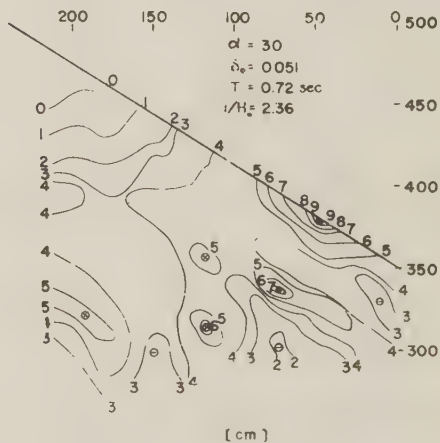


Fig - 16

Figure 15 shows a comparison between the calculated and measured value which, despite a wide scatter, seems to demonstrate the general trend.

b) Reflecting waves on the front side of the jetty.

Figure 16 shows the distribution of wave heights in the vicinity of the jetty where the zones of exceedingly large wave heights are clearly distinguished from those of small wave heights. The rate of reflection, k , has been calculated with measured values with reference to the following formula:

$$k = \frac{H_{\max} - H_{\min}}{H_{\max} + H_{\min}} \dots\dots\dots(12)$$

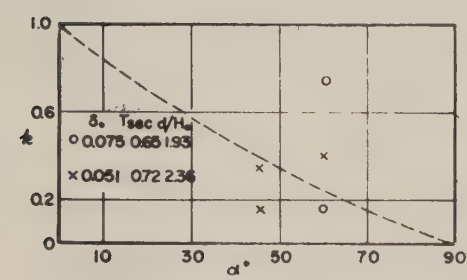


Fig - 17

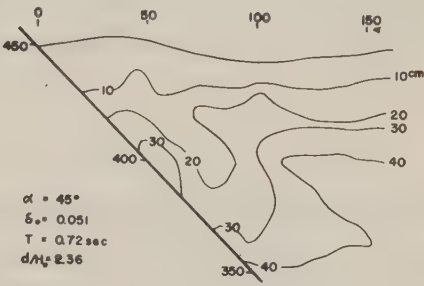


Fig - 18

Figure 17 shows the relationship between k and α . Nothing definite could be derived from this diagram; the assumed trend is given by the dotted curve. Further investigation is needed on this problem.

c) Flows and wave-height distribution on the lee-side of the jetty.

The flows and wave-height distribution constitute the most outstanding aspects of the lee-side of the jetty. The lee-side of a breakwater is generally protected from the direct impact of waves but is not completely free from wave disturbances caused by diffraction. A number of studies are available on the problem of diffraction in the constant-depth basin, but not much has been done for the case of varying depth. Our case is further complicated owing to the flows clashing against the progressing waves, and therefore it cannot be fully explained only by diffraction. Figure 18 gives an example of the wave height distribution.

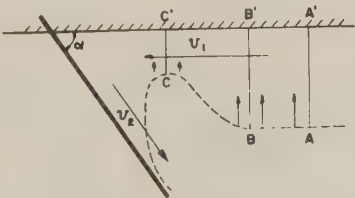


Fig - 19

We now proceed to consider the generation of flows along and toward the jetty (Figure 19). In the zone AB that is considerably removed from the jetty the waves are high and consequently the mass transport by breakers is

great; in the zone BC that is closer to the jetty the waves are small and so is the mass transport. Accordingly, the level of the zone ABB'A' generally exceeds that of the zone BB'C'C, causing an inclination of water surface and a flow, v_1 , toward the jetty. This may also give rise to a flow, v_2 , along the jetty to compensate for v_1 . Figure 20 shows the mean elevations of the zones which contain these flows, obtained by averaging the elevations of wave crests and troughs. The existence of an inclination of water surface, though not uniform, is clearly demonstrated, justifying the previous reasoning. Assuming that this inclination of water surface may be represented by I, i.e. that of the open channel, and denoting the still-water depth by h , the flow velocity v_1 may be computed by analogy to the Chézy formula for mean flow velocity:

$$v = C \sqrt{h I} \dots \dots \dots (13)$$

Considering that the degree of both disturbance and resistance is much greater for an oscillating movement than for an open channel flow, the value of C has been set at 20. The result is shown in Table 2, which indicates a fairly good agreement between the computed and measured values.

Table - 2

α	$\delta_o = 0.094$		$\delta_o = 0.075$		$\delta_o = 0.051$	
	v_{cal} (cm/s)	v_{exp} (cm/s)	v_{cal}	v_{exp}	v_{cal}	v_{exp}
45°	15.1	17.7	26.3	21.0	22.7	20.0
60°	17.4	16.3	20.0	22.3	22.9	19.2
78.7°			18.3	16.2	23.3	15.0

A quantitative analysis has been made of the generation of this water-surface inclination. Computing for the wave of $\delta_o = 0.094$ and $T = 0.53$ sec, the equi-phasic and breaker lines have been obtained as shown in Figure 21. A further computation of mass transports Q_b at the points A and B, and of the elevations at AA' and BB' leads to the following results:

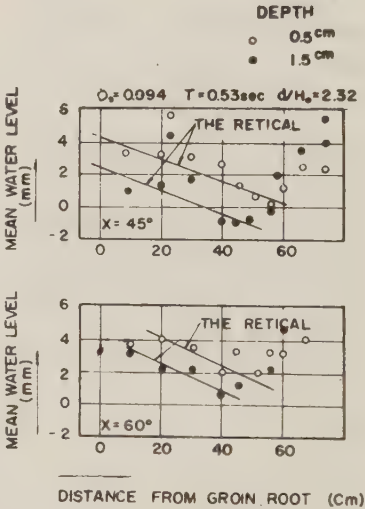


Fig - 20

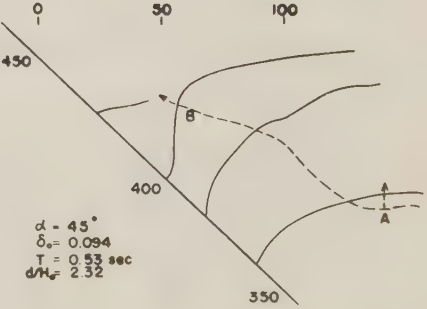


Fig - 21

per unit width at A: $42.5 \text{ cm}^2/\text{sec}$, $AA' = 55 \text{ cm}$, $H_A = 42.5/55.0 = 0.77 \text{ cm}$
 per unit width at B: $6.75 \text{ cm}^2/\text{sec}$, $BB' = 15 \text{ cm}$, $H_B = 6.75/15.0 = 0.45 \text{ cm}$

By subtraction, 3.2 mm is obtained as the difference in water levels which is nearly equal to the measured value of 3 mm. This result seems to justify the previous analysis of the generation of the inclination of water surface.

There still remain uncertainties concerning the relationships between both the size of the alongshore flow and of the seaward flow along the jetty, and the other factors. A methodical analysis has been impossible due ot lack of the necessary data; the results of the measurements are given for reference in Figure 22 which correlates v_1 and α , and in Figure 23 which correlates v_1 and v_2 thus seemingly satisfying the relationship $v_1 = v_2$.

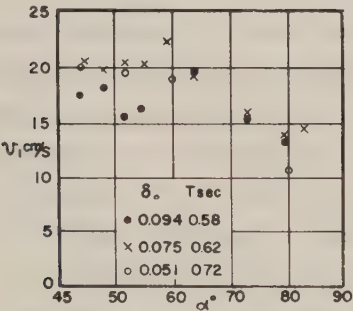


Fig - 22

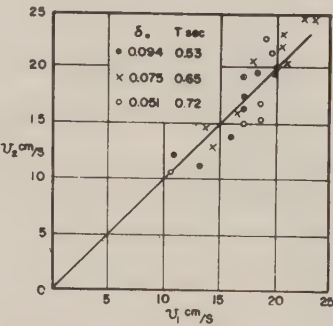


Fig - 23

The wave-height distribution has been diagramed following three different procedures:

- 1) Neglecting the water-surface inclination and assuming a uniform depth of water at the tip of the jetty, a preliminary diffraction diagram has been drawn with respect to the wave orthogonal and the direction of the jetty, as suggested By the diffraction theory.
- 2) The preliminary diagram has been modified to introduce the influence of the depth on wave heights using a formula of the small-amplitude theory:

$$H/H_0 = (h_0/h)^{1/4}.....(14)$$

Where H and h are the wave height and depth of water respectively, and $H = H_0$ for $h = h_0$. Since this formula gives an infinitely increasing wave height, the position of the breaker line has been determined by locating the intersectinh point of the values given by the small-amplitude theory and the values computed form Dr. Sato's maximum

shoaling wave height theory. For convenience the computation from the latter theory has been carried out by tracing the values from the shore-line.

- 3) The effects of the flows have been considered. The along the jetty decreases in velocity as it moves away from the jetty, and at its boundaries a progressing movement of water mass predominates. In applying a further modification to the wave heights the assumptions have been made that the flow velocity linearly decreases from the jetty side to the edge of the flow width, and that the results of Yi-Yuan Yu' research on the breaking of waves by an opposing current is applicable to our case. The width of the flow has been adopted from the values obtained from the experiments. The theoretical and experimental curves employed in this computation are shown in Figure 24.

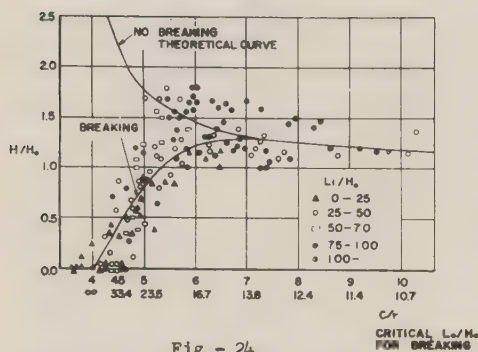


Fig - 24

An example of the above procedures is introduced for the case of $\alpha=45^\circ$, $\delta_0=0.051$, $T=0.72$ sec, $d=9.5$ cm. Figure 25 is a diagram drawn by procedures 1 and 2. In applying the modification of procedure 3, the wave celerities C at various depths are obtained first for use in computing the corresponding value of $-C/V$. According to Figure 24, the breaking occurs at $-C/V$ 4, while for $-C/V$ larger than approximately 7

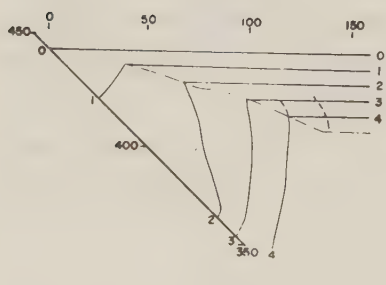


Fig - 25

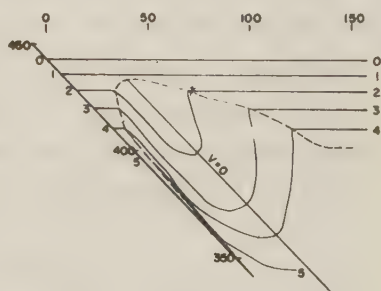


Fig - 26

the waves without breaking, undergo the variation of heights following the theoretical curve. For $-C/V$ ranging between 4 and 7 the actual curve departs from the no-breaking theoretical curve, presumably because of the partial breaking of the waves. Figure 26 has been finally obtained on the basis of the interpretations

of the above relations that the maximum shoaling wave height theory may be applicable to the cases of clear breaking, that the waves whose heights H obtained from the theoretical curve exceed the maximum shoaling wave height at the same depth may be regarded as post-breaking even for $-C/V^4$, and that the theoretical curve may be applicable to the remaining cases. Figure 26 shows a fairly good agreement with Figure 18, and seems to account for all the complications involved. According to Figure 26 the wave heights are greater near the jetty and the breaker line is more complicated than in the case of simple diffraction. Strictly speaking, the effects of refraction should have been considered but it has been omitted as negligible.

The analysis is not complete, but the unresolved uncertainties remaining will be investigated in the future.

5. Conclusions

Although handicapped by the inconveniences of the experiment conditions, some results have been obtained and they may be recapitulated as follow:

- a) The movement of beach material has been partially clarified by observation.
- b) The flows on the front side of the jetty have been found to depend largely on d/H_0 , α , and the wave characteristics. For $d/H > 3$ the effects of d/H_0 seem to be reduced, and α and the wave characteristics generally seem to exert the most significant influences. For the same wave characteristics, the velocity of the flow sharply varies according to α , and tends to attain a maximum for a larger α as d/H_0 is decreased. According to our experiments where d/H_0 lay between 0.9 and 3.0, the maximum for the flow velocity appeared for α lying between 55° and 45° .
- c) On the lee-side of the jetty, the generation of flow has been clarified. The distribution of wave heights has been found to be subject to the influences of diffraction, depth of water, and the wave-height distribution made on the basis of these considerations has explained the phenomenon fairly well.

References

- 1) Grantham, K. N. : Wave Run-up on Sloping Structures; Trans. A.G.U., Vol. 34, 1953.
- 2) Tanaka, K. : Dohatei no Suiiri "Hydraulic Characteristics of Breakwaters": Suikogaku No Saikin No Shimpo "Modern "Developments of Hydraulic Engineering," 1953.

On the Sea Waves: Technology Reports of the Osaka University, Vol. 3, No. 65. 1953.

On the Distribution of Waves in Harbor, *ibid*, Vol. 3, No. 81.

- 3) Blue, F. L. and Johnson, J. W. : Diffraction of Water Waves Passing through a Breakwater Cap; Trans. A.G.U., Vol. 30, 1950.
- 4) Johnson, J. W.: Generalized Wave Diffraction Diagrams, Coastal Engineering II, 1951.
- 5) Johnson, J. W.: Engineering Aspects of Diffraction and Refraction; Proc. of A.S.C.E., Separate No. 122, Vol. 77, 1952.
- 6) Hamada, T.: Breakers and Beach Erosions; Report of Transportation Technical Research Institute, No. 1, 1951.
- 7) Sato, S. and Kishi, T.: Experimental Study on the Height of Seawall; Journal of the Public Works Research Institute, Vol. 1, July, 1954.
- 8) Sato, S.; Kaigan Teibo No Sekkei Ni Tsuite: "On the Design of Seawall"; Kaigan Kogaku Hapuyokai Rombunshu "A Symposium of the Council of Coastal Engineering", 1954.
- 9) Yi-Yuan Yu: Breaking of Waves by an Opposing Current; Trans. A.G.U., Vol. 33, 1952.

(The same content has been published in Japanese in the 2nd Proceedings of Coastal Engineering in Japan, 1955.)

AN EXPERIMENTAL STUDY ON THE EFFECT OF COASTAL GROINS

K. HORIKAWA, Assistant Professor, University of Tokyo

C. SONU, Postgraduate Student, University of Tokyo

Introduction

Groins are widely regarded as one of the most useful means of protecting or building up beach. Essentially, they are walls of various lengths placed inside the surf zone at various distances and are more or less perpendicular to the shore line. They are expected to influence movement of littoral drift and prevent erosion. They may be built with steel sheet piles, boulders, concrete blocks, rocks, asphalt, or other materials. When classified by their function they are roughly divided into three main categories:

- a) Permeable or impermeable
- b) high or low
- c) fixed or adjustable

The impermeable groins are apt to cause erosion on the lee-side beach while a considerable accretion of beach material can be expected on the up-current beach. This is characterized by a sharp growth in the discontinuity of the shoreline on both sides of the groin. The use of permeable groins is believed to compensate for the disadvantage of impermeable groins because they facilitate the passage of accreted material from the up-current to the lee-side beach and maintain a smoothly connected shoreline. Moreover, when properly designed the permeable groins

can be built more cheaply. However, there remain uncertainties: can the permeable structures withstand the powerful shocks of storm waves; and how effectively can they detain the beach material around them to prevent it from being washed away and lost in deep water by storm waves.

As long as there is no need to check the sand at the up-stream sides of the groins, the height of the groins should be kept as low as possible so that the storm waves or waves at high tide may surpass the groins supplying beach material to the lee-side. Consequently, the lower groins may resemble permeable groins and may also be built more cheaply.

Most groins are of the fixed type. It is also reported that the so-called "adjustable groins" have been successful in England (Case and Du-Plat-Taylor).¹ Their specifications are now unavailable for us but it is supposed that the height of these groins may be "adjustable" so as to keep it at a certain value above the beach surface.

The fundamental consideration to be made in the problem of beach erosion is, primarily, to determine whether or not groins should be employed. When this decision has been made, there next arises the need to determine the desired functions, i.e., the structure of the groins. Further, the lengths, intervals, and alignment of the groins must be determined because they should work in unison. As a matter of course these procedures of groin field design must be based on an adequate knowledge of the effects of the coastal groin. In this respect American engineers have been developing a theory which suggests a criterion to anticipate a desired shoreline assumed to be perpendicular to the direction of predominant waves as a basis for groin field design. In Japan we have not yet succeeded in providing an appropriate guide for design. Dr. Nagai, of the University of Osaka City, proposes² that the groins, whose most proper length is 40% of the shoreline-to-breaker-line distance, must be aligned at an interval of three times the groin length and in a direction slightly inclined away from the dominant wave orthogonal and toward the lee-side.

We have been impressed that the existing theories on groin design, for all their outstanding successes, seem to overlook the significance of the flows influenced by the littoral current as well as by the shoaling waves. This report is not to present design formulae for groins, but intends to point out that the flow patterns in the vicinity of coastal groins are far more complicated than has generally been realized.

2. Experimental equipment and procedures

The experiments were carried out in the model basin of the Transportation Technical Research Institute, Ministry of Transportation, at Kurihama; its working section was 10 m long,

wide, and 50 cm deep. At one end of the basin was built a mortar-coated beach of 1/15 slope so that the incident wave crossed the bottom contour of the slope at 30° ; at the other end of the basin a flutter type wave generator was installed which could reciprocate around the bottom hinges. The depth of the water was kept at 30 cm in the constant-depth portion of the basin throughout the experiment. At times "Onahama" sand (150μ in mean diameter, specific gravity of 2.64) or coal slugs (mean diameter of 200μ ; specific gravity of 1.5) were used to trace the littoral drift or indicate the flow pattern.

The deep water characteristics were determined by resistance-type profile wires connected to an oscillograph recorder, the height of the shoaling waves by a bar gauge equipped with electrodes fixed 1 mm apart and connected to neon lamps, and the current velocity by a propeller-type current meter consisting of four blades 25 mm in diameter and an axis 15 mm above the bottom. The length of the groins was varied and the directions ranged from 45° to 135° against the shoreline at 15° intervals. Three different heights were used: 3 cm, 4 cm, and approximately 20 cm (denoted by ∞) which was not over-topped by any wave used in the experiment. For the runs the groins were flanked on both sides with rubble mounds; and in order to simulate a permeable groin an iron crib 5 cm thick and 10 cm high filled to a certain height with glass beads of two different diameters was used. All the model groins had the same thickness of 1.5 cm except for the iron-crib type, and were made completely water-tight by seating on sponge supports.

The waves used in the experiments were selected so as to represent three typical cases consisting of a flat wave (a gentle wave), a steep wave (a storm wave), and a medium wave.

(Table 1)

Table - 1

WAVE	H_{30}	T	λ_0	H_0	δ_0	α_0	α_b
I	1.50	1.18	216	1.64	0.0076	39	11
II	2.40	0.81	102	2.56	0.025	32	14
III	3.60	0.73	82.9	3.72	0.045	31	17

In advance of the main runs of the experiments, careful calibrations were made in order to determine the nature of fluctuations of the waves available in this basin. For each representative wave a 2-

minute record was taken of the height and period at the constant-depth water, 30 cm, and of the current velocities at the tip of the groins placed perpendicular to the shoreline, by an oscillograph recorder which was started 15 seconds after the first wave was generated. The results of

Table - 2

DURATION OF RECORDING (sec)	TYPE OF WAVE		
	I	II	III
120	—	—	—
60	—	± 0.5	± 2.6
30	± 1.8	± 0.5	—
25	—	—	± 3.6
15	± 2.5	± 2.7	—
10	—	—	± 4.5
7.5	± 10.3	± 5.1	—

Table - 3

DURATION OF RECORDING (SEC)	TYPE OF WAVE		
	I	II	III
15	± 11.3	—	—
10	± 10.2	± 3.1	± 1.4
5	—	± 5.4	—

the calibration records are given in Table II and III which show maximum deviations of flow velocities and wave heights from the mean values taken over 2 minutes. For Wave I the measured heights showed a considerable fluctuations for the first 15 seconds of recording, tended to stabilize during the succeeding 1 minute, and then finally gave way to a gradual but steady increase. This seems to result from the fact that the waves of less steepness, i.e., longer or flatter waves, have a larger rate of reflection at the slope than the waves of higher steepness. For Waves II and III no remarkable fluctuations were observed except for an almost negligible swell extending over a period of 30 seconds. An examination of the calibration records revealed that the flatter waves had more fluctuations and that precision of measurement could be improved by a longer duration of recording. It was concluded from the preceding results that the recording of wave heights and flow velocities should be taken for 10 seconds beginning 30 seconds after the first wave strikes the shoreline. The deviation in data expected from this procedure can be confined to approximately $\pm 5\%$, both for the wave heights and the flow velocities, which is satisfactory for the purposes of our experiments. The deviation of wave period data resulting from this recording procedure was about $\pm 0.5\%$ which was practically negligible. The duration of recording the flow velocities was 30 seconds using a simple ink recorder.

3. Distribution of the velocities of littoral current

We can see numerous research papers already published,^{3,4,5} treated the littoral current on a flat, uniformly sloping beach where measurements were conducted using floats of potassium permanganate grains. Most of these studies failed to give the distribution of the current velocities in the surf zone, the stretch lying between the shore and breaker lines. We employed the propellar-type current meter for this purpose. The values obtained in extremely shallow water, where the propellar blades partly protruded beyond the water surface, had to be corrected by applying modification factors found in extra calibration tests, but they seemed less

table as compared with the values which did not require modification.

Figure I shows the relationship between V and r , where:

V is the velocity of the littoral current,

r is the ratio (expressed as a percentage) of L' to L , where L' is the distance between the point of measurement and the shoreline, and L is the width of the surf zone.

mean values obtained by floats are given comparison. The general trend is for a rapid variation in velocities over the surfzone to the maximum value at $r=30\%$. The values themselves seem so large that they may not be immediately applicable to field conditions without various modifications. As a matter of fact, this is an ideal case which would not actually occur in field conditions; most natural beaches

have far more complicated bottom topographies characterized by long-shore bars, troughs and varying slopes, and fluctuations in the breaker characteristics. It is believed that these factors are interrelated and produce a distribution of littoral current velocities that is unique for every beach.

It was found in the experiments that a considerable amount of sand could be transported along the bottom at the observed velocities, the amount varying according to the location, but the sand transported in suspension by littoral drift was all but negligible probably because the waves used, generally small, were unable to produce disturbances strong enough to cause suspension of beach materials. But in field conditions, the suspended materials would constitute an important portion of the littoral drift, depending upon the deep-water wave steepness, wave energy, and properties of beach materials. It must also be pointed out that the longitudinal movement of beach materials oscillating perpendicularly to the shoreline as well as the critical limit of eroding and accreting waves must be influenced not only by beach characteristics but by the grain size of beach materials.^{6,7}

These complications, together with other numerous factors involved in surf-zone

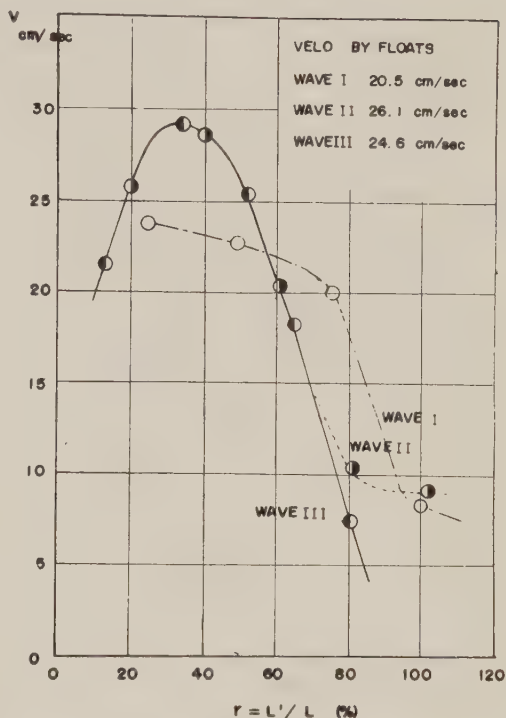


Fig - I

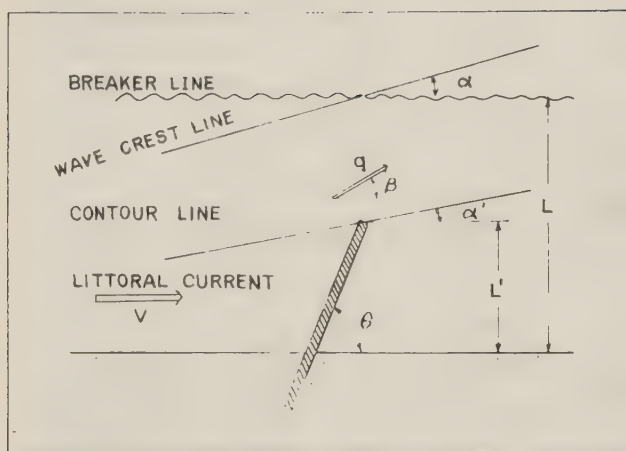


Fig — 2

toward the breaker line.

4. Velocities and directions of flow at the tips of groins

a) Single groin

Each recording of the velocities and directions of flow was taken at a point slightly (5 cm) seaward from the tip of the groin. The direction finder was a simple device consisting of a semi-circular protractor equipped with a rotating vane. An extreme fluctuation was found in the directions of flow measured with this finder; the flow deviated sharply in a direction parallel to the shoreline during the wave crests accompanying mass transport, while the flow was directed toward deep-water during the ensuing troughs. These two directions were measured and averaged to obtain mean directions, denoted by β . The current velocities, denoted by q , are given as the average of the values measured in the directions of β . Figures 3 and 4 show the results of the measurements for Wave II and the groin height ∞ . In Figure 3 the curves give a fairly clear trend correlating current directions, β , and groin lengths, denoted by $r = L'/L$ (%), provided that the precision of measurement has been strongly effected by fluctuation in flow directions. These results indicate that:

- 1) as r increases, the flow directions tend to veer more and more seaward.
- 2) there seem to exist two different types of curves represented approximately by $\beta > 90^\circ$

hydraulics, would dominantly influence the effects of coastal groins and it is to this end that our experiments are directed. This constitutes the principal difficulty of model studies on littoral drift and unless it can be overcome, the reliability of model experiments can not be improved. It therefore appears highly desirable to conduct a measurement of the characteristics of littoral current in the field for a considerably longer duration, at several fixed distances from the shoreline

and $\theta < 90^\circ$; the trend of variation differs on both sides of θ coinciding with the direction of oncoming waves; for $\theta > 90^\circ$ a remarkable increase of β occurs with the increase of r until the flow is directed against the littoral current, while for $\theta < 90^\circ$ the relationship of β and r is not as clear.

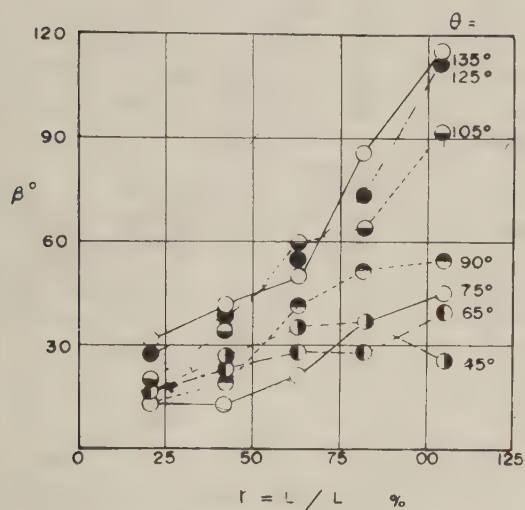


Fig - 3

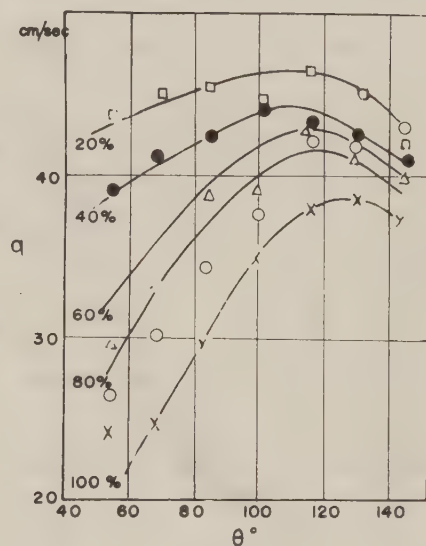


Fig - 4

According to Figure 4, which relates flow velocities and θ , an increase in groin length companies a decrease in flow velocities and for each groin length the velocity reaches a maximum between $\theta=100^\circ$ and 130° .

Figures 5 and 6 show the results of the preceding analysis for the two components of flow velocities, denoted by v and u , perpendicular or parallel to the shoreline, respectively. The perpendicular component, v , attains a maximum at approximately $r = 75\%$ and between $\theta=100^\circ$ and 130° . For a larger θ , the component v shows a greater variation with respect to r . On the other hand, the parallel component u rapidly decrease as θ increases but is less than 90° , and for $\theta > 90^\circ$ the trend is reversed.

The observations made above were found to apply also to the other cases of different types of waves, groin heights, and structures.

Now, by correlating flow directions for the three different types of waves (I, II, and III) with groin heights (3cm, 4 cm, and ∞) with θ , it was found that the values are densely scattered around straight lines drawn through the middle of the plotted points, and that β increases as groin heights are decreases, i.e., in the descending order of ∞ , 4 cm, and 3 cm,

probably because the overtopping water may cause a head of water on both sides of the groins accelerating the seaward flow on the lee-side.

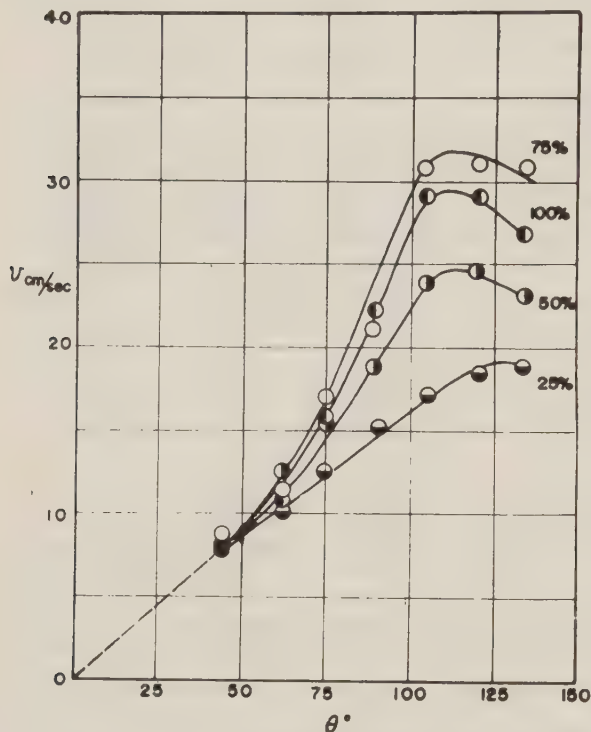


Fig - 5

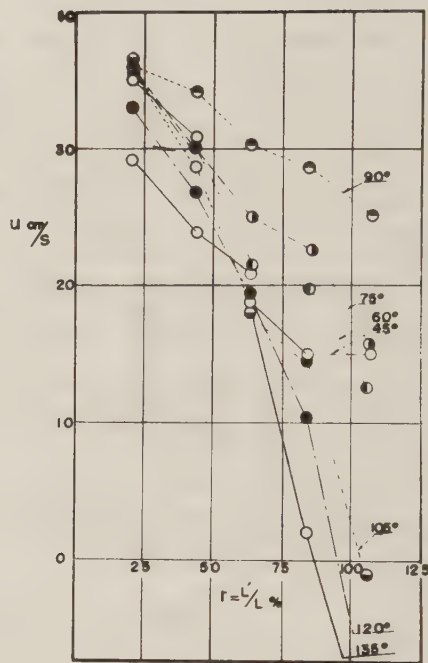


Fig - 6

Comparing the influences of groin structures, i.e., of permeable, impermeable, and rubble-flanked tubes of equal height, 4 cm, over the flow directions, little or no distinction was found to exist between them except that β became very slightly larger for permeable, rubble-flanked, and impermeable groins in the order named. An example is shown in Figures 7 (a) and (b) for the case $\theta = 90^\circ$, where a thick straight line may be added to represent the general, mean trend of the plotted points. By checking the tangents of the straight lines, n , for each value of θ , n was found to be correlated with θ in the manner shown in figure 8 and, consequently, in figure 9. These results confirm that r may be regarded as a representative factor of wave characteristics, and further that β depends upon r and θ .

The different flow-velocity trends in relation to r were found for the case of Wave II and $\theta = 90^\circ$, as shown in Figure 10, one for impermeable groins (denoted by A) and the other for rubble-flanked groins (denoted by B). It was found that rubble-flanked or permeable groins

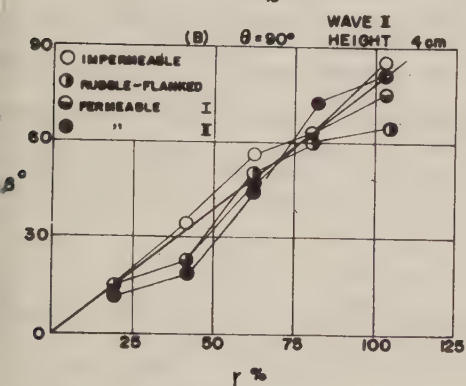
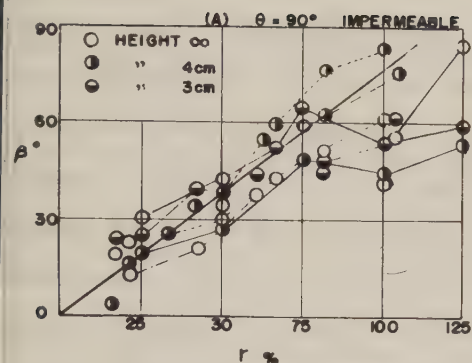


Fig - 7

slightly more effective in impeding flows at tips than impermeable groins, and that this became outstanding with an increase in r , though the effects of the surf-zone geometry consisting of r and α seemed more pronounced than those of the groin structures. On the other hand, rubble groins seemed to correspond to smaller velocities but this was not conclusive because of the disturbances resulting from reflection and overtopping of oncoming waves. The influences of groin structures may be regarded as secondary, however.

Figure 11 is a non-dimensional expression of velocities designed to further clarify the effects of wave characteristics for impermeable groins or height ∞ . The mean value, V , of the

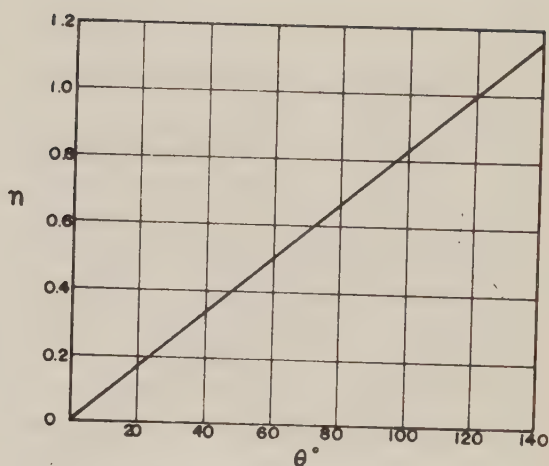


Fig - 8

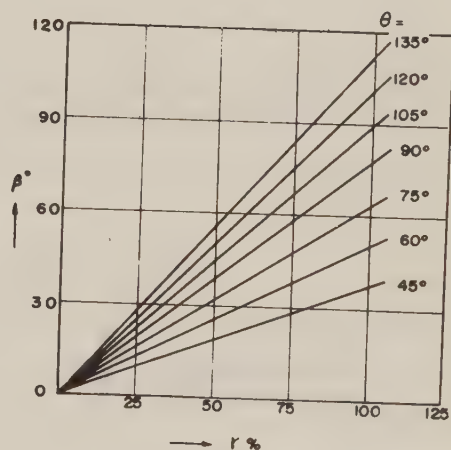


Fig - 9

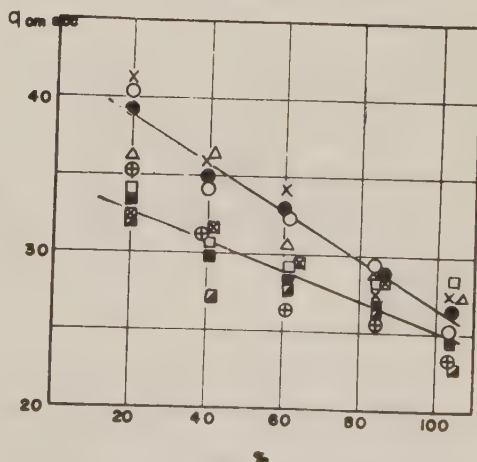


Fig - 10

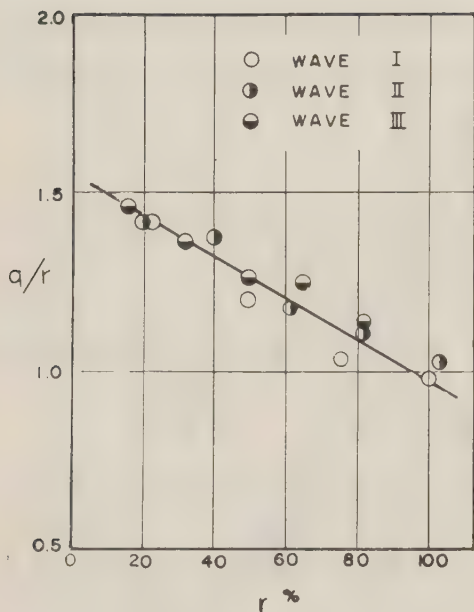


Fig — 11

current velocities measured by floats had to be adopted as the basis for non-dimensional expression, q/V , since the other existing formulae of longshore current velocities seemed to involve uncertainties. Figure 11, in which non-dimensional flow velocities, q/V , are plotted against r in relation to θ , shows a good concentration of points along a straight line. As θ increases from 45° to 135° , the tangent of the line gradually decreases and all the lines coverage at $r = 20\%$ trend was found for permeable groins.

b) Two groins

Independent groins are not fully effective unless they are deployed in numbers and in proper alignment. Because of the lack in beach length available in the experiment basin, the

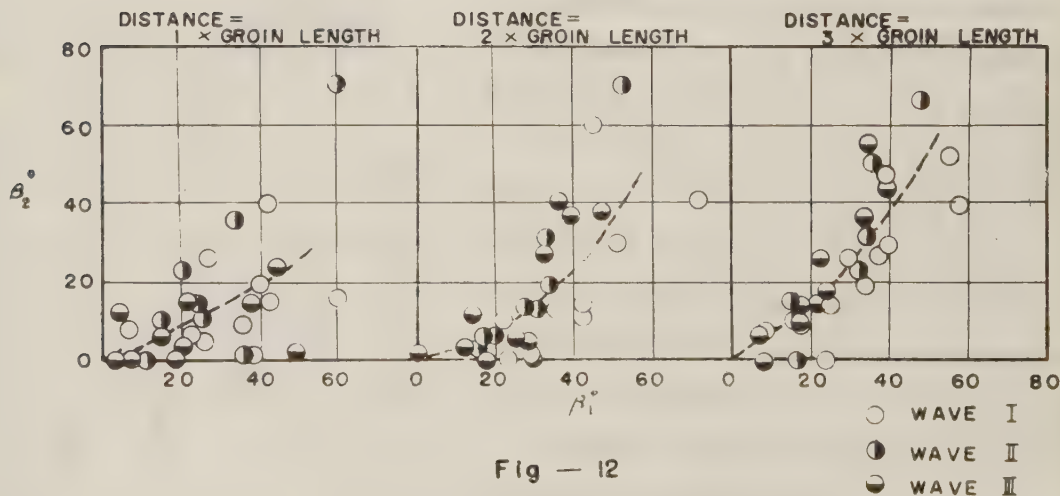


Fig — 12

distance between the two groins was confined to three times the groin length. Figure 12 shows a comparison of flow directions at the two groin tips for the groin distances of one, two, and three times the groin length, where the Suffix 1 and 2 denote the upstream and downstream

ns respectively.

the scatter is considerable but it may be generally described:

- (1) $\beta_1 > \beta_2$
- (2) With and increase in groin distance, β_1 and β_2 tend to converge. It has been a widely accepted theory that the distance of groins should not be decreased below a certain limit, as might be the case in river groins, because the groin-tip flows may be directed more and more seaward with an increase in groin length. but the result of our experiment seems to conflict with this theory, in fact, the widening of groin distance reduced mutual interference between the groins, resulting in the convergence of β_1 and β_2 .

Figure 13 shows the relationship between the velocity ratio q_2/q_1 and groin length r . Flow velocities at the tip of downcurrent groin are considerably lower than those of the upcurrent groin, particularly for a larger value of r . Consequently, the velocities for the downcurrent groin would not be likely to return to those of a single groin until the two groins are separated far enough. It must also be added that the values of β_1 and β_2 are approximately equal to those of single groin.

Characteristics of flows and sand movement in the vicinity of groins.

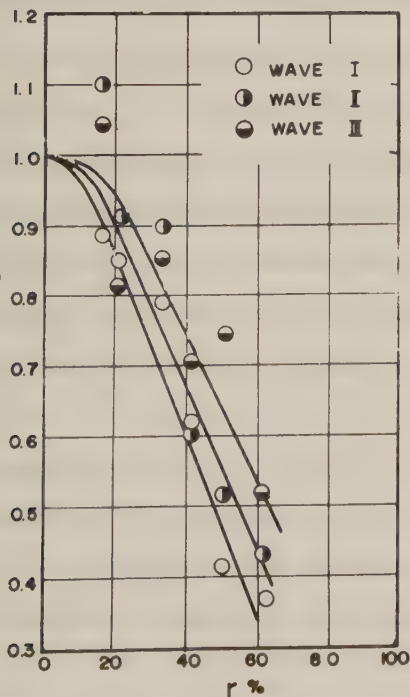


Fig-13

The sloping beach of the experiment basin was covered in uniform thickness with sand or coal slugs and redistribution of these materials was sketched after the waves washed the beach for 30 minutes.

In considering the relationship between the littoral drift and the effect of coastal groins, the first factor to be considered must be the movement of beach materials along the bottom or in suspension, which is immediately influenced by littoral current and flows resulting from the existence of groins. Waves may come as the next problem to be considered. They constitute the ultimate cause of littoral current and flows, set bed materials in a state liable to suspension by

turbulent action of breakers, and are also related to the change of beach topographies due to shore-ward and sea-ward movements of beach materials. Accordingly waves must be considered as the cumulative effect of all these factors, where also lies, as previously pointed out, the main difficulty of model studies on littoral drift. As a matter of fact, the results of our experimental studies could hardly be called final, but they would only give findings obtained with due reflection to the preceding considerations.

According to the results made clear in the experiments, it is stated in common to all three types of waves used;

a) The effects of groins on the littoral current were relatively lessened by a smaller r . Complicated local changes in bottom topography took place but most characteristic was the appearance of an approximately continuous trough lying in front of the tips of the two groins. The longshore bars were curved near the groin tips due to the flows veered seaward by the groins.

b) The trough disappeared when r was generally greater than 40%. The flow near the tip of the upstream groin was diffused and decelerated, consequently dispersing the bed materials in a wide range. This range of dispersion extended, for a small groin distance, beyond the down-current groin, but remained between the groins for approximately $r = 50\%$ and the groin distance equal to twice the groin length.

c) A very complicated pattern of flows was observed to occur in the inter-groin field when separated beyond a certain amount. This flow pattern was found to consist of a circulating flow directed against the littoral current near the downcurrent groin, and of a zigzagging flow following a catenary slightly shoreward of the groin tips. The latter could be observed with the aid of coal slugs which tended to gather in this flow and were carried in the direction of the littoral current. This must have come to exist as a result of mutual interference of shoreward and seaward flows running out of the inter-groin field, and would probably prevent sand drift from reaching the shore.

d) Remarkable scouring was observed at the groin tips. This was not so severe, however, at the downcurrent groin where the velocity of the groin-tip flow was comparatively low (Figure 13). Scouring took place also along the groin sides which were directly exposed to rushing waves, and at the groin roots which were washed by concentrating waves. The damage of scouring at the sides and roots of groins varied with β .

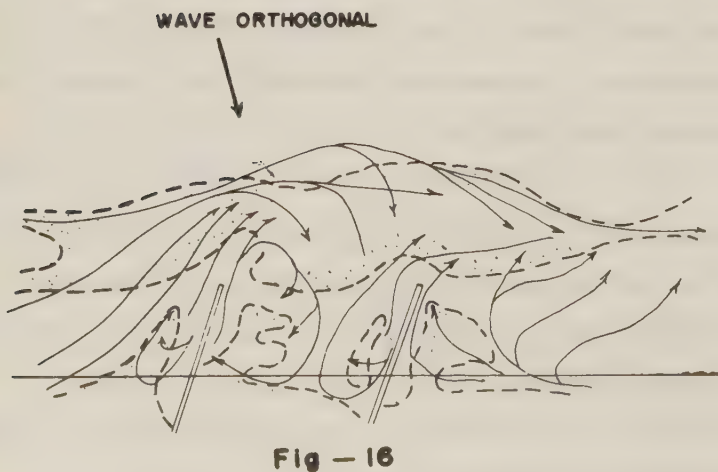
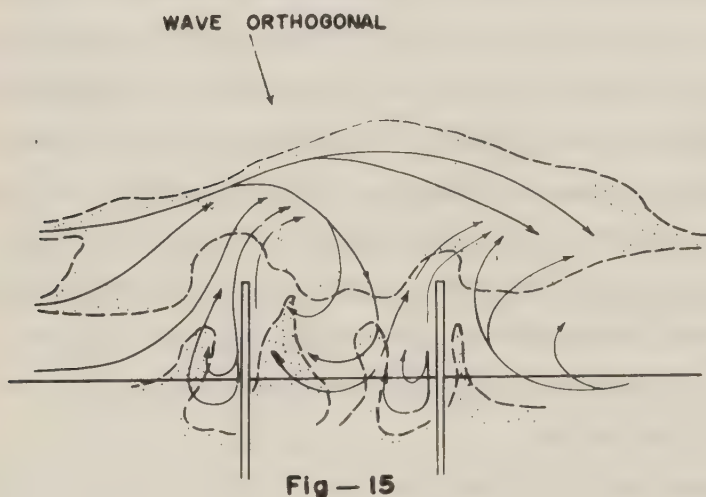
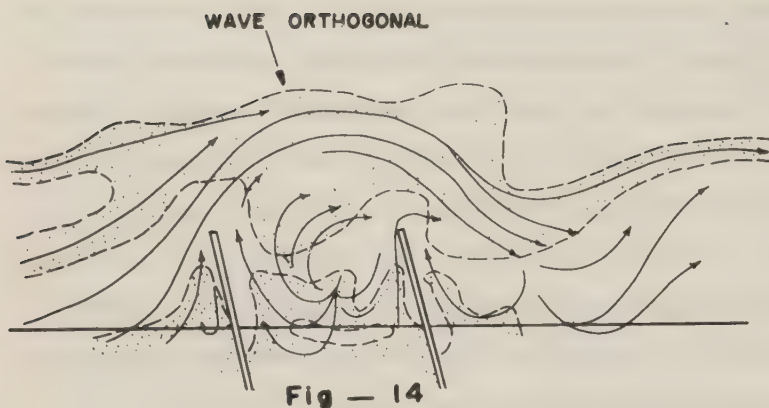
The results of the experiments led us to conclude that it would be far more realistic to

on the contributions by flatter waves which would push up sand and nourish the beach, and water overtopping the groins which would accompany a part of the sand accreted on the up-beach beach, than to expect the littoral current to transport sand drift in the inter-groin field. It would unlikely to prevent the beach from being eroded by steep storm waves, but the use of groins may alleviate the erosion to such an extent that the eroded materials could be retained within a certain distance of the beach to be carried back again by the flatter waves. As a consequence, the groin length, r , should not be too small nor too large lest the seaward transport of beach materials (Figure 5) and the groin-tip scouring by breakers be increased. The most desirable range of r is considered, therefore, to lie between 40 and 60 %.

It is true that groins, when separated too far, act only independently, exposing the inter-groin field to the damaging effects of waves, and that undesirable flows therefore result, accompanying movements of sand. It is also true that the groin distance must not be arbitrarily increased for the beach materials which were carried seaward can hardly return to the inter-groin field. Moreover, groins, when placed too close, would only act as independent groins and result in increasing the construction cost. Accordingly, the most desirable groin distance must lie between these two extremes. The results of our experiments proved that this distance is related to groin length and that a larger groin length generally allows a decreased groin distance.⁸ A groin distance of three times the groin length is more desirable than one equal to the groin length although the former is a little excessive.

The effects of groins were further examined by comparing their directions at $\phi = 75^\circ, 90^\circ, 105^\circ$. The examples are given in Figures 14, 15, and 16 which show the flow patterns in the vicinity of the groins separated twice their length, for the case of Wave III, $r = 50\%$, and the three different values of groin direction, ϕ . The phenomenon was observed with the use of sand and coal slugs, but it must be noted that their redistribution, as shown in the figures, does not necessarily represent the actual pattern of a deformed beach. For $\phi = 105^\circ$, where the waves strike the beach unimpeded, the velocities of groin-tip flows were found to be considerably higher, and the probability of erosion in rough weather seemed inevitable. Further, the rate of sand accretion by flat waves, i.e., calm weather waves, seemed lower than in the other two cases of 90° and 75° , the following facts were observed:

1) Scouring at the groin tips as well as along the groin sides was more noticeable at $\phi = 75^\circ$, presumably due to strikes by waves and to accelerated flows along the groins.



- b) The upcurrent sides near the groin roots were washed by concentrating waves more severely at $\theta = 75^\circ$. This shows the possibility of scouring there in rough weather.
- c) When judged by the rate of accretion in calm weather, $\theta = 90^\circ$ seemed preferable, but $\theta = 75^\circ$ showed less possibility of erosion in rough weather.

Since groins are subject to strong influences not only by flows but by waves, their directions should not coincide with those of the oncoming waves. However, owing to the complications involved, the most adequate values of θ cannot be simply determined.

Although our examination of the effects of groin structures were far from comprehensive, the

observations made in the experiments agreed with the general concept that permeable groins could be credited, principally, for their effectiveness in building up a well-aligned beach. It was further observed that rubble-flanked or permeable groins are superior to impermeable groins in accelerating flows and also in impeding the rushing waves along the groin sides. However, the advantage of rubble-flanked or permeable structures must not be accepted without due consideration. In fact, the rubbles, which proved so effective against flows and waves, were rapidly scattered at the groin tips by flows and waves. In order to make coastal groins fully effective and feasible, this type of structural difficulty must also be overcome.

Conclusions

It was strongly felt throughout this research that without field surveys laboratory study could only partly contribute to an advancement in our knowledge of the effects of coastal groins, more particularly, the problems concerning littoral drift. The coastal groins involve far more complicated factors than the river groins because they are influenced by the inseparable relations of flows and waves. Our knowledge of river groins should not be simply translated to the problems of coastal groins, nor should the influences of waves be under-emphasized.

We have avoided attempting to draw any hasty conclusions from this laboratory research with the thought that our knowledge, enriched by this research, should be tested under actual field conditions.

Acknowledgements

We wish to express our appreciation to Prof. T. Shimano and Prof. M. Homma, University of Tokyo, for their valuable advice and suggestions during this research. Dr. T. Hamada, Harbor Engineering Department of the Transportation Technical Research Institute, kindly provided us with the experiment basin and other conveniences and joined discussion on the problems involved in this research.

We are also deeply indebted to Dr. R. Schwantes, Asia Foundation, and Mr. Russel, Geography Survey, U. S. Army, for assistance in obtaining reference materials. We extend our thanks to N. C. Lees for invaluable assistance in obtaining reference materials and preparing the manuscript.

References

Shore Protection Planning and Design; Beach Erosion Board, Technical Report No. 4, 1954.

Nagai, S.: Arrangement of Groins on a Sandy Beach: Journal of the Waterways and Harbors Division, ASCE, Vol. 82, No. WWE, Sept. 1956.

- 3) Putnam, J.A., Munk, W. H., & Traylor, M.A.: The Prediction of Longshore Current; Trans. Am. Geophy. Union, vol. 30, No. 3, June, 1949.
- 4) Shepard, F.P. & Inman, D.L.: Nearshore Circulation; Prod. of 1st Conference of Coastal Engineering, Chap. 5.
- 5) Inman, D.L. & Quinn, W.H.: Currents in the Surf Zone, Proc. of 3rd Conference of Coastal Engineering, Chap. 3.
- 6) Hayami, K.: Saiha No Kiko (II) "On the characteristics of Breakers" Proc. of 2nd conference of Coastal Engineering of Japan, 1955.
- 7) Rector, R.L.: Laboratory Study of Equilibrium Profiles of Beaches: Beach Erosion Board, Technical Memorandum, No. 41, August 1954.
- 8) Horikawa, K.: Kaigan Susei No Koka "On the Effects of Coastal Groins", Presented at Annual Convention of J.S.C.E., 1956.

Experimental Study on the Equilibrium Slopes of Beaches and Sand Movement by Breaker

Y. Iwagaki, Dr. Eng., Kyoto University
T. Sawaragi, " "

Synopsis In this paper, the basic research of the equilibrium slope of beach and the sand movement by wave actions, contributive to the establishment of dynamics in beach process, is treated.

The effects of sands in grain size and the characteristics of incoming waves on the equilibrium beach were made clear by the experimental research at the Hydraulics Laboratory, Kyoto University and the field observations at the Sen-nan coast and the Amino coast, Japan.

1. Introduction

Before the thorough investigation of beach process as the combined feature of physics of waves and beach materials is attempted, the basic problems like the equilibrium slope of beach and the mechanism of sand movement due to breaker must be solved.

It is of common observation that the definite beach profile, assumed to be substantially in a state of equilibrium, has been reached by attacking of incoming waves of constant characteristics. And it is a significant problem that it makes unclear whether the natural beach has the substantial equilibrium slope or not.

Since J. W. Johnson¹⁾(1949) published the experimental results concerning the equilibrium slope of beaches, the systematic experimental research projects of large scale on the equilibrium slope were conducted at the Beach Erosion Board²⁾.

It may be, however, said that there are still few engineering attempts to study the clear formulation of the dynamic significance on the equilibrium slope and the relationship between the equilibrium slope and the beach erosion phenomena. Furthermore, the future development of this study is confronted with an analytical difficulty because of the complexity of the dynamics of breaker and the physics of sediment transport.

The establishment of the relationship between the dynamics of sand transportation and the characteristics of waves, the relation between the movement of beach material and the resulted variations in

bottom elevation, the effect of grain size of beach material on the variation of bottom elevation and the critical water depth for sediment transportation, defined as the depth where the rate of transportation of sands will be suddenly changed, are considered as the first step contributive to the further progress of beach process in coastal engineering.

In this paper, at first, the experimental results on the equilibrium slope of beach in cases of the beach material with size frequency curves shown in Fig. 1 are compared with the experimental results of University of California and natural beach profiles observed by authors at the Sen-nan coast in Osaka Prefecture and the Amino coast in Kyoto Prefecture.

Furthermore, the distributions of rate of on- and offshore transportations of sand due to wave actions, the behaviours of bottom variation of beach, and the change of distributions of rate in the process of approach to the equilibrium profile of beach are presented.

Finally, the relationship between the critical water depth for sediment transportation and the characteristics of waves is explained.

2. Experimental Equipment and Procedure

(1) Experimental Equipment

The experimentation was conducted in a concrete tank with a visible side wall of glass and lucite, which is 11 m long, 0.5 m wide, and 1.3 m deep, at the Hydraulics Laboratory, Kyoto University.

This tank was used by setting the wooden slab in 0.9 m deep and the test section was divided into 4.9 m horizontal part and 4.0 m sloping part, (1 : 10), and the sloping slab was covered by sand of uniform grain size in 10 cm thickness.

Waves were produced by the flutter type of wave generator which had a 1/4 HP motor and a non-step control machine for speed. Wave heights were controlled by changing the length of arm of the variable scoop, and the wave periods were adjusted through the control of speed of the machine.

For trapping sands transported by the

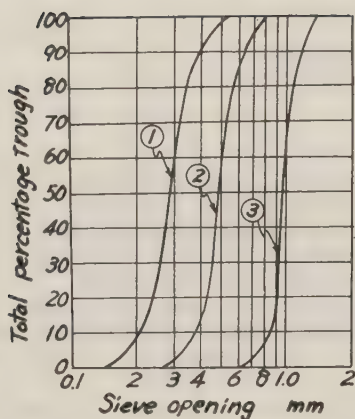


Fig. 1 Sieve analysis curves of used sands

action of incoming waves, lucite rectangular conduits of 3 cm x 5 cm in area were placed in zigzag along the center line of channel bed (Fig. 2 (a)).

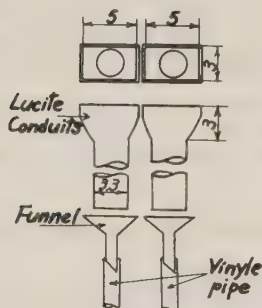


Fig. 2 (a) Collecting equipments transported sediment

The transported sands were dropped from these rectangular entrances and collected by the funnels and led out of the tank with water by the vinyl pipe.

16 sets of above described trapping equipments were placed at intervals of 20 cm in the onshore part and 35 - 50 cm in the offshore part for the test section of 5 m from the shoreline. Each set is composed of two conduits to obtain separately continuous records of transported sands by the up- and backrushes.

Fig. 2 (b) indicates the locations of arrangements of these conduits. Three different sizes of sands were used for performing the present program, and the medium diameters of sands were 0.30, 0.52 and 1.0 mm, and similar in size to fine sands commonly found at beaches.

The characteristics of these sands are indicated graphically in Fig. 1. Their specific weights are also 2.63, 2.56 and 2.65.

(2) Procedure

The experiments on the equilibrium slope were started from the initial state of beach of 1 : 10 in slope and the records of variations of beach profiles resulted from the wave action in every one hour were measured from the side wall.

The observation of the beach profiles was continued until the beach slopes had reached stable and the maximum duration required for obtaining the equilibrium slope was about 15 hours.

For each run of experimentation, the measurement of the rate of transported sands was carried out four times at 4 hours, 7 hours, 10 hours and 15 hours after the start of operation.

(3) Characteristics of Experimental Waves

Wave heights (H_0) measured during the experimentation were ranged from 2.32 to 6.90 cm, and the wave lengths (L_0) from 78.6 to 260 cm.

The values of wave steepness measured

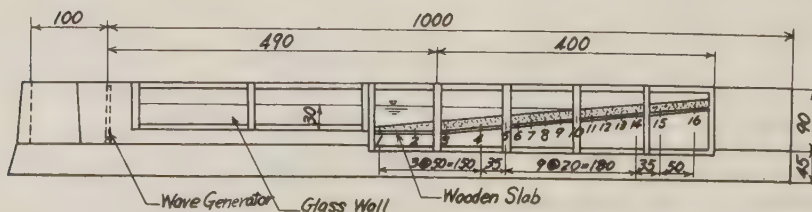


Fig. 2 (b) Side view of wave tank showing location of equipments

Table 1

Case I, $d_m = 0.30$ mm :	0.0092, 0.0185, 0.0325, 0.0328, 0.0488, 0.0594
Case II, $d_m = 0.52$ mm :	0.0092, 0.0234, 0.0331, 0.0457, 0.0498, 0.0574, 0.0680, 0.0770
Case III, $d_m = 1.00$ mm :	0.0093, 0.0250, 0.0322, 0.0426, 0.0524, 0.0534, 0.0580, 0.0815

in all runs of a series of experimentation the offshore zone.
are indicated in Table 1.

The wave length in deep water (L_0) was determined from the relationship of

$$L_0 = gT^2/2\pi,$$

and the wave period, T , was also determined by the measurement of frequency of wave generator. As the physical condition of deep water waves had not been obtained in the model tank, so the deep water wave height (H_0) was estimated from the wave height of constant depth (H) by means of the table of Wiegel.

3. Analysis of Equilibrium Slopes

The experimental beaches of initial slope 1 : 10 were gradually approached to the state of substantial equilibrium with the lapse of time.

The determination of required time of operation until the beach profile becomes stable and the observation of its process are interesting problems.

Selecting the shoreline as a reference point, Fig. 3 (a) and 3 (b) show the variation of hourly change of bottom elevation for runs of $H_0/L_0 = 0.0092 - 0.0093$ and $H_0/L_0 = 0.0574 - 0.0594$ as parametric expressions of grain size and location.

In both figures, (A) indicates the onshore zone, (B) the surf zone and (C)

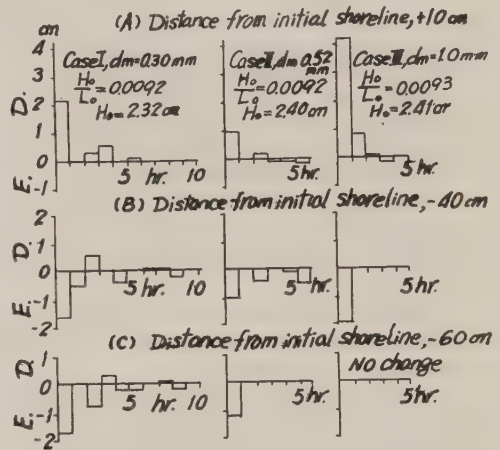


Fig. 3 (a) Variation of hourly change of bottom elevation in case of $H_0/L_0 = 0.0092 - 0.0093$ (D : Deposition, E : Erosion)

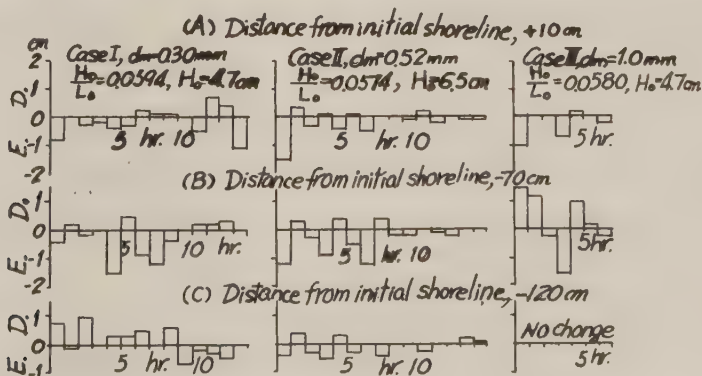


Fig. 3 (b) Variation of hourly change of bottom elevation in case of $H_0/L_0 = 0.0574 - 0.0594$ (D : Deposition, E : Erosion)

In cases of small waves of $H_0/L_0 = 0.0092 - 0.0093$, it is evidently seen the onshore zone was always deposited, and on the contrary, the surf and offshore zones were eroded, and the rate of variation of bottom elevation was gradually decreased with the lapse of time.

On the other hand, in cases of higher waves of $H_0/L_0 = 0.0574 - 0.0594$, the onshore zone was strongly eroded after the initiation of operation in experiment, and thereafter the repetitions of deposition erosion in the process of variation of beach were observed, while the distinguished tendency in the bottom variation has not been observed at the surf zone.

In case II, however, it should be noticed that two zones of (B) and (C) were located off the breaking point due to the generation of higher waves than in cases of I and III.

These results⁵⁾ coincide well with the experimental results on the variation of beach by T. Hamada^{3), 4)}.

It is also understood from Fig. 3 that the duration time of wave action until the beach slopes reached stable, becomes shorter for smaller steepness and for larger size of bed material.

The dimensionless equilibrium profiles as a parametric expression of steepness for several runs of experimentation under the condition of constant bed materials are indicated in Fig. 4. In the figure, the origin of coordinate system is the shoreline and the ordinate indicates the dimensionless depth h/L_0 and the abscissa the dimensionless distance x/L_0 , and L_0 the wave length of incoming wave in deep water.

It is also observed from Fig. 4 that a sand ridge is formed at some distance from the shoreline under the action of higher waves of greater steepness than 0.03, and it is not developed for waves of less steepness.

To explain the effect of grain size of sands on the equilibrium profiles for various grain sizes of sands are shown in Fig. 5. In the figure, furthermore, these profiles are compared with the experimental result of Johnson.

Evidently in inspection of Fig. 5, in case of experiment for less steepness, the beach profiles for different sizes of sands are commonly similar but with some local differences in shape (in case III, the sand moving area is restricted very narrow, and the beach profile is distorted, compared with the other cases of I and II).

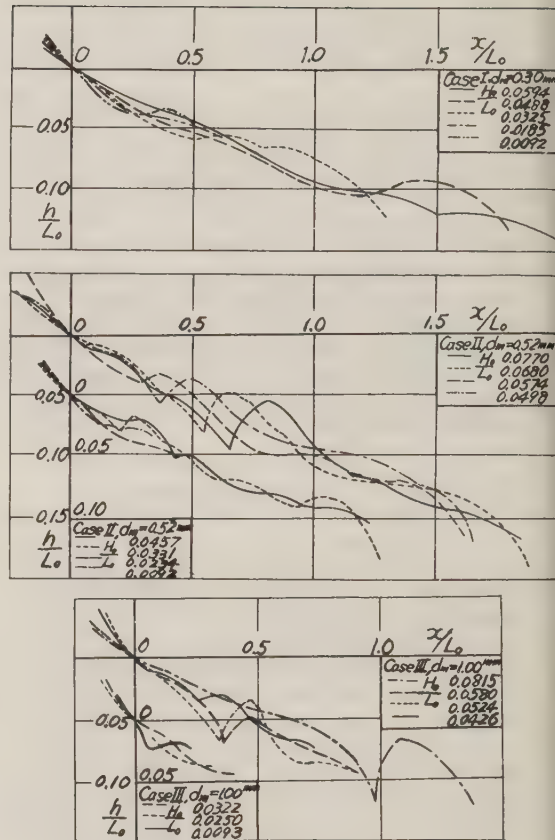


Fig. 4 Dimensionless representation of equilibrium profiles of beach

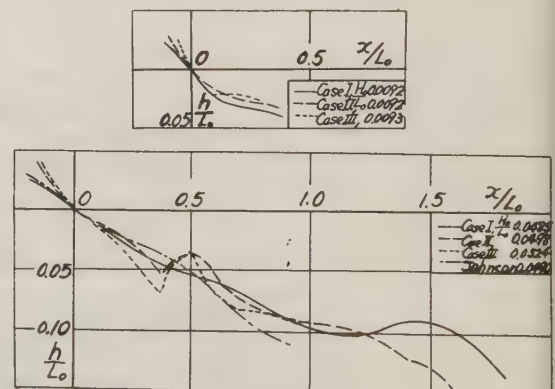


Fig. 5 Effects of grain sizes of beach sand on equilibrium profiles of beach

On the other hand, the beach profiles of waves of greater steepness is considerably similar, but the location and the shape of the longshore bar in a particular case are different from each other. These differences are supposed to be caused by the dynamic mechanism of transported materials of different sizes in grain. Fine materials will be suspended at the breaking point by the strong agitation of incoming surfer waves and easily transported even by a slow fluid velocity and a longshore bar will be formed at the breaking point. On the contrary, coarse sands will not be suspended, even by the strong action of surfer waves, and therefore they form a longshore bar in the neighbourhood of plunging point.

Fig. 6 indicates the relationships between wave steepness and foreshore slopes, which is considered to initiate a significant characteristic of equilibrium slopes.

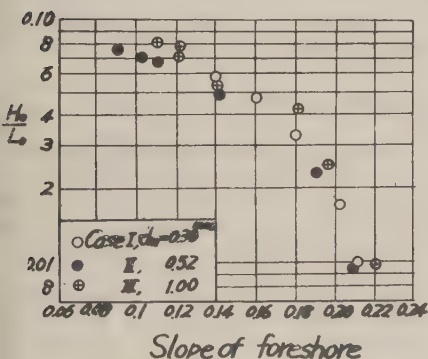


Fig. 6 Relationships between slopes of foreshore and wave steepness

As illustrated in Fig. 6, the flatter foreshore is clearly formed by higher waves of greater steepness and the effects of grain size on the foreshore of stable equilibrium is not distinguishably seen for the sedimentation of these grain sizes.

When these experimental results are applied to the natural beach influenced by both active and diffractive waves, the equivalent wave height H_0' which is multiplied by the wave height in deep water by the refractive or diffractive coefficients may be substituted as the initial wave height H_0 in Fig. 4 and Fig. 6.

When the wave height and the wave length at the breaking point are observed, the best indication of beach profiles with the relationship between h_b/L_b and x/L_b

as a parametric expression of wave steepness at the breaking point, H_b/L_b , will be obtained instead of using the above described relation between h/L_0 and x/L_0 shown in Fig. 4, in which h_b is the breaking depth.

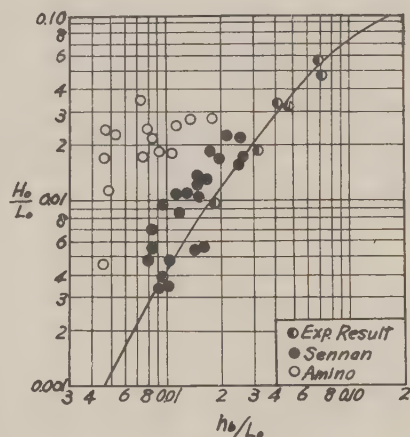


Fig. 7 (a) Relationship between dimensionless breaking depth and wave steepness in deep water by experimental results of Kyoto University and field observations at Sen-nan coast and Amoni coast

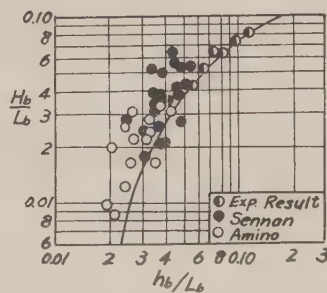


Fig. 7 (b) Behaviours of wave steepness of breakers to dimensionless breaking depth in terms of breaker characteristics

Fig. 7 (a) indicates the relationship between H_0/L_0 and h_b/L_0 from the experimental and observed results at the laboratory, Sen-nan and Amino coasts.

In Fig. 7 (a), it is seen that the observed results at the Amino coast, where the incoming waves are greatly refracted and dif-

fracted, do not coincide with the results in cases of non-diffraction and non-refraction by the expression used the characteristics of deep water.

Consequently, the results expressed in terms of the characteristics of breaking wave height H_b and breaking wave length L_b are indicated in Fig. 7 (b) and it is understood such expressions may be applied to the natural beach influenced by refractive waves.

Fig. 8 indicates the dimensionless plots of the experimental equilibrium beach in case I by the use of the expression of characteristics of breaking waves.

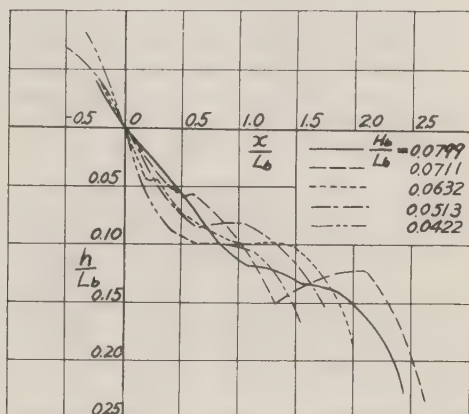
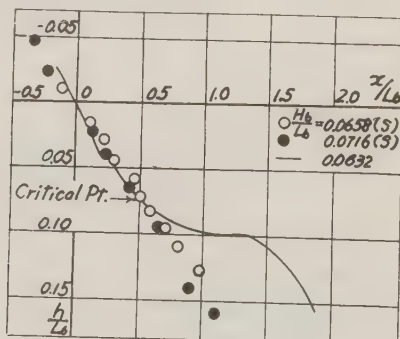
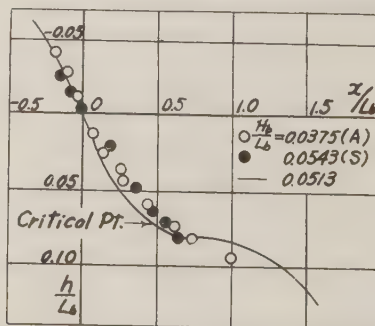


Fig. 8 Dimensionless representation of equilibrium profiles of beach by characteristics of breaker in case I

The comparison of these experimental results at the Sen-nan coast and the Amino coast are presented in Figs. 9 (a) and 9 (b).



(a)



(b)

Fig. 9 Comparison of experimental profiles of beach with natural beach profiles

It is evidently seen in these figures that these experimental profiles closely coincide with natural beach profiles in the onshore side from a certain definite depth, do not agree with natural profiles in the offshore side from that depth. The critical depth of sand movement is indicated in Fig. 9 (a) and 9 (b). As illustrated in the figures, this critical depth may be considered the boundary of limitation in agreement between the equilibrium slope resulted from experimentation and the observed profiles of natural beaches.

The difference in coastal behaviour between artificial and natural beaches will be explained as follows; owing to greater volume of bed material transported in the onshore side from the critical depth at the natural coast, the beach profile of this part remains quickly stable, while the beach profile in the offshore part from the critical point is not readily influenced, due to less volume of materials transported in this part, so it will be supposed the beach profiles of this part is still similar to the equilibrium profile for the previous incoming wave with a different steepness.

4. Sand Movement by Breakers

- (1) Distribution of rate of transported beach sands and wave steepness

Fig. 10 (a), 10 (b) and 10(c) show the distributions of onshore and offshore of transported beach sand in case I, II and III, respectively.

The distributions of transportation of beach sands have a tendency to become of similar shape. Namely, the transported sand due to flatter waves relatively concentrates in the neighbourhood of the shoreline, but the distribution of beach sands tends to a flatter shape by higher waves of greater steepness.

[S: Sennan, A: Amino]

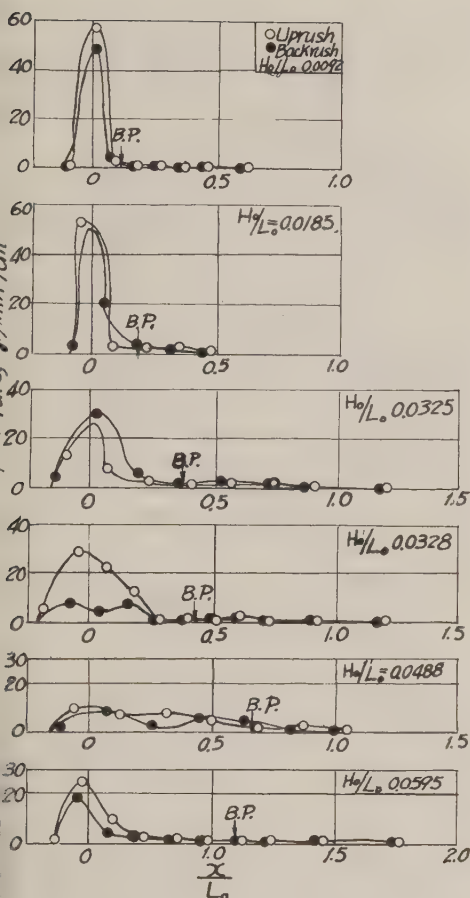


Fig. 10 (a) Distributions of on- and offshore rates of sand transportation in case I

The remarkable significance of difference in the shape of distributions for different sands in size is that two peaks in distribution of rate of sediment transportation exist for coarse sands of case II. In case II by attacking of higher waves of greater steepness than 0.03, while for fine sands in case I it does not become clear, compared with both cases of II and III. One of these two peaks situates near the shoreline except a few cases, and the other in the vicinity of the plunging point between shoreline and breaking point. As it is assumed the local distributions of velocity near the bed or the local distribution of shearing stress cause the

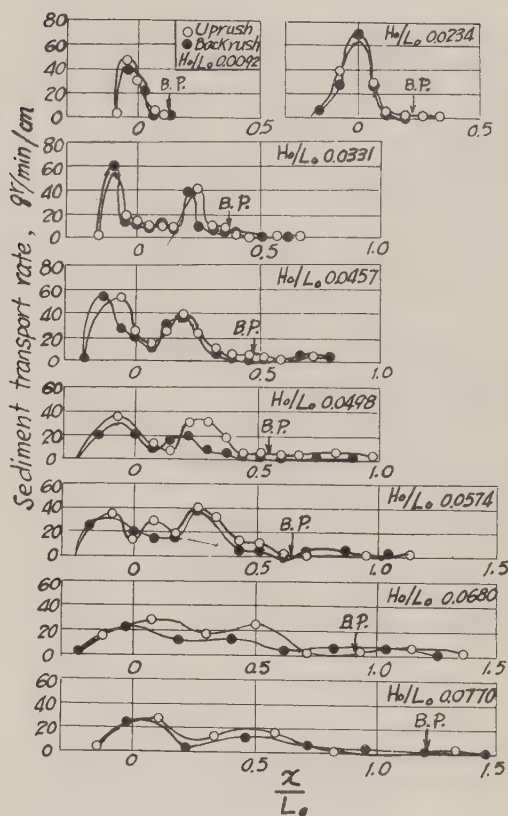


Fig. 10 (b) Distributions of on- and offshore rates of sand transportation in case II

above behaviours in beach process, so it will be of significance for the further study to establish the dynamics of wave action in coastal engineering.

Fig. 11 indicates the hourly change of distributions of rate of sediment transportation in the process of approach to the equilibrium profile of beach in the case of wave steepness, 0.0331, and grain size, 0.52 mm.

This figure indicates both changes of distributions of rate of sediment transportation by up- and backrushes.

When the beach reached the equilibrium profile of beach, the rate of sediment transportation by uprush has to coincide with that by backrush.

Evidently as shown in Fig. 11, both distributions of rate of sediment transportation are agreed.

Consequently, until the profile of beach

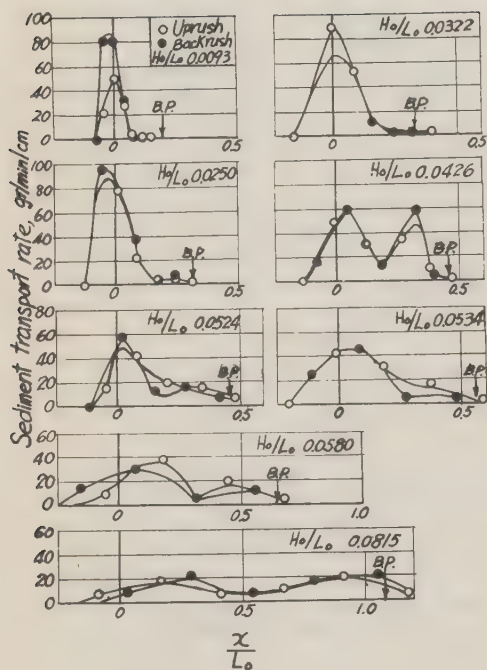


Fig. 10 (c) Distributions of on- and offshore rates of sand transportation in case III

does not reach stable, the distribution of rate of sediment transportation differs from each other, and thus three regions of erosion, deposition and equilibrium are estimated with the aid of difference in the rate of sediment transportation.

The part of oblique line in Fig. 11 shows the sediment transportation rates subtracted the sediment transportation rates by uprush by that of backrush. The positive zone indicates the transportation rates by uprush are larger than that by backrush, while in the negative zone more sands are transported by backrush than by uprush.

As the increasing part of transportation rates in the direction of incoming waves represents the zone of erosion, and the decreasing part that of deposition, so the coast is divided into two regions of erosion and deposition as shown in Fig. 11.

(2) Critical Water Depth for Sediment Transportation

The location of a remarkable decrease of sand transportation exists in the im-

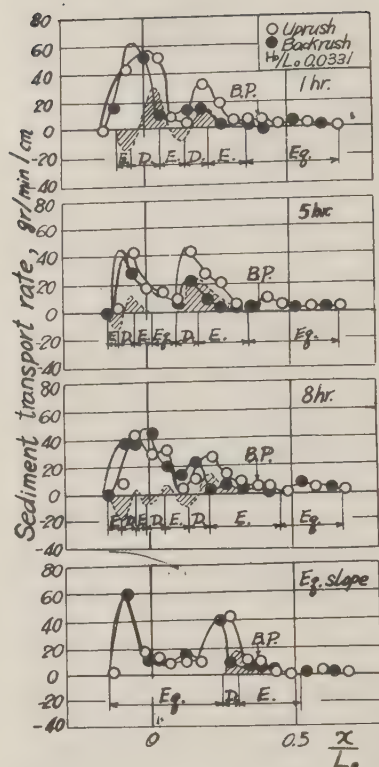


Fig. 11 Changes of distributions of rates of sediment transportations in the process of approach to equilibrium profile of beach (E_g : Equilibrium, D: Deposition, E: Erosion)

mediate vicinity of breaking point on the distribution of transportation rate, as illustrated in Fig. 10. Rate of sediment transport in the offshore region from this point become less.

Except in cases that beach sands are fine and the resulted sediments are easily transported by littoral current, the sediment transportation resulted from the turbulent action of incoming waves may not influence on the variation of the beach profile.

This point is called the critical point of sediment transportation by authors and the depth for this point is also called the critical water depth, as described in the former section.

It should be noticed that the depth is different from the depth of initiation of sand movement by shoaling waves, and of course, the

latter depth is deeper than the former.

The relationship between the critical water depth for sediment transportation and wave steepness is plotted in Fig. 12.

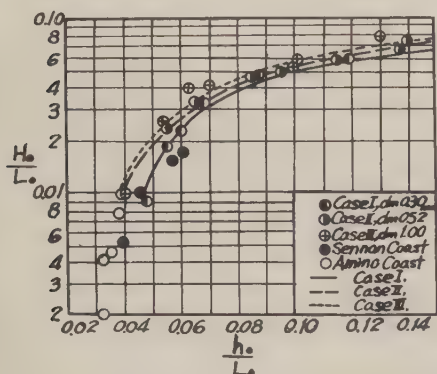


Fig. 12 Dimensionless representation of critical water depth for sediment transportation

Fig. 12 is the dimensionless representation of the critical water depth for the sediment transportation and the experimental results for three kinds of grain size and the observed results at the Sen-nan coast and the Amino coast are shown. When the natural coast influenced by the incoming refractive and diffractive waves, as at the Amino coast, the dimensionless representation of the critical water depth, as to be used in terms of the equivalent wave steepness or the characteristics of breaker, as described in the preceding section.

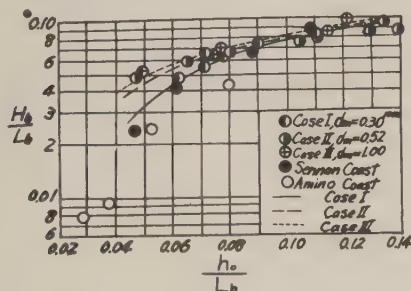


Fig. 13 Dimensionless critical water depth for sediment transportation expressed by characteristics of breaking waves

Fig. 13 indicates this critical water

depth for sediment transportation in terms of latter representation.

The observed results in natural beaches are closely agreed with the two dimensional experimental results conducted in the indoor tank.

As seen in the figure, the observed results at the Sen-nan coast approximately coincide with the experimental results in case I, but the observed results at the Amino coast is deeper in depth for the critical transportation than the other observed results and the experimental results.

It may be due to the effects of grain size, and the sediment at the Amino coast is fine sands of 0.3 mm in medium diameter, while the sediment at the Sen-nan coast is coarse sands of 2 - 3 mm in medium diameter. Consequently, it may be considered the experimental results in case I correspond with the results at the natural beaches of 2 - 3 mm in medium diameter.

Furthermore, as the curve in case I approximately corresponds with the breaker index, so it is understood the initial point of remarkable sediment transportation at natural beaches of bed material of several mm in grain size is near the breaking point, and on the contrary, at natural beaches of fine sands the critical point for sediment transportation will be far from the breaking point.

The possible way to make the clear formulation of this problem is to study the details of suspension of bed material in dynamics.

5. Conclusion

In this paper, the experimental results on the equilibrium slopes of beaches and sand movement by breaker are reported and the engineering attempts concerning the clear formulation of beach process in terms of the effects of grain size and the characteristics of waves are performed.

As the conclusion of the research program, the following statements regarding the formation of beach and sand movement are described.

a. The wave steepness is an important factor governing the variation of bottom profile and the distributions of rate of sediment transportation.

b. The location and scale of the longshore bar are influenced by the grain size of beach material.

c. The critical water depth for sediment transportation in the case I (medium size of sand is 0.30 mm) approximately coincides with the observed results at the Sen-nan coast where the beach material has the medium diameter of 2 - 3 mm.

d. The critical water depth for sediment transportation in case I approximately corre-

sponds with the breaking depth.

Furthermore, many fundamental problems to make the further development of study for the mechanism of beach erosion sure have to be solved. Concerning the present purpose of project, many experimental studies as well as observations in field, and the verification of the similarity for these results are required.

Acknowledgments

The present experimental program was performed by the financial grant of aid for fundamental scientific and cooperate research of the Ministry of Education.

The authors are very grateful to Prof. T. Ishihara who guided this research program and also greatly indebted to the devoted assistance of Messrs. Y. Suzuki, T. Kita and H. Mitsui.

References

- 1) Johnson, J. W., Scale Effects in Hydraulic Model Involving Wave Motion, Trans. AGU, Vol. 30, No. 4, Aug., 1949, pp. 517 - 525.
- 2) Rector, R. L., Laboratory Study of Equilibrium Profiles of Beaches, Beach Erosion Board, Tech. Memo., No. 41, Aug., 1954, pp. 1 - 38.
- 3) Hamada, T., Breaker and Beach Erosions, Report of Transportation Tech. Res. Inst., Report No. 1, 1951, p. 116.
- 4) Hamada, T., and Shibayama, A., Experimental Study of Breaker for Two Dimension and Beach Erosion, Report No. 3, 1951, pp. 248 - 283.
- 5) Iwagaki, Y., Beach Erosion, Proc. 1st Conf. Coastal Engg. of Japan, Nov., 1954, pp. 69 -80.

Study on Littoral Drift and Longshore Current

Yasuo Mashima.

Dr. Eng., M.J.S.C.E., Prof.

Civil Engineering Department, Defence Academy, Yokosuka, Japan.

Index.

Introduction

Littoral drift

- (a) Geology of coast
- (b) Sorting by sea water
- (c) General properties of driftsand
 - (1) Curve of size distribution
 - (2) Sand layer of coast
 - (3) Turbulence of coast seawater
 - (4) Coastal forces
- (d) Classification of littoral drift

Variation of sand size distribution curve

Relation between the littoral drift and the longshore current

Conclusion.

Introduction.

Along the coast line, there are sandy beaches, rocky beaches and cliff, and between them many river mouths. On the section of normal line on the coast line, the geology of beach and seabottom consists of the moving part due to the littoral processes and the fix part under the former part. The seaside boundary of the moving part is considered the limit of moving region of bottom sand by the coastal effects of sea water. The practical boundary is considered the contour depth of about half the wave length. The general section of sandy beach is showed in Fig.-1. Outside of this width of the section, the sands are often transported by winds on land and the suspended fine sands and mud in the sea water are transported by tidal and ocean currents and deposited on the deep sea bottom, but there are little practical effects as coast process.

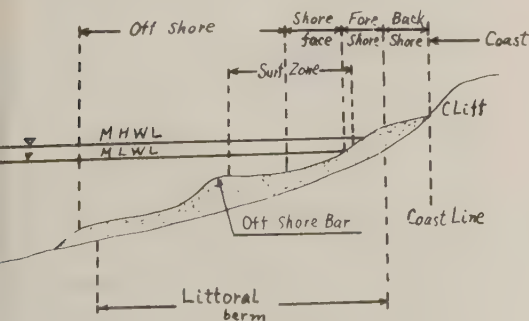


Fig.-1

Accordingly the main area where coast processes are most active is relatively narrow and very long region along the coast. A littoral drift is defined as the travelling of movable clay, sands and cobbles etc. by the flow of sea water in this region, and as the result, coast topographies remain unaltered or are eroded and deposited. In the region of littoral drift, sea water is moving and the drift is active at any time. Considering the flow in and out of movable materials in this region, there are mud and sand etc. transported by river flow suspending or sweeping which are made by erosion of the river drainage area. And the coast materials are eroded and disintegrated by the continuous actions of weather and sea water and supplied in this region. Among them, the former should be much larger in volume than the latter, for it is supplied by the erosion in larger drainage area than the narrow basic layer of the coast line. But the arrived materials by river flows are controlled by wash load and bed load, therefore their sizes and specific gravities are considerably sorted due to the effects of geology, weather, topography, slopes and discharges of rivers etc. in the district. On the other hand the eroded and disintegrated materials of coast basic layer exist there primarily and are moved and sorted by the mechanism of littoral drift, that is to say, the supply regions are cliff coast, rocky beach, and the basic layer of coast revealed by the development of coast erosion.

Then the flow out materials from the littoral drift region are the fine mud and the similar that flow out suspending in sea water and deposit in deep sea, and the deposit sand and mud in the part that could not be considered the littoral drift region after the development and stabilization of deposit.

The equilibrium between the supply and flow out of drift materials has the principal effects on the stability of coast topographies, and moreover the variation of continuous movement of sea water in the littoral region arises littoral drifts and erodes some part

or deposits on another part, and even at the same part erode or deposit occurs seasonably, then after a long period the difference of supply and decrease of materials in some scope of coast and sea bottom determines the stability of that scope.

But after the geological long time, it is considered that accompanying to the stabilization of the inland, the flowing and depositing fine materials far from the littoral drift region, increases more and more as the result of developments of the disintegration of coast debris, and accordingly forms the stable coast where the coast deposits would be consisted of larger size materials. Namely the coast will be usually transformed to the stable one where would be formed of rocky beach, cliff, cobble and stone that could not be moved resisting to the acting forces, and the sandy coast would be the intermediate transient state. Moreover, littoral drift moves not only to the normal direction of coast, but along the coast, so as long as the whole region of littoral drift area between the discontinuous points such as a cape or a head land where separate the littoral drift region will not be stable, there will be large littoral drift even on rocky beaches between any river mouth or sandy beach.

Therefore on the consideration of littoral drift about an artificial coastal work, the natural coast process should not be disturbed in order to match the intermediate state of coast development, or the incongruity of littoral drift should not be occurred by the structure and if it is occurred, the damage due to its erosion and deposit should not be grown by the precise interpretation of the littoral drift mechanism at the coast respectively, and a reasonable project and its construction.

All the coastal structures we have necessity for any purposes must be built almost in the region of littoral drift and many coast protections must be constructed where the coast erosions are discovered everywhere as the result of natural coast process. These erosion protection works must also be constructed in the littoral drift region. Consequently the interpretation of littoral drift has to study over the whole coast area and with the continuous observation data during a long time. Such structures may give some effects to the

natural coast process and to the other states subsequently, ultimately vary the condition of stabilization of the coast.

2. Littoral drift.

The littoral drift is the movement process of sand, gravel and mud etc. caused by the flow of sea water where they move suspending in sea water, sliding, rolling or with saltation on the sea bottom. Therefore they may be divided into two main parts, the suspended drift and the tractive drift.

And the movements of sea water in the narrow littoral drift region surrounding the ocean are the waves and the currents in open sea extremely complicated under the influences of coast topography, sea depth and flowing out river water. The causes of waves and currents of sea water are mainly the weather (wind, temperature), specific gravity and tides, etc., and those that arrive at the coast among them are the wind waves, swells propagated from the far wave generating area, ocean current, tidal currents, longshore currents accompanying waves, and the currents due to the vibration of sea water in a bay, etc.. They generate littoral drift by their acting forces on the coast material, so that the interpretation of drift process necessitates the properties of sand and gravel, movement of sea water, weather, ocean current, tide current and their relations, and then with the statistic data of the weather, ocean current, tidal current, seiche over the neighbouring sea, we get the statistical movements of sea water off the littoral drift region.

These movements undergo some changes by the effects of coast elements (position, topography, depth, geology, river, coast structures, etc.) on the way to the coast. Then if applying the relation of the movement of sea water and littoral drift, we calculate a statistical volume of littoral drift and the balance of moving in and out materials at the coast area, we may decide the statistical stability of the coast region by these measure and degree.

Accordingly the littoral drift is connected intimately with not only all over the coastal engineering, but also climatology, river engineering, geology, oceanography and geophysics.

The most of the preceding phenomena and their relations are not yet solved

and are on the way of enthusiastic study in many countries in the world.

In the next, I will make clear some part of the relations between littoral drift and longshore currents.

(a). Geology of Coast.

As it has been previously stated, the erosion and deposit occur as the result of littoral drift, so that the materials on sea bottom and coast consist of movable solids. These movable solids in this littoral drift region travel by the force of motion of sea water that overcomes the resistant force of stable limit and become the littoral drift. Those active forces are called Coastal forces and have their direction.

The coast materials are classified by their resisting force of travel as follows:

1. Rock (igneous rock, aqueous rock, etc.)
----Rocky beach, Rocky cliff.
2. Cobble and gravel-----Gravel beach.
3. Sand-----Sandy beach.
4. Clay, silt, etc.-----Muddy beach.

At the contact surface of these beach to sea water receive the above described coastal forces. The resistance of sand to move concerns with its size, specific gravity, form and surface roughness, especially the role of size and specific gravity are important. Specific gravity varies in a pretty range due to its original rock, so that one of the smallest is about 1.1 for volcanic gravel which is much mixed in the coast sand at FUNKA Bay and IBURI Coast in HOKKAIDO, Japan.

Now assume the sand as a sphere and its diameter including its specific gravity, form and surface roughness as an equivalent diameter d_t or d_t' which indicates the degree of stability.

At suspension; $k_1 \frac{\pi d^2}{4} = k_1' \frac{\pi d_t^2}{4}$ $d_t = \left(\frac{k_1}{k_1'} \right)^{\frac{1}{2}} d$ (1)

At tractive state;

$$\frac{k_1 \frac{\pi d^2}{4}}{k_2 \frac{\pi d^3}{6} (\rho - \rho_0)} = \frac{k_1' \frac{\pi d_t^2}{4}}{k_2' \frac{\pi d_t^3}{6} (\rho' - \rho_0)}$$

$$d_t = \frac{k_1 k_2}{k_1' k_2'} \frac{\rho - \rho_0}{\rho' - \rho_0} a \text{ ---- (2)}$$

where k_1 : Coefficient concerning the form of sand

k_2 : Coefficient concerning the surface roughness

ρ : Density of standard sand

ρ_0 : Density of sea water

k_1' : Form coefficient as a sphere

k_2' : Surface roughness coefficient of standard sand

ρ' : Density of the sand.

the density does not concern with the

horizontal movement of sand in suspension, but concerns with ascending, settling or traction on sea bottom.

For example, volcanic gravel;

$$d_t = \frac{1.1 - 1.03}{2.7 - 1.03} d \approx 0.42 d$$

it is very movable and has larger volume. And flat form sands are very suspendable for its large k_1 and more movable in comparison of these size. Thus if the diameter indicates the stability of sand, above stated classification of coast may be considered the one by the size of diameter. At rocky beaches, the surfaces of rocks are gradually eroded by the forces of water movements and movements of sand and gravel forced by the water flow. This process is named the rock erosion of the sea. By this action, rocks are gradually broken from their weakest parts and smashed to fine sizes so that they can be expressed the source of sands and gravels. Then the sand and gravel collide and rub each other by the water movement, so that the gravels are broken to sand and sand to more fine particle and then to clay. In the same manner, mud, sand and gravels flowed down in rivers are broken to smaller particles at the coast. That is to say, coast materials are moved and broken by the motion of sea water. So that there must exist all sizes from larger rocks to smaller clay on coast. But the sea water travels in very wide ranges and the strength of movement varies by times and places, and in addition the stability of the sand and gravels are not uniform, so that by the constant coastal forces the particle smaller than some sizes will suspend or move and one larger than the other size will rest in their places. As such the so-called sortings take place perpetually.

The size distribution of usual coast materials has generally some uniform tendency and are possible to be classified as previously mentioned. This fact shows that the average state of the movement of the coast sea water may have some approximately uniform coastal forces. Moreover the coast materials are really moving in suspension or traction. Therefore it is clear that the stability of coasts depends on the balance between the flow in and out of coast material and the erosion and deposition may be occurred whenever the balance is broken.

There are sometimes the case that the protection works for coast erosion damages must be constructed abruptly where the coast is hitherto about stable for long time. These cases seem to be that the accumulation of slight continuous erosion for long time attracts our attention or some coast structures have been constructed in the neighbourhood or the extraordinary storm might break the balance of the coast.

(b) Sorting by sea water.

The size distribution curve of the coast materials shows that the materials of some size range are most and the weight of larger or smaller sizes abruptly decrease. The movement of sea water causes this results. Now if assume l_c the largest diameter among which can be moved by the velocity V only, the larger sizes than l_c cannot be supplied to the point from the other. The larger one than l_c that exist previously in this point remains as before. The smaller one than l_c will be wholly removed, for the ratio of active force to resistance, such as $k_1 d(\rho - \rho_0)$ from (2) in tractive state, is larger for smaller diameter. If the sands are not at all supplied there, all smaller size than l_c are lost there and the smallest size remains there is l_c . And when the smaller sizes flow in there from upper reaches constantly, all size volume does not vary in suspension and traction.

But because of the variation of travelling velocity due to the state, the travelling volumes are not constant according to each state or size. In addition, the smaller size than l_c are travelling in turbulent motion, so if V suddenly become smaller, the larger size will rest more quickly than smaller one and l_c for smaller V will become small. When the volumes of flow in and out are balanced, that is, V does not change, neither erosion nor accretion will occur respectively if V become larger or smaller. Namely there is a critical diameter to rest in response to each V and if V change to V_2 , the size between l_1 and l_2 will begin to move or rest. If we suppose that at the coast, all sorts of size are supplied from the source of sand and gravel, and transported due to the movement of sea water and the beaches are formed, there must be the smallest velocity that can move the largest size l_{max} among the sand at one place and it must be the largest velocity in that place. (Of course it is assumed that there is sufficient large sizes at sources.)

med that there is sufficient large sizes at sources.)

However the specific gravity, the shape etc. of sand are converted to an equivalent diameter and the effects by topography, slope etc. are assumed to be uniform. And the velocity is the resultant of the velocities in all movements of sea water as waves, longshore currents, tidal currents and breaker etc. in same time.

By the previously described thought, next relation is considered,

$$l_c = f(V) \quad \dots\dots(3a)$$

If V is uniform,

$$l_c = f(S) \quad \dots\dots(3b)$$

S = other factor excepting V .

When V will change from V_2 to V_1 , the equivalent diameter will change from l_c to l_{c1} consequently, and its range will be $l_{c2} - l_{c1} = f(V_2) - f(V_1)$, so that variation of V could be estimated by the change of equivalent diameters. (Fig.-2)

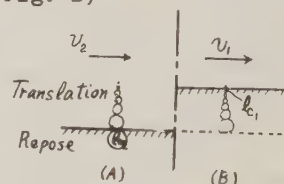


Fig.-2

And if V diminishes from V_2 to V_1 , from the sizes smaller than l_{c2} to l_{c1} , the larger will deposit more quickly and the smaller than l_{c1} , will not deposit and continue to move. So in this transition part, the size distribution curve of deposit will have some tendency. For example in Fig.-2 B part, the sizes smaller than l_{c2} to l_{c1} , will deposit in the situation that the largest will be at upper stream and lower layer, and smaller sizes at lower stream of B part.

The direction and velocity of sea water vary at times and places, and such sorting will be performed according to every variation. Near coast, the turbulence occurred by breakers will suspend more finer particles more easily. If the turbulence varies, one time suspended particles may settle instantly and may suspend at other time again. Suspended particles will move with sea water velocity. Now if V represents the movement velocity including the turbulence and minimum size that is

for U in a tractive state is l_{tc} , particles smaller than l_{tc} will end.

Generally $l_{tc} < l_c \dots \dots \dots (4)$ and l_{tc} will become larger when v increases and smaller when U decreases. the velocity will decrease from U_2 to U_1 , l_{tc2} will decrease to l_{tc1} , and particles between them will settle in tractive state on the sea bottom then the particles between l_{c2} and l_{c1} will rest.

the next relation $l_{tc} = f_t(v) \dots (5)$ be estimated, the range

$$l_{tc2} - l_{tc1} = f_t(v_2) - f_t(v_1) \dots \dots (6)$$

indicate the variation of the flow circumstances. As showing in Fig.-3, U arises from (A) to (B), the sizes of tractive particles and suspended particles shall be very nearly equal according to their sizes in the form turbulence state and larger particles shall be situated at lower layer. the velocity and the direction at this situation according to the size is necessarily uniform, the particles will be sorted and deposit at every direction, and the size distribution in littoral drift will display discontinuities.

General properties of drift sand.

(1) Size distribution curve.

the movement characteristics of water is almost uniform, and its direction and velocity distribution is clear, the volumes of transportation, accretion and erosion shall be estimated to some extent by the calculation using the sorting processes described in preceding article and the size distribution curve of the source. However there is few clear and simple relation like this and the movement characteristics, and consequently the littoral drift will change from time to time as the resultant results during a long period, erosion, accretion or stable state will produce in a region, and the size distribution curve at a certain place in some region is affected by innumerable various factors to some range of size and is estimated as to match the most effective results. The size distribution curve will display consequently on Log-probability law.

assume $F(y)$ to be a distribution function for $y = \log_e l$,

$$\log_e l = \sum_{n=0}^{\infty} \log_e l_n \dots (7)$$

$$F(y) = \frac{1}{\sqrt{2\pi} \sigma_y} e^{-\frac{(y-\bar{y})^2}{2\sigma_y^2}} \dots (8)$$

where σ_y is the standard deviation of $y = \log_e l$
 \bar{y} is the mean value of $\log_e l$.

Fig.-4 is the size distribution curve of the sample at the fore shore surface of TOMAKOMAI sandy beach, Hokkaido which shows approximately to maintain the preceding relation.

The range of this size distribution curve, mean size, its distribution and standard deviation, etc. shall depend on the neighbouring sand through the

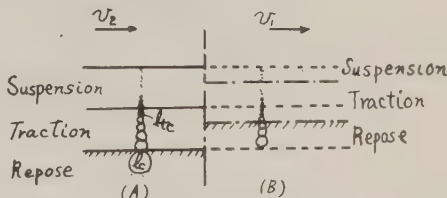


Fig.-3

movement of sea water and the variation of these items should come from the effects of many processes, especially depend on the principal elements of the movement of sea water.

It is considered that the principal elements of the movement of sea water are wave heights, wave steepness, velocity of longshore currents, near shore currents, tidal current, water depth, sea bottom slope, roughness of sea bottom, and topography of sea bottom, etc., though they should be selected to fit every situation in the littoral drift.

(2) Sand layer of coast.

It is considered that the sand layer depth disturbed by the maximum movement of sea water in a certain period will be approximately constant. This thickness is assumed D_s . D_s will be vary corresponding to the degree of movement.

If the sand particles in the volume of depth D_s and unit area are disturbed, finer particles will be suspended and larger particles will rest on the surface of the layer and more layer ones under the surface and so on, so that the distribution of the sand will correspond to the velocities at every situation and be transported in suspension or traction.

Moreover the finer particles under D_s may be moved by the permeating water and

TOMAKOMAI Coast, Aug. 1955.

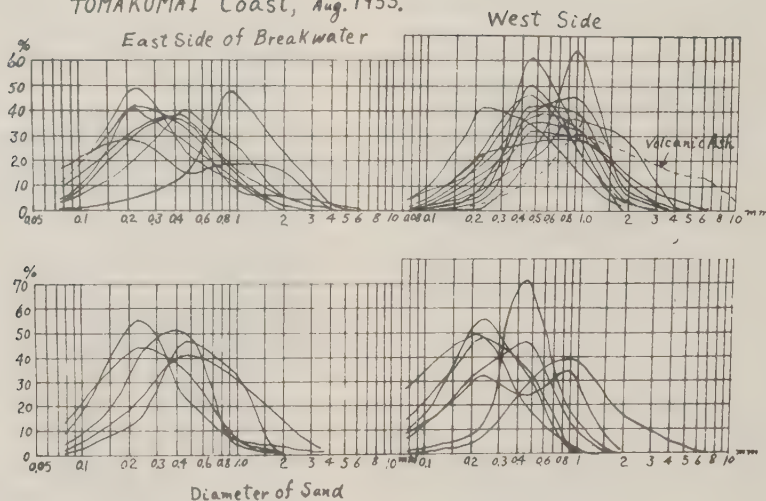


Fig.- 4

appear to the surface. When the water movement continues a long time, suspended particle will be lost from the D_s layer, and the moving particles in traction will also flow out as long as there are supplied from upper reaches, then D_s will be penetrate to lower layer, and the particle P_c which cannot be moved in traction will be remained in the thickness D_s , so the thickness of larger particles than P_c will be grown up and the penetration of D_s to lower layer will be over when there is no particle movable by the disturbances. If the tractive particles will be supplied from the neighbouring region, D_s does not penetrate to lower layer and stay at about the initial situation.

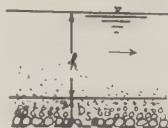


Fig.- 5

Large particles under surface can be considered the resistible part to erosions. If the geology at the existing coast does not contain such larger particles, for example when a groin as coast protection is constructed on the coast where supplied sand hitherto, the erosion will advance to the part where the movement of sea water is weak. As this transformation demand some time lapse, for the larger sand stability, it will be more slower, but the erosion by the extraordinary violent storms may be very rapid.

Next the accretion may occur mainly when the movement of sea water become mild and where is more sand supplied than flew out, or the flew out sands are intercepted by some coast obstruction, only supplied from upper reaches. But the path of sand is not always same in suspension and traction, and the size distribution varies by the intensity of movement of water, so that at some time, finer particles may deposit or at other time coarser may do, and suspended sand may deposit or traction sand may do. Anyhow deposited sands form generally some stratification corresponding with the movement of water. The most sensitive part to erosion and accretion is the surface of D_s , so we should examine the vertical section of sand layer in the case when we consider a long period variation.

The velocity of D_s penetration may relate to the storm duration time and advance and retreat of coast line. Moreover in the case of accretion on the gentle region, the proportion of finer particles will increase with time as the travelling velocity of finer particles is usually larger than that of coarser. The accretion material in a calm harbour may be so fine clayey materials that explain the fact that the covering effects of breakwater have been sufficient, but it should be noted that the coarser material does not necessarily flow in

harbour.

(3) Turbulence of coast sea water. It causes that sand-particles suspended in water at coast are not only the driving force due to the horizontal velocity along the sea bottom, but the turbulent motion by breakers, especially at the breaker line, the beach and the region between these two. Many observations have ever shown that the turbulence diffuses and moves the sea bottom materials. But though the volume and sizes of suspended materials are provided principally by breakers, their travel is at the velocity of coastal current. Namely for estimation of suspended volume and sizes, the velocity and condition of breakers should be considered at the situation of the littoral drift patterns. Such suspended drift sands can be carried along the coast or off shore by longshore currents or rip currents respectively, and they are suspended only by the turbulence of horizontal current accompanying the decrease of breaker turbulence. Therefore only finer particles will be transported away. But when the coastal region has a uniform turbulence of breaker, the sands shall be carried a long way. Johnson indicated that the circulation of wave particles increase the same character when the open sea approaches to the shore, on the contrary near the shore line, the off shore currents due to the rip current and the reflected waves are very prominent, so that the situation of their motion tends to become the situation of long-shore bars to be formed. This situation will be fixed by water depth, bottom slope, bottom materials and wave characteristics, but the position will be changed and therefore the longshore current cannot be formed when the tidal range is great or the wave characteristics are not uniform. This bar restricts the breaker position to some extent and the longshore current is received into the trough. These results promote the littoral drift of sand. Above there is a pretty difference between the surf zone and the fast side of break line and the off shore region outside. Then off shore there will be chiefly tractive drift and suspended drift due to rip current at surf zone tractive drift and other suspended drift due to longshore current and rip current will be dominant.

(4) Coastal forces.

If the forces that may act upon and move the materials what constitute the coast is defined the coastal forces, they will contain the gravity force and the forces due to the movement of sea water. When they act to urge the littoral drift, it can be said that the coastal force is strong.

Accordingly the main elements of coastal forces are

1. Current due to wave (wave current). The current caused by the mass transport of wave.

The current caused by the momentum of breaker.

2. Wave force.

Velocity difference during going and returning of water particles of waves.

Velocity difference during going and returning of water particles of breaker

3. Return current of mass transport

(Rip current)

4. Current due to the mass transport of reflective wave.

5. Gravity force on the slope of sea bottom.

6. Tidal current, the direction and velocity turn between low water and high water.

7. Ocean current, that is about steady, but varies seasonably.

8. Counter current or eddy current accompanying the main longshore current due to the topography and coastal structures (breakwater, groin, etc.)

9. Current due to beach line breaker (final breaker at plunging point), contains uprush, backwash and near shore current.

Among them, 1 and 2 act on shore in the direction between normal and parallel to the coast according to wave directions. 3, 4, and 5 have off shore forces and act in the direction normal and parallel changed by the topography or longshore bar. 6 and 7 are the characteristics of the coast itself. 8 varies according to main currents and relates essentially to the littoral drift in part. 9 acts on and off shore and relates to the cusp formation by the directions of wave and coast, and to the direct erosion and accretion at fore shore or backshore. Finally 1, 2, 3, 4 and 9 have relations to waves. 5 to the gravity on slope and the others are the characteristic of every coast.

Waves in the whole year can be approximately by the weather data and weather charts treated statistically. After estimating the longshore currents

by the waves, the direction, volume, sizes, and the season of littoral drift should be solved by the relation between them and bottom materials.

However many relations between wave, longshore current and bottom materials have been not ever solved, so that the volume of the littoral drift can not be yet concluded.

As the summarily approximate method of estimation, volume of littoral drift has been studied using the vectorial resultant of wave energy and work done, but this is not so sufficient that must more studied hereafter.

And Johnson¹³ defined an equilibrium size that does not run out of circuit of go and return motion of water particle when the depth, bottom slope and wave are constant, and indicated it by diameter only assuming the density, shape and position are constant. And then he established the following hypothesis.

(1) When slope and wave are uniform:- The equilibrium size is larger according to decreasing the depth. (For the on shore current is intensified in this case.)

(2) When depth and wave are uniform:- The equilibrium size is larger where the slope is steeper. (For as the gravity effect is larger where the slope is steeper, the same size can be pushed up higher on a flat slope.)

(3) When depth and slope are uniform:- The equilibrium size is larger as the bottom velocity decreases, that is to say, wave period or wave height decreases. (For the larger size can not be pushed up as the current velocity is weakened.)

On account of the complexities of the variation of tidal water surface, wave (shape and direction, etc.) and size distribution of sea bottom material, this hypothesis only indicates the approximate tendency and cannot yet give the quantitative estimation.

This equilibrium size may be corresponded to *etc* at the preceding 2 (b).

(d) Classification of littoral drift.

Taking above mentioned elements into consideration, the littoral drift may be classified as follows.

By the travelling state,

- (1) Suspended littoral drift
- (2) Bottom moving tractive drift
- (3) Saltation drift

By the situation,

- (1) Rip current drift or Undertow drift.
- (2) On shore drift

(3) Breaking point drift

(4) Surf zone drift

(5) Off shore drift

(6) Beach drift

Normal Beach drift

Storm beach drift

(7) Longshore drift

(8) Plunging point drift

(9) Rocky shore drift

(10) Sandy shore drift

By the special situation or state,

(1) Estuary drift

(2) Pass over drift, which is the drift passing in front of river mouth, harbour entrance or the end of groins, etc.

(3) Guided drift which travels along breakwaters, groin or jetty and is considered as a kind of longshore drift.

(4) Over splash drift which travels with over splash water at breakwater,

(5) Push up drift which is the drift sand that is pushed up on the sea wall with wave spray.

(6) Intrusion drift (or invasion drift) which enters into harbour passing through the entrance.

(7) Permeation drift which passes through the gaps of rubble mound or breakwater and deposits in harbour.

(8) In harbour drift, which is the drift that the bottom materials in harbour are moved by waves or currents.

(9) River birth drift which is transported in the sea through rivers.

(10) Scouring drift which is the movement of fine sand under the sea bottom by the permeating water in the neighbourhood of breakwater.

By the properties of drift materials,

(1) Ordinary drift (sand, gravel, etc)

(2) Special drift (volcanic ash, volcanic gravel, pumice-stone, iron sand, etc.)

(3) Clay drift, mud drift

(4) Sea- weed fragments, floating drift, which are not usually contained in the littoral drift, but sometimes have an essential effects in harbour or coast.

The sources of these materials are divided in

(1) Inland transported mud and sand etc.

(2) Coast and sea bottom eroded materials, sand and gravel, etc.

By the states of accretion of drift materials,

(1) Sand ridge, longshore bar, or off shore bar.

- (2) Sand bar
- (3) Shoal, bar or shallows
- (4) Sand bar at river mouth, sand ridge at river mouth, sand bar at entrance of lagoon.
- (5) Deposit at the root of groin
- (6) Deposit at the root of breakwater.
- (7) Sand bar at the entrance of harbour.
- (8) Pushed up sand on breakwater
- (9) Pushed up sand on coast or sea-wall.
- (10) Harbour deposit
- (11) Sand spitz
- (12) Sand dune which is formed by winds or coast upheavals.

The coast erosions is classified by its situation as follows.

- (1) Erosion of sandy beach (Regression of coast line)
- (2) Erosion of rocky beach (Cliff, flat rocky submerged beach)
- (3) Erosion at the foot of groin and breakwater.
- (4) Erosion of sea bottom (Trough, scouring along a breakwater)
- (5) Erosion at river mouth
- (6) Erosion of coast line
- (7) Erosion at the entrance of harbour. (Scouring at the entrance of harbour.

The causes of erosion are mainly the littoral drift by the sea water, but in special cases there are erosions by drifting ice, erosion by freezing and by some floating drifts such as timbers or log etc.. And there are also the erosions at river mouth by the river water, the surface erosion of inland by rain and snow, the aeolian erosion and the erosions by freezing, melting and weathering, etc..

6. Variation of sand size distribution curve.

As described above, the size distribution of littoral drift indicates approximately Gauss's normal distribution of $y = \log_e l$, so-called Log-probability law assumed l as the size diameter through many sorting processes. This distribution indicates a normal distribution on a semi-log paper and can be expressed by the following formula.

$$F(y) = \frac{1}{\sqrt{2\pi} \sigma_y} e^{-\frac{(y - \bar{y})^2}{2 \sigma_y^2}} \dots \dots (8)$$

The distribution curve of l is

$$\phi(l) = F(y) \left| \frac{dy}{dl} \right|$$

$$\begin{aligned} \frac{dy}{dl} &= \frac{1}{l} = e^{-y} \\ \text{so } \phi(l) &= \frac{1}{\sqrt{2\pi} l \sigma_{\log_e l}} e^{-\frac{(\log_e l - \overline{\log_e l})^2}{2 \sigma_{\log_e l}^2}} \\ &= \frac{1}{\sqrt{2\pi} e^y \sigma_y} e^{-\frac{(y - \bar{y})^2}{2 \sigma_y^2}} \dots \dots (9) \end{aligned}$$

$$\sigma_y^2 = \frac{1}{N} \sum_{i=1}^n f_i (l_i - \bar{l})^2$$

$$\bar{l} = \frac{1}{N} \sum_{i=1}^n f_i l_i$$

where f_i is the number of times that l_i occurs.

N is the total number of times. and the scope of this distribution is

$$\int_{-\infty}^{\infty} F(y) dy = \int_{-\infty}^{\infty} \phi(l) dl = 1 \dots \dots (10)$$

If such size distribution of a sample of drift sand is changed by the sorting process of sea water, for example from (2) to (1) in Fig.-6, the rates of loss and increase of each size are shown explicitly in this figure.

Here consider $y_{tc} = \log_e l_{tc}$ concerning with sorting process. l_{tc} is assumed the minimum size diameter of tractive movement. If larger sizes than y_{tc} are stayed and smaller than y_{tc} are wholly washed away, the hatched part in Fig.-6 remains and this area will be uniformly enlarged to be 100 per cent, but there remains more or less smaller sizes than y_{tc} due to the turbulence of natural sorting process and also is washed larger than y_{tc} , so that the curve will be indicated by the broken line in Fig.-6.

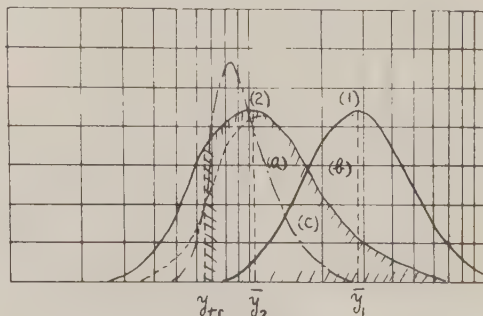


Fig.- 6

Then if the sample has been taken from the bottom surface, it will be exposed to the disturbances with time and finer particles will move to the surface and larger to lower. Some

times later, smaller particles than y_{tc} will decrease more and more, and y_{tc} and a little larger than y_{tc} will come to the surface to have a tendency that the proportion of a little larger part increases. Such distribution is the chain line in Fig.-6. So if the samples are taken from the surface thin layer, \bar{y} is to approach to y_{tc} . In natural movements of sea water, y_{tc} will vary from time to time, so that it has no time to match to the size distribution corresponding to every y_{tc} . Accordingly \bar{y} in the surf zone will be considered as the mean standard critical size during a certain period. But at the tractive regions where the circumstances have small variations relatively as off shore, \bar{y} will be considered very nearly to y_{tc} . By such consideration, the variation of size distribution curves of the surface layer at coast will be presumed as follows.

- (1) The variation with time at same point.

(a) When y_{tc} become larger.
 \bar{y} will become larger, so this will indicate the movement of sea water to strengthen and to have a tendency of erosions. Accordingly the supplies from the adjoining reaches will be decide whether the erosion will happen.

(b) When y_{tc} become smaller.
 \bar{y} will become smaller. The movement will weaken and it will indicate a tendency of accretion.

(c) When y_{tc} does not vary.
 \bar{y} will be constant and it will be considered the movement of sea water is unaltered. If the existing coast material is assumed to have only a same size, \bar{y} will not change even if the movement of sea water will change. But such coast will exist not at all, so an accretion or an erosion will be occur corresponding to the increase or decrease of supply respectively.

- (2) The variation of size by the situation on coast.

It is assumed that the littoral drift varies from y_2 on upper reach to y_1 on lower in the general course of its movement.

(a) When $y_{tc2} < y_{tc1}$, namely $\bar{y}_2 < \bar{y}_1$
 The sizes of coming particles will be smaller than y_{tc1} , so all of them will move out of the lower reach and not supply on the surface to happen erosion

If the movement of water is uniform, the lower reach is stable.

(b) When $y_{tc2} > y_{tc1}$, namely $\bar{y}_2 > \bar{y}_1$
 The sizes of coming particles contain larger than y_{tc1} and they will stay on the lower reach, but one smaller than y_{tc1} will continue to move as ever. In this case the velocities of transport decrease and occur an accretion. If the movement of water is uniform, lower reach will be eroded.

(c) When $y_{tc2} = y_{tc1}$, namely $\bar{y}_2 = \bar{y}_1$
 The coming particles continue to move as before and there are neither erosion nor accretion.

Generally either (1) or (2) is considered to be able to apply through the estimation of the direction of littoral drift, but it is noted that the volume of transportation on the direction of normal to the coast line is considerably large.

- (3) When the course of transport of littoral drift differs according to the size.

This fact will be happen when the main direction of littoral drift at heavy storm day differs from the direction at milder storm, or the water layer containing some suspended materials separates from the direction of tractive movement. In such case the hypothesis (1) and (2) will not be applied altogether, for the size distribution curve will be discontinuous.

After the precise investigation of the direction and velocity distributions of longshore currents and other over all the adjoining water regions, the effect of littoral drift should be examined from the size distribution of drift sand.

4. Relation between the littoral drift and the longshore current.

As described above, the gravity force on sea bottom slope has a large effect upon the stability of bottom materials and it is supposed that there is (3 b) relation between the slope of fore shore and the material sizes on that place.

On this problem, the author studied along TOMAKOMAI Coast in Hokkaido. On the coast of 70 km distance where TOMAKOMAI harbour is now under construction in its center, the slopes of fore shore are measured by 2 m long bubble level and the sands on the surface are analysed by sieves. Fig.-4

icates their size distribution curves
Fig.-7 is the relation between the
n diameters and the fore shore slopes.

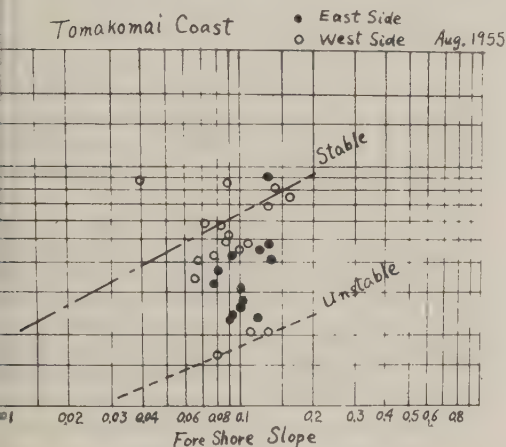


Fig. - 7.

MAKOMAI coast is a storm beach with
gshore bars and was recognized to
e the minimum slope⁽²⁾ stated by Bascom.
ew points out of the scope was the
cial case in the neighbourhood of
er mouths. This figure shows that the
t side coast of breakwater is erodible
the west side is more stable. The
e erodible localities at the west
e are supposed to exist from the
n direction of the longshore current.
re it is assumed that the position of
minimum slope showed by the chain
e in Fig.-7 indicates the stable
te and is more unstable or erodible
uniform movement of sea water so far
ward from the line that the broken
e is an erosion line. It is recog-
ed by the assumption that the states
observation points coincide roughly
h the positions of the points in the
ure.

reover this property coincides with
hypothesis of Johnson and the hypo-
sis(2) in 3 in this paper. This
imum possible slope will be shifted
the degree of progression of erosion,
the degree that is found slightly
e erosion on the beach may have the
ition of the broken line in Fig.-7.
this unstable line will indicate
coast where happens the accretion
smaller movement of sea water and
stable line will indicate the coast
re happens the erosion by stronger

movement of sea water.

At TOMAKOMAI the velocities of long-
shore currents were observed at the
same time using wooden rod floats which
length 30cm and section was 4.5x4.5cm
and hung a weight of stone at the
lower end. The velocity of a longshore
current is controlled by the longshore
component of the momentum of waves and
so has an important relation with the
longshore transportation of the litto-
ral drift. By this idea, the relation
between the velocities of the measured
longshore currents and the sizes of
surface sand at that beach is indicated
in the logarithmic paper of Fig.-8,
where the chain line may be a stable
velocity line and the broken line an
erodible velocity line and the inter-
mediate position of these two lines
may indicate the erodible degree. The
broken line shows the relation of the
formula (5).

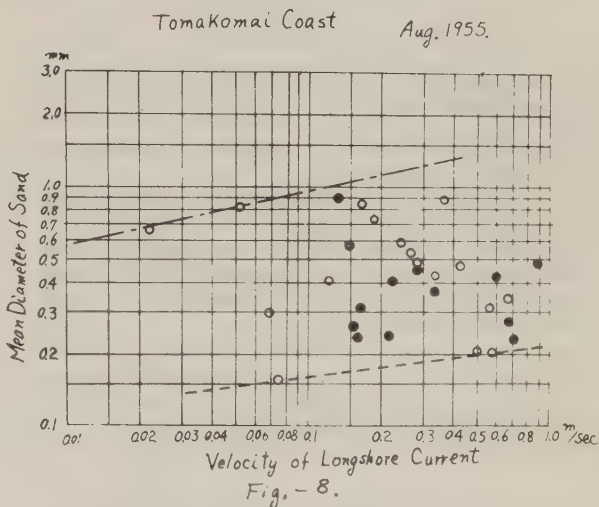


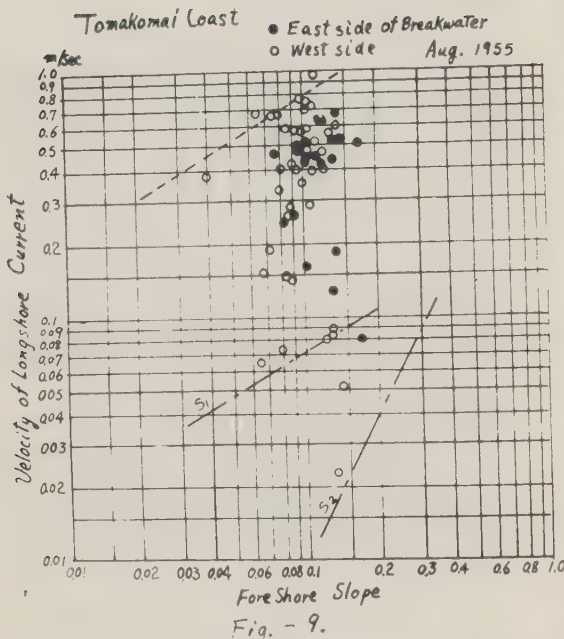
Fig. - 8.

The relation between the velocities of
longshore currents and the slopes of
fore shores is indicated in Fig.-9 in
the same method as above.

In Fig.-9 the upper broken line may
point out the erosion and the lower
chain line the stable beach, and the
lower part is more stable.

This erosion line indicates the rela-
tion of formula (3b). If it is assumed
to be able to express this relation in
a straight line on this figure,

$$S = a v^c \quad \dots\dots(11)$$



The smaller Q , the stronger the erosion develops. In Fig.-9

$$S = 0.153 v^{1.71} \dots \text{erosion line} \dots (12)$$

$$\left. \begin{aligned} S &= 8.7 v^{1.71} \\ S &= v^{\frac{1}{2}} \end{aligned} \right\} \dots \text{stable line} \dots (13)$$

It was difficult to determine the value of power C , for the observation data was inclined to one part and so must be investigated hereafter.

5. Conclusion.

In this report, the author stated the general problems of littoral drift. But there are many unsolved parts in quantity relations and it is yet difficult to estimate the volume of littoral drift. However it is believed that the present qualitative method is possible to be advanced to the quantitative estimation by the cooperative studies.

Acknowledgments:- This study was performed under the assistance and cooperation of the synthetic science research fund of Japan Education Ministry, The Civil Engineering Experiment Laboratory of Hokkaido Development Bureau, TOKAKOMAI City and Faculty of Technology in Hokkaido University.

References

- (1) J.W.Johnson: Proceeding of the Council on Wave Research on Coastal Engineering I, 1950.
- (2) Japan Society of Civil Engineers, Kansai Branch: Transaction of the Research Meeting on Coastal Engineering No. 1, Nov., 1954.

This report was published in Japanese on Transaction of the Research Announcement Meeting on Coastal Engineering, No.2, Nov.1955.J.S.C.E.

On the Investigation of Beach Erosion along
the North Coast of Akashi Strait

Tojiro Ishihara, Dr. Eng., Kyoto University
Yuichi Iwagaki, Dr. Eng., " "
Masashi Murakami, " "

Synopsis Sandy beaches are defensive zones created by nature, protecting the land against aggressive oceanic forces. They are very flexible and their configurations are varying daily, seasonally and annually, depending on many factors, such as wave characteristics, beach materials, shore structures and the others. The investigation of beach erosion is one of the most important and difficult subjects in coastal engineering.

In this paper, a method for investigating the mechanism of beach erosion is presented, concerning the investigation practice of beach erosion along the north coast of the Akashi Strait, and the author's opinion of the following three subjects to be investigated is described:

- (a) Distribution of sand drift along the coast,
- (b) Distribution of sand drift along the beach profile, and
- (c) General characteristics of sand drift, such as the type of sediment transport, the direction of drift and the others.

1. Introduction

Sandy beaches are defensive zones created by nature, protecting the land against aggressive oceanic forces. They are very flexible and their configurations are varying daily, seasonally and annually, depending on many factors, such as characteristics of incoming waves, beach materials, shore structures and the others. It is of common observations that during storms, the shore line is receded, the slope becomes gentle, and the offshore bar is formed, while in calm weather, the shore line is advanced, the slope becomes steep, and the offshore bar is gradually disappeared. It may be, therefore, said sandy beaches hold their virtual equilibrium by the repetition of erosion and deposition. Nevertheless, some sandy beaches lose their virtual equilibrium for a long time and are gradually eroded, resulted in becoming the non-defensive or wasted zone in utilities. Why do such beach ero-

sions happen? What and what kind of investigation shall we do for the analysis of behaviours in beach process?

The erosion of beaches, of course, is caused by the movement of beach materials, resulted from the dynamic behaviours of water particles by incoming waves. Two types of fluid motion in the onshore side from breaking point are mostly related to the movement of beach sands: One is the reciprocation of water caused by the progression of incoming waves and the other is the longshore currents caused by waves broken obliquely to the shore line. The former motion influences on sand movements along the beach profile and directly contributes to the formation of profile of sandy beaches. Variations of sandy beaches in short periods, such as the recession of shore lines caused by the attack of storms and their progress in calm sea, are resulted from the former action. Herewith, it may be called as the deformation of configuration at sandy beaches.

The littoral drifts, caused by the latter action, may be considered one of the fundamental factors of dynamic behaviours in beach process for a long time, and are similar to the sediment transportations in channels resulting in the deformations of river beds. Consequently, the primary requirements for the clear formulation of beach process in coastal engineering are to investigate thoroughly the characteristics of littoral drifts in forms of

1. Distribution of sand drifts along the coast
 2. Distribution of sand drifts along the beach profile, and
 3. General characteristics of littoral drifts.
- Hence, the field investigation for beach erosions should be orientated to the completion of above engineering requirements. Nevertheless, in the present stage, no general methods available for field observations and theoretical analysis in beach process have not been established, and the present possible way to make the behaviour in beach process clear is the estimation of qualitative tendency by the systematic consideration through direct or indirect observations. Herewith, the engineering requirements for the analysis of beach process will be described as follows.

- (1) Distribution of sand drifts along the coast

If the rate of sediment transportation is uniform along the entire region of beach, the beach may be called stable for a long time, except the short period deformation in progression or regression by the action of incoming waves. When the distribution of sand drifts along the beach, however, increases gradually in the direction of movement, the beach will be eroded little by little, while the beach will be deposited and its shore line will be advanced, by the decrease of littoral drifts in volume. The most important two factors influential to the rate of littoral transportation in sand are the littoral component of wave energy and the bottom materials. Therefore, the distribution of littoral drifts will be estimated for given bed materials of coasts under investigation and velocity of longshore currents determined by dynamic characteristics of incoming waves like the height of breaker, the incident angle of breaker and geological characteristics of beaches like bottom configuration and beach profiles.

(2) Distribution of sand drifts along the beach profile

The measurement of distribution of sand drifts along the beach profile, resulted in the estimation of critical water depth for sediment transportation of sands, is of primary significance for the engineering contribution to design and construction of coastal structures as well as efficiency for erosions by constructed structures. The engineering practice for measurement of this distribution along the beach profile will be possible to some extent and some collecting equipments of sand drifts have been designed and used at Hokkaido University¹⁾. It is, however, still difficult to measure sand drifts in the neighbourhood of

shore line where the wave action by higher waves becomes distinguishably intense under the condition of rough weather. As described in (1), the possible approach is the estimation of distribution through considerations of dynamic and geological factors influential on the beach process with the aid of experimental results. Consequently, field observations of the distribution of longshore current velocity, bed materials, and wave characteristics like wave steepness and beach profile closely related to the distribution of sand drifts may be of most importance.

(3) General characteristics of sand drifts

The primary subject of investigation contributive to the clear formulation of dynamics in beach erosion and the practical application to design and construction of coastal structures is to reveal the general characteristics of littoral drifts such as the direction and dynamic process of movement of drift. The direction of movement of sediment is commonly estimated by the incident angle of incoming waves. However, in case which incoming waves are deflected and refracted by the complicated feature of coasts and the offshore structures, the refraction diagram for obtaining the direction of breaker, the direct methods by measuring littoral drifts by tracing of floats or radio-isotope²⁾ or by collecting equipments for sand drifts should be used. Consequently, dynamic behaviours in littoral movements will be estimated by the field measurements of sand drifts along the beach profile and mechanical properties of bed materials as well as characteristics of incoming waves.

The foregoing description is the outlines of basic subjects for the investigation of beach process, and the procedure of investigation will be accentuated in the light of past field observation conducted by authors at the north coast of the Akashi Strait since Aug., 1955.

2. Beach Profiles at the North Coast of the Akashi Strait

The detailed soundings to obtain the bottom configuration were conducted at about 100 sections of beaches along the shoreline in 15 km between the Myohoji River, which was at the east end of the Suma beach and the Akashi River stood at the west end of Akashi City, from July 20 to August 30, 1955. Fig. 1 indicates some typical beach profiles in the north coast of the Akashi Strait.

The slope at the coast under investigation is generally 1/10 or steeper than 1/10 in the neighbourhood of the shore line. Especially, at Nishi Tarumi, Shiroya and Higashi Tarumi, no littoral sand bars are developed and the water depth is 7 - 8 m off the coast of 100 m from

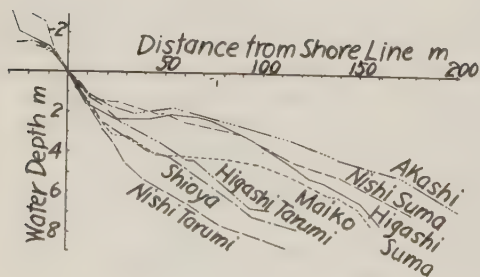


Fig. 1 Some typical beach profiles at the north coast of Akashi Strait

the shoreline. At Akashi, Nishi Suma, Higashi Suma, and Maiko, sand bars are located at 50 m in distance from the coast and 2 - 4 m in water depth. Selecting three beaches of Akashi, Nishi Tarumi, and Nishi Suma as reference points, the relation between equilibrium profiles at these locations and estimated wave steepness of incoming waves generated by the S-E wind will be considered.

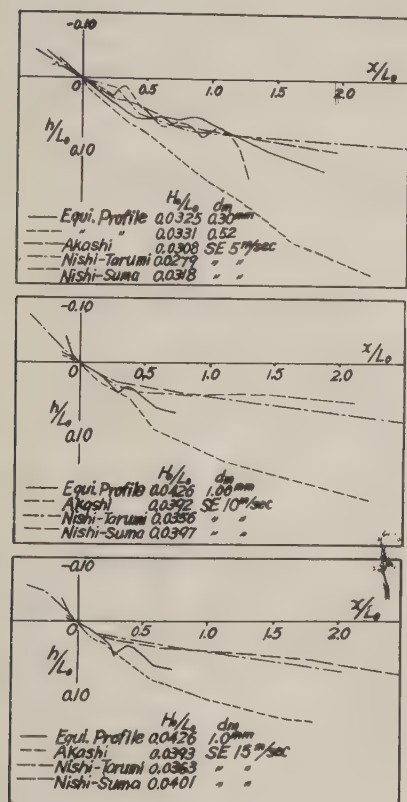


Fig. 2 Dimensionless representation of beach profiles

Fig. 2 indicates the dimensionless representation of these beach profiles divided the distance from the shore line and the water depth by the wave length estimated, with the aid of the following fetch graph (Fig. 7), for 5 m/sec, 10 m/sec, and 15 m/sec of winds in velocity. Furthermore, for comparison with observed profiles, the equilibrium profiles experimentally obtained at Kyoto University are also described^{3), 4)}.

In the figure, the wave steepness is corrected through multiplication of wave

steepness estimated from the fetch graph by refraction coefficients calculated from the refraction diagram at these locations.

Evidently, it is seen that the beach profiles at Nishi Suma and Akashi are closely related to the experimental equilibrium profiles in case of wind velocity, 5 m/sec, or equivalent steepness, 0.03. On the contrary, the behaviours of beach at Nishi Tarumi seems to be different and in case of 10 - 15 m/sec in wind velocity and equivalent steepness of 0.04, the beach profile seems to approach stable. However, the details of stable beach profile is

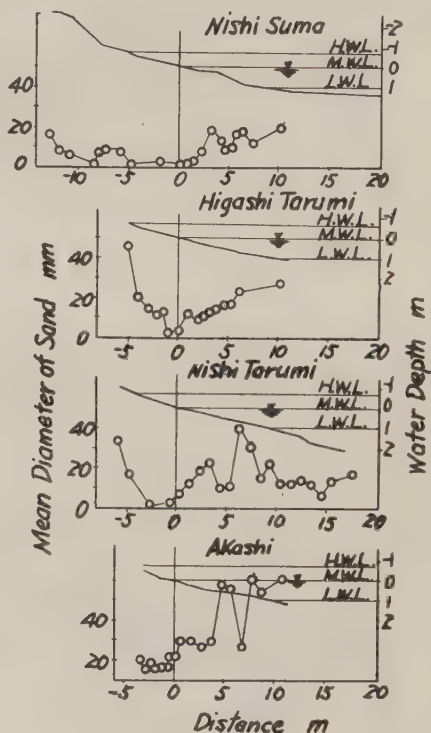


Fig. 3 Relations between mean diameters of beach sand, water depth and distances from shoreline at some typical beach parts

very different from that of experimental profile. Further study to make dynamics of detailed movements of sand clear should be considered.

3. Bed Materials of the Coast

At the same time when the sounding were conducted, bed materials were also collected at about 40 points and every mouth of river and sieved by JIS sieves. Fig. 3 indicates rela-

tions of mean diameters of beach sands and water depth to distances from the shoreline at four typical beaches. It is seen in this figure that the mean diameter of sand is small in the neighbourhood of shoreline and onshore where the wave action is distinguishly violent and becomes larger in the offshore part. W. H. Pascon⁵⁾ obtained similar results in some parts of the Pacific Coast, and the maximum diameter of sand were measured at two zones of the last breaking point and ordinary berm. Field observations at the Senan coast indicate the maximum size of bottom material exists at the breaking point, resulted in poor sorting of sands. The same conclusion for sorting at the westward beaches from Higashi Tarumi is obtained by the present observations. Table 1

the coast are not less than several mm in minimum mean diameter except at Nishi Suma, and the common tendency in the distribution of grain size is not obtained.

4. Frequency of Wind in Kobe and Akashi

As the north coast faces the Osaka Bay and the Inland Sea and its fetch is less than about 80 km as mentioned afterward, so it is considered the coast is hardly influenced by swells even if they enter from the Pacific Ocean through the Kitan Strait, and wind waves will play a primary role to the beach process. The investigation of wind characteristics, therefore is of essential importance for understanding the characteristics of sand drifts at the coast. Fig. 5 indicates that the frequency diagrams of wind velocity for each wind direction in Kobe (

Table 1 Sorting coefficients of beach sand near the shoreline at some typical beaches

	Nishi Suma	Nishi Tarumi	Maiko	Akashi
	No. 26	No. 64	No. 74	No. 97
Sorting Coefficient	1.45	4.85	2.58	2.15

indicates the sorting coefficient of bed materials, $\sqrt{d_{25}/d_{75}}$, near the shoreline at various beaches along the Akashi Strait. It is seen that the coefficient is maximum at Nishi Tarumi. Fig. 4 shows the distribution of minimum mean diameters of beach sands near the shoreline along the north coast of the Akashi Strait and at mouths of rivers. Coastal sands at most parts of

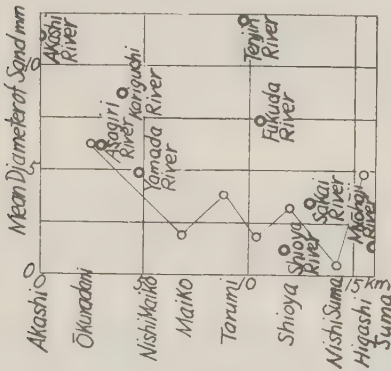
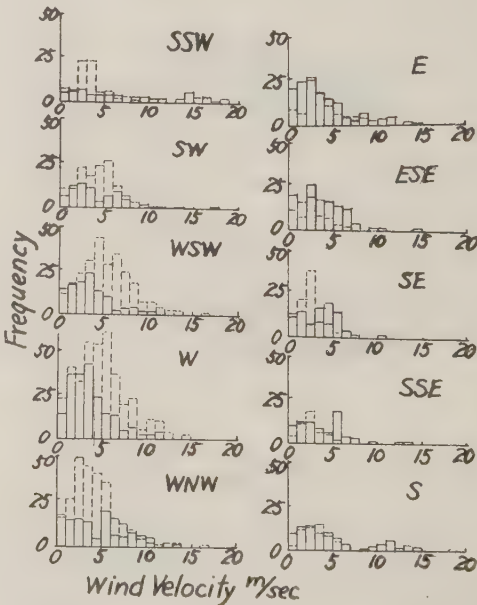


Fig. 4 Distribution of mean diameters of beach sand near the shoreline along the north coast of Akashi Strait



Kobe : Dotted line, Akashi : Full line

Fig. 5 Frequency diagrams of wind velocity for each wind direction at Kobe and Akashi

Dec. 1954 to Nov. 1955) and Akashi (from Jun. to Nov. 1955). Frequent directions of winds are E, S, SSW, and W and winds bring strong velocity. The conclusion is also derived in Fig. 6, which indicates the frequency diagram of wind velocity for east and west winds in Kobe. Nearly all winds of velocity over

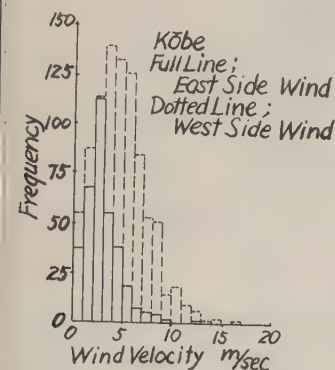


Fig. 6 Frequency diagram of wind velocity for east side wind and west side wind in Kobe

/sec are in the direction from west. Therefore, it may be assumed the great part of sand drifts move from west to east.

Waves at the North Coast of the Akashi Strait

Characteristics of deep water waves
The characteristics of waves in deep water generated within several decade km fetch are determined by fetch and wind velocity. Fig. 7 is the diagram of wave height, H_0 , wave length, L_0 , and wave period, T , in deep water obtained by C. L. Bretschneider⁷⁾ after correcting the fetch graph of Sverdrup and Munk. In the figure, L_0 , and T are calculated directly for given values of wind velocity and fetch. Fig. 8 is the diagram of wave steepness H_0/L_0 in deep water obtained from the fetch graph. Therefore, two values of U and F are required for obtaining the characteristics of deep water waves. Fig. 9 describes the changes in directions of frequent winds at Shi Suma, Tarumi and Akashi beaches, and they are ranged from 30 - 40 km in the direction from SSW to E, to 70 - 80 km in the direction from SW to W. Table 2 shows the approximate values of wave height, period and steepness in deep water for relatively long and frequent winds at the coast.

Refraction of waves and equivalent

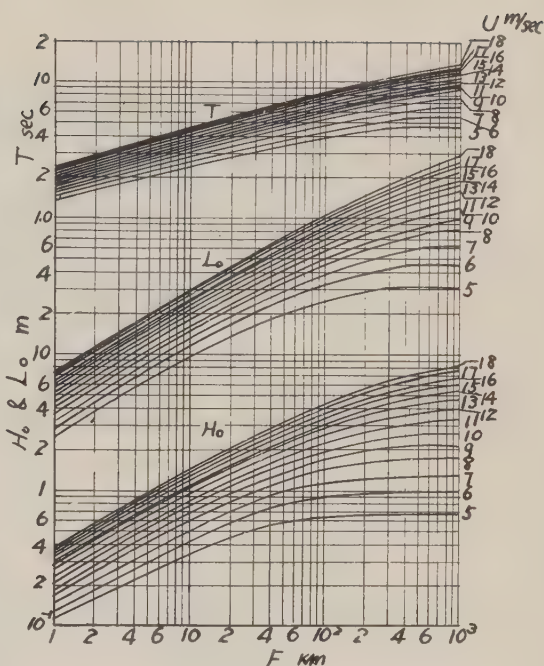


Fig. 7 Diagram of wave height, wave length and wave period in deep water obtained from the fetch graph by Sverdrup-Munk-Bretschneider

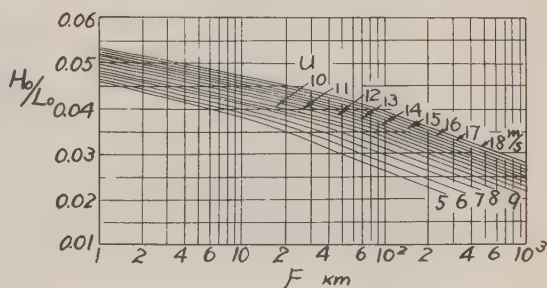


Fig. 8 Diagram of wave steepness in deep water obtained from the fetch graph by S.M.B.

wave steepness

The characteristics of waves in deep water are gradually changed by refraction and diffraction resulted from the bottom variations in configuration. Consequently, the refraction and diffraction coefficients are required for the determination of the characteristics of re-

Table 2 Approximate values of wave height, period and steepness in deep water for selected wind velocities at the north coast of Akashi Strait

	E	SE	S	WSW	W	WNW
U m/sec	8	5	12	8	8	10
H_0 m	1.0-1.2	0.5-0.6	1.8-1.9	1.4	1.4	1.5-1.7
T sec	4.0-4.4	3.1-3.2	5.2-5.4	5.0-5.2	5.0-5.2	5.1-5.5
H_0/L_0	0.036-0.037	0.031-0.032	0.040-0.041	0.032-0.033	0.032-0.033	0.037-0.039

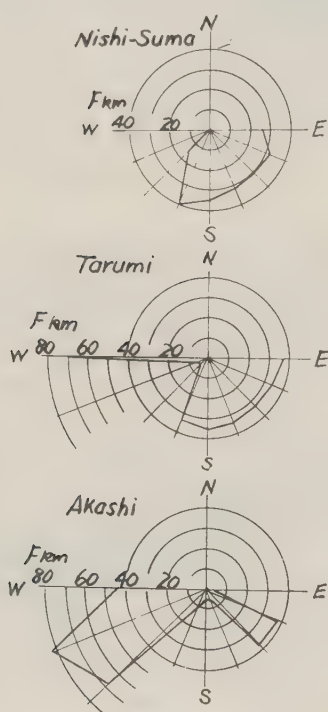


Fig. 9 Fetches for each direction at typical beaches of the north coast of Akashi Strait

fracted and diffracted waves through the refraction and diffraction diagrams.

Fig. 10 is an example of refraction diagram for the wave of 4 sec. in wave period from east drawn by the wave crest method. In the same manners, five refraction diagrams for waves of directions, SE, and wave period 3 sec. and directions

of S, WSW, W and NW with wave period 5 sec. (the diffraction by the Awaji Island is also considered) were drawn and refraction coefficients at several beaches under consideration were estimated. The refraction coefficient is used as the square root of the ratio of distance S_0 between two orthogonals in deep water to distance S_b in breaking point.

Let the equivalent deep water wave be an assumed incoming wave in deep water, perpendicular to the shoreline, of which characteristics at the beach are equivalent to those of refracted waves. Then the wave steepness for such equivalent waves in deep water, which is called the equivalent steepness, is readily calculated by the product of H_0/L_0 to $\sqrt{S_0/S_b}$ and are indicated in Table 3.

It is seen in the table that the equivalent wave steepness at the coast is commonly small and the classification of storm beach of wave steepness more than 0.025 - 0.030, for which the littoral sand bar is formed, are as follows: for SE winds, Akashi and the east coast from Nishi Tarumi, for S winds, the east coast from Nishi Tarumi, for WSW winds, Akashi. The most significant behaviours, which characterize the seasonal beach profile in summer and winter and the movement of sand drifts, are that the S wind forms higher waves of large steepness while the W - WNW winds generate lower waves.

(3) Depth and height of breakers

The breaker depth is calculated by the breaker index⁹⁾ for a given equivalent wave steepness and Table 4 indicates the breaker depth for particular wind velocities occurred most frequently at typical beaches of the coast, and it is understood that at some beaches the breaker depth for the S wind is over 2 m and the littoral sand bar at the Suma beach will be formed under above described particular circumstances. The breaker height is approxi-

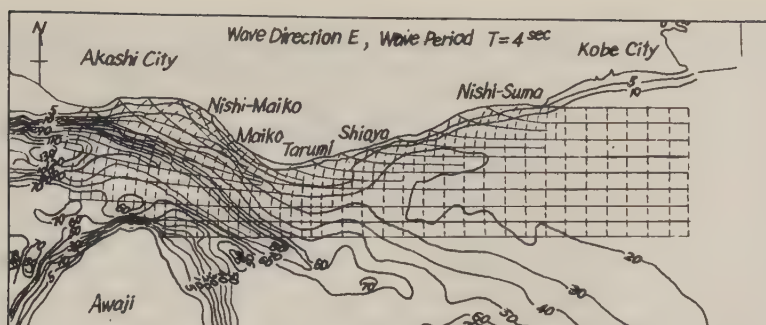


Fig. 10 Refraction diagram for the wave of direction E and period 4 sec.

Table 3 Equivalent initial steepness in deep water for selected wind velocities at typical beaches of the north coast of Akashi Strait

Wind direction	E	SE	S	WSW	W	WNW
Akashi	0.005	0.031	0.017	0.013	0.008	0.027
Yamada	0.005	0.025	0.023	0.017	0.006	0.022
Nishi Maiko	0.008	0.028	0.025	0.030	0.008	0.014
Nishi Tarumi	0.022	0.030	0.040	0.001	0.010	0.009
Shioya	0.023	0.031	0.040	?	0.010	0.006
Nishi Suma	0.021	0.032	0.041	?	0.008	0.003
Higashi Suma	0.026	0.032	0.040	?	0.004	0.002

Table 4 Breaking depth for selected wind velocities at typical beaches of the north coast of Akashi Strait (unit: m)

Wind direction	E	SE	S	WSW	W	WNW
Akashi	0.4	0.8	1.1	0.9	0.7	1.4
Yamada	0.4	0.6	1.5	1.1	0.6	1.3
Nishi Maiko	0.5	0.7	1.6	1.7	0.7	1.0
Nishi Tarumi	1.0	0.7	2.4	0.4	0.8	0.8
Shioya	1.0	0.7	2.4	?	0.8	0.6
Nishi Suma	0.9	0.8	2.4	?	0.7	0.4
Higashi Suma	1.0	0.8	2.4	?	0.5	0.3

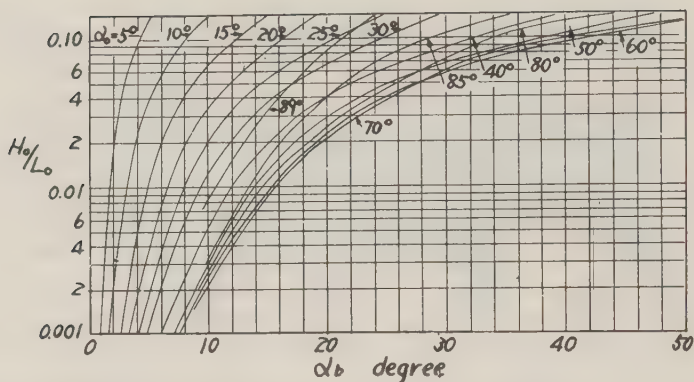


Fig. 11 Diagram for obtaining the breaker angle α_b from the initial steepness H_0/L_0 and the crest angle α_0 in deep water

mately calculated by the following relation.

$$H_b = H_0 (S_0/S_b)^{\frac{1}{2}} \quad (1)$$

Or strictly, it is expressed, with the aid of $H_b/H_0 = f(h_b/L_0)$, in a form of

$$H_b = H_0 f(h_b/L_0) (S_0/S_b)^{\frac{1}{2}} \quad (1')$$

Along the coast, however, the diameter of bottom materials is relatively large and it is expected the wave height will be decreased by the percolation through the sea bottom, and therefore, Eq. (1) will be used as an engineering approximation to calculate the breaker height.

Dotted line in Fig. 12 indicates local distributions of the breaker height calculated by Eq. (1) for various winds.

6. Longshore Current at the Coast

J. A. Putnam, W. H. Munk and M. A. Traylor¹¹⁾ derived the relation of the longshore current in a form of

$$V = (a/2) \left[\sqrt{1 + (4c/a) \sin \alpha_b} - 1 \right],$$

where

$$a = (2.61 H_b \cos \alpha_b) / kT, \quad (2)$$

$$c = (2.28 g H_b)^{\frac{1}{2}}$$

D. L. Inman and W. H. Quinn¹²⁾ obtained the friction coefficient k in Eq. (2) as a function of V based on the experimental and field observations, and finally presented rather empirical formula of velocity of longshore current in a form of

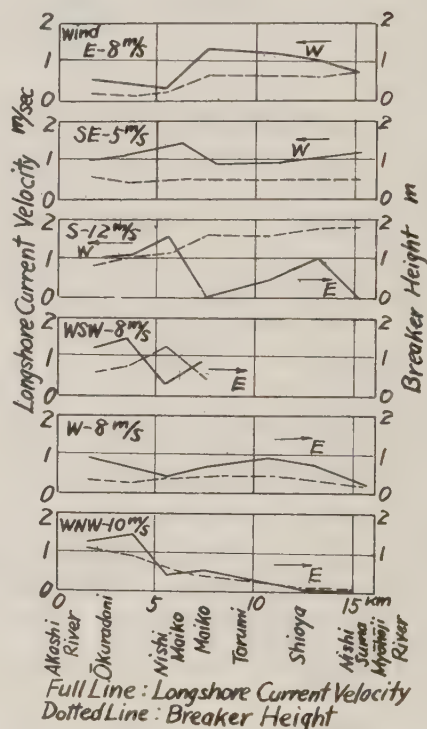


Fig. 12 Distributions of longshore current velocity calculated by Eq. (3) and the breaker height for selected wind velocities along the north coast of Akashi Strait

$$V = \left[\left\{ \frac{1}{4x^2} + y \right\}^{\frac{1}{2}} - \frac{1}{2x} \right]^2 \quad (3)$$

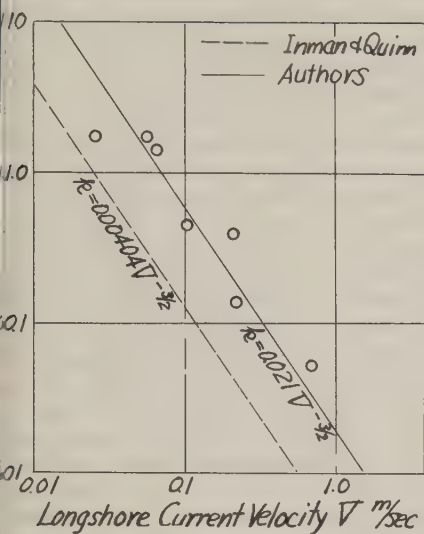


Fig. 13 Relation between coefficient of friction k and longshore current velocity V

$$(646H_b \cos \alpha_b) / T,$$

$$c \cdot \sin \alpha_b, \quad (\text{m} \cdot \text{sec} - \text{unit}),$$

which V is the velocity of longshore current, α_b : the angle of shoreline to wave crest at the breaking point, i : mean beach slope between the breaking and the shoreline, and g : the acceleration of gravity.

The breaker angle, α_b , may be determined by the refraction diagram of Fig. 10, but the desirable accuracy for α_b obtained by the diagram of large scale is not expected. Therefore, for obtain-

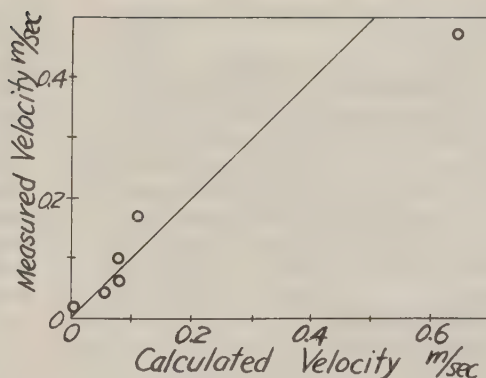


Fig. 14 Relation between calculated values by Eq. (6) and observed data

ing the possible values of α_b in accuracy, Fig. 11, which indicates the relation between α_b and the wave steepness of deep water waves as a parametric expression of crest angle, α_0 , in deep water, is used.

This figure is calculated by means of the law of Snell and the breaker index, while P. Groen and M. P. H. Weenik¹³) made the same diagram with the aid of Snell law and the hydraulic characteristics of solitary waves.

The angle of the crest line, thus, to the shoreline at the breaking point is estimated for given values of H_0/L_0 and α_0 . As the deep water waves at the Akashi coast are short in wave length and changed to the shallow water waves at the water depth of 15 - 20 m, the value of α_b in first approximation may be obtained under the condition of locally straight coast.

Fig. 12 indicates the distribution of velocity of the longshore current calculated by Eq. (3) and the breaker height.

This figure is of primary importance to

Table 5 Tendency of beach process at each part of the coast for various wind directions

Part along the coast	E	SE	S	WSW	W	WNW
Akashi-Yamada	NC	D	NC	E	D	E
Yamada-Nishi Maiko	NC	D	D	D	D	D
Nishi Maiko-Nishi Tarumi	D	E	E	E	E	E
Nishi Tarumi-Shioya	NC	NC	E	?	E	D
Shioya-Nishi Suma	E	NC	E	?	D	D
Nishi Suma-Higashi Suma	E	D	D	?	D	D

investigate the characteristics of littoral drifts and the dynamic behaviours in beach erosions.

In October, 1955 and August, 1956, the field observations of longshore current velocities were performed by the authors at Higashi Tarumi, resulted in a poor agreement with the empirical formula of Inman and Quinn. Then, the reexamination of behaviours of frictional coefficient, k , in the empirical formula (3) is considered with the aid of field observations.

The transformation of Eq. (2) yields the following equation,

$$k = 2.61H_b \cos \alpha_b (c \sin \alpha_b - V) / V^2 T \quad (4)$$

Insertion of the observed data of longshore current velocities and characteristics into Eq. (4) leads to the determination of k , as seen in Fig. 13.

The first approximation of k as a function of V is expressed in a form of

$$k = 0.021V^{-\frac{2}{3}} \quad (5)$$

Thus, the revised formulas for V and x becomes

$$V = \left[\left\{ \frac{1}{4x^2} + y \right\}^{\frac{1}{2}} - \frac{1}{2x} \right]^2 \quad (6)$$

$$x = (124H_b \cos \alpha_b) / T, \quad y = c \sin \alpha_b$$

Fig. 14 indicates the relation between calculated values by Eq. (6) and observed data.

7. Consideration of Mechanism of Erosion and Littoral Drift along the Coast

(1) Distribution of littoral drift along the coast

The most important factors influential on the littoral drift are the longshore current velocity and the grain size of bottom materials. At the coast the grain size of bottom materials are large, and the equivalent wave steepness is comparably small, and therefore, it is supposed that the littoral drifts are mostly composed of beach drifts near the shoreline. As the grain size of bed materials near the shoreline at the coast is several mm in diameter, as seen in Fig. 4, so the velocity of longshore current will mainly influence on the littoral drifts. If the distribution of littoral drifts is related to the distribution of velocity of long-

shore shown in Fig. 12, the dynamic behaviours of erosion and deposition in beach process will be considered with the use of the figure. Although such behaviours at the Sen-nan coast have been discussed by the distribution of breaker height, the better estimation along the irregular coast will be obtained with the aid of knowledge of velocity of longshore current. Considering in Fig. 12 that the beaches where the longshore velocity increases in the direction of longshore current is eroded while the beach of decreasing velocity is deposited, Table 5 indicates the dynamic behaviours of erosion and deposition in beach process will be obtained.

Evidently in inspection of Table 5, it is of significance that beaches between Nishi Maiko and Nishi Tarumi are eroded for all winds except E while beaches between Nishi Suma and Higashi Suma, and Nishi Maiko and Yamada will be deposited. As strong winds are frequently blown from west and south, so particular beaches along the Akashi Strait will be fundamentally characterized by the above described behaviours in beach process.

(2) Distribution of sand drifts along the beach profile

T. Saville, Jr.¹⁵⁾ and one of the authors¹⁶⁾ revealed experimentally the sand drifts were transported as bed load movement for less wave steepness not more than 0.025 and the movement was limited in a very narrow zone near the shoreline. As seen in Table 3, the equivalent wave steepness at this coast is very small except for cases of wind directions, S and SE, and the grain size of bottom materials is considerably large. Therefore, it is supposed nearly all sand drifts are transported in the onshore side from the breaking point. At this coast, however the tidal current is very fast, so that the sand drifts due to the tidal current should be considered. As the highest velocity of tidal current observed at the coast is $V = 1.6$ m/sec, and the water depth is 10 m, so the movable largest size of bottom materials is estimated 2 - 6 mm in diameter, with the aid of following relation of critical tractive force.

$$\sqrt{\tau_0 / \rho} = U^* = nVg^{\frac{1}{2}} / h^{\frac{1}{2}}, \quad (7)$$

where τ_0 : frictional force on the bottom, ρ : density of sea water and n : Manning roughness assumed 0.01 and 0.02 (m-sec).

The detailed observations of tidal current velocity near the shoreline and the establishment of the relation between tidal current and longshore current were performed by the authors in October, 1955. Fig. 15 is an example of current velocity distribution, and it is seen that the breaker height is very low and the clear distinction between the longshore current in the

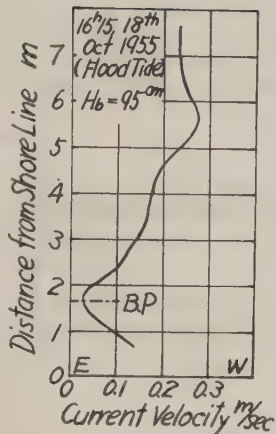


Fig. 15 Example of current velocity distribution at the onshore of Higashi Tarumi beach

shore and the tidal current in the off-shore exists at the breaking point. It is also recognized that the velocity of tidal current increases with the distance from the breaking point, while the velocity of longshore current is not uniformly distributed and increases near the shoreline.

Although the tidal current is larger in velocity than longshore current in this zone, the tidal current carries no bed materials, because the running direction of the tidal current is parallel to the shoreline.

The sand drifts are transported by the actions of longshore current and breakers, and therefore, there exists sand within the zone of bed materials disturbed by the disturbance of breakers near the coast.

Fig. 16 is an example of the distribution of the rate of sediment transportation near the shoreline at the Higashi Tarumi beach. The sand trap (sampler) used had a mouth of 4 cm and 2 cm in area and a clothsack was attached at the back of it. It is seen in Fig. 16 the movement of sediment is almost limited in the on-shore zone from the breaking point, maximum in the rate of transportation is at the shoreline, and its distribution is similar to the experimental results in the case of small wave steepness.

General characteristics of sand drifts

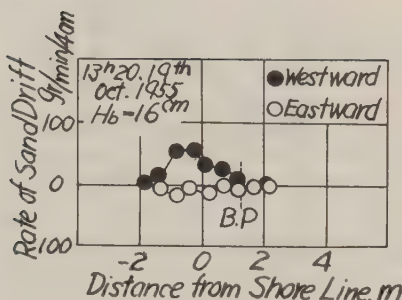


Fig. 16 Example of distribution of rate of sediment transportation near shoreline of Higashi Tarumi beach

As nearly almost strong winds come from west, so it will be supposed that the littoral drifts are carried from west to east. However, most volumes of drifts may be deposited by many coastal structures like jetties in case of small incoming waves, so that the speed of erosion and deposition in beach process will also be slow.

Already described, as the coastal behaviours at the Akashi Strait are essentially characterized by incoming waves of small equivalent wave steepness and large grain size of bottom materials, so the type of drift movement is classified as the movement of beach sand drifts near the shoreline. Therefore, the most parts of sands will be deposited by comparably short jetties. However, in case of the wind direction, S, the breaker depth and the wave steepness are large at the east coast from Nishi Tarumi, so that careful consideration contributive to engineering satisfaction of prevention from beach erosions should be required for the construction of coastal structures.

(4) Estimation of rate of littoral drifts

Concerning the estimation of rate of littoral drifts, J. M. Caldwell¹⁸⁾ (1956) and G. M. Watts¹⁹⁾ (1953) published the following empirical relation between the energy of incoming wave and the rate of sand transportation, based on observed data at South Worth Inlet, Florida and Anaheim Bay, California.

$$Q_i = k E_i^m, \quad (8)$$

in which k and m are constant, Q_i is the rate of sand drifts per hour, and E_i is the coastal part of transmitted wave energy along the coast per unit length per hour.

For engineering purpose of establishment of the relation between the energy of incoming wave and the rate of sand transportation at the north coast of Akashi Strait, the hydraulic behaviours of erosion and deposition in beach process were

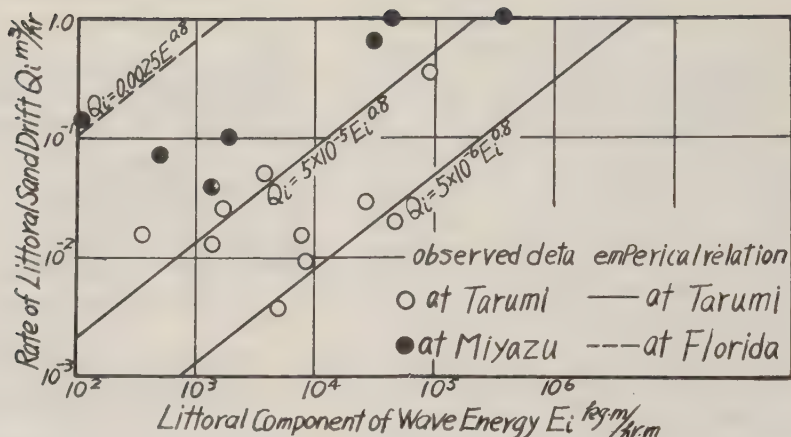


Fig. 17 Relation between shoreline part of wave energy and rate of sand transportation



Plate 1 Temporary jetty for observation of rate of beach drifts

observed from August 18 - 30, 1956, at Higashi Tarumi. The measurement of the rate of transported materials was conducted twice a day at 9 am, and 3 pm, by setting a temporary jetty of small scale as seen in Plate 1.

Fig. 17 indicates the observed data at Higashi Tarumi and the results at Miyazu coast are plotted, and furthermore, the empirical relation obtained by Caldwell and Watts is also drawn in the same figure and it is in a form of

$$Q_i = 0.0025 E_i^{0.8} \quad (\text{m}^3/\text{hr.}, \text{kg.m/hr.}, \text{m})$$

It is seen the rate of littoral drifts at Higashi Tarumi is less than that at the other coasts.

It is supposed this may be due to the fact that the grain size of bottom material at the north coast of Akashi Strait is larger than that at other coasts. The scattering of observed data in Fig. 17 will be resulted from the difference in the rate of sand transportation due to the characteristics of incoming waves, which has been made clear by Saville and J. W. Johnson.

Consequently, the observed data at Higashi Tarumi are involved within two limits of empirical relations derived by the same procedures as Caldwell and Watts did.

8. Conclusion

In this paper, the investigation procedures on hydraulic behaviours of erosion and deposition in beach process are accentuated in the light of modern knowledge in hydrodynamics and past experience in coastal engineering and the methods described here are also considered less in labour and more in efficiency.

There still remain unsolved problems like simple method of observation of incoming waves, influences of tidal currents to refracted waves, effects of jetties, supply source of sands, artificial nourishments and so on.

The research procedure described in the present paper may be considered the most systematic method for engineering purpose of complete establishment of investigation contributive to the further development in coastal engineering.

Acknowledgments

The present investigation program was conducted as a part of the research project at the Akashi Strait with the sponsorship of the Harbour Bureau, Kobe City. The investigation was con-

ected under the direction of Dr.
jiro Ishihara, Director of the Hydraulics Laboratory and the field observation was mainly performed by Masashi Murakami. Acknowledgment is also made to the assistance of Messrs. T. Sawaragi, Kita, A. Ogo, and T. Matsuoka.

References

Fukushima, H., and Mizoguchi, H., On littoral drift and its measurement, Proc. 2nd Conf. Coast. Engg., Japan, Nov., 1955, pp. 155 - 161.

Inose, S., On field measurement of littoral drift by using radio-isotope, Proc. 2nd Conf. Coast. Engg., Japan, Nov., 1955, pp. 163-174.

Iwagaki, Y., and Sawaragi, T., Experimental study on the equilibrium slopes of beaches and sand movement by breaker, Proc. 2nd Conf. Coast. Engg., Japan, Nov., 1955, pp. 99-105.

Iwagaki, Y., and Sawaragi, T., Some problems on the equilibrium slopes of beaches, Dis. Prev. Res. Inst., Bulletin, Memo. Issue, 5th Anniversary, Nov., 1956, pp. 233 - 240.

Bascom, W. N., The relationship between beach width and size and beach-face slope, Trans. AGU, Vol. 32, No. 6, Dec., 1951, pp. 866 - 874.

Hayami, S., Adachi, S., and Tsuchiya, A., Fundamental study on beach erosion along Sen-nan coast, No. 4, On sediment materials along Sen-nan coast, Report of Investigation, Beach Erosion along Sen-nan coast, Vol. 2, Oct., 1952, pp. 3 - 26.

Bretschneider, C. L., Revised wave forecasting relationships, Proc. 2nd Conf. Coast. Engg., 1951, pp. 1 - 5.

Dunham, J. W., Refraction and diffraction diagrams, Proc. 1st Conf. Coast. Engg., Oct., 1950, pp. 33 - 49.

Mason, M. A., The transformation of waves in shallow water, Proc. 1st Conf. Coast. Engg., Oct., 1950, pp. 22 - 32.

Putnam, J. A., Loss of wave energy due to percolating in a permeable sea bottom, Trans. AGU, Vol. 30, No. 3, Jan., 1949, pp. 359 - 356.

Putnam, J. A., Munk, W. H., and Traylor, L. A., The prediction of longshore currents, Trans. AGU, Vol. 30, No. 3, Jun., 1949, pp.

337 - 345.

12) Inman, D. L., and Quinn, W. H., Currents in the surf zone, Proc. 2nd Conf. Coast. Engg., Nov., 1951, pp. 24 - 36.

13) Groen, P., and Weenik, M. P. H., Two diagrams for finding breaker characteristics along a straight coast, Trans. AGU, Vol. 31, No. 3, Jun., 1950, pp. 398 - 400.

14) Ishihara, T., Iwagaki, Y., and Tsuchiya, A., Fundamental study on beach erosion along Sen-nan coast, No. 5, On the beach slopes and the distribution of wave height along the Sen-nan coast, Report of Investigation, Beach Erosion along Sen-nan coast, Vol. 2, Oct., 1952, pp. 27 - 40.

15) Saville, T. Jr., Model study of sand transport along an infinitely long straight beach, Trans. AGU, Vol. 31, No. 4, Aug., 1950, pp. 555 - 565.

16) Sawaragi, T., and Murakami, M., Estimation of the rate of littoral drifts, Proc. 2nd Conf. Coast. Engg., Japan, Nov., 1957, pp. 41 - 49.

17) Iwagaki, Y., and Tsuchiya, Y., Fundamental study on critical tractive force, Trans. JSCE, No. 42, Dec., 1956, pp. 1 - 21.

18) Caldwell, J. M., Wave action and sand movement near Anaheim Bay, California, Beach Erosion Board, Tech. Memo., No. 68, 1956.

19) Watts, G. H., A study of sand movement at South Lake Worth Inlet, Florida, Beach Erosion Board, Tech. Memo., No. 42, 1953.

SAND TRANSPORT ALONG A MODEL SANDY BEACH
BY WAVE ACTION

Kinji SHINOHARA, Tōichirō TSUBAKI, Masuo YOSHITAKA,
and Chiaki AGEMORI

1. Introduction

In this report, an attempt has been made to clarify the mechanism by which the sandy beach profile changes due to waves and to evaluate the beach sediment moving thereby, i.e., the amount of beach drift. Beach drift is supposed to move on the beach surface by waves near the shore, especially by the breakers, or to float and transport by longshore current. Such phenomena of the beach drift moving by waves and changing shore line as this have been already given three dimensional experiment by Saville¹⁾ and Johnson²⁾. And Dr. Iwagaki³⁾ has also conducted measurement of two dimensional equilibrium profile and the distribution of sand transport which is in normal direction to shore line, obtaining interesting result respectively. In these experiments, however, sand of 0.3mm was used for beach sediments and the properties of the waves of deep water were so much alike, and if the result is applied to actual sandy beach, it seems to correspond to the case where the beach sediment size is comparatively large. Judging from the important part played by the sediment size upon the non-dimensional representation of tractive force of flow, the distribution of concentration of suspended load and its amount in sediment problem in rivers, the effect of beach sediments is considered to be extremely great. Accordingly, when experi-

mental results are to be applied to actual sandy beach, it is necessary to enlarge the sediment size to a wider range and to establish similarity between the property of beach sediments and that of waves. From such viewpoint as this, the authors have tried in this experiment to investigate sand transport by wave action at the beach of small sediment size by reducing the specific gravity, using pulverized coal instead of small size of sand. If classified roughly as in the case of river sediment, the form of sediment transport may be divided into the traction near the bottom and suspension, and in view of little attention hitherto paid to it despite of its practical importance as the cause for beach drift, they also measured the amount of bed-load as well as that of suspended load.

2. Experimental Apparatus and Method

The experiment was carried out in a water tank of organic glass, stiffened steel frame works, 50cm wide, 50cm tall and 20m long. The wave making machine was of flut-ter type and its general view is seen by the photographs 1 and 2. In this tank was made a model sandy beach, 4.5m long in the part of slope and 1/10 in gradient, as shown in the photograph 3. The depth of the water was made 35cm at all cases. As to the

measurement of wave property, wave length and mean wave height were evaluated at the adjacent part of the beach end by an electric point gauge, transforming it into the quantity of wave of deep water by the theory of waves with small amplitude. Height of breakers, breaking depth and the change of wave height near the plunge point were determined by piecing together the results of measurement from the side as well as those from pictures and electric point gauge. ^{The} Photographs 4 and 5 show the electric point gauge used for measurement devised by Mr. Awaya of this Institute. With a view to catching the sand that moves near the bottom, the authors adopted the method to bury at the bottom a sand trap which is provided with a rectangular opening, about 5cm long and 3cm wide, nearly the same with the apparatus used by Dr. Iwagaki. The sand trap was allotted one per a section, and measurement was carried out while sucking out the sand that fall through the opening together with water by means of siphon, putting no distinction between uprush and back rush. In using siphon, it is desirable to make its absorption rate as small as possible, because it leads to overestimate sand amount due to the generation of downward velocity on the surface of the sand trap. However, as the pipe becomes choked if velocity is too small, the standard for this experiment was placed at the condition where the velocity at the sand trap is almost equivalent to the settling velocity of sand and pulverized coal respectively. By the way, in order to prevent sand

from falling into the hole sideways, flanges were installed at the sides; 2mm one for sand, 1cm one for pulverized coal.

As it is impossible to sample sand with siphon on the land-side from the shore-line and as amount of transport also changes considerably according to the distance from the shore-line, measurement was made by burying a sand trap of 2cm long and 3cm wide for a given time and taking it up by hand. These sand-traps are shown in the photograph 6

The distribution of sediment concentration in depth direction of each section was examined, sampling suspended load with siphon by arranging glass tubes of 2mm inside diameter 4 ~ 10 per a section in zig-zag lines, covering the entire range in which sand moves from the beach-line. The photograph 7 shows the condition of sampling suspended load.

The beach sediments used for experiment are sand and pulverized coal with such grading curves as shown in Fig. 1, whose mean diameter is respectively 0.2mm and 0.3mm and almost uniform. Specific gravity of sand was 2.66 and that of pulverized coal 1.29. The settling velocity of sand and pulverized coal which was evaluated by dividing both according to diameter and was averaged by adding weight to grading distribution were respectively 2.19cm/s (water temperature 15°C) and 1.14cm/s (water temperature 25°C).

The property of wave submitted to experiment was 0.59 ~ 1.65 sec. in period, 1.49 ~ 5.68cm in wave height and 0.00922 ~ 0.0685 in initial steepness.

As to the method and order of experiment,



Photo.-1 Wave making apparatus (1)



Photo.- 2 Wave making apparatus (2)

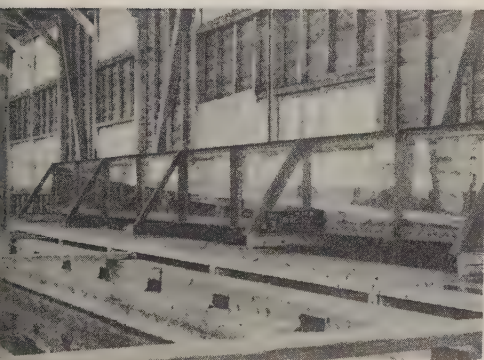


Photo.-3 Water tank



Photo.-4 Electric point gauge (1)

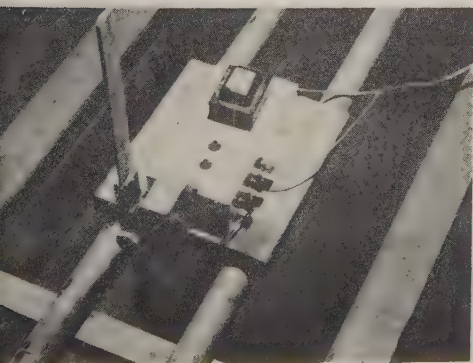


Photo.-5 Electric point gauge (2)



Photo.-6 Sand traps catching for bottom transport

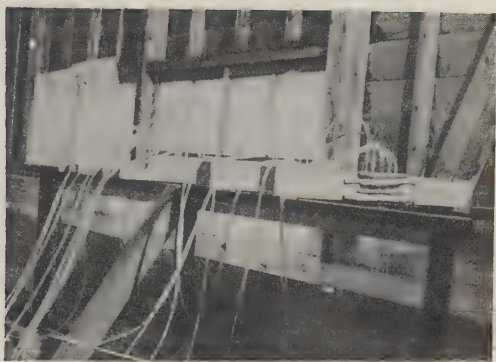


Photo.-7 Sampling suspended load

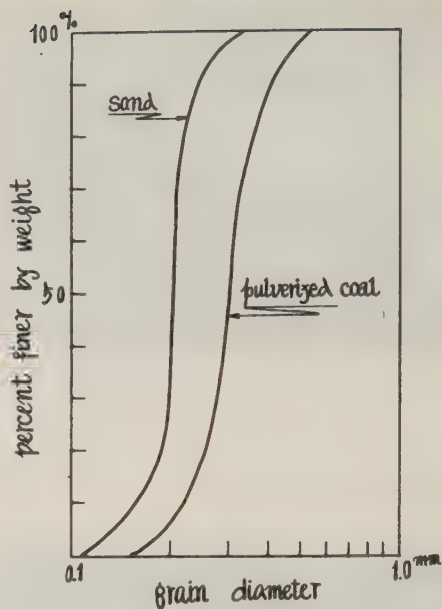


Fig.- 1 grading curve for beach sediments

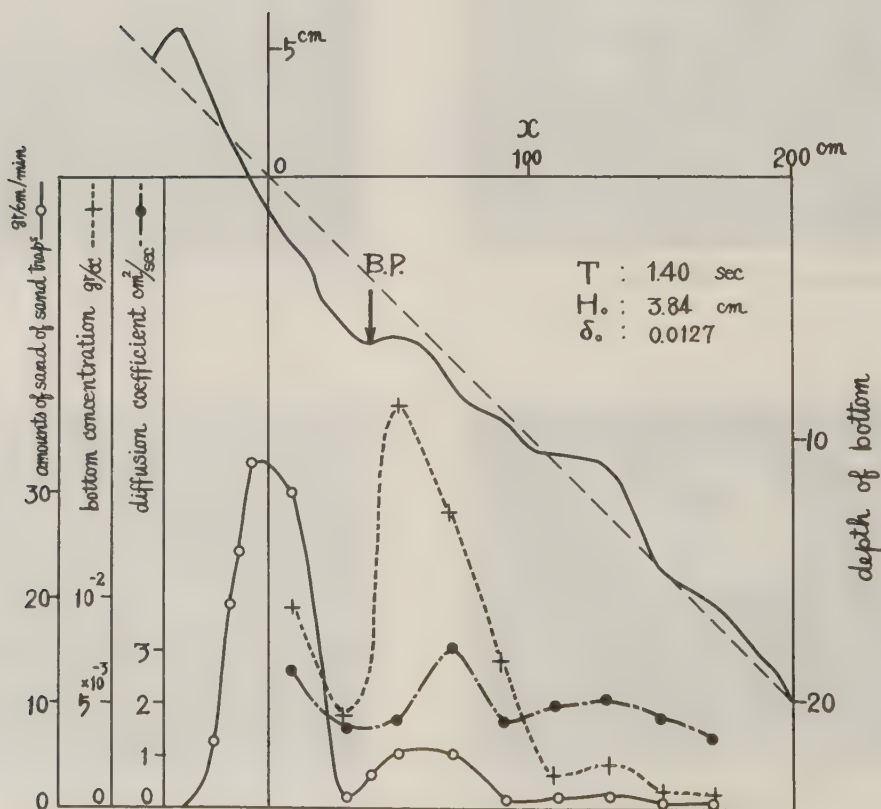


Fig.- 2.a Beach profile and sand transport (1)
(sand)

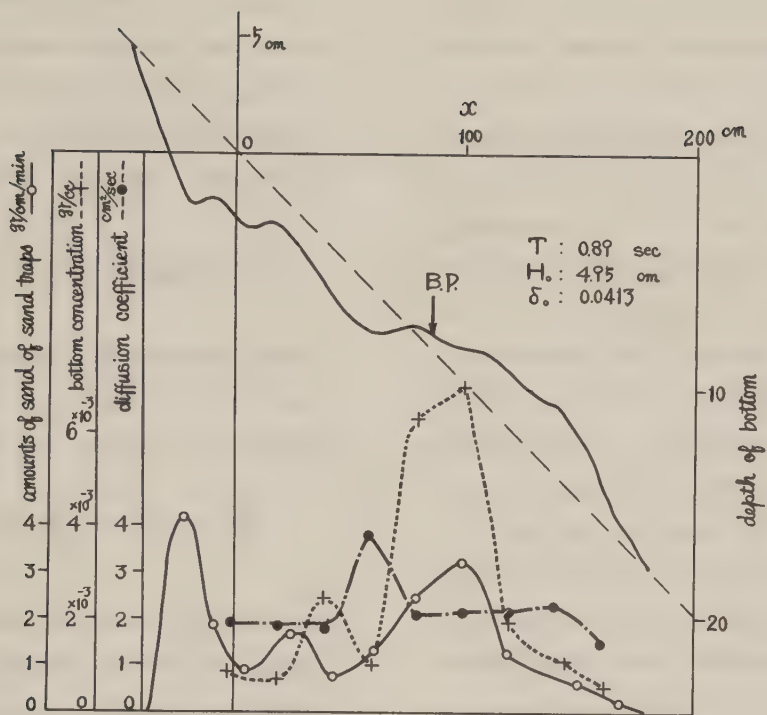


Fig.- 2.b Beach profile and sand transport (2)
(sand)

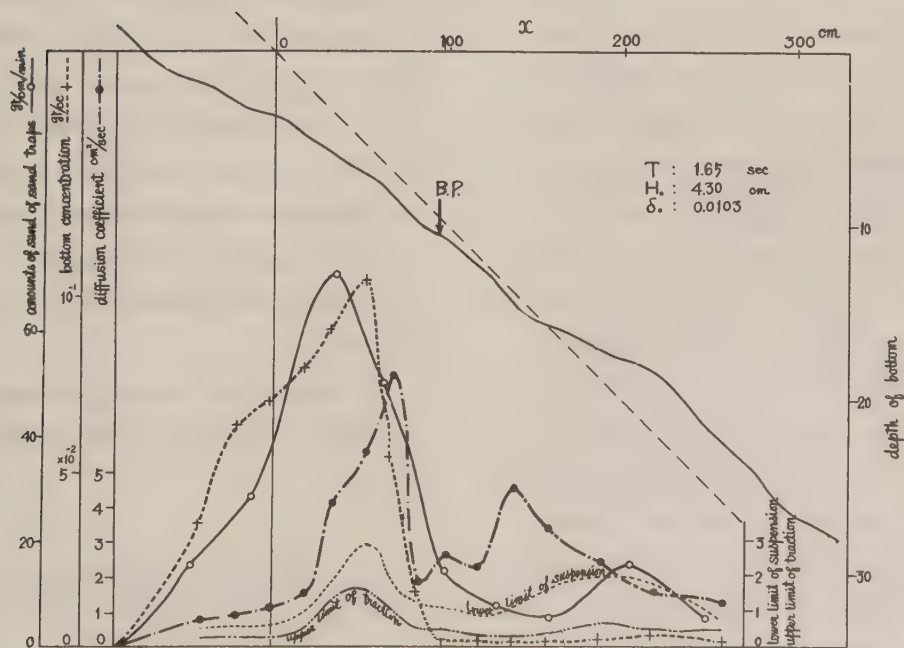


Fig.- 2.c Beach profile and sand transport (3)
(pulverized coal)

suspended load was measured after four hours from the beginning, when the beach was assumed to have nearly reached to its equilibrium condition, then beach profile was measured after 5 ~ 7 hours both at the sides and the central section and after that, measurement of the amount of sand transport on the bottom was done by means of sand traps. The result of experiment obtained by the above-mentioned method looks like the attached table, a part of which will become Fig. 2, when illustrated.

The original points in the figure are the shore line on the slope 1/10, and what is called "the amount of sand trap sand" represents the amount of sand that moves back and forth near the bottom. Explanations concerning to bottom concentration and diffusion coefficient will be given in later chapters.

3. Beach Profiles

When a given wave of deep water is sent to beach of a slope 1/10, it is gradually changed, approaching to a equilibrium condition corresponding with the characteristics of wave of deep water and the properties of beach sediment. Letting the depth from still water surface to the bottom be h to express this profile (Fig. -3), h is considered to be the function of (1) the property of waves, (2) the property of beach sediment, (3) the distance x from shore line which is made origin. As the properties of waves, wave height H_0 , period T , gravitational acceleration g or wave length L_0 are considered, and as the properties of sediment, specific gravity of beach sediment in the water δ and granular diameter D are

considered. Accordingly, taking axis x to the open sea making shore line origin, the beach profile reaching to a equilibrium condition is considered to be expressed by the following functional form:

$$\frac{h}{T^2g} = f\left(\frac{x}{T^2g}, \frac{H_0}{T^2g}, \frac{H_0}{\delta D}, \delta\right) \quad (1)$$

Letting wave length of the waves of deep water be L_0 , then $L_0 = gT^2/2\pi$, and, therefore, the equation (1) becomes

$$\frac{h}{L_0} = f\left(\frac{x}{L_0}, \delta_0, \frac{H_0}{\delta D}, \delta\right) \quad (2)$$

where $\delta_0 = H_0/L_0$ is initial steepness which is considered to be the parameter governing the property of breakers. Since height of breakers and depth of breaking are considered to be expressed as function of δ_0 according to the past studies, it is most important as the parameter providing for beach profile. It is also possible to consider $H_0/\delta D$ as follows, i.e., non-dimensional expression of the tractive force of stream flow is $U_*^2/\delta g D$ putting U_* for friction velocity. As for the velocity corresponding to U_* in case of waves,

(i) assuming δ_0 as small and having the property of long wave at plunge point, we get

$$U_* \sim \sqrt{g H_b} = \sqrt{g H_0} f_1(\delta_0)$$

H_b : height of breakers

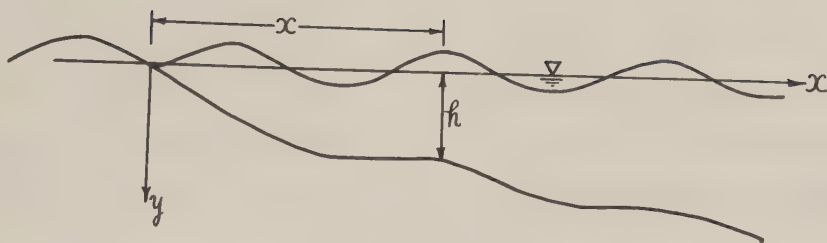


Fig.- 3

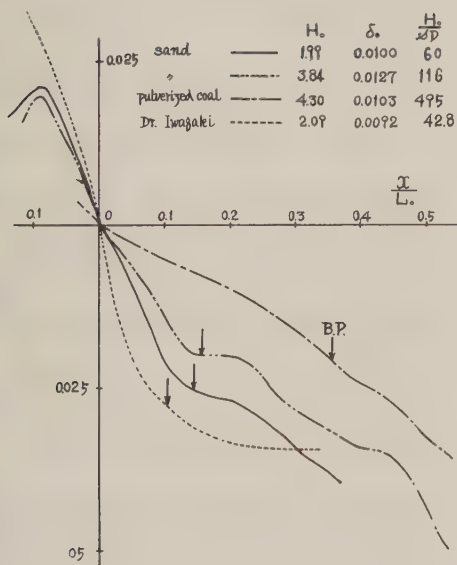


Fig.- 4.a equilibrium beach profile (1)

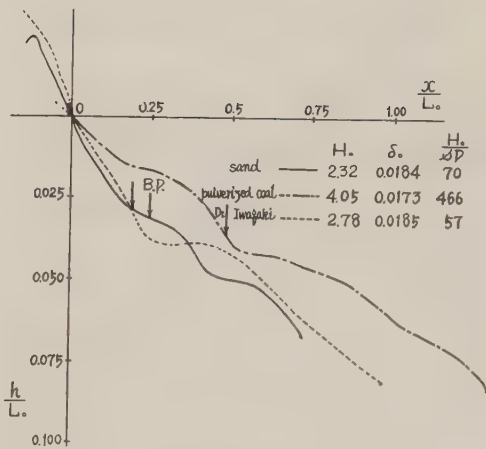


Fig.- 4.b equilibrium beach profile (2)

(11) and assuming it as having the property of surface wave, we get

$$U_x \sim H_b / T \propto H_b / T f_1(\delta_0) \sim H_b / L_b f_1(\delta_0) = \sqrt{g H_b} \delta_0^{1/2} f_1(\delta_0)$$

in any cases, the tractive force in case of waves will be expressed by

$$\frac{g H_b}{g D} f_1(\delta_0) = \frac{H_b}{D} f_1(\delta_0)$$

where H_b/D becomes parameter indicating the magnitude of tractive force in case of waves.

When beach profile of an actual shore where waves suffer such local effect as refraction and other is compared to an experimental one, it is desirable to express beach profile non-dimensionally with the property of breakers as Dr. Iwagaki has pointed out. In this case, it will suffice to represent beach profile with H_b instead of H_0 in the equation (1).

The experiment on equilibrium beach profiles has been made in full details by Dr. Iwagaki, but the sand used being 0.3mm in mean diameter and H_0 within the range of 2.05 - 5.88cm, the value of H_b/D in the equation (2) becomes 42.7 - 122.5 assuming $\mathcal{A} = 1.6$, and if applied to actual beaches, it corresponds to the case of beaches with the sediment of large granular diameter. As it is difficult in the experiment of sand to maintain similarity between the shore where beach is composed of fine sand and the experiment, pulverized coal was used to remove this difficulty, with success to enlarge the range of H_b/D for the same δ_0 five times.

According to the authors' experiments, it was $H_b/D = 59.9 \sim 170.8$ when sand was ^{used} and

$H_b/D = 350 \sim 640$ when pulverized coal was used.

With respect to the change of beach profile, the difference of equilibrium beach profile due to the change of initial steepness δ_0 , the effect of H_b/D and the relation δ_0 with the slope of foreshore were examined.

Fig. -4 shows beach profile expressed non-dimensionally when steepness is approximately 0.01, 0.18, 0.03 and 0.06, where the result of Dr. Iwagaki's experiments is also shown in broken lines for comparison. In Fig. -5 is given the relation of slope of foreshore I with δ_0 . These figure reveal that the slopes of foreshore and surf zone are considerably different according to beach sediment. That is to say, while both the results of Dr. Iwagaki's experiment and of the authors' experiment using sand for beach sediment correspond very well due to nearly the same H_b/D , the slope in the case of pulverized coal whose H_b/D is as large as about 4~6 times of sand is pretty small compared to sand. This seems to reveal that beach profile is subject not only to the steepness but to the effect of H_b/D . Since \mathcal{A} is nearly constant at an actual shore, it is considered to be due to this that the smaller the size of beach sediment is, the slower beach slope becomes.

In the experiment with sand as beach sediment, there the boundary becomes apparent between the part where beach profile has changed from its initial slope 1/10 and the part that suffered no change. The end

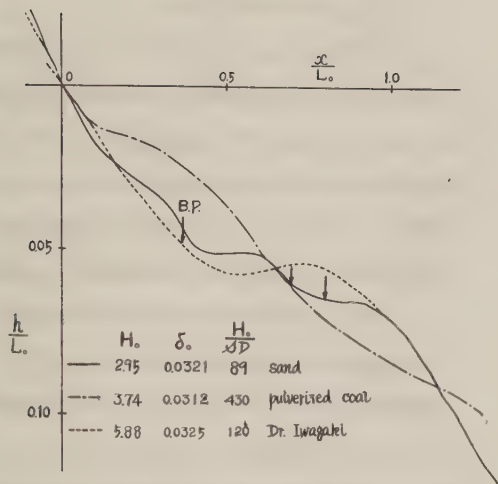


Fig.- 4.c equilibrium beach profile (3)

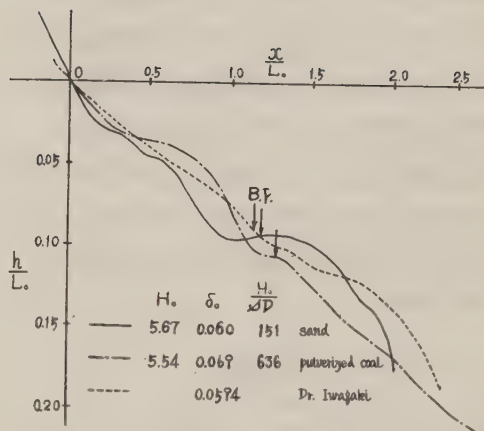


Fig.- 4.d equilibrium beach profile (4)

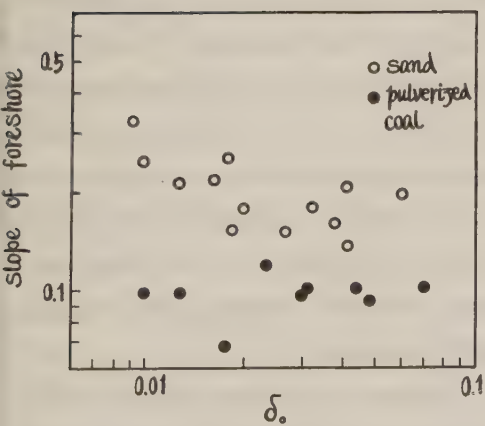


Fig.- 5 relation of the slope of foreshore I with δ_0

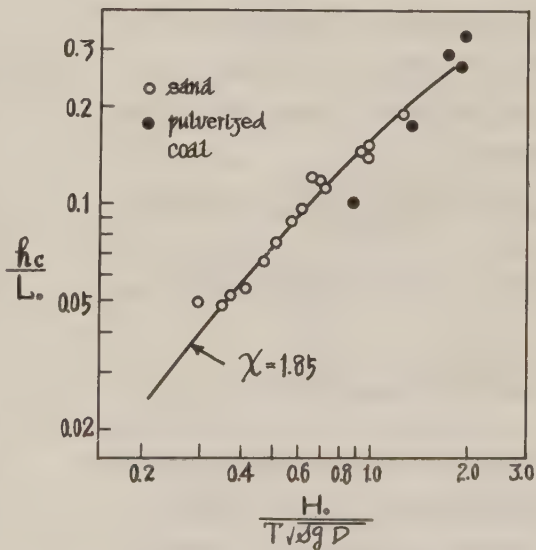


Fig.- 6 relation between $\frac{h_c}{L_0}$ and $\frac{H_0}{T\sqrt{gD}}$

point of the change of this beach profile is also considered to indicate the limit of sand transport. Dr. Seichi Sato⁴⁾ who assumed the transport limit of sand to be equivalent to the boundary condition in which shearing stress by waves can move sand has proposed following equation for transport limit depth h_c putting H for wave height of that point, L for wave length, and U_m for mean value of semicycle period of water particle velocity at the bottom,

$$\sqrt{\frac{D}{2.5}} U_m = \frac{\pi H}{2T \sinh \frac{2\pi h_c}{L}} \quad (3)$$

where, U_m is expressed in m/sec and D in mm . As for the definition of transport limit of sand, the points based on practical view are that transport grow less conspicuous or it entirely goes out, but the equation (3) corresponds to the former definition and the end point of the change of beach profile in the authors' experiment to the latter.

Letting velocity of water particle in x direction be u

$$u = \frac{\pi H}{T} \frac{\cosh \frac{2\pi}{L}(h+y)}{\sinh \frac{2\pi h_c}{L}} \sin\left(\frac{2\pi x}{L} - \frac{2\pi t}{T}\right)$$

accordingly, maximum velocity at the bottom is

$$u_{max} = \frac{\pi H}{T} \frac{1}{\sinh \frac{2\pi h_c}{L}}$$

When we consider the maximum fluid resistance due to maximum value of velocity of water particle $u_{max} \sqrt{\frac{D}{2.5}} = X$ is expected to take a given value X_c at the end point of the change of beach profile. Substituting, therefore, the value of wave of deep water for H and L , h_c/L will be given by the following equation

$$\begin{aligned} \text{tion as the function of } H/\sqrt{D} &= \sqrt{\frac{H}{D}} \sqrt{\frac{D}{2.5}} \\ \frac{u_{max}}{\sqrt{D}} &= X_c = \frac{\pi H}{T \sqrt{D}} \left[\tanh \frac{2\pi h_c}{L} \left(1 + \frac{4\pi h_c/L}{\sinh \frac{2\pi h_c}{L}} \right) \right]^{-\frac{1}{2}} \frac{1}{\sinh \frac{2\pi h_c}{L}} \\ \frac{\frac{2\pi h_c}{L}}{\frac{2\pi h_c}{L}} &= \tanh \frac{2\pi h_c}{L} \quad (4) \end{aligned}$$

According to the experiment of critical tractive force at rivers, the ratio of critical friction velocity U_{xc} to \sqrt{D} is $0.18 \sim 0.28$, though it varies according to sediment size.

Again adopting the velocity at the place detached one grain from the bottom, assuming it as representative velocity with respect to the sand transport at the bottom, it is considered to be $U_b/U_{xc} = 8.5$ and therefore, the value of U_b/\sqrt{D} will be $1.53 \sim 2.38$.

In case of waves using maximum value u_{max} of velocity of water particle at the bottom as the U_b , the result is to be $X_c = u_{max}/\sqrt{D} = 1.53 \sim 2.38$. Now evaluating the relation of h_c/L with H/\sqrt{D} assuming $X_c = 1.85$, it will be like Fig. -6, presenting a close resemblance with actual measurement. Putting again $X = 1.66$, $X = 4.04$ in the equation (4), we can get the equation (3). The fact that the value of this X is more than twice as large as the value of X_c which represents the authors' end point of the change of beach profile leads to a presumption that Dr. Sato's standard of transport limit indicates such depth where sand transport practically ceases to be conspicuous.

Examining the difference in beach sediment of sand and pulverized coal in the next place, while in the former, the larger δ_c grows, the more distinct longshore bar is shaped, in the latter, there is no growth of longshore bar, only assuming the linear shape

of nearly 1, 10 gradient. The longshore bar is considered to be formed by the sand that had been carried from surf zone to the part of waves of deep sea due to the back rush from plunge point and deposited from plunge point to transport limit point owing to the existence of transport limit of beach sediment. Accordingly, for the growth of bar, the distance of plunge point and transport limit is considered to be one of the important factors. In case of pulverized coal, the reason why it fails to form longshore bar may be ascribed to the fact that the preceding distance is long because of its large H_0/D and transport of beach sediment is observed all over the beach in most cases, being devoid of the function to hold beach sediments which are carried toward deep sea.

4. Sand Transport along the Bottom

As in the case of sediment of rivers, sediment transport by waves will be studied, dividing it into traction and suspension. There is the transition region between the bed load layer along the bottom and the suspended load layer above it, and it will be theoretically difficult to separate the sediment transport of the bed load layer and that of the transition region. The amount of sediment in suspension layer can be evaluated pretty accurately by absorbing sediment along with water through siphon and measuring concentration distribution, but it is empirically very difficult to measure sand transport in the bed load layer and transition region. In order to measure the amount of these sand transport, there seems to be, for the present,

no better method than to represent it with sand that fall into the sand trap buried in the bottom, but this method makes it difficult to prevent mixing of suspended load. On the other hand, by absorbing the sand that fell into sand trap along with water the amount of sand will depend upon the rate of absorption.

There is thus considerable difficulty in the experiment due to sand trap, especially in the case of pulverized coal, measurement error is great at the section where the amount of transport is larger, for the thickness of bed load layer and transition region amounted to a few centimeters, making it also hard to give it theoretical significance. The authors will tentatively assume here for simplicity that the sand that entered into sand trap represents the amount of the sand transported along the bottom.

Beach sediment forming beach seems to be transported by various reasons such as the current after plunge resulting from velocity of water particle of a wave or mass transport, disturbance due to impact, backrush and others, but amounts of transport and their distribution are extremely complicated. In this study, therefore, it has been made an object to examine its property through experiment, shelving any attempt to clarify theoretically sand transport along the bottom for future study.

Now the amount of sand transport (in absolute volume) that passes back and forth across unit width in unit time will be assumed here as $q (L^3/LT)$. Since the parameters related to q are H_0 , T and g will respect to waves of deep sea and s , D to beach

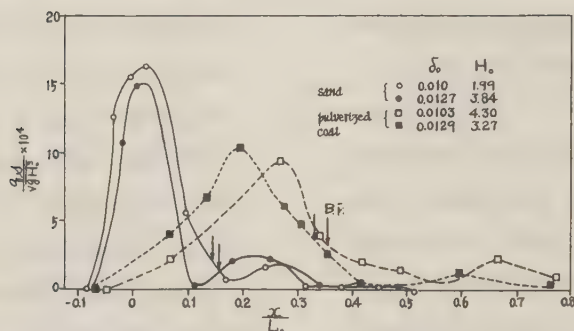


Fig.- 7.a relation between bottom sand transport (ϕ) and $x/L_o(1)$

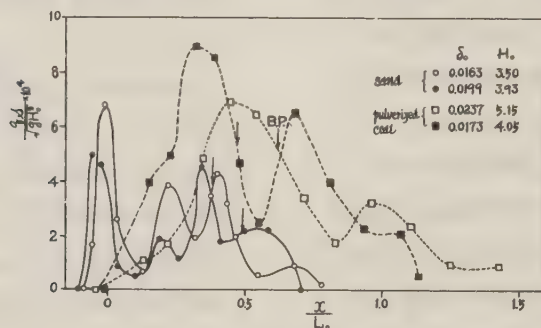


Fig.- 7.b relation between bottom sand transport (ϕ) and x/L_o

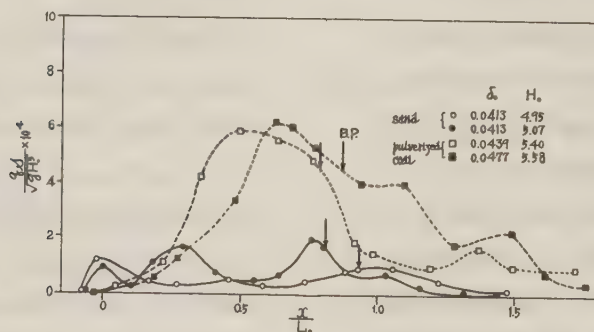


Fig.- 7.c relation between bottom sand transport (ϕ) and x/L_o

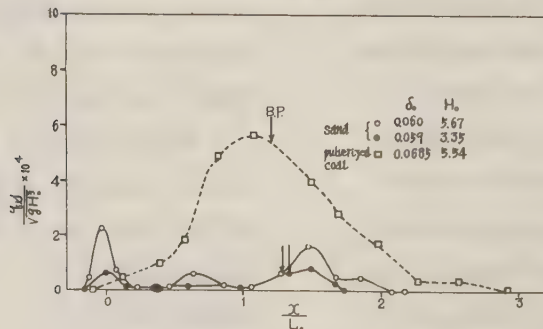


Fig.- 7.d relation between bottom sand transport (ϕ) and $x/L_o(4)$

sediment, following equation is conceivable for q :

$$\frac{q}{\sqrt{gH_0^3}} = f(\delta, \frac{H_0}{sD}, \frac{x}{L_0}, s)$$

On the other hand, in the case of rivers which are in equilibrium condition with respect to sediment, when tractive force is considerably larger than its critical value, the amount of sand transported along the river bed will be expressed as follows:

$$\frac{q}{\sqrt{s g D^3}} \propto \left(\frac{U_*^2}{s g D} \right)^{\frac{3}{2}} \left(\frac{U_*^2}{s g D} \right)^m$$

where the value of index m is $m = 1$ according to C.B. Brown,⁵⁾ and when it is only bed load, it is said to become $m = 0$. The above equation may be transformed as $q s g / U_*^3 = (U_*^2 / s g D)^m$.

In the case of sand transport by waves, it presents extremely unbalanced condition unlike the case of river sediment, and it seems to have sand transport mechanism different river sediment, being subject to such great influence as disturbance from impact beside the shearing stress due to current. Assuming tentatively, however, that an analogous inference is to be admitted, the amount of sand transport may be expressed by the following equation considering what corresponds to U_* as $\sqrt{gH_0} f(\delta_0, x/L_0)$.

$$\Xi = \frac{q s}{\sqrt{gH_0^3}} = f(\delta_0, \frac{H_0}{sD}, \frac{x}{L_0}, s) \quad (5)$$

Fig. -7 shows the relation of Ξ with x/L_0 by various steepness, from which it is proved that, when the beach sediment is composed of sand, sand transport is concentrated to the shore line in the case of a wave of small δ_0 , whereas, with the increase

of steepness, transport along the shore line is reduced, sand transport at the step of surf zone as well as at the longshore bar becomes conspicuous, and longshore drift predominates over all others. On the other hand, in the case of pulverized coal, no matter how large δ_0 is, sediment transport is seen to grow maximum at foam line just after plunge point, considerably affected by disturbance resulting from impact. It is also worth attention that sediment transport at foreshore is so extremely small that shoreline drift is negligible and that transport at the part of waves of deep sea is pretty large compared to the case of sand. As the reason for these, in the former, exhaustion of wave energy in the course of its ascent along mild slope is accounted for, while in the latter, considering from the well-known theory of sediment transport that sediment load rapidly increases with the increase of tractive force in the neighborhood of the critical tractive force, it is presumed to be possibly due to the largeness of $\frac{H_0}{T\sqrt{s g D}}$ or $\frac{H_0}{sD}$ which represents tractive force from waves in the case of pulverized coal compared to that of sand.

Fig. -8 gives the relation between non-dimensional expression of the total amount of transport Q of beach sediment and δ_0 .

In the case of pulverized coal, since the transport at the part of waves of deep sea becomes distinguished with the increase of δ_0 as mentioned above, the value of $\frac{Q s}{\sqrt{gH_0^3} L_0}$ increases with δ_0 , giving quite opposite result from the case of sand. What are

accountable for this in the two experiments are the difference in equilibrium beach profile due to the disparity of $\frac{H}{\delta D}$ for a given wave of deep sea by 5 times, that in the degree of effect suffered by the disturbance resulting from impact and that of sediment transport at the part of wave of deep sea. Some more reasons may be considered beside this, for instance, the facts that the shape of pulverized coal is flatter than that of sand and that specific gravity δ in the water exerts its influence directly, because sand transport by waves is periodic accelerated motion and suffers impact from the breaker. These problems, however, should be submitted to future study.

By the way, when sand is adopted for sediment, the value of $\frac{Q\delta}{\sqrt{gH^3}L_0}$ has decreased with the increase of δ_0 , provided that δ_0 is more than 0.02. According to Saville's three-dimensional experiment of drifts, the maximum amount of drift was produced at $0.02 \sim 0.025$ of δ_0 , but in the authors' experiment, whether maximum value is produced or not ^{has not} been clarified because of scattered measurement values.

5. Suspended load transport

The sand that is suspended by waves is expected to play an important role to long-shore drift as it keeps on drifting along the current as it is, but it seems that suspended load of this sort has been seldom taken up for study up to date. In this experiment, the authors conducted measurement at the area between the shore line and the end point of transport limit of sand, though they were unable to measure suspended load because of

small depth at the part of foreshore to the land-side from shoreline.

Fig -9 shows the relation between the concentration in the depth direction of each section C and the distance from the bottom y . In the case of sand, linear relation is held between $\log C$ and y , while in the case of pulverized coal, the phenomenon is extremely complicated, showing thin layer that is moved by waves in a condition close to saturation over the layer of settled sediments. The top of this layer will be tentatively called upper limit of traction. The concentration forms, as seen in Fig. -9 (C), the distribution of two straight lines of different slope. If the upper straight line is looked upon as suspension zone, the lower one is considered to be showing transition zone. Calling the intersecting point of these two straight lines as lower limit of suspension, the concentration of this point will be assumed as C_0 . In Fig. -2.C are given upper limit of traction and lower limit of suspension.

Since there exists linear relation between logarithm of concentration and depth with every case of sediment, as mentioned above, the concentration distribution may be expressed as follows:

$$\frac{C}{C_0} = e^{-\alpha y}$$

The distribution of suspended load by waves is considered to be determined by diffusion equation of unsteady and non-equilibrium state. Since the validity of the above equation has been empirically acknow-

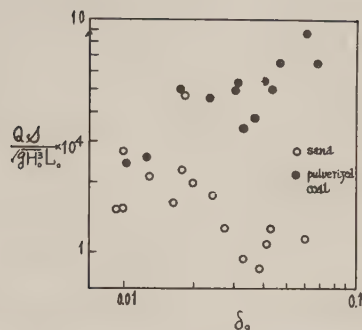


Fig.- 8 relation between $\frac{Q\delta}{\sqrt{g}H^2L_0}$ and δ_0

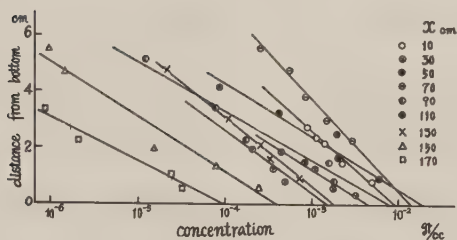


Fig.- 9.a Concentration distribution of suspende load (1)

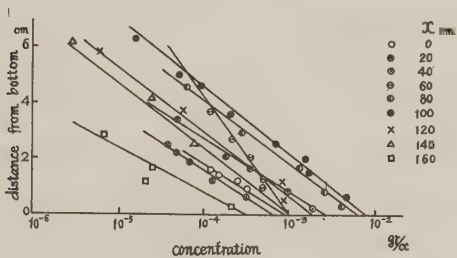


Fig.- 9.b concentration distribution of suspended load (2)
(sand)

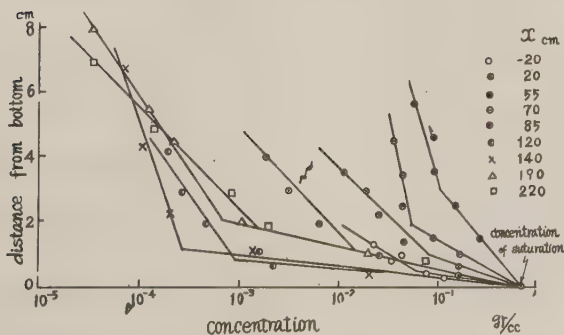


Fig.- 9.c Concentration distribution of suspended load (3)
(pulverized coal)

ledged, however, considering concentration distribution as steady and equilibrium state in average and putting U_s for settling velocity and \mathcal{E} for diffusion coefficient, concentration distribution is assumed to be in accordance with following equation,

$$C/C_0 = e^{-\alpha y}, \quad \alpha = U_s/\mathcal{E} \quad (6)$$

where, \mathcal{E} is explained as apparent diffusion coefficient in which is included the effect of the state of current or the effect of non-equilibrium state beside diffusion coefficient of turbulence. From concentration distribution of Fig.-9 is evaluated $\gamma = 0$ or concentration of lower limit of suspension C_s and from the slope of straight line, the value of α or \mathcal{E}/U_s is obtained. U_s being known, the value of \mathcal{E} is also obtainable. In Fig.-2 is given the change of C_0 and \mathcal{E} in X direction, which proves that \mathcal{E} slowly increases with the decrease of depth, more increasing before breaking. This is considered to be due to the current as if it were drawn up at the crest of breakers. This is pretty distinctly observed when sediment is composed of pulverized coal. Moreover, after breaking, it grows at a point which is considered to be foam line, especially it is conspicuous in the case of pulverized coal, forming almost uniform distribution in the direction of depth due to an intense disturbance. While at surf zone, in the case of pulverized coal, it gradually decreases, in the case of sand, it seems to decrease for once, suddenly increasing again when δ_0 is small.

Though the authors failed to conduct mea-

surement at the shore line, it is possibly estimated that a large \mathcal{E} will be obtained there independently of the value δ_0 owing to uprush and backrush advancing in piles to the steep slope of approximately 1/5.

The bottom concentration C_0 is expected to be larger where disturbance is stronger, and as transport along the bottom is subject to two kinds of actions of tractive force and disturbance, there is observed considerable correlation between the two.

Neglecting upward movement of still water surface by waves with longshore drift as object, when sediment is sand, suspended load S_b contained in the area between the shore line and plunge point as well as the total amount of suspended load S between the shore line and offshore side will be as follows from equation (6) :

$$S_b = \int_0^{l_b} \frac{C_0 \mathcal{E}}{U_s} (1 - e^{-\frac{U_s h}{\mathcal{E}}}) dx,$$

$$S = \int_0^{l_c} \frac{C_0 \mathcal{E}}{U_s} (1 - e^{-\frac{U_s h}{\mathcal{E}}}) dx$$

where it is provided that l_b , l_c are the distance between the shore line and the plunge point or the end point of transport limit.

In the above equation, diffusion coefficient \mathcal{E} can be transformed non-dimensional at $\mathcal{E}/\sqrt{gH_0^3}$ making δ_0 as parameter, and assuming C_0 as absolute volume of sediment in the unit volume, C_0 receives the effect of $\sqrt{gH_0}/U_s$ and δ_0 . Especially $\sqrt{gH_0}/U_s$ expresses the rate of the strength of disturbance due to waves and the settling velocity and is considered to play a most important role to C_0 .

Referring to Kalinske's theory concerning^{e)} to bottom concentration of suspended load in

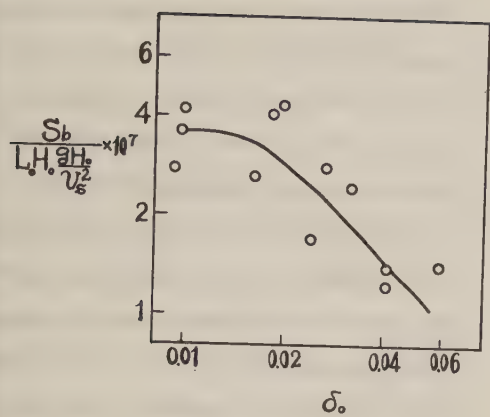


Fig.- 10.a

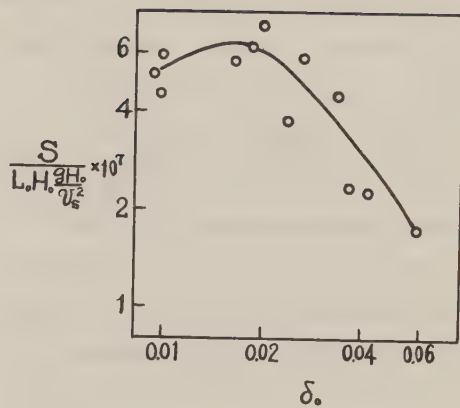


Fig.- 10.b

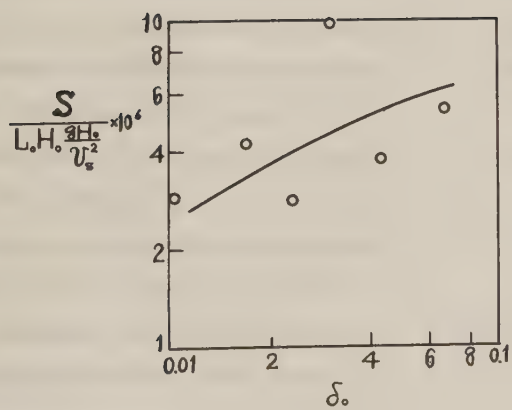


Fig.- 11

rivers, C_0 is considered to be in proportion with the index above 1 of $\sqrt{gH_0}/V_s$ to equivalent δ_0 . Hence non-dimensional forms of S , S_b may be put as

$$S \text{ or } S_b = L \cdot H_0 \frac{gH_0}{V_s^2} f(\delta_0, \sqrt{gH_0}/V_s) \quad (7)$$

In Fig. -10 is shown the result of test in the case of sand and in Fig. -11, that is the case of pulverized coal. The case of pulverized coal is about ten times of the case of sand. The latter is noticeable where it presents a tendency closely resembled to the relation in the case of non-dimensional expression of bed load in Fig. -8 and where maximum value is turned up with respect to the total amount of suspended load similar to Saville's^D experiment on beach drift.

As mentioned above, the clue to suspended load by waves is considered to depend on the clarification of characteristics of diffusion coefficient E and bottom concentration C_0 , but it is the authors' wish to wait for future experiments for the study of quantitative property of the both.

6. Summary

The most difficult problems in the application of the results of experiment on the change of profile of a model sandy ^{beach} A by waves and sand transport to actual beaches will be the establishment of the similarity due to difference in the size of beach sediment. In this study, as the important factor representing the characteristics of beach sediment besides the steepness of wave, the authors considered the ratio of hydraulic force of wave upon sand to frictional force or weight of

sand, H_0/LD and conducted tests on the profile of sandy beach and sand transport, using pulverized coal besides sand in order to bring this value close to sandy beach of smaller sediment size. As the value of H_0/LD in the case of pulverized coal is 4~6 times larger than that in the case of sand, it has been testified from the experiments about the profile of sandy beach that, expressing the relation of the distance and depth from shore line in non-dimensional form, H_0/LD grows large for the same initial steepness while beach slope of surf zone becomes slow, thereby approaching to the profile of actual sandy beach of small sediment size. And as to the sediment transport along the bottom, in the case of pulverized coal, it has been proved that transport near foam line is predominant, independently of initial steepness, that its distribution is considerably different from the case of sand and that the relation of non-dimensional expression of the total bed load with δ_0 (initial steepness) is extremely at variance with the case of sand. Furthermore, in the measurement of concentration distribution, what interested the authors in dealing with pulverized coal was that transition condition from traction to suspension zone has been distinctly apparent as well as the fact that concentration distribution in suspension zone can be expressed by a simple exponential form. Besides, the shapes of grains of pulverized coal which are somewhat flat seemed to affect more or less the mechanism of sand transport.

The fact that there was striking differ-

ence in the change of profile of sandy beach according to sediment size is considered to be probably caused by disparity in $H_0/\lambda D$ mainly, even if partially admitting the effect of the shape of sediment.

As mentioned above, the problem of sand transport by waves is difficult not only in giving theoretical treatment, being related with the current by breakers or the disturbance from impact, but also in depending only upon experiment, because more than two factors such as initial steepness or $H_0/\lambda D$ are involved in it. In order to get a general conclusion, therefore, it is necessary to clarify the mechanism of sand transport as well as to conduct many experiments and observations at actual sandy beach.

Acknowledgements

This study is a part of the result of the allotted work of the synthetic research, "Fundamental Researches on Coastal Engineering" which is now being pursued by researches headed by Prof. Ishihara of Kyoto University and financed by the Scientific Research Fund of Education Ministry. The authors express their warm thanks to Messrs. Ikeda, Susuki and Katashima for their assistance in equipping experimental apparatus.

Literature Cited

- (1) T. Saville, Jr.,: Model Study of Sand Transport along an Infinitely Long, Straight Beach. Trans. Amer. Geophys. Union, Vol. 31, No. 4, Aug. 1950.
- (2) J. W. Johnson: Sand Transport by Litteral Currents. Proc. of the Fifth Hydraulics

Conference, Bulletin 34, State University of Iowa Studies in Engineering, 1953.

- (3) Y. Iwagaki: Kaihin no Heikōkōbai to Saiha niyoru Sunaidō nikansuru Jikken. (Experiments on the Equilibrium Profile of a Beach and Sand Transport by the Breaker.) Kaigankōgaku Kōenkai Kōenshū, 1955.
- (4) S. Sato: Hyōsa ni Kansuru Kenkyū (7). (Researches on the Sand Drift.) Doboku Kenkyusho Hōkoku No. 85, 6, 1952.
- (5) H. Rouse: Engineering Hydraulics. PP. 799.
- (6) A. A. Kalinske: Movement of Sediment as Bed Load in Rivers. Trans. Amer. Geophys. Union, Vol. 28, No. 4, 1947.

Authors, SHINOHARA, YOSHITAKE,
AGEMORI; Kyushu University, Fukuoka
Tsubaki; Yamaguchi University, Ube.

Appendix

Beach Sediments	δ_0	H_0 cm	H_b cm	L_0 cm	$\frac{H_0}{\delta D}$	I	$\frac{R_c}{L_0}$	$\frac{H_0}{T\sqrt{gD}}$	$\frac{Q\delta}{L_0\sqrt{gH_0^3}}$	$\frac{S_b}{L_0H_0\frac{2H_0}{\gamma_s^2}}$	$\frac{S}{L_0H_0\frac{2H_0}{\gamma_s^2}}$
Sand	0.0092	2.84	4.20	308	84.6	0.318	0.0487	0.356	1.54	0.279	0.516
	0.0097	3.07	4.50	316	92.2	0.256	0.0522	0.378	1.57	0.368	0.459
	0.0100	1.99	3.85	200	59.8	0.240	0.050	0.301	2.77	0.423	0.593
	0.0127	3.84	5.64	302	114.5	0.218	0.0678	0.483	2.11	0.120	-
	0.0163	3.50	4.25	215	104.4	0.225	0.0766	0.522	1.64	0.266	0.566
	0.0179	2.11	3.71	118	63.4	0.264	0.0550	0.421	2.24	0.341	-
	0.0184	2.32	3.70	126	68.9	0.159	0.0675	0.498	4.78	0.412	0.630
	0.0199	3.93	5.66	197	118.4	0.181	0.0966	0.616	1.99	0.437	0.733
	0.0241	2.96	3.53	123	88.4	0.290	0.0895	0.583	1.75	0.171	0.383
	0.0268	4.10	5.40	153	122.5	0.155	0.1175	0.720	1.29	0.288	0.582
	0.0321	2.95	3.52	192	87.8	0.182	0.125	0.664	0.925	0.245	0.443
	0.0378	2.85	3.29	75.5	85.0	0.167	0.119	0.714	0.831	0.0711	0.239
	0.0413	5.07	5.10	123	153.8	0.140	0.142	0.988	1.09	0.123	0.229
	0.0413	4.95	6.00	120	148.8	0.212	0.150	0.976	1.24	0.140	0.289
	0.0588	3.35	3.80	57.0	100.0	0.115	0.149	0.976	0.501	0.142	0.178
	0.0600	5.67	5.98	94.5	171.6	0.200	0.190	1.29	1.13	0.205	0.457
Pulverized Coal	0.0103	4.30	7.8	418	495	0.100		0.892	2.45	2.83	2.89
	0.0129	3.27	4.2	254	376	0.100		0.875	2.55	-	-
	0.0173	4.05	5.3	234	466	0.070		1.128	4.96	4.09	4.16
	0.0237	5.15	6.3	217	592	0.122		1.494	4.61	2.72	2.81
	0.0305	3.12	3.2	102	359	0.100		1.336	4.92	-	-
	0.0312	3.74	4.2	120	430	0.105		1.472	5.28	9.71	9.80
	0.0371	4.44	4.5	120	510	-		1.738	3.72	-	-
	0.0407	4.80	5.3	120	552	-		1.847	5.38	-	-
	0.0439	5.40	6.0	123	621	0.105		2.078	4.94	3.67	3.69
	0.0477	5.58	5.8	117	641	0.095		2.197	6.41	-	-
	0.0618	3.40	3.0	55.0	391	-		1.973	8.62	-	-
	0.0685	5.54	5.6	80.8	636	0.105		2.598	6.46	5.13	5.30

FIELD INVESTIGATION OF SUSPENDED LITTORAL DRIFT

Hisao FUKUSHIMA
Yutaka MIZOGUCHI

Introduction

There are various methods which have been employed for investigating the suspended sediment in the sea. In the laboratory a pumping method is often used. Some researchers have employed samplers made of cotton cloth to gather the suspended sediment in the sea as well as in the river. A pump-type sampler was designed by G. W. Watts to procure sediment samples by pumping a quantity of sediment-laden water from a selected point. It was used for gathering the suspended sediment in the surf zone at Pacific Beach near San Diego.

In Japan there are many sand beaches in natural condition. Erosion and sedimentation in or around the harbours is constantly occurring, but no piers are found as suitable places from which to sample the sedimentation. Within the past several years, the present authors have designed a convenient sampler which has proved to be satisfactory for the purpose. The apparatus consists of bamboo poles with small holes and concrete blocks to anchor to the sea bottom. Such apparatus can, on account of its low cost, be set at many points over the surf zone where the observer wants to gather data. At each point, the vertical distribution of suspended materials can also be procured easily. The

sampler is a kind of integrator. It stands erect in the sea on account of its buoyancy, and acts as a buoy, also it can be easily drawn up.

Apparatus and Procedure

The lower part of the sampler is shown in Fig. 1. Below the joints, elongated holes 5^{cm} in length and 5^{mm} in breadth are made through the pole. The whole length of the bamboo poles is about 5 meters or so; they are about 5^{cm} in diameter.

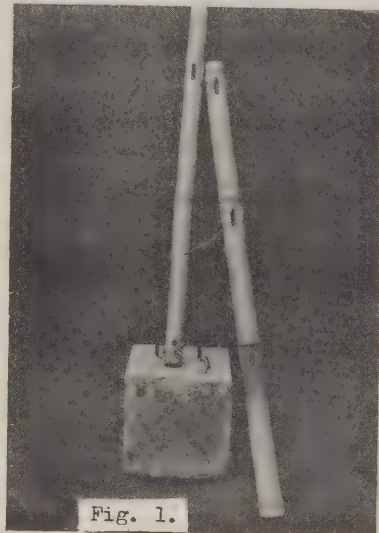


Fig. 1.

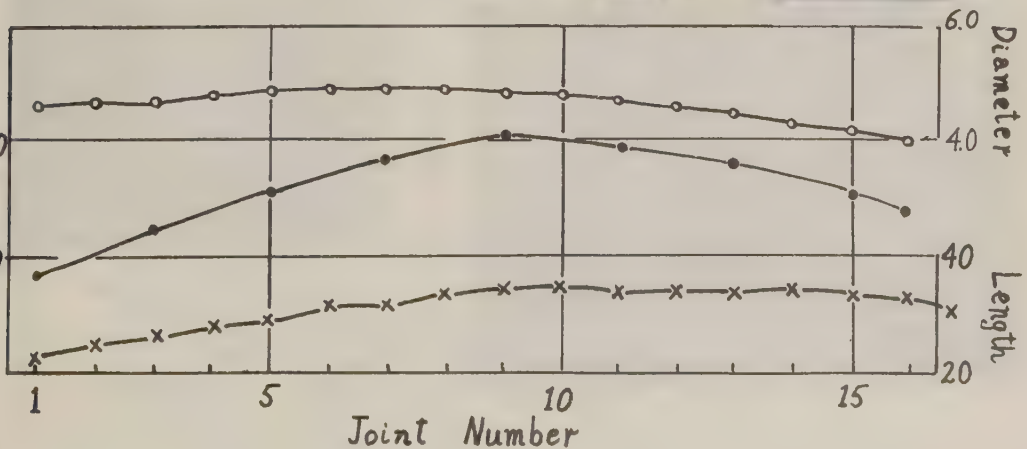


Fig. 2

In Fig. 2 an example for the characteristics of a pole is shown. The interval between two successive joints, mean outside diameter, and the volume of the hollow space are plotted against the joint number. The interval increases with the joint number. The curve of the volume V has its maximum at a joint higher than the middle one.

The lower end of the pole is connected to the block of concrete which weighs about 20 kg in the air.

Sounding the depth of the sea at the station where the observer wants to set the sampler, he selects bamboo poles which are about 1 m longer than the depth and sinks them from his boat with their blocks. The bamboo pole stands vertically in the calm sea. The poles are almost incessantly inclined and even swung by the winds and waves; the elvation of the holes which are under the water surface also varies by the tides. But unless the sea is very shallow, the fluctuations of the elvation can be neglected; tolerable masses of sediment are obtained.

After one week or so, when the sea is calm, the bamboo poles are drawn out of the sea water and are cut carefully in lengths of about 1 m . The holes must be closed as quickly as possible with ordinary black tape commonly used for electric insulation, lest the contents should run out of the hole.

The poles are taken to the laboratory, where the sediment materials in the bamboo hollows are taken out by cutting the joint. Then they are desiccated and weighed.

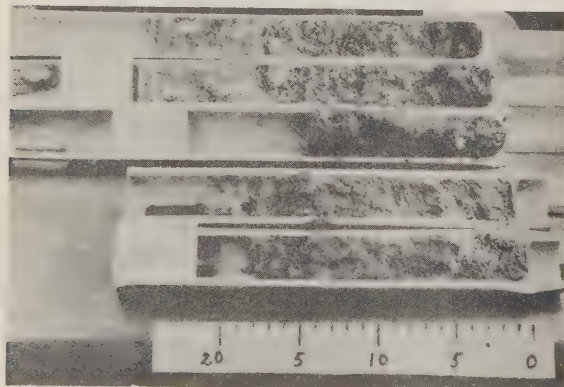


Fig. 3.(a).

The concentration of the suspended load is generally the largest near the bed of the sea. To sample the materials near the bed where the block is anchored, a short pole is specially readied and adapted as shown in Fig. 1. Actually this short pole gathers the most materials.

Results

By the procedure above mentioned, observations have been carried out at many points along the coast of Hokkaido. The contents gathered in the poles have been taken out by cutting the bamboos lengthwise. In most cases, rich rough sands are taken as a soft block. Sometimes these blocks consist of some strata, which are distinguishable each other. Fig.3 shows such stratified contents. These are samples obtained on the coast at Tomakomai. The white strata are volcanic sand which seemed to drift on the bed during certain intervals of time.

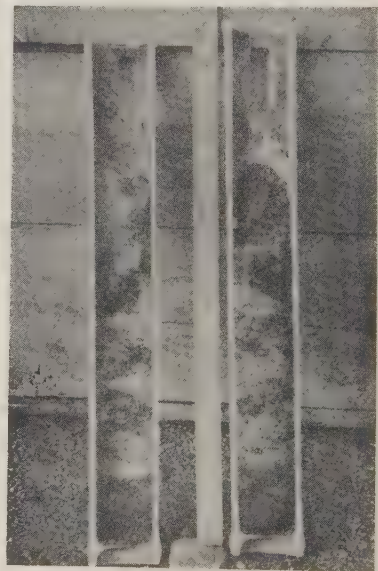


Fig. 3. (b).

A profile of vertical distribution of the mass of material obtained by the sampler on the coast at Tomakomai is shown in Fig. 4. Distribution curves generally may be classified in the following three types.

(I) At the shorelines where the depth is a few meters and the waves stir up the sands, the curves are much apart from the ordinate, showing that the "Austausch" coefficient is very large.

(II) Within the surf zone the quantities of the sampled materials are much less than those gathered at the bottom; in the latter region masses of material gathered by sampler rapidly increase, showing that the sand is drifting in large quantities along the bed.

(III) Outside shore of the area of the sand ridges where the depth is over 10^m , sand drift is still observed, but the distribution curves show very small values, and the bed load is something more than a suspended one.

In Fig. 4 types II and III appear somewhat alternately.

In the zone beyond the ridges, drifting seems to be remarkable. Some of the distribution curves which were obtained by plotting the depth against the logarithms of the mass of the sampled material, are shown in Fig. 5. These examples have been observed at Tomakomai in 1954. The

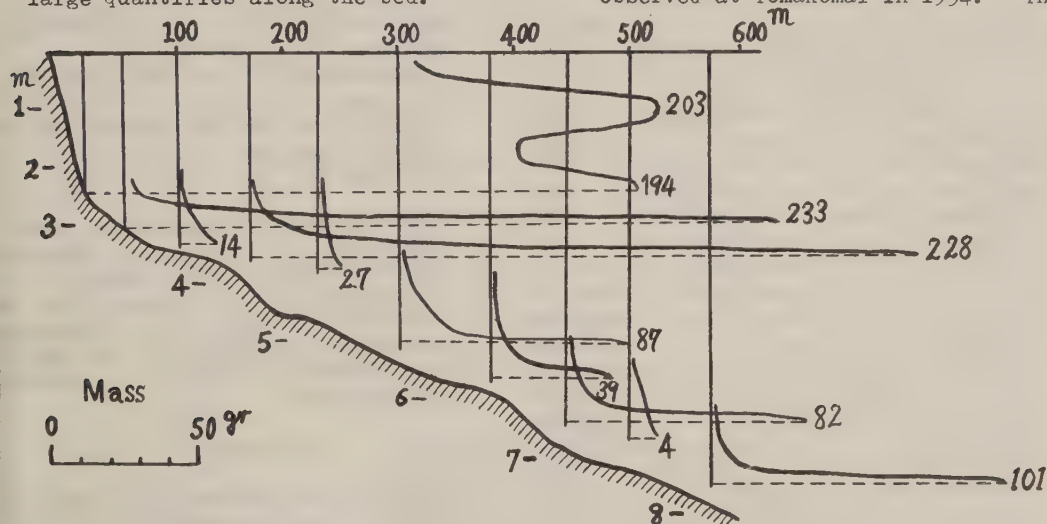


Fig. 4

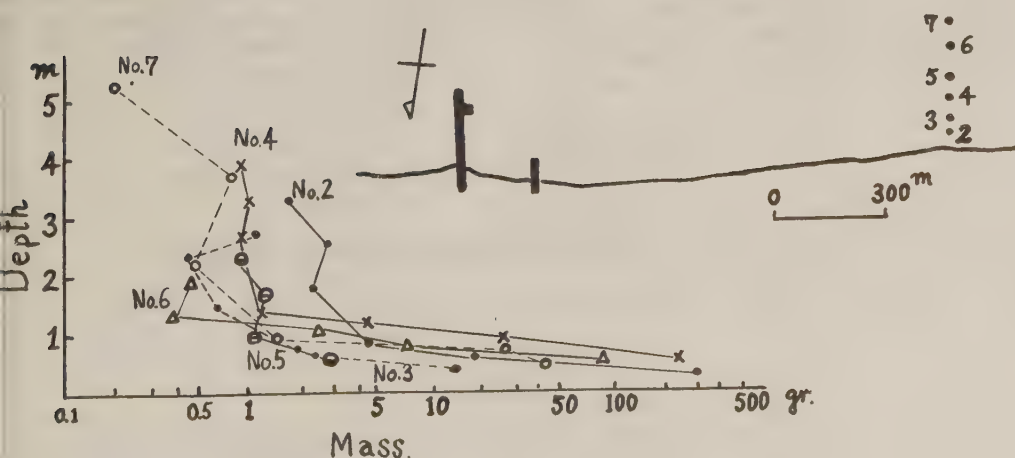


Fig. 5

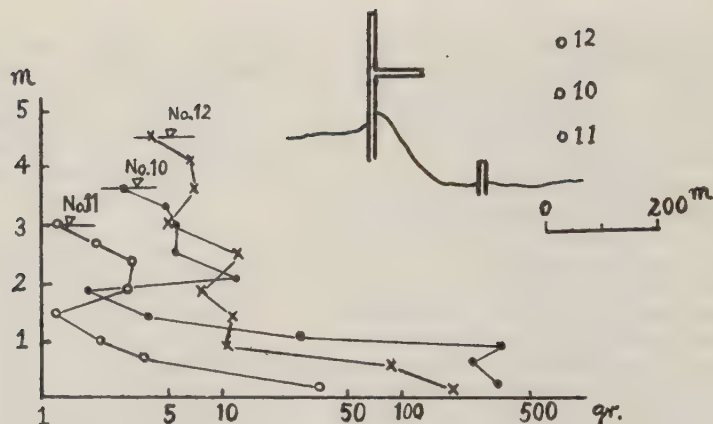


Fig. 6

samplers were set on the 22nd of August and taken in after four days. The surfs were not observed during that period. The curves consist of two parts. In the layer of about 1 m thickness above the bottom, the mass increases exponentially with the depth. The inclinations of the lower part of the curve are almost the same for each station. Those characteristics have been observed in many data. The upper parts of the curves are somewhat zigzagged, but these fluctuations can be smoothed practically.

If the concentration of suspended load is simply assumed to be proportional to the sampled mass, the upper part of the curves correspond to the small value of the ratio W_0/η , where W_0 and η represent the terminal velocity of the particle and the "Austausch" coefficient respectively.

Similar three curves which were obtained at the same coast, are shown in Fig. 6. Although they seem to be complicated, the values plotted are not randomly distributed. They show the upper layer of the sea transport-

ing suspended materials stirred up at the beach to the westward.

Experiments on the sensitivity of the sampler for the grain size of the sediment and for the current velocity passing through the hole are now under way.

In conclusion the authors wish to thank Prof. Y. Ikeda who encouraged them and gave suggestions. The investigation was supported in part by a Grant in Aid of a Fundamental Scientific Research from the Ministry of Education, which is gratefully acknowledged.

References

- 1) Ikeda, Y. T. Soeya and Y. Mizoguchi (1952). Drifting Sand in the Sea; Journal of the Faculty of Science, Hokkaido Univ. Series II, Vol. IV, No. 2.
- 2) Watts, G. M. (1953). Field Investigation of Suspended Sediment in the Surf Zone; Proc. Fourth Conf. on coastal Engineering.

Authors. Hisao FUKUSHIMA

Professor of Hokkaido University, Sapporo.

Yutaka MIZOGUCHI

Professor of Defence Academy, Yokosuka.

CONSIDERATION BY FUNDAMENTAL TEST OF JETTY IN RIVER MOUTH

Tamotsu KUBO *

1. General Consideration

In the different direction of model tests of small scale of the prototype, this hydraulic experiments of the jetty in a river mouth (or an estuary) are so fundamental, small and not specific. Hydraulic model tests are not generally satisfied with the law of similitude of the water flow and the movement of sandy loads. But this test is so fundamental that the results from it have no relation with such law of similitude. Therefore results of this paper are valuable not only for the phenomenism, but also for fundamental establishment of the design of a jetty.

Forces to such jetties are the action of river flow, wave attacks etc., but in this paper are limited to actions of a river flow only.

The water tank for this test is as Fig.1.

The water is circulated by the

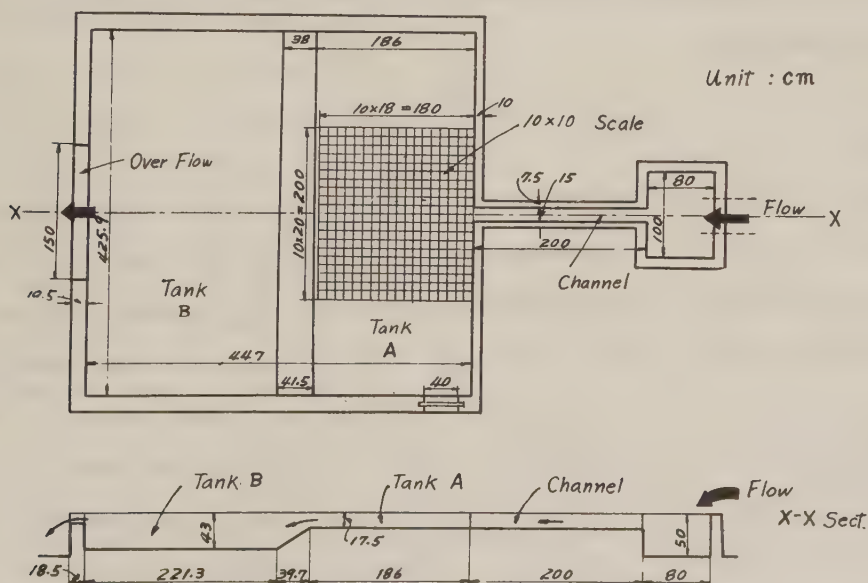


Fig.1

* Member of the Japan S.C.E.; Faculty of Engineering, Tokushima University; Tokushima City, Japan

3 inches pump which is connected to the 3 horse powers electric motor, and fine sands which were made from Toyoura (Japan) are entrained by the water flow. Features of water flow and sand sediments are taken by 35 mm films of a camera and analysed from the developed photos. Sandy loads out of a river mouth are entrained by the flood which is a jet flow (or super critical flow) by this jetty. And deltas by the growth with sandy sediments at a river mouth show as following three types; (1) Delta type in a sea bed; in this type the sea water is denser than the river water, (2) Delta type by Gilbert; in this type the density of sea water is equal to that of the river water, and (3) Delta type at the sea coast; in such type the river water is denser than the sea water. [1]. Actually the information of the sedimentation of sandy load is difficult fundamentally, but it seems that in the actual feature deltas show often the Gilbert type.

And in this test the river bed has the same height of the sea bed, and both beds are made of cement mortar. Therefore, though the actual bed is scoured by water flow, the bed in this case is fixed and not scoured, but from the results of this experiment it is perhaps understood in what way by the effect of the jetty in a river mouth the sandy loads move.

2. Jet Flow

The jet flow of water from the outlet can be researched by the method that had been studied by Tollmien [2], Albertson [3] and S. Chiaki [4] etc. But these studies were on the steady and mean average values on the flowing time. But as the flows in which the breadth of water channel are suddenly broad, are shown often the type as Fig. 2. a, b, and c, main stream is so meandering, moderately bending or nearly straight. And the part of jet flow in the coast is straight and perpendicular to the shore line. These parts of straight line and meandering of the main flow should have relation to the motion of sandy loads. The part of straight line of flow is due to the inertia of jet flow in the river mouth, and the meandering flow depends on the vortex motion of sea water.

Those vortices are seemed to depend on the law of Karman's row; or the steady

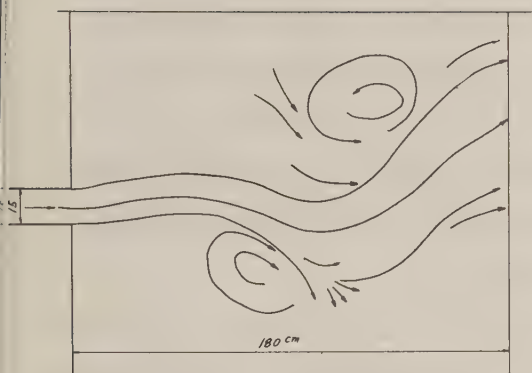


Fig. 2.a

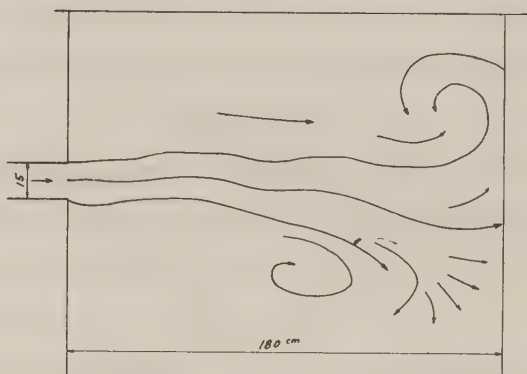


Fig. 2.b

vortex by him were shown that the ratio of breadth h to distant l had $\cosh^{-1}\sqrt{2}/\pi$ (or $h/l = 0.2806$).

From many photos in this experiment on jetties of various kinds, the mean value of the coefficient h/l is nearly equal to 0.2806 by Karman. The motion of sandy loads at the sea bed must depend on this vortices and the meandering of the main stream from the river. In stead of these

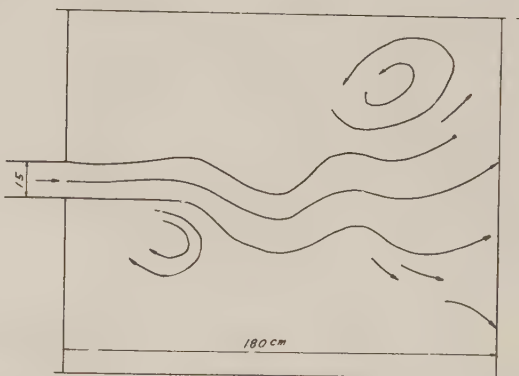


Fig. 2.c

vortices and meanders, if the main

flow of a river is steady and diffused to the sea water, the end of the main flow which parts from the outlet or a river has low speed and a little tractive force, and therefore can not scour the sea bed or flush the sandy loads. But since the stream is concentrated on the main flow and meanders left and right, the beds part from the coastal line may be scoured.

If the flow out of a river is not a jet flow, the scouring feature differs from that above mentioned. At the jetties in the estuary, for the purpose of the bed loads, the flows must be accelerated and made jet flows. For the flow becomes a jet, the breadth B of a jetty mouth must be as a following equation; that is

$$B < Q/\sqrt{gy}$$

where, Q; discharge from the river, g; gravity acceleration, and y; depth. Since jet flows are more straightened to the offshore than a tranquil flow, the tracted sandy loads are flushed away from the river mouth.

In a jet flow, the length of the straight part of main flow depends on the velocity or the discharge at the mouth of a jetty. Following Fig.3 shows the relation between the length and the velocity

in this test. From this figure, it is found that the length straightened becomes long as the velocity increases.

Perhaps in this straight part of the main flow the tracted sandy loads may be impossible to sediment immediately.

Or it seemed that the flushing of the sandy loads by the water depends essentially on this straight part of a

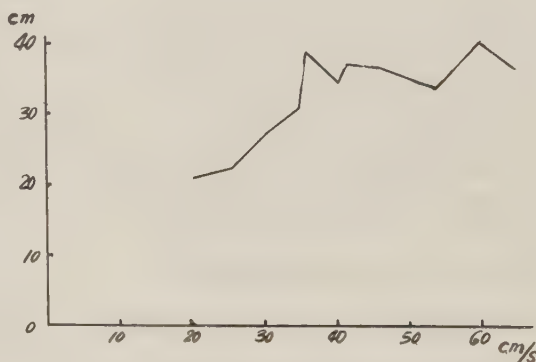


Fig.3

jet flow. Therefore if the width of jetty mouth is smaller, the straight part is longer for the same discharge of the river, and the sandy loads may be flushed far away from the coast.

3. Diffusion of a Jet Flow

As the main flow from the estuary appreciably meanders, the velocity of any point is so variable by the time. And as the water surface is disturbed and vortices are not fixed, therefore the velocity at any time is difficult to measure. By the home-made Pitot tube, high speeds and low speeds velocities were measured at each ten times continuously in this test. Mean values of these velocities are shown as follow-

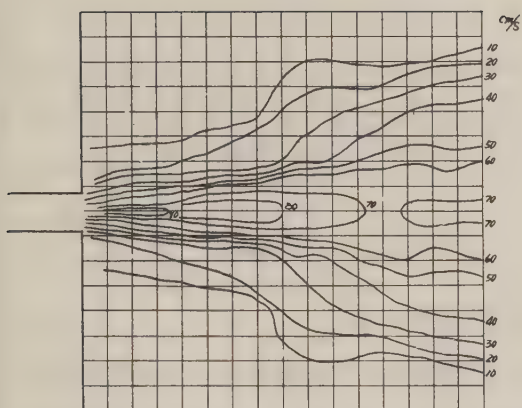


Fig.4.a

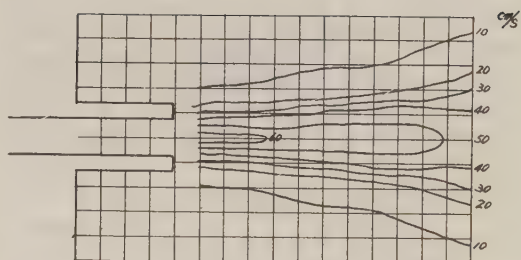


Fig.4.b

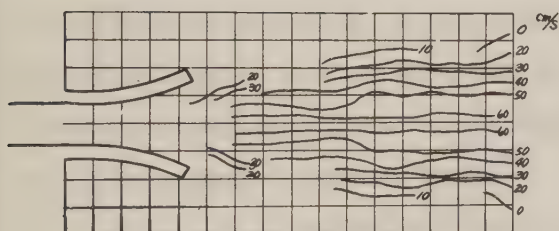


Fig.4.c

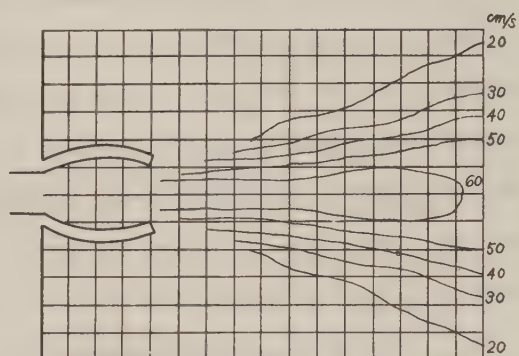


Fig.4.d

Mean Value of High Velocities

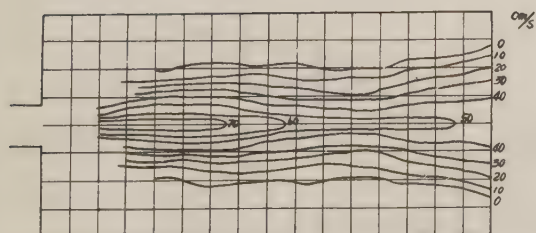


Fig.5.a

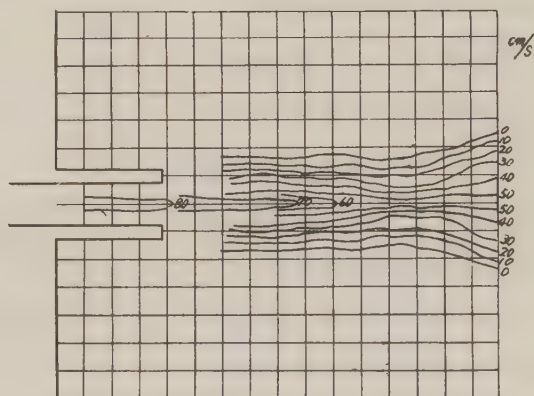


Fig.5.b

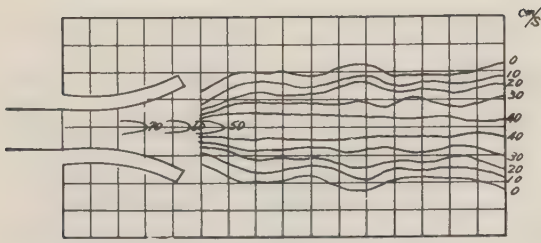


Fig. 5.c

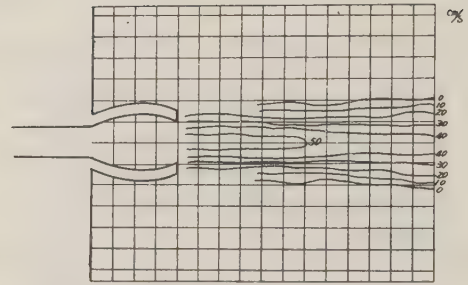


Fig. 5.d

Mean Value of Low Velocities

owing Fig. 4.a, b, c, d and Fig. 5.a, b, c, d. From these figures it thinks that in comparison with four shapes of jetties, the no jetty type has the highest velocity at the center line in the main flow at the same distance from the river mouth, and it seems that the angle of diffusion is largest in the case of no jetty. The author thinks the reason why the flow has the highest velocity and the largest angle of diffusion in the case of no jetty as following; that is, by little secondary flow or little energy-loss in no jetty at the river mouth, the jet flow is flushed away from the river mouth, but in the other jetty types a secondary flow at the mouth grows and the energy-loss of a flow increases. Therefore jetties for flushing away sediment loads must be constructed with the broad and massive body.

The curve of boundary of the jet flow from a small orifice has a parabolic shape in that of the jet flow by Tollmien's theorem. From

photos by this test the shape of the diffusion of the jet flow from the jetty is as following Fig. 6 and 7. Or Fig. 6 shows the relation between the breadths B_2 of the boundary of diffusion and the distances from the mouth by several discharges.

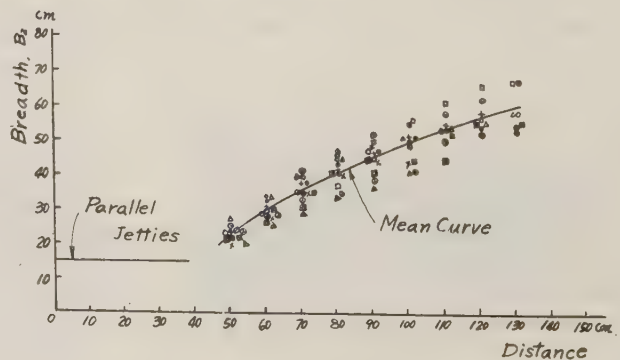


Fig. 6

$$1/D = (B_2/D)^2 / k_1 - k_2$$

the width of the channel, B_2 : the breadth

of the diffusion, and k_1 and k_2 are coefficients varied with the discharge (in this test $k_1 \approx 2.4$, $k_2 \approx 0.458$).

The feature of the sedimentation of sands is shown in Fig.8. And the width of sedimentational part B_1

and B_2 (in the figure) are variable by the discharge and the durational time of this test. In

Fig.9, 10, 11, 12 and 13
these variations are
shown. From these fig-
ures it is seemed that

in the quantity of discharge which is larger than 3.5 lt/sec, after

several minuits from the beginning of the experiment, B_1 , B_2 and $(B_1 - B_2)$ are not so variable by discharges and times. The relation between the ratio of l and the width D of

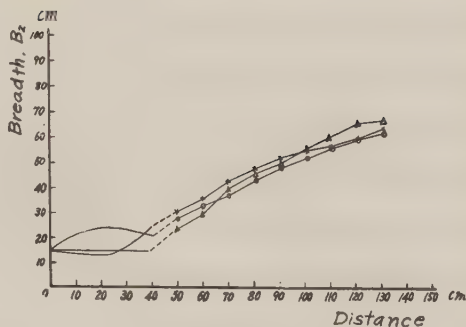


Fig. 7

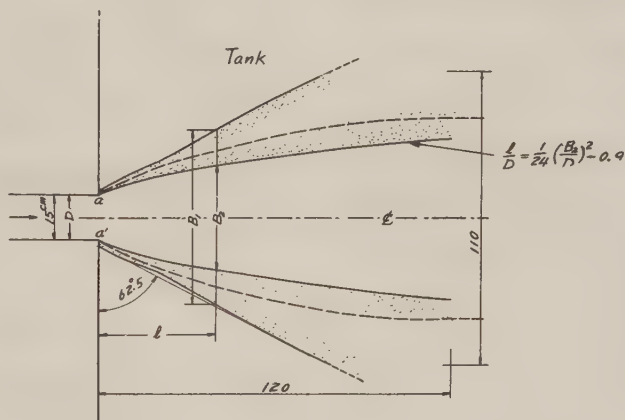


Fig.8

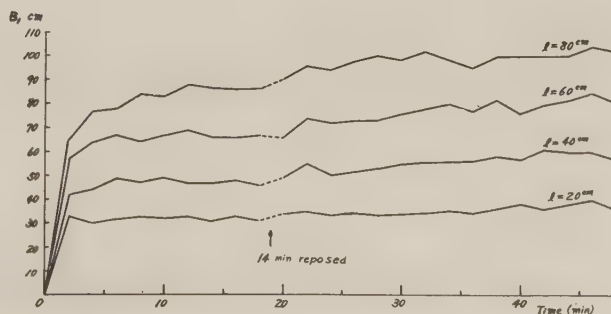


Fig. 9

the river mouth and B_2/D may be required from this test as following equation; that is

$$1/D = (B_2/D)^2 / k'_1 - k'_2$$

where k'_1 and k'_2 are coefficients that depend on the time, the discharge and other actual factors of the feature of jetty (in this test k'_1 and k'_2 are 2.4 and 0.9 respectively

). From this test,

$$k'_1 \approx k'_2$$

and then the diffusion curve is seemed to correspond to that of the sediment.

Therefore the author thinks that by the parallel jetty or no jetty, the sediment is diffused effectively from the mouth in such way.

But of course the flushing of the sandy loads depends on the position of the mouth of jetty. Or the long jetty is more useful than a short jetty.

Therefore it is concluded that the parallel, straight and long jetty may be used to good purpose.

4. Single Jetty

By the direction of a single jetty, types are classified as following two types;

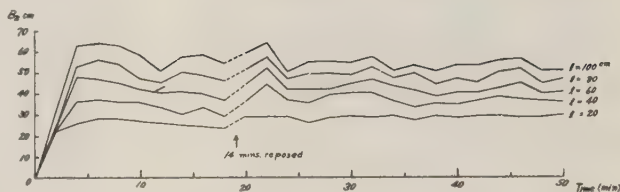


Fig.10

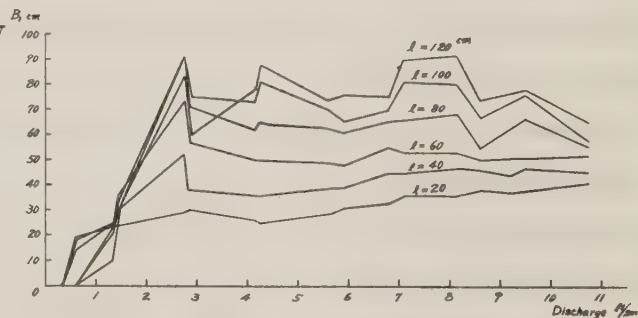


Fig.11

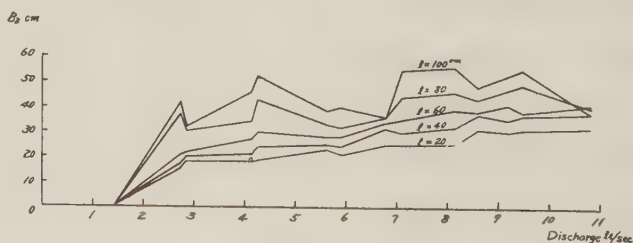


Fig.12

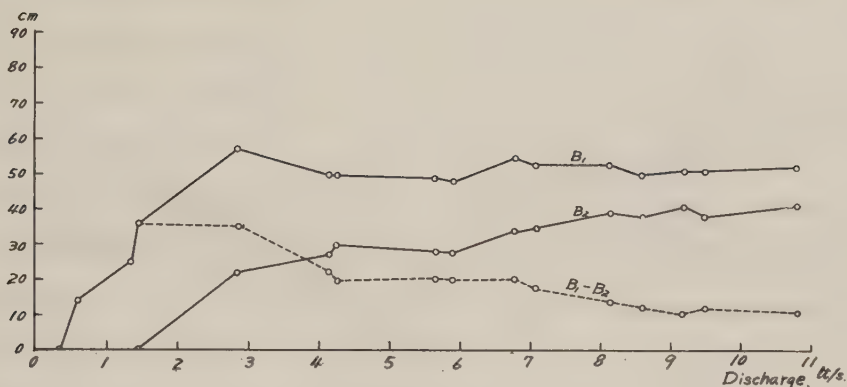


Fig.13

(1) the checked type to the main stream from a river as Fig.14 and
 (2) the unchecked type to the main flow as Fig.15. In these types the angle of the diffusion or the breadth of the sedimentation of sandy loads depends on the quantity of the discharge. Fig.16 and 17 show the breadth variation by the discharge. From these figures it is seemed that the checked type of a jetty pushes the main stream and sandy loads to the coast and the jetty of the unchecked type pulls the stream and sands.

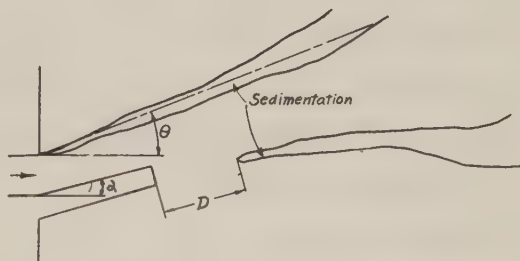


Fig.14

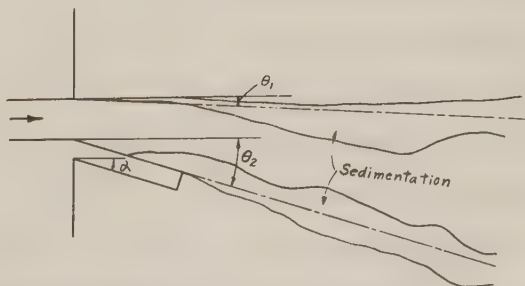


Fig.15

5. A Pair of Jetties

If parallel jetties are perpen-

dicular to the coastal line, the phenomenon of the stream and the sand movement are above mentioned as (3). But the action of the parallel jetty of the skewed type to a coast as Fig.18 and 19 may differ slightly from the perpendicular type. Fig.18 and 19 show respectively the diffusion of water stream and the feature of sandy sedimentation. The results are shown in Fig. 20 (the relation between the breadth B of the diffusion and the discharge), Fig.21 (the relation between the breadth B'_2 of the diffusion and the discharge), Fig.22 (the relation between the average breadth $\overline{B'_1}$, $\overline{B'_2}$ or $\overline{B'_1} - \overline{B'_2}$ of various angles and the discharge), and

Fig.23 (the relation

between the diffusion angle of sedimentation φ_1 or φ_2 and the discharge). From these figures it is understood that the parallel jetties have a little variation

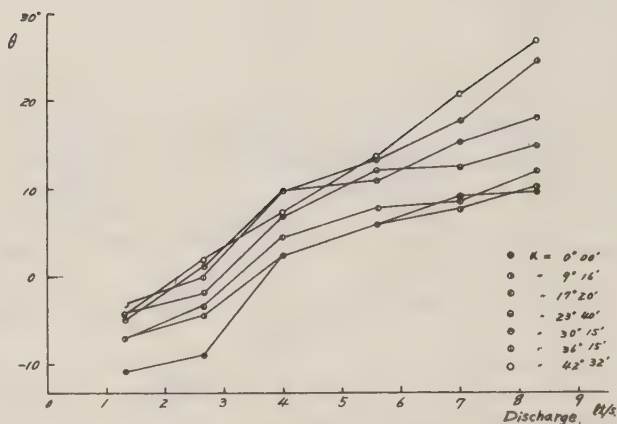


Fig.16

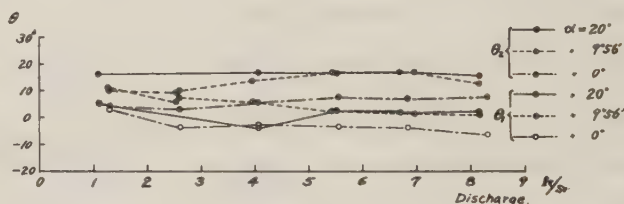


Fig.17

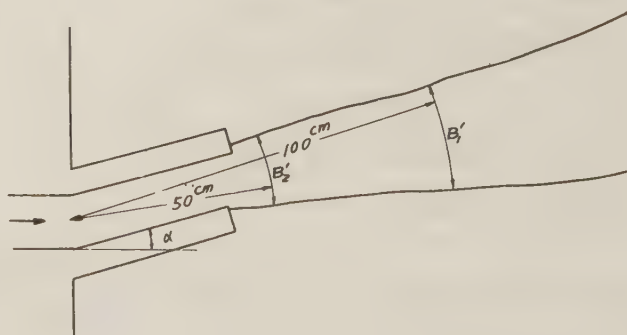


Fig.18

by the discharge, but does not so depend on the angle of the direction of jetty α and the skewed and parallel jetty is hardly found to the difference from the perpendicular type.

Not parallel jetties may differ from parallel types. For examples, the results of the test are shown in Fig.24. a, b, c, d and e. There are two types of the jetties of the breadth of mouth being reduced and enlarged.

In the enlarged breadth of the mouth of jetties, the diffusion of the main stream may becomes larger than that in the parallel jetties and may flush away the sandy sediment in the near of the river mouth. On the contrary, in jetties to be reduced the mouth, main stream may become a high velocity flow and sandy loads are entrained to the off-shore. But in the other hand, reduced jetties have the tendency which the energy of the flow decreases by frictions at

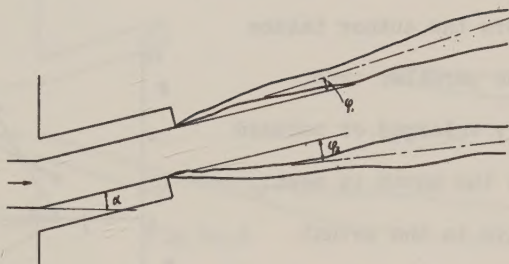


Fig.19

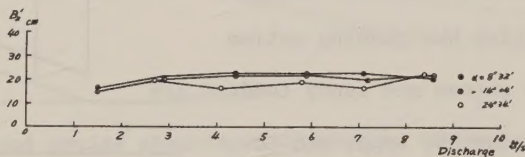


Fig.20

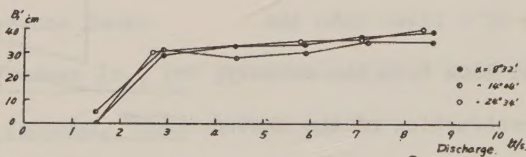


Fig.21

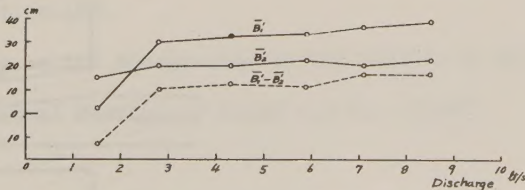


Fig.22

the wall side and by the scouring in the part of jetties. Therefore the author thinks that the parallel type, slightly enlarged or reduced type at the mouth is most effective in the actual estuary.

Skewed and parallel jetties have two actions of each side of jetties; that is, one side of jetties has pushing action of the stream and sandy loads as the checked type, and another side has pulling action of those as the unchecked type. Therefore for the introduction of the sandy loads and the stream of a river into the coastal line from the estuary, the construction of the skewed jetties of a pair may be adapted for this purpose of an actual work.

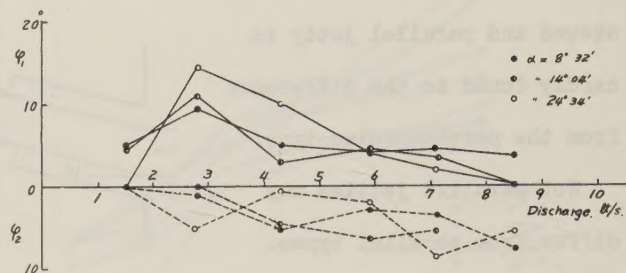


Fig.23

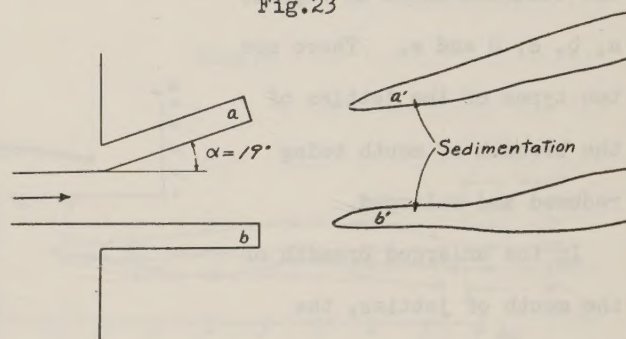


Fig.24.a

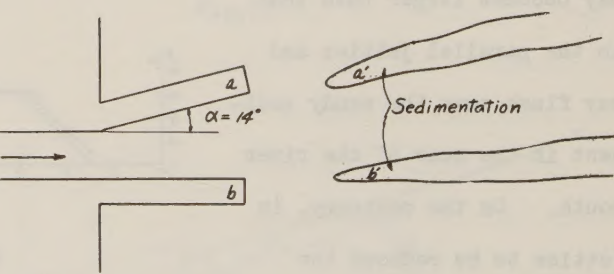


Fig.24.b

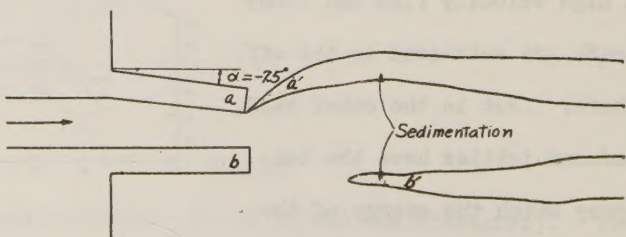


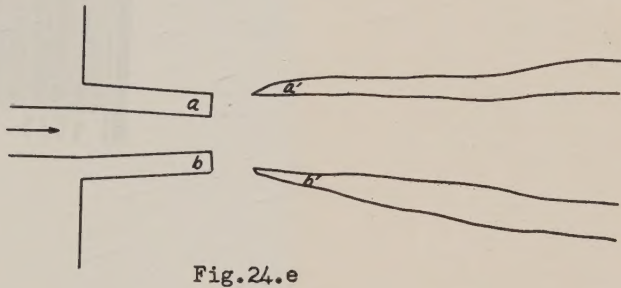
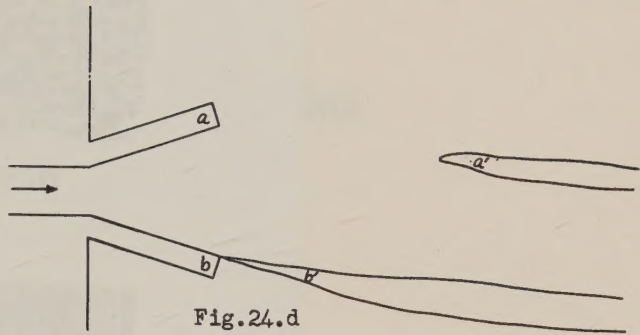
Fig.24.c

6. Conclusion

The author thinks that the parallel jetties are beneficial to guide the water flow and introduce the sandy loads sediment. But the prevention from the encloement in an estuary by sandy loads is not effective by only such jetty, and the sandy loads of the drift along a coast often close the mouth of the jetty.

Therefore, it is concluded

from these test, parallel jetties and groins checking the movement of the sandy drift must be effectively used for the prevention from the encloement at the river mouth.



Reference Books

- [1] Charles C.Bates and John C.Freeman Jr., The 3rd Conference of Coastal Engineering, Oct., (1952), by J.W. Johnson, "Coastal Engineering".
- [2] W.Tollmien, "Berechnung turbulenter Ausbreitungsvorgange", Z.a.M.M., Bd.6, (1926), S.468.
- [3] M.L.Albertson, Y.B.Dai, R.A.Jensen and Hunter Rouse, "Diffusion of submerged jets", Proc. A.S.C.E., Dec., (1948), p.468.
- [4] M.Homma and S.Sensyu, "Study on the energy-loss at the outlet of falling water and channel flow", The 8th Annual Meeting of Japan S.C.E., (1952).

